

**Identification of novel interactions between the proline- rich motif
on Receptor Tyrosine Kinases and the SH3 domain of cytoplasmic
proteins under non-stimulated conditions**

Janne Evjen Darell

Submitted in accordance with the requirements for the degree of
Doctor of Philosophy

Astbury Centre for Structural Molecular Biology

School of Molecular and Cellular Biology

The University of Leeds

November 2018

The candidate confirms that the work submitted is her own and that appropriate credit has been given where reference has been made to the work of others.

This copy has been supplied on the understanding that it is copyright material and that no quotation from the thesis may be published without proper acknowledgement.

The right of Janne Evjen Darell to be identified as author of this work has been asserted by her in accordance with the Copyright, Designs and Patents Act 1988.

© 2018 The University of Leeds and Janne Evjen Darell

Acknowledgments

I would like to thank my supervisor Professor John Ladbury for his guidance throughout my project and time in his lab. I would also like to thank all current and former members of the group for all their help and advice. In particular I want to thank Dr. Chi Chuan-Lin for his help with protein production, biophysical assays and other resources.

I would also like to thank my co-supervisor Dr. Andrew Macdonald for all his help with my project, and also his guidance as a tutor. An extended thank you to current and former lab members from the Macdonald group for all advice you have given me. In particular I would like to thank Ethan Morgan for his support during all my rants about project things and non-project things.

I've been funded by the Wellcome Trust and I am extremely grateful to have been given this opportunity to carry out a 4-year long studentship. A big thank you to the Wellcome Trust cohort here at the University of Leeds, former and current students, but particularly everyone in my year who I've had some incredible times with, both on and off campus. Whenever I have had a bad day, meeting up with any of you has always lifted my spirits. So a massive thank you to Anna, Dan, Ethan, Hugh, Ieva and our adopted member Becky.

Nicola Jane Taylor, you have been a solid friend. Thank you for all your advice and putting everything into perspective. And the Baileys. And Toni Braxton.

Francis, thank you for being so patient with me. Thank you for saying all the right things and making me calm. I will repay it when it's your turn.

Lastly I want to thank my family and friends back home in Norway. Tusen takk mamma og pappa, dere har støttet meg hele veien helt ubetinget og alltid vært der for meg. Det er alltid trygt og godt å komme hjem, og den roen jeg har fått har hjulpet gjennom alle årene jeg har holdt på. Jeg lover jeg er ferdig nå...

Tusen takk til tante Lise som har vært en uvurderlig støtte som jeg alltid har sett opp til.

Abstract

A “second tier” regulation of signalling from Receptor Tyrosine Kinases (RTK) has been uncovered where the receptor can be activated without ligand stimulation. This is mediated from an interaction between SH3 domains and proline-rich motifs in the RTK C-terminal tail. Most RTKs have one or more proline-rich motifs in their C-terminal tail. The outstanding question remains as to what is the importance of these interactions. Several high-throughput screens have been carried out to discover novel interactions between proline-rich motifs and SH3 domains. One potential candidate is the oncogenic LIM and SH3 domain protein 1 (LASP1). Work presented here demonstrates that LASP1 directly interacts with the C-terminal tail of several RTKs. The oncogenic RTK ErbB2 has been shown to directly interact with LASP1 via the ErbB2 C-terminal tail. More importantly an endogenous interaction was demonstrated in the breast cancer cell line SkBr3. Both LASP1 and ErbB2 are found in the vicinity of each other on the chromosome, and co-overexpression of both proteins has been shown in breast cancers. LASP1 has also been shown to directly interact with Fibroblast Growth Factor Receptor 2 (FGFR2). This interaction happens via the C-terminal tail of FGFR2, which has previously been shown to be important in “second tier” signalling and regulation. Preliminary data suggests that the LASP1 and FGFR2 interaction may impact cell growth and migration. In another example of a “second tier” interaction, the SH3 domains from SRC family kinases FYN and SRC are shown to interact with ErbB2 under starved conditions, and the interaction between SRC and ErbB2 is mediated by a proline-rich motif in ErbB2. Taken together these data demonstrate a role for the C-terminal tail of several RTKs in interacting with proteins in a non-stimulated background, and challenges the canonical view of RTK signalling.

Contents

Acknowledgments	ii
Abstract	iii
Contents	iv
List of Tables	viii
List of Figures	ix
Abbreviations	xi
Chapter 1: Introduction	1
1.1 Cell signalling	1
1.2 Receptor Tyrosine Kinases	2
1.3 FGFR family	4
1.3.1 FGFR signalling	4
1.3.2 MAPK/ERK pathway	7
1.3.3 PI3K/Akt pathway	7
1.3.4 FGFRs role in cancer	8
1.3.5 FGFR2	8
1.3.6 SH2 domain	9
1.3.7 SH3 domains and Proline-rich motifs	10
1.3.8 FGFR2 under non-stimulated conditions.....	12
1.4 ErbB family.....	15
1.4.1 ErbB2 signalling	17
1.4.2 The role of ErbB2 in cancer	18
1.4.3 ErbB2 regulates the cell cycle	19
1.4.4 ErbB2 interacts with a member of SRC family non-receptor kinases	21
1.5 SRC family kinases	21
1.5.1 SRC structure and conformation	22
1.5.2 The role of SRC in cancer.....	24
1.6 LASP1 domains and interacting partners	25
1.6.1 LASP1 function and role in cancer	26
1.7 Aims and objectives	28
Chapter 2: Materials and Methods	30
2.1 Bacterial cell culture	30
2.1.1 Bacteria growth and storage	30

2.1.2	Transformation	30
2.1.3	Preparation of plasmid DNA.....	30
2.2	Molecular cloning	31
2.2.1	Polymerase chain reaction (PCR)	31
2.2.2	Agarose gel electrophoresis and gel extraction.....	32
2.2.3	DNA ligation reactions.....	32
2.3	Protein expression and purification	32
2.3.1	Maltose Binding Protein (MBP)	33
2.3.2	Glutathione-S-Transferase (GST)	33
2.4	Protein biochemistry.....	35
2.4.1	Protein concentration determination.....	35
2.4.2	SDS polyacrylamide gel electrophoresis (SDS-PAGE)	35
2.4.3	Western blot.....	35
2.4.4	Dot blot.....	37
2.5	Mammalian cell culture	37
2.5.1	Cell lines and maintenance	37
2.5.2	Transient transfections	38
2.5.3	Cell lysis	39
2.6	Immunocytochemistry	40
2.6.1	Growing cells on coverslips and fixation	40
2.6.2	Proximity ligation assay and ICC.....	40
2.6.3	Microscopy	41
2.6.4	Statistics for PLA.....	41
2.7	Immunoprecipitation and pull downs	42
2.7.1	Sample preparation for Mass Spectrometry	42
2.7.2	Co-IP.....	42
2.7.3	GFP/RFP pull down	42
2.7.4	GST/MBP pull down.....	43
2.8	Microscale thermophoresis (MST)	43
2.8.1	Protein labelling.....	43
2.8.2	Microscale thermophoresis	44
2.9	Growth and migration assays.....	46
2.9.1	Growth assays	46
2.9.2	Scratch wound assay	47

Chapter 3: High-throughput analysis to detect SH3 containing proteins which interact with the proline-rich motifs of receptor tyrosine kinases	48
3.1.1 The use of mass spectrometry to detect SH3 domain containing proteins	53
3.1.2 Using purified peptides of the C-terminal tails of RTKs in a dot blot	59
3.1.3 Verifying LASP1 binding to selected receptors from the dot blot	63
3.1.4 Discussion.....	68
Chapter 4: Interaction between LASP1 and FGFR2 proline-rich motif and physiological significance of the interaction in cells	71
4.1.1 FGFR2 C-terminal tail interacts with LASP1 SH3 domain in cells	73
4.1.2 Further characterisation of the FGFR2 and LASP1 interaction using MST and mutants	78
4.1.3 Physiological relevance of the LASP1 and FGFR2 interaction	82
4.1.4 Discussion.....	90
Chapter 5: ErbB2 and SRC interact in starved conditions in a breast cancer cell line	94
5.1.1 SRC and ErbB2 interact in the breast cancer cell line SkBr3 under starved conditions	98
5.1.2 ErbB2 interacts with the SH3 domain of SRC and FYN	103
5.1.3 A proline-rich motif in ErbB2 C-terminal tail interacts SRC	109
5.1.4 Binding affinities between ErbB2 peptides and SRC SH3 domain suggest a weak interaction	112
5.1.5 Discussion.....	115
Chapter 6: Discussion	118
Chapter 7: Conclusions and further directions	126
Bibliography	128
Appendix A: All identified proteins from MS screen using peptides with proline-rich motifs from RTKs	151
ALK-1	151
ALK-2	154
ErbB2-1-1.....	158
ErbB2-1-2.....	163
ErbB2-2-1	167
ErbB2-2-2.....	171

FGFR1-1	173
FGFR1-2	176
FGFR2-1	181
FGFR2-2	184
FGFR2-3	186
IGFR-1	189
IGFR-2	193
PDGFRB-1	199
PDGFRB-2	202
Control peptide 1	207
Control Peptide 2	210
Appendix B: Table of accession numbers from MS.....	214
Appendix C: C58 amino acid sequences	228

List of Tables

Table 1 Oligonucleotides for mutagenesis.	31
Table 2 PCR reagents for mutagenesis.....	31
Table 3 PCR steps for mutagenesis	31
Table 4 Proteins expressed and purified	33
Table 5 Primary and secondary antibodies used for detection of Western blots	36
Table 6 Cell lines used in mammalian cell culture	38
Table 7 Plasmids for mammalian transfection	38
Table 8 High-throughput screen of C-terminal tails and SH3 domains done by Prof. M. Bedford. Relative fluorescence for each SH3 domain was measured and here are the top five hits presented.	50
Table 9 Interactions between RTK C-terminal tail and LASP1 with and without the SH3 domain based on relative intensity from dot blot (Figure 3.3).....	61
Table 10 List of C-terminal tail peptides and molecular weight used in dot blot	63
Table 11 MST binding affinities. Labelled proteins are listed first and always at a concentration of 100 nM	82
Table 12 Peptides containing proline-rich motifs from ErbB2 C-terminal tail and NS5A. MST was used to determine binding affinity between the peptides and SH3 domains from SRC and FYN	113

List of Figures

Figure 1-1 RTK subfamilies and domain structures.....	3
Figure 1-2 FGFR-FGF structure.....	5
Figure 1-3 Signalling pathways activated by FGFRs.	6
Figure 1-4 FGFR2 isoforms binds to different FGFs.	9
Figure 1-5 SRC SH2 domain.....	10
Figure 1-6 LASP1 SH3 domain (PDB 3i35).....	12
Figure 1-7 Proline-rich motifs form helices that interacts with pockets on the SH3 domain surface.	12
Figure 1-8 GRB2 C-SH3 domain can interact with FGFR2 C-terminal tail.	13
Figure 1-9 GRB2 interaction with FGFR2.....	14
Figure 1-10 ErbB domain organisation.	17
Figure 1-11 Cell cycle phases and components.....	20
Figure 1-12 SRC family kinase structure and domains.....	23
Figure 1-13 SRC family kinase open/active and closed/inactive conformation structure.....	23
Figure 1-14 LASP1 structure and domains. At the N-terminal there is a LIM domain, followed by two nebulin repeats and at the C-terminal an SH3 domain.	26
Figure 1-15 In a complex with ZO-2, LASP1 translocates to the nucleus after phosphorylation by PKA. LASP1 is dephosphorylated by PP2B.	26
Figure 2-1 A typical experimental setup of Microscale Thermophoresis interface.	45
Figure 2-2 Soft agar assay illustration. A typical well for Soft agar assay consisted of a base layer of 1% agarose mixed with 2X DMEM. Cells were mixed with a top layer of 0.7% agarose and 2X DMEM.....	47
Figure 3-1 Fluorescent screen with purified SH3 and WW domains incubated with peptides containing proline-rich motifs from various RTKs.....	52
Figure 3-2 Number of unique peptides from each protein that were pulled down by proline-rich peptides from receptors.....	58
Figure 3-3 Dot blot with purified MBP-tagged C-terminal tails of RTKs.	62
Figure 3-4 Validation of LASP1 interactions.....	67
Figure 4-1 Preliminary fluorescent screen with FGFR2 peptide	73
Figure 4-2 GST pull downs shows LASP1 interaction with FGFR2	76

Figure 4-3 PLA demonstrated that FGFR2 and LASP1 interacts in HEK293T cells and that it is through the C-terminal tail.....	77
Figure 4-4 Mutations in the C58 construct. The last 25 amino acids are used here to highlight the different deletion mutants and point mutations used in the MST experiments.	79
Figure 4-5 Binding affinities determined by MST	80
Figure 4-6 Western blot analysis of protein changes under LASP1 and FGFR2 overexpression.....	85
Figure 4-7. Growth assays for FGFR2 and LASP1 interaction	88
Figure 4-8 Migration assay for LASP1 and FGFR2 interaction.	89
Figure 5-1 ErbB2 proline-rich motifs and Src/Fyn homology.....	97
Figure 5-2 ErbB2 and SRC interact endogenously in breast cancer cell line SkBr3.	100
Figure 5-3 ErbB2 and SRC interact endogenously in breast cancer cell line SkBr3	101
Figure 5-4 ErbB2 and SRC interact in absence of EGFR	102
Figure 5-5 The SH3 domain of SRC is interacting with ErbB2.	106
Figure 5-6 SRC interaction with ErbB2 could be dependent on SRC conformation.	107
Figure 5-7 The C-terminal tail of ErbB2 is interacting with SRC.	110
Figure 5-8 MST was used to determine binding affinities between peptides based on sequences in the C-terminal tail of ErbB2 containing proline-rich motifs and the SH3 domains of either SRC or FYN.	114
Figure 5-9 Proposed model for SRC and ErbB2 interaction. Both SH2 and SH3 can interact with the receptor, either with pTyr or a PXXP motif on the C-terminal tail of ErbB2.....	117

Abbreviations

ABL: Abelson murine leukemia viral oncogene homolog 1

ALK: Anaplastic Lymphoma Kinase

BCR: Breakpoint cluster region protein

CDKs: Cyclin dependent kinases

CSK: C-terminal SRC kinase

DAG: Diacylglycerol

EGF: Epidermal Growth Factor

EGFR: Epidermal Growth Factor Receptor

ERBB: Avian erythroblastosis oncogene B

ERK: Extracellular signal-Regulated Kinase

FBS: Foetal Bovine Serum

FGF: Fibroblast Growth Factor

FGFR: Fibroblast Growth Factor Receptor

FRS2: FGFR substrate 2

GPCR: G-protein Coupled Receptor

GRB2: Growth factor receptor-bound protein 2

GST: Glutathione-S-Transferase

HSPG: Heparan Sulphate Proteoglycans

Ig: Immunoglobulin

IGF1R: Insulin like Growth Factor 1 Receptor

InsR/INSR: Insulin Receptor

INSRR: Insulin receptor-related protein

IPTG: Isopropyl- β -D-thio-galactoside

KRP1: Kelch related protein

LASP1: LIM and SH3 protein 1

LPP: Lipoma preferred partner

MAPK: Mitogen-activated protein kinase

MBP: Maltose Binding Protein

MS: Mass spectrometry

MST: Microscale Thermophoresis

PBS: Phosphate buffered saline

PDGFRB: Beta-type platelet-derived growth factor receptor

PH: Pleckstrin homology

PI3K: Phosphoinositide 3-kinase

PIP2: Phosphatidylinositol-4,5-bisphosphate

PIP3: Phosphatidylinositol-3,4,5-trisphosphate

PKA: Protein Kinase A

PKC: Protein Kinase C

PLA: Proximity Ligation Assay

PLC γ : Phospholipase C, gamma

PP2B: Serine/threonine-protein phosphatase 2B

PTB: Phosphotyrosine binding domain

PTP1B: Protein-tyrosine phosphatase 1B

PTEN: Phosphatase and tensin homolog deleted on chromosome 10

RTK: Receptor Tyrosine Kinases

SH2/SH3: Src homology 2/3 domain

SOS: Son of Sevenless

STAT3: Signal Transducer and Activator of Transcription

TBS: Tris buffered saline

TGF- α : Transforming growth factor- α

Tyr/Y: Tyrosine

VASP: Vasodilator-stimulated phosphoprotein

VEGFR: Vascular Endothelial Growth Factor Receptor

ZO-2: Zonula occludens protein 2

Chapter 1: Introduction

1.1 Cell signalling

Cells have developed an astonishingly complex way of communication. There are a large number of components involved and there is need for highly specific interactions and regulation. Signalling events are mainly activated by extracellular stimuli binding to specific receptors resulting in intracellular responses such as receptor conformational changes. Signalling events can activate cellular processes including cell proliferation, migration and differentiation. Perturbations of these signalling events have dramatic consequences for the cell and are often found to be involved in many disease states such as cancers. There are three main groups of cell surface receptors; ion channel coupled receptors, G-protein coupled receptors (GPCRs) and enzyme coupled receptors. Ion channel receptor activation by ligand binding opens up the channel to allow flow of ions such as K^+ , Ca^{2+} , Na^+ or Cl^- leading to a change in membrane potential. GPCRs are the most abundant receptor type of the main groups. These have seven transmembrane helices and are activated by ligand binding in the extracellular loops (Trzaskowski et al., 2012). Conformational change from the ligand binding leads to G-protein activation and further downstream activation of pathways as determined by the G-protein subclass. Enzyme coupled receptors are transmembrane receptors and are activated by ligand binding at extracellular domains. The largest group among enzyme-coupled receptors are Receptor Tyrosine Kinases (Uings and Farrow, 2000).

1.2 Receptor Tyrosine Kinases

RTKs consist of an extracellular region, a transmembrane domain, an intracellular kinase domain and a cytoplasmic tail. Most RTKs are activated by a similar mechanism. Ligand binding of two monomeric receptors at the extracellular domain causes receptor dimerisation. The receptor dimer undergoes a conformational change and the intracellular kinase domain trans-phosphorylates tyrosine residues in the intracellular tail and kinase domain. This allows the recruitment of proteins to the phosphorylated tyrosines (pY/pTyr) and further activation of signalling pathways (Lemmon and Schlessinger, 2010). Proteins can be recruited to multiple regions of the intracellular receptor, although many tyrosines are found in the cytoplasmic tail. This is a highly flexible region and is important for protein docking. Some of the flexibility of the C-terminus tail is facilitated by prolines, although another important feature of prolines in the C-terminal tail is binding proteins when the receptor molecules are not activated, which will be discussed in detail later. The juxtamembrane region can also be important for downstream signalling activation, with both allosteric regulation and protein recruitment, which will be discussed later. The human genome encodes for 58 RTKs which are distributed into 20 subfamilies (Robinson et al., 2000). The subfamilies have variabilities in the extracellular ligand binding site, highlighting the specificity for binding the activating ligand (Figure 1.1). On the intracellular region all receptors contains a tyrosine kinase domain. Activated kinase domains are highly similar across all kinase domain containing proteins. They contain a catalytic subunit which transfers phosphate from ATP to tyrosines (Nolen et al., 2004). A glycine-rich motif close to a lysine is important for ATP binding. The lysine forms hydrogen bonds with oxygen molecules within phosphate groups, and is essential for ATP binding. A conserved aspartic acid is important for the enzyme

activity, potentially as a result of the negative charge of aspartic acid assisting in substrate binding (Knighton et al., 1991).

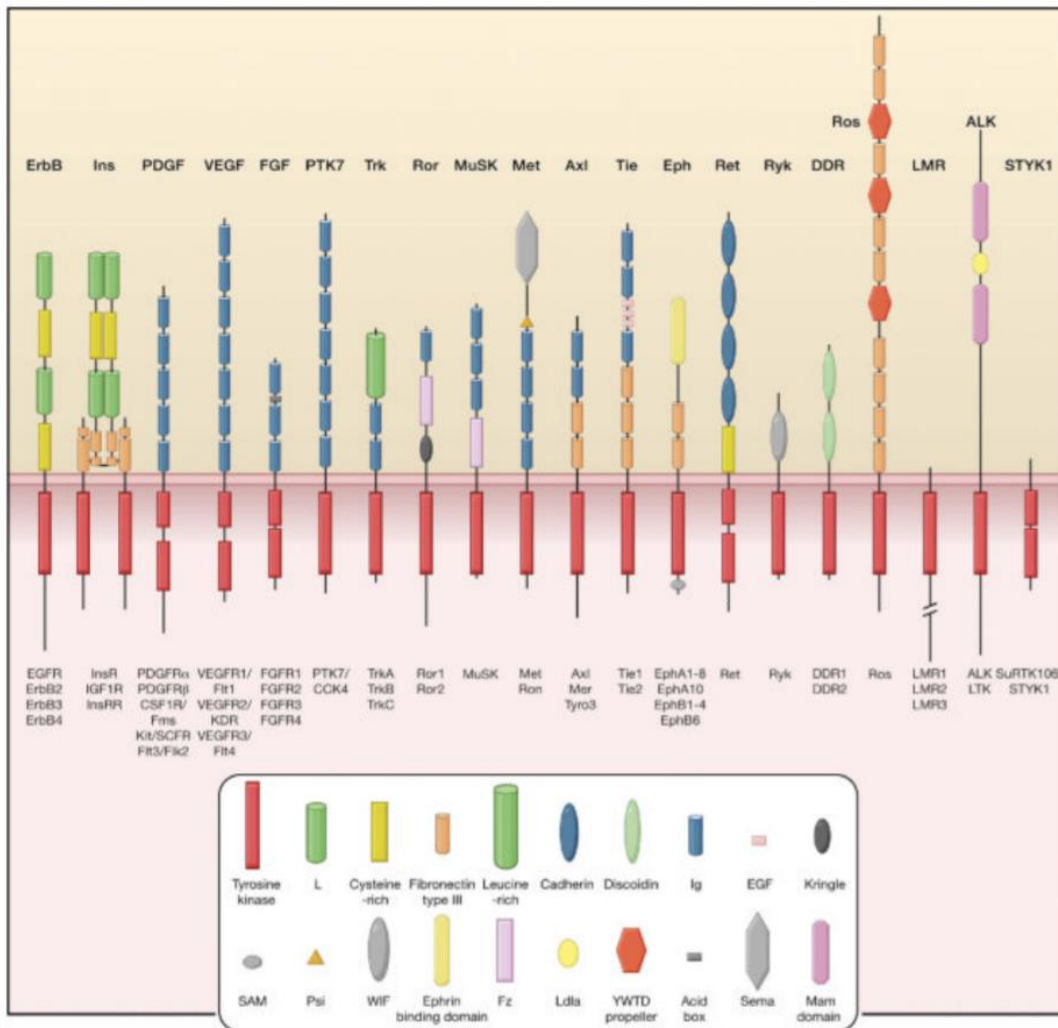


Figure 1-1 RTK subfamilies and domain structures

This includes families such as Epidermal Growth Factor Receptor family (EGFR/ErbB), Insulin receptor family (Ins, InsRR and IGF1R), Platelet-Derived Growth Factor Receptor (PDGFR), Vascular Endothelial Growth Factor Receptor (VEGFR) and Fibroblast Growth Factor (FGFR) family (Lemmon and Schlessinger, 2010).

1.3 FGFR family

The Fibroblast Growth Factor Receptor (FGFR) family consists of four members; FGFR1-FGFR4. A fifth receptor has been identified which is able to bind Fibroblast Growth Factors (FGF) but lacks a kinase domain (Sleeman et al., 2001). The FGF family contains 22 genes, out of which 18 members of the FGF family has been shown to bind to FGFRs on the extracellular domain and activate the receptor (Ornitz and Itoh, 2001; Ornitz and Itoh, 2015). The FGFs can be divided into subfamilies based on their function, such as paracrine or endocrine secretion or intracellular FGFs (FGF 11 and FGF13 are intracellular and does not bind FGFRs). There are 4 genes encoding FGFRs, but consists of 7 members from alternative splicing. Alternative splicing of the receptors produces different isoforms and the splicing can increase or decrease affinity of interactions with FGFs (Miki et al., 1992; Leung and Neal, 1997; Ornitz and Itoh, 2015)

1.3.1 FGFR signalling

The extracellular region of FGFRs consist of three immunoglobulin (Ig)-like domains which interact with FGFs and heparan sulphate proteoglycans (HSPGs). The FGF binding pocket is found between Ig II and Ig III (Figure 1.2). Alternative splicing of the Ig III domain determines FGF binding specificity. HSPGs sequester FGFs to the cell membrane by binding with low affinity and in a complex with FGFRs it increases the stability of the interaction (Turner and Grose, 2010). Once a dimer is formed by FGFRs, the intracellular kinase domain trans-phosphorylates tyrosine residues in a specific order, which serves as a docking site for proteins to activate a number of downstream pathways.

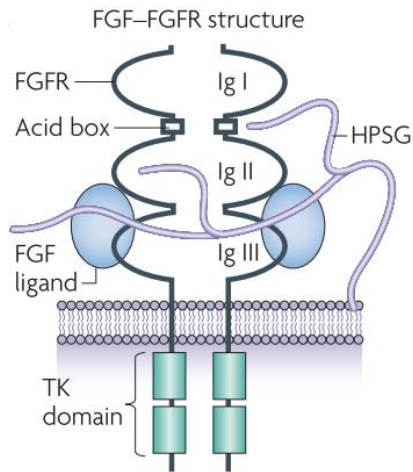


Figure 1-2 FGFR-FGF structure.

Two FGF receptors, two FGFs and a heparan sulphate proteoglycans (HSPGs) chain forms a complex in which is the activated receptor. FGFs interact with FGFRs in a binding pocket between Ig II and Ig III (Turner and Grose, 2010).

Pathways activated by FGFR include mitogen-activated protein kinase (MAPK) pathway, phospholipase C γ (PLC γ) and phosphoinositide 3-kinase (PI3K)-AKT signalling (Figure 1.3) (Turner and Grose, 2010; Brooks et al., 2012). FGFR substrate 2 (FRS2) binds at a NPXY motif (and not pTyr) in the juxtamembrane region of FGFR via the FRS2 phosphotyrosine binding domain (PTB). It is important to point out that FGFR1 and FGFR2 shows distinct mechanisms in interacting with FRS2. FGFR1 is found in a constitutive complex with FRS2 regardless of receptor activity, while for FGFR2 FRS2 is recruited upon receptor stimulation (Ahmed et al., 2008). Once FRS2 is recruited, FGFR2 phosphorylates FRS2 (Ong et al., 2000a). Once phosphorylated FRS2, provides a recruitment site for downstream proteins such as growth factor receptor-bound protein 2 (GRB2), which then recruits son-of-sevenless (SOS) and this leads to activation of the MAPK/ERK pathway via RAS (Kouhara et al., 1997). Additionally GRB2 can activate the PI3K/AKT pathway. PLC γ 1 can interact with pTyr of FGFR (pY769 in FGFR2) via its SRC homology 2

(SH2) domain, and activated PLC γ 1 hydrolyses phosphatidylinositol-4,5-bisphosphate (PIP $_2$) to Inositol trisphosphate (IP $_3$, denoted PIP $_3$ in figure 3, but they are not the same) and diacylglycerol (DAG) (Peters et al., 1992). DAG activates MAPK pathway via Protein Kinase C (PKC). Other pathways activated by FGFRs include Signal transducer and activator of transcription (STAT3) pathway (Hart et al., 2000).

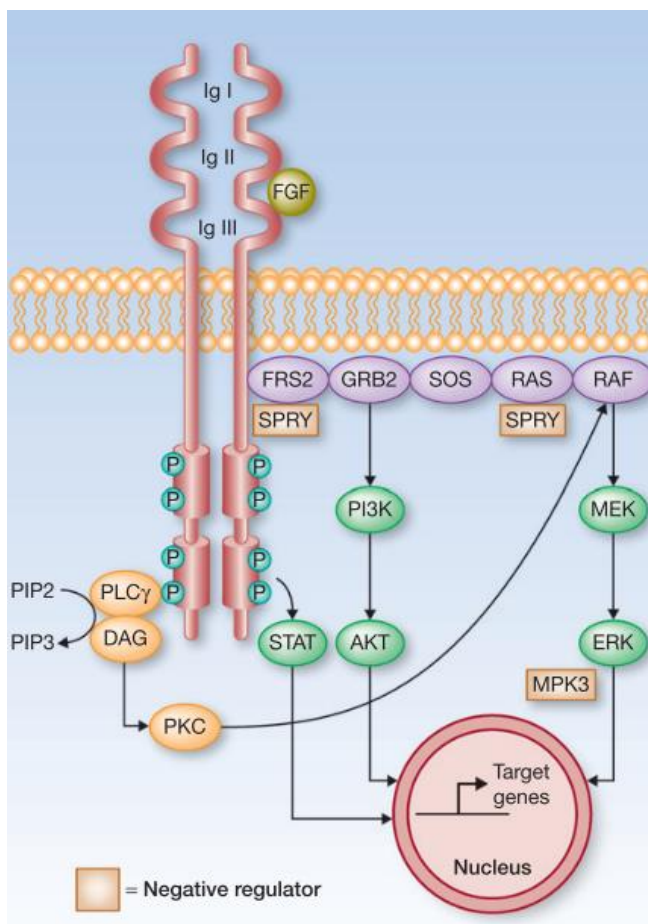


Figure 1-3 Signalling pathways activated by FGFRs.

FRS2 binds the FGFR2 juxtamembrane region and phosphorylation of FRS2 by FGFR sequesters GRB2 and SOS. The complex activated the MAPK pathway via RAS. GRB2 can also independently activate the PI3K/AKT pathway. PLC γ can interact with FGFRs via its SH2 domain and activated PLC γ hydrolyses PIP $_2$ to IP $_3$ (not PIP $_3$ like in figure) and DAG. DAG can activate MAPK pathway via PKC. Other pathways that are activated by FGFRs includes STAT pathway (Brooks et al., 2012).

1.3.2 MAPK/ERK pathway

MAPK pathways are activated by a number of receptors, including RTKs and GPCRs. Activation of these pathways leads to a wide range of cellular responses including proliferation, differentiation and apoptosis. Three different classes of MAPK pathways have been extensively studied; p38 MAPK pathway, JUN kinase (JNK) and Extracellular signal-Regulated Kinase (ERK), with ERK/MAPK being the best characterised RTK-activated signalling pathway. The three classes share the overall structure of the MAPK activation where phosphorylation drives the cascade. As previously mentioned ERK/MAPK can be activated in a number of ways, including by PKC and RAS, which activates RAF/MAPKKK. RAF/MAPKKK then phosphorylates MEK/MAPKK 1/2 which in turn phosphorylates ERK 1/2 (also known as MAPK p42/44). ERK 1/2 can further control protein activity or translocate to the nucleus to activate transcription (Zhang W, 2002; Roskoski, 2012).

1.3.3 PI3K/Akt pathway

Another pathway activated by a number of receptors is the PI3K/AKT pathway. PI3K phosphorylates PIP₂, which is found enriched at the plasma membrane, to produce PIP₃ (phosphatidylinositol-3,4,5-bisphosphate). PIP₃ can recruit proteins containing pleckstrin homology (PH) domains such as the protein kinase AKT. AKT is activated by phosphorylation and then serves as a downstream mediator of the pathway. AKT activity is negatively regulated by Phosphatase and tensin homolog deleted on chromosome 10 (PTEN), which dephosphorylates PIP₃ to PIP₂ and AKT can no longer be recruited to the plasma membrane (Franke et al., 1997; Campbell et al., 2003; Engelman et al., 2006; Redfern et al., 2008).

1.3.4 FGFRs role in cancer

Any perturbations of the signalling cascades that are regulated by FGFRs have the potential to induce detrimental effects in the cell. As a result, deregulated FGF signalling is often linked to cancers. Mutations of the receptors have been found in many human cancers including bladder, cervical and endometrial cancers (Turner and Grose, 2010). A single point mutation in the extracellular domain of FGFR3 replacing serine with cysteine results in a disulphide bridge being formed between monomeric receptors forming a constitutively active dimeric receptor without ligand activation (di Martino et al., 2009). Receptor gene amplification of FGFR1 and FGFR2 is found in a subset of cancers such as breast cancers and gastric cancers (Jacquemier et al., 1994; Courjal et al., 1997; Kunii et al., 2008). Chromosomal translocations in which FGFR1 forms a fusion protein with zinc-finger containing protein ZNF198 are found in lymphoma and myeloid leukaemia. The fusion protein forms dimers and is constitutively active (Xiao et al., 1998; Roumiantsev et al., 2004). Overexpression of growth factors is also linked to cancers. FGF1 was found to be overexpressed in ovarian cancer (Birrer et al., 2007) and inhibiting expression of FGF1/FGFR1 by antisense cDNA in mice with subcutaneous human melanomas showed tumour regression (Wang and Becker, 1997). These examples from multiple cancers and by various mechanisms illustrate the importance of the role of FGFR.

1.3.5 FGFR2

FGFR2 has two splicing variants, FGFR2 IIIb and FGFR2 IIIc which can interact with different FGFs (Figure 1.4). The isoforms are differentially expressed in tissues. The IIIb variant is predominantly found in epithelial cells while the IIIc isoform is expressed in mesenchymal cells (Katoh, 1992). FGFR2 mutations are associated

with a number of diseases. Missense mutations in the third Ig-domain or in the tyrosine kinase domain have been associated with congenital skeletal disorders (Katoh, 2009). FGFR2 gene amplification has been demonstrated in breast cancer and gastric cancer (Nakatani et al., 1990; Adnane et al., 1991). Missense mutations of FGFR2 are associated with several cancers such as breast cancer, lung cancer, gastric cancer and melanoma (Jang et al., 2001; Stephens et al., 2005; Davies et al., 2005; Gartside et al., 2009). The canonical signalling from FGFR2 is like other activated RTKs with PTB and/or SH2-domain containing proteins that interact with pTyr. Interestingly a second-tier activation has been discovered involving proteins containing SH3 domains binding a proline-rich motif in the FGFR2 C-terminal tail, which will be discussed later.

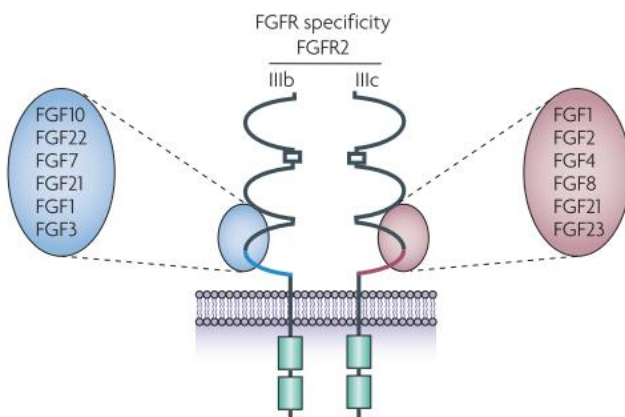


Figure 1-4 FGFR2 isoforms binds to different FGFs (Turner and Grose, 2010).

1.3.6 SH2 domain

SH2 domains are central in interactions with RTKs. Together with PTB domains they bind phosphorylated tyrosines. Proteins containing SH2 domains can be divided into two groups. One where the proteins also have enzymatic activity, like non-receptor tyrosine kinases such as the SRC family which contain both an SH2 and kinase domains. The second group often has single or tandem SH2 domains, sometimes in

conjunction with SH3 domains. These proteins act as adaptor or scaffold proteins, such as GRB2 (Schlessinger, 1994). The SH2 domain is structurally conserved amongst proteins and consists of a hydrophobic anti-parallel beta-sheet flanked by α -helices (Figure 1.5). It recognises a stretch of 3-6 amino acids, starting with pTyr. A conserved arginine interacts with the negative charge of the phosphate group and pTyr is buried into the pTyr binding pocket (Ladbury and Arold, 2000).

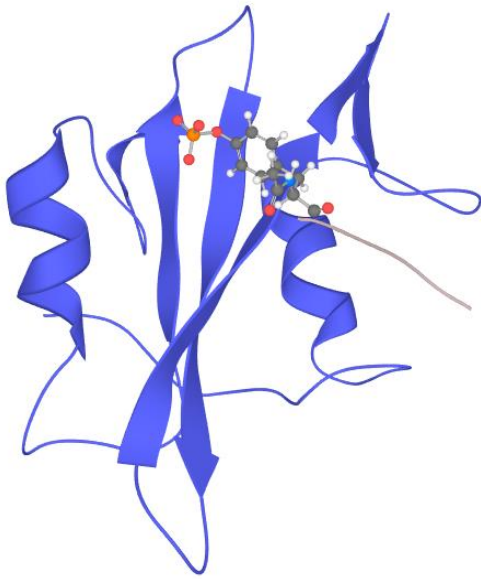


Figure 1-5 SRC SH2 domain

SRC SH2 domain consisting of three anti-parallel beta-sheets flanked by alpha-helices. A peptide containing a phosphorylated tyrosine (ball-and-stick) shows that pTyr interacts with the loop between two beta-sheets (Kohda et al., 1993).

1.3.7 SH3 domains and Proline-rich motifs

SH3 domains are abundant in the cell and about 300 SH3 domains are encoded by the human genome. Unlike SH2 domains, the SH3 domain interactions with proline-rich motifs are generally much weaker interactions, where SH2 domains can interact with a pTyr of the preferred motif pYEEI with an affinities between 0.1-1 μ M (Ladbury and Arold, 2000). For SH3 domains the affinities are weaker. For example, the SH3

domains of the GRB2 dimer interact with FGFR2 molecules with a K_D of 0.1 and 25 μM , while the PLC γ 1 SH3 domain binds FGFR2 proline-rich motif with a K_D of 40 μM (Lin et al., 2012; Timsah et al., 2014). Other examples include GRB2 interacting with peptides from SOS at affinities 5 and 21 μM (Ladbury and Arold, 2000). The structure of SH3 domains consists of a beta-barrel formed by two β -sheets (Figure 1.6). The hydrophobic surface of SH3 domains contains small pockets conserved by aromatic residues, which can be occupied by prolines. Proline-rich motifs form a unique helical conformation, Polyproline (PP) II. The PPII helix contains three residues per turn and the prolines are trans-conformation, so they can occupy the ligand-binding pockets. PPII helices have been divided into two classes; class I that binds in a plus orientation and class II that binds in a minus orientation (Figure 1.7) (Mayer, 2001; Kurochkina and Guha, 2013). A consensus sequence of prolines that often bind SH3 domains is PXXP which forms the PPII conformation. P is proline and X can be any residue but is often hydrophobic. However, there is evidence that a much larger variety of proline-rich motifs can interact with SH3 domains. A high-throughput analysis using a library of random peptides was used to identify binding partners of purified SH3 domains, and over half of the SH3 domains could interact with non-canonical peptides, and they also exhibited specificity for several peptides (Teyra et al., 2017).



Figure 1-6 LASP1 SH3 domain (PDB 3i35)

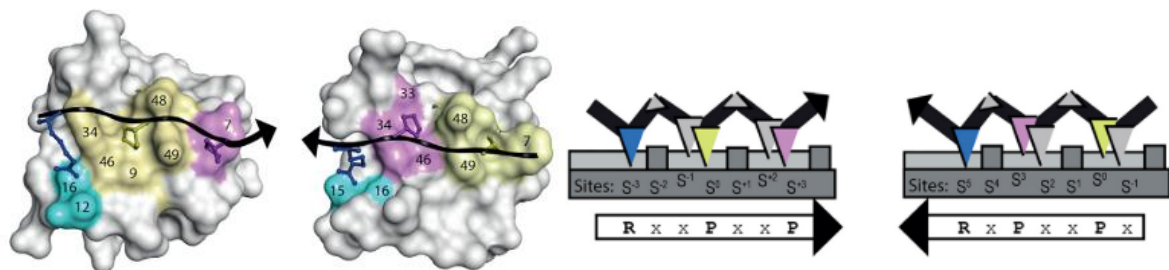


Figure 1-7 Proline-rich motifs form helices that interact with pockets on the SH3 domain surface (Teyra et al., 2017).

1.3.8 FGFR2 under non-stimulated conditions

The FGFR mediated phosphorylation of FRS2 serves as a docking site for the SH2 domain of GRB2, which activates downstream responses. GRB2 contains an SH2 domain flanked by two SH3 domains. Interestingly, it has been shown that under serum starved conditions the C-terminal SH3 domain of GRB2 can interact with a proline-rich motif found in the C-terminal tail of FGFR2 (Ahmed et al., 2010). After deleting this C-terminal sequence in FGFR2, which contains the proline-rich motif, an increase in MAPK activity coupled with decreased FGFR2 phosphorylation was observed. Furthermore, the presence of GRB2 impairs Dephosphorylation of FGFR2

by the phosphatase SHP2. SHP2 can interact with FRS2/FGFR1 complex and plays a role in activating MAPK, and this only occurs with the activated receptor and not in non-stimulated conditions (Ong et al., 2000b). Altogether this suggests that the GRB2 C-SH3 domain can regulate FGFR2 activity, possibly by sterically hindering the access of SHP2 phosphatase to FGFR2 (Figure 1.8).

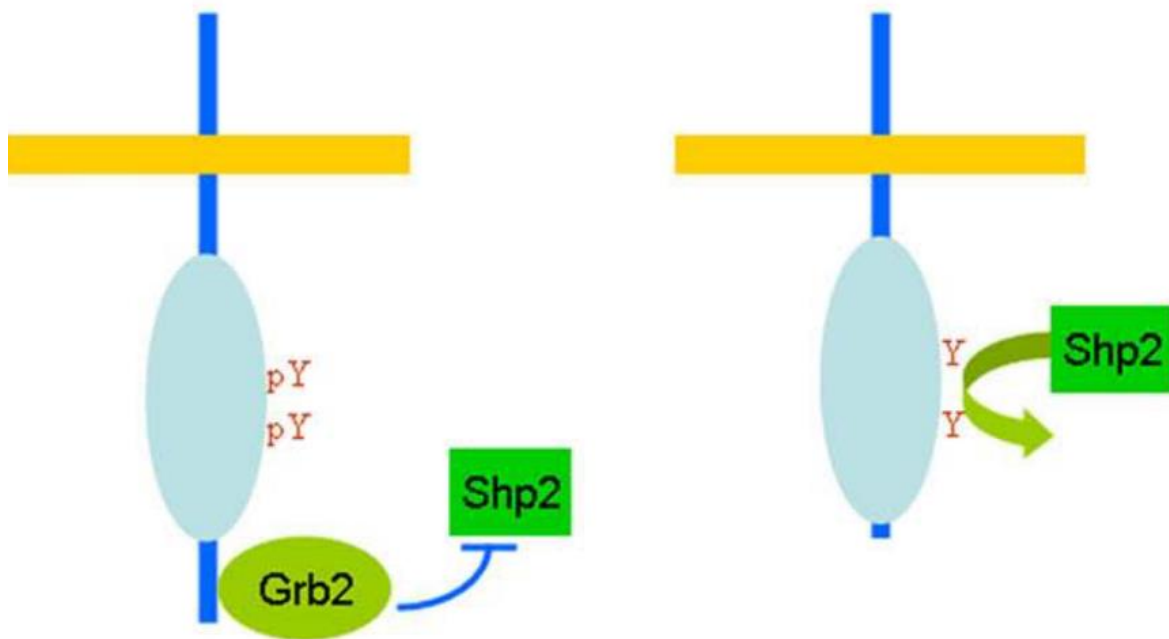


Figure 1-8 GRB2 C-SH3 domain can interact with FGFR2 C-terminal tail.

A mutant FGFR2 lacking the SH3 binding site shows increased dephosphorylation mediated by SHP2 phosphate (Ahmed et al., 2010).

Furthermore, under serum starved conditions a dimeric form of GRB2 can interact with the FGFR2 C-terminal tail and keep two receptor molecules in close proximity (Lin et al., 2012). The receptor maintains basal kinase activity in this state but is unable to activate any downstream MAPK pathway signalling. Upon ligand binding at the extracellular site, the tetramer undergoes a conformational change and phosphorylation of GRB2 Y209 causes it to be released from the receptor. In the absence of GRB2, FGFR2 then proceeds to its normal activated form (Figure 1.9). GRB2 can also be dephosphorylated by SHP2, allowing GRB2 to yet again form a heterotetramer with FGFR2 proteins (Ahmed et al., 2013). Altogether this demonstrates complex mechanisms controlling FGFR2 where GRB2 acts as a stabiliser of a dimeric state of FGFR2 under basal conditions.

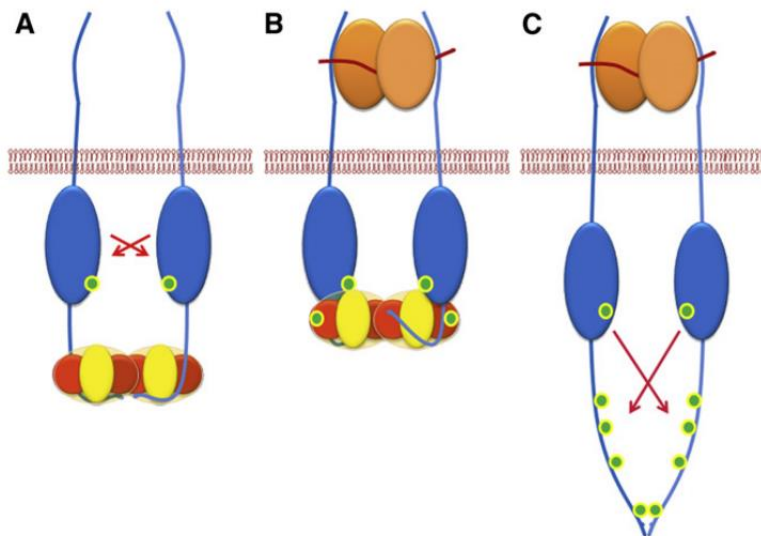


Figure 1-9 GRB2 interaction with FGFR2

Dimeric GRB2 can interact with the C-terminal tail of FGFR2 under starved conditions (a). Some “background” phosphorylation is maintained. Upon ligand binding a conformational change occurs resulting in GRB2 phosphorylation and release from receptor (b). FGFR2 cross-phosphorylates tyrosines in the C-terminal tail (c) (Lin et al., 2012).

The GRB2 SH3 domain interacts directly with a proline-rich motif on the C-terminal tail of FGFR2, including proline residues P810 and P813. Under serum starved conditions, the SH3 domain of PLC γ 1 competes for binding to the same proline-rich motif (Timsah et al., 2014). In serum starved cells, which are depleted of GRB2, recruitment of PLC γ 1 to FGFR2 occurs. This results in increased pathway activation as measured by PIP $_2$ turnover to IP $_3$ and an increase in Ca $^{2+}$ levels. Decreasing levels of PIP $_2$ as a result of PLC γ 1 activation leads to inhibition of PTEN. PTEN dephosphorylates PIP $_3$ to PIP $_2$, and negatively regulates AKT activity. Consequently inhibition of PTEN results in increased AKT activity as a result of PLC γ 1 activity (Timsah et al., 2015). GRB2 SH3 and PLC γ 1 SH3 interactions with the receptor are protein-concentration dependent as they bind to the receptor with similar affinities. GRB2-depleted cells showed increased cell migration and invasive behaviour as a result of phospholipase activity. Indeed, when comparing GRB2 and PLC γ 1 protein levels in cancerous tissues from for example breast cancer and colon cancer, an increase in metastatic potential is observed when there are low GRB2 levels and high PLC γ 1 levels (Timsah et al., 2014). Together these data suggest that complex regulation of FGFR2 exists and perturbations to this regulation result in consequences for downstream signal transduction. In this case, signalling events are controlled by protein concentration and occur under non-stimulated conditions, which challenges the canonical way of thinking of RTK signalling cascades.

1.4 ErbB family

The ErbB (from avian erythroblastosis oncogene B) family has four members, Epidermal Growth Factor Receptor (EGFR (ErbB1), ErbB2 (Her2), ErbB3 (Her3) and ErbB4 (Her4)). Like other RTKs they form dimers and can form either homodimers or

heterodimers (Lemmon and Schlessinger, 2010). The receptors can be activated by several growth factors such as EGF, transforming growth factor- α (TGF- α), amphiregulin and neuregulins 1-4. EGF, amphiregulin and TGF- α only activate EGFR whilst the neuregulins 1 and 2 can activate ErbB3 and ErbB4, neuregulins 3 and 4 activates ErbB4 (Linggi and Carpenter, 2006). ErbB3 is kinase impaired and consequently has less autophosphorylation activity, but can still be phosphorylated and activate downstream signalling (Wee and Wang, 2017). The extracellular part of the ErbB receptors contain four domains, two homologous large domains (L1 and L2, or I and III) and two cysteine rich domains (CR1 and CR2, or II and IV) (Figure 1.10 a). By forming disulphide bonds, the monomeric receptor is found in a tethered structure but upon monomeric ligand binding to domains I and III, the receptor undergoes a conformational change, exposing the extracellular domains, which then promotes dimerisation (Burgess et al., 2003). ErbB2 is an orphan receptor as it has no known ligand that binds the extracellular region. As a result of the receptor having its dimerisation arm constitutively exposed it is the preferred dimerisation partner of the other members of the ErbB family (Figure 1.10 b and c) (Tzahar et al., 1996; Burgess et al., 2003; Baselga and Swain, 2009). The activation of EGFR family receptors is different compared to other RTKs in which they do not require trans phosphorylation. An allosteric mechanism where the kinase domain of an EGFR receptor acts on the corresponding receptor kinase is important for activation, and the juxtamembrane region plays an important role in facilitating the allosteric activation (Red Brewer et al., 2009; Jura et al., 2009).

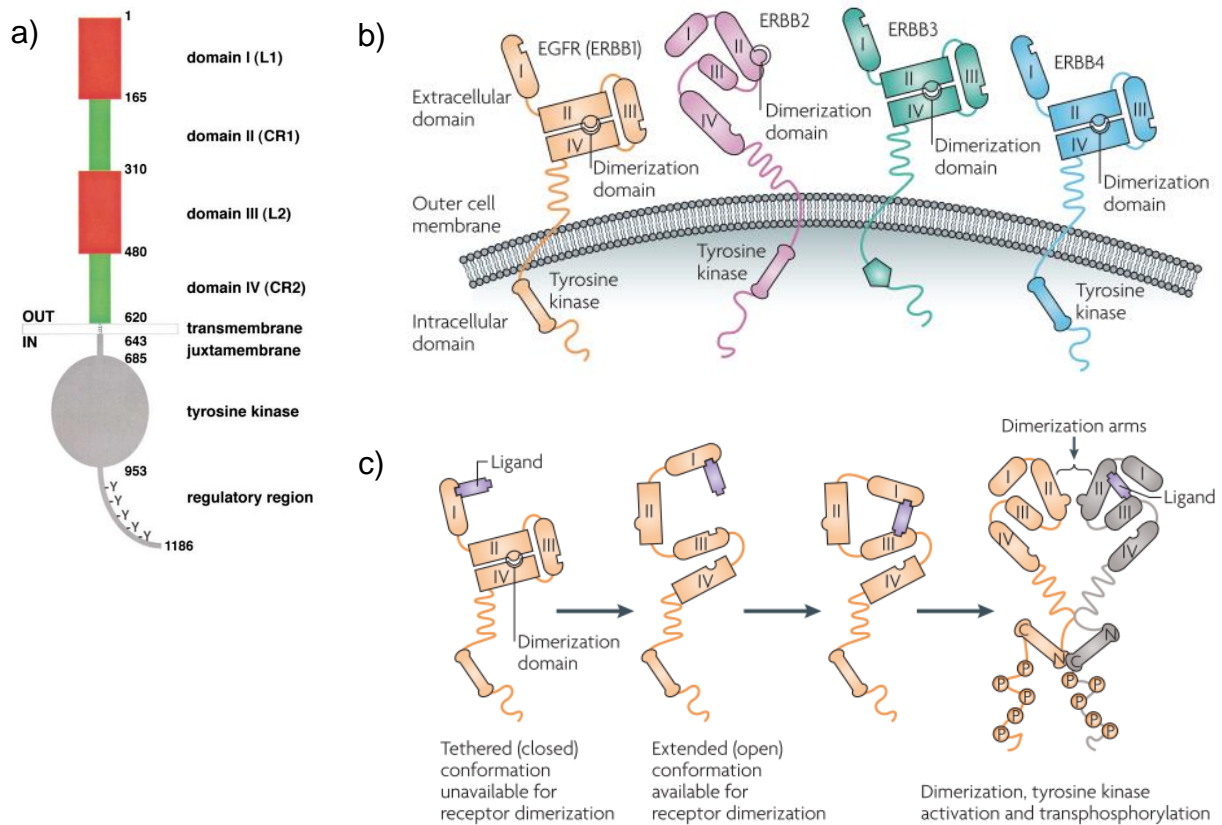


Figure 1-10 ErbB domain organisation.

a) The extracellular part contains four domains, two large and two cysteine-rich. The transmembrane domain is followed by a juxtamembrane and the tyrosine kinase domain. The C-terminal tail contains several tyrosines that upon activation is phosphorylated (Burgess et al., 2003). b-c) EGFR, ErbB3 and ErbB4 has a tethered conformation of the extracellular domains, while ErbB2 has an extended conformation. This allows ErbB2 to be a preferred heterodimerisation partner of the other ErbB family members. ErbB3 does not have an intracellular kinase domain (Baselga and Swain, 2009).

1.4.1 ErbB2 signalling

The orphan receptor ErbB2 forms heterodimers with other members of the ErbB family. Residues that are involved in ligand binding of the other ErbB family receptors are not conserved in ErbB2, potentially explaining why an ErbB2 activating ligand has yet to be discovered (Garrett et al., 2003). As a result of the constitutively exposed dimerisation arm, ErbB2 is the preferred dimerisation partner of the other

ErbB family receptors, and upon heterodimerisation downstream pathways are activated (Graus-Porta et al., 1997). Additionally there is evidence suggesting that overexpressing ErbB2 can activate downstream signalling without ligand (Wildenhain et al., 1990). Phosphorylation of key tyrosines in the kinase domain and C-terminal tail allows for protein binding via their SH2 or PTB domains. In a phosphotyrosine interactome study for the ErbB family, several phosphorylated tyrosines on ErbB2 and new interaction partners were identified (Schulze et al., 2005). GRB2 has been shown to interact with pY1139, the SH3 domain binding protein SH3BGRL at pY923, the phosphatase PTP-2c (also known as PTPN11) at pY1023, and finally SHC was found to interact with phosphorylated tyrosine residues in the C-terminus of the receptor (pY735, pY1005, pY1196, pY1222 and pY1248). SHC recognises an amino sequence NPXY which is incorporated into sequences proximal to both Y1196 and Y1248 (Campbell et al., 1994). Moreover phosphorylation of Y1248 is linked to the RAS-RAF-MAPK pathway (Ben-Levy et al., 2018). GRB2 plays an important role in linking SHC to the MAPK pathway. The SH2 domain from GRB2 interacts with pTyr on SHC, and activates MAPK pathway. And in the case of ErbB2, phosphorylation of pY1248 links the SHC:GRB2 complex to the MAPK pathway (Harmer and DeFranco, 1997).

1.4.2 The role of ErbB2 in cancer

ErbB2 is overexpressed in many types of cancers including ovarian, lung, stomach and most notably breast cancer (Holbro, Civenni, et al., 2003; Janni et al., 2015; Wolfson et al., 2016). ErbB2 has been shown to be overexpressed in 25-30% of breast cancer tumours and is correlated to increased aggressiveness and mortality (Slamon et al., 1987). ErbB2 overexpression is a result of gene amplification and breast cancers have been shown to have 25-50 gene copies, resulting in 40-100 fold

increase in ErbB2 expression (Moasser, 2007). The elevated levels of ErbB2 increase both homodimerisation and heterodimerisation with other ErbB members, and can lead to increased proliferation, invasiveness, survival and metabolic functions. Increased dimerisation between ErbB2/ErbB3 has been shown to activate the PI3K/AKT pathway, which controls a number of cellular responses such as proliferation, survival and invasiveness (Ram and Ethier, 1996; Holbro, Beerli, et al., 2003). Cell polarisation and adhesion have been shown to be dysregulated from either homodimerisation of ErbB2 or heterodimerisation with EGFR. In addition the EGFR/ErbB2 dimer promotes invasive behaviour through activation of PI3K/AKT, RAS/MAPK and PLC γ pathways (Muthuswamy et al., 2001; Zhan et al., 2006). The monoclonal antibody Trastuzumab (Herceptin) is used in treatment of ErbB2-positive breast cancer patients. Trastuzumab interacts with the extracellular part of ErbB2 with high affinity and leads to tumour regression, although the mechanisms behind it are not fully understood. Some studies suggests that Trastuzumab causes ErbB2 internalisation and degradation as an immune-mediated response, and also upregulation of cell cycle inhibitors (Bange et al., 2001). Administration of Trastuzumab on its own has a response in 30-40% of ErbB2-positive metastatic breast cancers. The overall efficiency of Trastuzumab suggests that there is some initial and acquired resistance to the drug (Vogel et al., 2002; Pohlmann et al., 2009).

1.4.3 ErbB2 regulates the cell cycle

Regulation of the cell cycle is controlled by a large number of components, primarily cyclins and cyclin dependent kinases (CDKs) and drives the cell into the different cell cycle phases, Gap 1 (G₁), Synthesis (S), Gap 2 (G₂) and mitosis (M) (K. A. Schafer, 1998). Protein levels of cyclins rise and fall throughout the cycle in an orderly fashion, and as a result periodically activate specific CDKs, which in turn initiate cell

cycle progression (Figure 1.11). G₁-phase entry is controlled by Cyclin Ds (D1, D2 and D3), where the cell prepares for DNA synthesis. Cyclin E is important in the transition from G₁ to S-phase. Cyclin A is expressed during S-phase and G₂-phase, but in complex with different CDKs. In the S-phase DNA replication occurs and the intermediate phase G₂ prepares the cell for M phase. CDK1/Cyclin A complex drives the cell into M-phase and a complex formed by CDK1 and Cyclin B continues to regulate mitosis (Vermeulen et al., 2003).

Deregulation of D-type cyclins and consequently G₁/S transition leads to cell proliferation. Overexpression of ErbB2 and Cyclin D1 has been reported in breast cancers, and overexpression of ErbB2 in various cell types was followed by an upregulation of Cyclin D1 (Harari and Yarden, 2000).

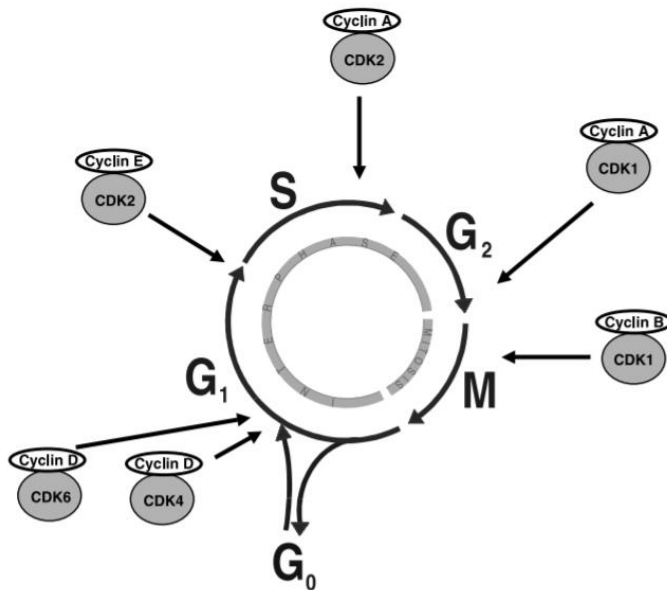


Figure 1-11 Cell cycle phases and components.

Cyclins are expressed at various stages and regulates CDK activity, which in turn regulate cell cycle phases (Vermeulen et al., 2003).

1.4.4 ErbB2 interacts with a member of SRC family non-receptor kinases

The C-terminal tail of ErbB2 is enriched in proline residues, and several of them form canonical proline-rich motifs. This could suggest that the C-terminal tail of ErbB2 could exhibit similar responses as FGFR2 by interacting with cytoplasmic SH3 domains. Indeed, one proline-rich motif near the C-terminus has been shown to interact with the SH3 domain of the SRC family kinase FYN (Bornet et al., 2014). The authors used Surface Plasmon Resonance (SPR) and Nuclear Magnetic Resonance (NMR) to determine that a peptide based on a proline-rich motif in ErbB2 consisting of the amino acid sequence R₁₁₄₆PQPPSPRE₁₁₅₄ interacts with the SH3 domain of FYN with a K_D of 0.9 mM. Using mutants of the peptide it was decided that the important residues in binding the SH3 domain were Arg1146, Pro1149 and Pro1152 (R₁₁₄₆PQP₁₁₄₉PSP₁₁₅₂RE). The physiological importance of this interaction is yet to be determined. It would be interesting to speculate whether an interaction via the SH3 domain of SRC family kinases can be a tumour escape mechanism. In the absence of ligand activation where SRC SH3 domain interacting with the C-terminal tail of ErbB2, and the ErbB2 kinase can activate SRC by phosphorylation. This could be a possible explanation to how some patients develop resistance to Trastuzumab.

1.5 SRC family kinases

SRC was first discovered as an oncogene encoded by Rous sarcoma virus. The oncogene could insert itself into chicken genome and cause cancer, which gave the protein its name, SRC short for sarcoma (Stehelin et al., 1977). Since the discovery of viral SRC, several homologues have been found in the human genome. SRC family kinases are non-receptor tyrosine kinases and consist of at least 14 members

including SRC, FYN, YES, LCK and LYN. Some of the members are ubiquitously expressed, such as SRC, FYN and YES, while other members are expressed in specific cell types and tissues such as myeloid cells, B-cells, NK cells, T cells and brain (Parsons and Parsons, 2004). SRC kinases play an important role in cell signalling and regulate key cellular processes. SRC can activate the cell survival pathway PI3K/AKT, and cell proliferation via MAPK/ERK pathway.

1.5.1 SRC structure and conformation

Members of the SRC family kinases have similar domains and conformation, including SRC (c-SRC or cellular SRC). In the cell, SRC is found in either a closed conformation, an inactive form or an open and active conformation. SRC kinases consist of an SH2, SH3 and a kinase domain (Figure 1.12). At the N-terminus there is a myristoylation site (Myr) which is responsible for recruiting SRC to the cell membrane. There is a proline-rich motif in the linker region between the SH2 domain and kinase domain which interacts with the SH3 domain when SRC is in its inactive form (Figure 1.13). There are two regulatory phosphotyrosine sites, 416 and 530 (Tyr416 or Y416 and Tyr530 or Y530). Phosphorylation of Tyr530 inactivates SRC by its interaction with the SH2 domain, causing SRC to fold up on itself. In this inactive form the SH2 and SH3 domains are less accessible for binding ligands, and under basal conditions 90-95% of SRC is found in closed conformation (Zheng et al., 2000). Dephosphorylation of Tyr530 opens up the protein to its active form. The kinase domain adopts the typical kinase structure having an N-lobe and a C-lobe. The N-lobe anchors and orientates ATP while the C-lobe binds the protein substrate. The catalytic site of the kinase lies in a pocket between the two lobes and movement of the two lobes can open or close the pocket. In the open form ATP can be catalysed by the kinase transferring one phosphate group to the tyrosine residues of

the substrate protein. A tyrosine (Y416) sits in the activation loop, which is buried in the pocket between the lobes in the closed conformation and which can be autophosphorylated by the kinase domain, leading to a hyperactive protein (Roskoski, 2004).



Figure 1-12 SRC family kinase structure and domains.

They contain a kinase domain, SH2 and SH3 domains and a myristoylation site which allows the protein to be anchored to the membrane.

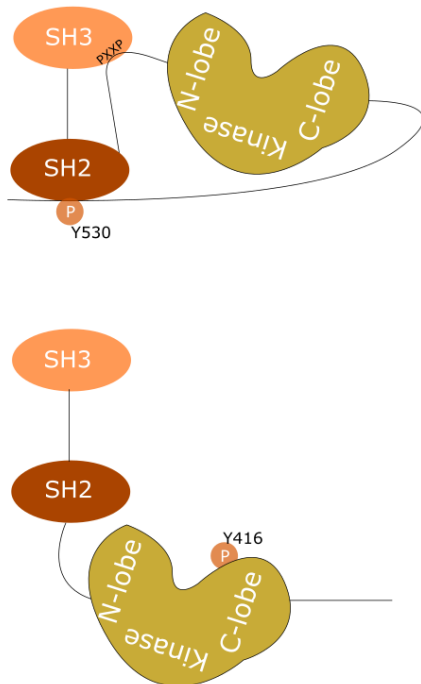


Figure 1-13 SRC family kinase open/active and closed/inactive conformation structure.

A phosphorylated tyrosine at the C-terminal tail (Y530) binds the SH2 domain while a proline-rich motif in the linker region between the SH2 domain and kinase interacts with the SH3 domain. Dephosphorylation of Y530 opens up the protein and the kinase domain can autophosphorylate Tyr416.

1.5.2 The role of SRC in cancer

The functional role of activated SRC is linked with several cellular processes such as proliferation, survival and invasion. Consequently disruption of these processes could potentially lead to abnormal growth and migration, which are hallmarks of cancer. SRC is overexpressed in several cancers, including colon and breast cancers (Frame, 2002). It has been demonstrated that expression of the phosphatase PTP1B (protein-tyrosine phosphatase 1B), which has been shown to dephosphorylate Y530, is elevated in breast cancers (Bjorge et al., 2000). The tyrosine kinase CSK (C-terminal SRC kinase) inactivates SRC by phosphorylating Y530 and in hepatocellular carcinoma the expression of the kinase CSK is reduced, suggesting a tumour suppressor role for CSK (Masaki et al., 1999). Overexpression of SRC in breast cancers is seen with and without ErbB2 overexpression. Overexpression of ErbB2 in mammary epithelial cells resulted in activation of SRC, suggesting that ErbB2 can activate SRC in tumourigenesis (Sheffield, 1998). In addition, it appears that SRC functions upstream of ErbB2. SRC can phosphorylate ErbB2 on its activation loop (Y877) and in doing so activate ErbB2 (Xu et al., 2007). SRC also enhances ErbB2/ErbB3 dimerisation and activity (Ishizawa et al., 2007). SRC and ErbB2 directly interact via the SRC SH2 domain and ErbB2 phosphorylated tyrosines, and the formation of the heterocomplex is suggested to be the cause of enhanced growth in the breast cancer cell lines UACC-12, MDA-MB-361 and MDA-MB-453. Additionally recruitment of SRC to ErbB2 results in modulation of cell polarity (Muthuswamy and Muller, 1995; Belsches-Jablonski et al., 2001; Kim et al., 2005). It is clear that SRC plays a role in several cancers, with or without ErbB2 overexpression.

1.6 LASP1 domains and interacting partners

LIM and SH3 domain protein 1 (LASP1) was first discovered as a gene amplified and overexpressed in breast carcinomas. It is located in close proximity to the *ErbB2* and *BRCA1* genes on chromosome 17, two known oncogenes in breast cancers (Tomasetto, Régnier, et al., 1995). It contains a LIM domain, two nebulin repeats and an SH3 domain (Figure 1.14). The nebulin repeats have been shown to directly interact with filamentous actin (Schreiber et al., 1998). The nebulin repeats have also been shown to interact with Kelch related protein 1 (KRP1), which is involved with cell migration (Miao et al., 1994). LASP1 SH3 domain has been shown to interact with many proline-rich motif containing proteins, such as dynamin, Lipoma preferred partner (LPP), palladin, Vasodilator-stimulated phosphoprotein (VASP) and Zonula occludens protein 2 (ZO-2). Additionally Zyxin interacts with LASP1 SH3 domain (Okamoto et al., 2002; Kwiatkowski et al., 2003; Li et al., 2004; Keicher et al., 2004; Rachlin and Otey, 2006; Grunewald et al., 2009; Mihlan et al., 2013). LIM domains have acquired its name from the proteins it was discovered in, LIN11, LSL-1 & MEC-3 (Bach, 2000). The LASP1 LIM domain has been shown to interact with the chemokine receptor CXCR2 (C-X-C motif chemokine receptor 2, also known as Interleukin 9 receptor, beta), a GPCR which is activated by the chemokine Interleukin-8. The LASP1 LIM domain binds specifically to the LKIL motif in the carboxy-terminal domain of CXCR2 (Raman et al., 2010). The LIM domain is structurally a zinc-finger domain, and it is interesting to speculate whether LASP1 LIM domain interacts with DNA. Especially as phosphorylation of serine 146 by Protein Kinase A (PKA) causes the release of LPP, Zyxin and actin, and LASP1 can be translocated to the nucleus in a complex with the nuclear shuttling protein ZO-2 (Figure 1.15). Dephosphorylation by Serine/Threonine-protein phosphatase 2B

(PP2B) relocates LASP1/ZO-2 complex to the nucleus (Mihlan et al., 2013; Orth et al., 2014). Additionally the cytoplasmic kinases SRC and ABL phosphorylate tyrosine residue 171 in LASP1 (Schreiber et al., 1998; Lin et al., 2004).



Figure 1-14 LASP1 structure and domains. At the N-terminal there is a LIM domain, followed by two nebulin repeats and at the C-terminal an SH3 domain.

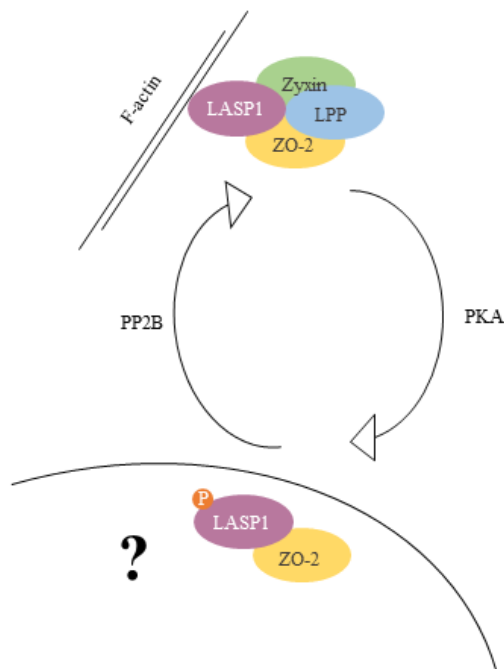


Figure 1-15 In a complex with ZO-2, LASP1 translocates to the nucleus after phosphorylation by PKA. LASP1 is dephosphorylated by PP2B. Adapted from (Orth et al., 2014).

1.6.1 LASP1 function and role in cancer

LASP1 interacts with filamentous actin directly and several of the interaction partners of LASP1 are also involved in actin organisation. LASP1 locates in focal adhesions, leading edges of lamellopodia and filapodia, which are involved in cell migration, adhesion and signalling events (Chew, 2002). Phosphorylation of LASP1 by SRC in

activated platelets relocated LASP1 to leading lamellae of a migrating cell (Lin et al., 2004). LASP1 is overexpressed in various cancers such as ovarian, bladder, prostate and also breast cancer where LASP1 was originally identified. In Chronic myeloid leukaemia (CML) patients, phosphorylation of Y171 in LASP1 was reported by the oncoprotein BCR-ABL which leads to interactions between pY171 and CRK-like protein (CRKL). BCR-ABL is a fusion protein between breakpoint cluster region protein (BCR) and Abelson murine leukemia viral oncogene homolog 1 (ABL). BCR-ABL activates MAPK/ERK and PI3K/AKT pathways, which leads to cell proliferation (Frietsch et al., 2014). LASP1 is overexpressed in 8% of breast carcinomas, and overexpression correlates with tumour size, suggesting LASP1 can be related to worse prognosis (Grunewald et al., 2007). LASP1 expression is higher in patient breast cancer tumours that are also ErbB2-positive (Glynn et al., 2012). Additionally there is evidence that LASP1 is localised to the nucleus in breast cancer patients and is correlated with poorer survival. In breast cancer cell lines this was confirmed and also an increase of protein expression was seen in S-phase and G2/M-phase (Grunewald et al., 2007; Frietsch et al., 2010). Silencing LASP1 expression by siRNA in breast cancer cell lines caused reduced migration, proliferation and the cells were arrested in the G2/M-phase of the cell cycle. Consequently overexpression of LASP1 in cells with no endogenous LASP1 lead to increased cell motility (Grunewald et al., 2006). Taken together it is clear that LASP1 plays a role in several cancers and not surprisingly cell migration is increased when LASP1 is overexpressed.

1.7 Aims and objectives

A second tier of signalling has been discovered for FGFR2. Unlike canonical RTK signalling this second tier signalling happens in the absence of extracellular stimuli. The interactions occur between SH3 domains and proline-rich motifs in the C-terminal tail, and not the canonical SH2/pTyr which requires receptor ligand binding. Additionally an interaction between FYN SH3 domain and ErbB2 proline-rich motif has been demonstrated using NMR, demonstrating another possible RTK interacting with SH3 domain. Investigation of these interactions between ErbB2 and FYN, and FYN homologue SRC would be important to investigate. SRC and ErbB2 have been shown to interact directly in breast cancer cell lines but there is no evidence of this interaction in the breast cancer cell line SkBr3 (Belsches-Jablonski et al., 2001). Several examples of RTKs interacting with proteins containing SH3 domains could suggest that there might be a second tier receptor modification which has gone largely unnoticed because of the weak and transient nature of these interactions. One can speculate if any deregulation of this system in cancers can play a role in cellular processes leading to tumour formation. The aims and objectives for this thesis are:

Aim 1: Identify novel interactions between SH3 domains and proline-rich motifs from RTKs.

Using mass spectrometry (MS) serves as a high throughput method to identify these novel interactions. Combined with peptides containing proline-rich motifs from RTKs and lysates from cells, MS will be utilised in order to discover novel proteins containing SH3 domains interacting with the proline-rich motifs.

Additionally a dot blot will be carried out to identify direct interactions. In this work purified C-terminal tails of several RTKs and purified LASP1 with and without the SH3 domain will be used to identify novel interacting partners for LASP1 SH3 domain.

Further verification and characterisation of some of the potential interactions will be carried out using immunofluorescence, pull down experiments and biophysical methods.

Aim 2: Prove interaction between FGFR2 proline-rich motif and LASP1.

Preliminary data suggest that LASP1 and FGFR2 interact. This will be carried out using a range of techniques including pull-down experiments and immunofluorescence to verify this interaction in a cellular context. A biophysical assay will be utilised to characterise the interaction further.

In addition to interaction verification and characterisation, cell motility and growth assays will be carried out to determine whether this interaction has any impact on cellular responses, and if it is physiologically relevant.

Aim 3: Verify the interaction between ErbB2 proline-rich motif and the SH3 domain from SRC in SkBr3 cells.

Cellular techniques such as co-immunoprecipitation and fluorescence in SkBr3 cells will be used to verify an interaction between SRC and ErbB2 in starved conditions, and demonstrating it in a cellular context.

Further characterisation of this interaction will be carried out using pull-down experiments, immunofluorescence and biophysical methods in order to determine the domains of SRC and region of ErbB2 involved in this interaction.

Chapter 2: Materials and Methods

2.1 Bacterial cell culture

2.1.1 Bacteria growth and storage

Amplification of DNA plasmids was performed in the *Escherichia coli* strains DH5 α or XL10. *E. coli* were grown on lysogeny broth (LB) agar and in liquid shaking cultures in LB medium overnight at 37°C. Appropriate antibiotics were used for selection (50 μ g/ μ l Kanamycin, 100 μ g/ μ l Ampicillin). Long-term storage bacterial cells were suspended in 50% liquid overnight culture/50% glycerol and stored at -80°C. Protein expression was performed in the *E. coli* strain BL21. Similar growth conditions were used for BL21, DH5 α and XL10 strains of bacteria, unless otherwise stated.

2.1.2 Transformation

E. coli was transformed by adding 2 μ l of plasmid DNA to 25 μ l competent DH5 α , XL10 or BL21 cells. The cells were incubated on ice for 10 minutes followed by heat shock treatment at 42°C for 45 seconds, before additional incubation on ice for 2 minutes. LB medium was then added to the cultures followed by 1-2 hour incubation shaking at 37°C. The culture was then plated on LB agar plates containing the appropriate antibiotic.

2.1.3 Preparation of plasmid DNA

Commercially available kits were used for the small and large-scale purification of plasmid DNA (Qiagen), following the manufacturers' guidelines. Overnight cultures varied between 5-20 ml for miniprep and 50-200 ml for maxiprep purification, depending on the copy number of the plasmid.

2.2 Molecular cloning

2.2.1 Polymerase chain reaction (PCR)

Point mutations in ErbB2 was done using In-Fusion Mutagenesis kit (Clontech, 639648). Primers were designed to contain all three mutations (Table 1). The polymerase chain reaction (PCR) mastermix (CloneAmp HiFi

Polymerase, dNTPs, and optimized buffer) was prepared according to protocol (Table 2) and PCR was run for 35X cycles (Table 3).

Table 1 Oligonucleotides for mutagenesis.

Overlapping nucleotides in green, point mutations in yellow

Gene	Forward primer	Reverse primer	Comments
ErbB2 triple mutant	5'AATATGTGAACCAGCCA GATGTT GC GCCCCAG GCC CCTTCGG 3'	3' GCGCCCCAG GCCCC TT CG G CCCCGAGAGGGCCC TCTGCCTGCT 3'	R1146A/P1149A/ P1152A

Table 2 PCR reagents for mutagenesis

Reagent	Volume/concentration
CloneAmp HiFi PCR Premix	12.5 µl
Forward primer	250 nM
Reverse primer	250 nM
Template DNA	0.1 ng
H ₂ O	To make total volume of 25 µl

Table 3 PCR steps for mutagenesis

Step	Temperature	Time
Denaturing	98°C	10 sec
Annealing	55°C	5 sec
Elongation	72°C	5 sec/kb

2.2.2 Agarose gel electrophoresis and gel extraction

To check whether the mutagenesis had worked the PCR product was run on an agarose gel and the DNA was extracted (Zymoclean Gel DNA Recovery kit, D4007). The agarose gel was run at 80 V. DNA was extracted by cutting out the DNA band from the gel, agarose dissolving buffer was added followed by heating at 55°C until completely dissolved. The mixture was then run through the spin columns to capture the DNA, then washed twice with wash buffer before eluting with elution buffer (8 µl). Recovered DNA was then ligated.

2.2.3 DNA ligation reactions

Linear DNA from PCR was ligated by adding ligase (1 µl) and ligation buffer (1 µl, 50 mM Tris-HCl, 10 mM MgCl₂, 10 mM Dithiothreitol, 1 mM ATP) to the extracted DNA (8 µl, ~10 µg). The ligation reaction was left at room temperature overnight before being transformed into Stellar competent *E. coli* cells (Clontech, 636763).

2.3 Protein expression and purification

Starter cultures of BL21 (DE3) were incubated overnight at 37°C, and then used to inoculate larger cultures of 1-2L. Larger cultures were grown to OD₆₀₀ = 0.8-1.0 and expression was induced by adding IPTG (0.1 mM) to the cultures. Cultures were then grown at the indicate temperatures and harvested at the designated time points. Cells were pelleted by centrifugation at 1990xg at 4°C for 20 minutes and either stored at -20°C or resuspended in appropriate buffer for further experiments (see below). Resuspended pellets were sonicated prior to centrifugation at 1990xg at 4°C for 30 minutes to separate cell debris and supernatant containing the protein. Protein integrity was then analysed by SDS-PAGE.

2.3.1 Maltose Binding Protein (MBP)

MBP tagged proteins (Table 4) were purified by resuspending the bacterial pellet in HEPES buffer (20 mM HEPES pH 7.5, 150 mM NaCl, 1 mM β -mercaptoethanol). After sonification and centrifugation the supernatant was incubated with 100 μ L amylose resin (New England Biolabs, E8021S) overnight at 4°C. Beads were then washed 5x with HEPES buffer to remove unbound proteins and beads were either stored in 20% glycerol at -20°C for further use in MBP pull downs, or the bound proteins eluted using 10 mM maltose in HEPES buffer.

2.3.2 Glutathione-S-Transferase (GST)

GST tagged proteins (Table 4) were purified by resuspending the bacterial pellet in Tris buffer (20 mM Tris pH 8, 150 mM NaCl, 1 mM β -mercaptoethanol). After sonification and centrifugation the supernatant was incubated with either 100 μ L (purification for GST pull down) or 1 mL (purification for MST) glutathione agarose beads resin (Sigma, G4510) overnight at 4°C. Beads were then washed 5x with Tris buffer to get rid of unbound proteins and beads were either stored in 20% glycerol at -20°C for further use in GST pull downs, or the bound protein were eluted using 20 mM reduced glutathione in Tris buffer, pH 8.

Table 4 Proteins expressed and purified

Protein	Tag	Molecular weight	Plasmid of expression vector origin
LASP1 wild type	GST	38 kDa	Elke Butt, Universitätsklinikum Würzburg
LASP1 Δ SH3	GST	23.1 kDa	Elke Butt, Universitätsklinikum Würzburg
LASP1 Δ LIM	GST	23.5 kDa	Elke Butt, Universitätsklinikum Würzburg
SRC SH3	GST	6.9 kDa	Andrew Macdonald, University of Leeds
FYN SH3	GST	8.0 kDa	Andrew Macdonald, University of Leeds

FGFR2 C58	GST	6.5 kDa	Chi-Chuan Lin, University of Leeds
FGFR2 C58 P800A	GST	6.4 kDa	Chi-Chuan Lin, University of Leeds
FGFR2 C58 P802A	GST	6.4 kDa	Chi-Chuan Lin, University of Leeds
FGFR2 C58 P804A	GST	6.4 kDa	Chi-Chuan Lin, University of Leeds
FGFR2 C58 P807A	GST	6.4 kDa	Chi-Chuan Lin, University of Leeds
FGFR2 C58 P810A	GST	6.4 kDa	Chi-Chuan Lin, University of Leeds
FGFR2 C58 P813A	GST	6.4 kDa	Chi-Chuan Lin, University of Leeds
FGFR2 C58 Δ 3	GST	6.1 kDa	Chi-Chuan Lin, University of Leeds
FGFR2 C58 Δ 6	GST	5.9 kDa	Chi-Chuan Lin, University of Leeds
FGFR2 C58 Δ 9	GST	5.5 kDa	Chi-Chuan Lin, University of Leeds
FGFR2 C58 Δ 12	GST	5.1 kDa	Chi-Chuan Lin, University of Leeds
FGFR2 C58 Δ 15	GST	4.8 kDa	Chi-Chuan Lin, University of Leeds
FGFR2 C58 Δ 23	GST	3.9 kDa	Chi-Chuan Lin, University of Leeds
C-terminal EGFR	MBP	25.6 kDa	Chi-Chuan Lin, University of Leeds
C-terminal ErbB2	MBP	28.3 kDa	Chi-Chuan Lin, University of Leeds
C-terminal ErbB3	MBP	41.0 kDa	Chi-Chuan Lin, University of Leeds
C-terminal ErbB4	MBP	36.6 kDa	Chi-Chuan Lin, University of Leeds
C-terminal INSR	MBP	9.2 kDa	Chi-Chuan Lin, University of Leeds
C-terminal INSRR	MBP	4.6 kDa	Chi-Chuan Lin, University of Leeds
C-terminal IGF1R	MBP	10.7 kDa	Chi-Chuan Lin, University of Leeds
C-terminal VEGFR1	MBP	20.0 kDa	Chi-Chuan Lin, University of Leeds
C-terminal VEGFR2	MBP	21.2 kDa	Chi-Chuan Lin, University of Leeds
C-terminal VEGFR3	MBP	21.1 kDa	Chi-Chuan Lin, University of Leeds
C-terminal FGFR1	MBP	7.2 kDa	Chi-Chuan Lin, University of Leeds
C-terminal FGFR2	MBP	6.8 kDa	Chi-Chuan Lin, University of Leeds
C-terminal FGFR2 C2	MBP	2.8 kDa	Chi-Chuan Lin, University of Leeds
C-terminal FGFR3	MBP	4.5 kDa	Chi-Chuan Lin, University of Leeds
C-terminal FGFR4	MBP	4.7 kDa	Chi-Chuan Lin, University of Leeds
C-terminal PDGFRA	MBP	16.0 kDa	Chi-Chuan Lin, University of Leeds

C-terminal ALK	MBP	30.0 kDa	Chi-Chuan Lin, University of Leeds
MBP	MBP	42.0 kDa	Chi-Chuan Lin, University of Leeds

2.4 Protein biochemistry

2.4.1 Protein concentration determination

Total protein concentration from cell lysates was determined using Coomassie Assay reagents (ThermoFisher, 23238) and measuring absorbance at 595 nm. 30-50 µg total protein was used for western blot analysis. For purified proteins concentration was quantified using a Nanodrop spectrophotometer by measuring absorbance at 280 nm (Thermo Scientific, NanoDrop 2000).

2.4.2 SDS polyacrylamide gel electrophoresis (SDS-PAGE)

Cell lysates or purified proteins were mixed with 4X sample buffer (Biorad, 1610747), boiled for 5-7 minutes at 95°C and loaded onto 4-20% Mini-PROTEAN Precast gels (Biorad, 4561096) for analysis. Gel tanks were filled with running buffer (35 mM SDS, 250 mM Tris Base, 192 mM glycine) and a constant voltage (120V) for 65 minutes.

2.4.3 Western blot

Proteins separated by SDS-PAGE were transferred from the gel to PVDF membranes via semi-dry transfer (Biorad Trans-Blot). Membranes were activated by methanol and membranes and filter papers were soaked in transfer buffer (25 mM Tris Base, 192 mM glycine, 10% methanol). The filter papers and membrane were made into a "transfer sandwich" and a constant voltage was applied at 20V for 55 minutes. Membranes were then blocked by incubating for 1 hour at room

temperature in blocking solution, 1X Tris buffer (10X 0.40 mM Tris HCl, 0.1 M Tris Base, 1.5 mM NaCl) containing 5% skimmed milk powder and 0.2% Tween-20. Primary antibody in blocking solution (Table 5) was added to the membrane and incubated overnight at 4°C. Membranes were washed 3x10 minutes in TBS-T at room temperature before incubation with secondary antibody in blocking solution for 1 hour at room temperature. The membranes were then washed again in TBS-T 3x10 minutes before briefly incubated with enhanced chemiluminescence (ECL) substrate. Proteins were detected by exposure onto X-ray films for an appropriate length of time.

Table 5 Primary and secondary antibodies used for detection of Western blots

Antibody	Size of target	Manufacturer, catalogue number
ALK	220 kDa/140 kDa	CST, #3633
ErbB2	185 kDa	CST, #4290
ErbB2 pY1221/1222	185 kDa	CST, #2243
ErbB2 pY1248	185 kDa	CST, #2247
FGFR2 (Bek C17)	150 kDa	Santa Cruz, sc-122
Fyn	59 kDa	CST, #4023P
GAPDH	35.8 kDa	Santa Cruz, sc-47724
GFP	37 kDa	CST, #2956
GFP	37 kDa	Santa Cruz, sc-9996
GST	26.7 kDa	CST, #2622S
LASP1	38 kDa	Santa Cruz, sc-374059
MBP	42 kDa	CST, #2396S
P42/44 MAPK	42/44 kDa	CST, #4370S
RFP/mCherry	25 kDa	Abcam, ab167453
Src	60 kDa	CST, #2108
Src	60 kDa	Santa Cruz, sc-19

Src	60 kDa	Santa Cruz, sc-5266
Src pY416	60 kDa	CST, #2101
Src pY530	60 kDa	Santa Cruz, sc-101803
β -actin	42 kDa	CST, #4970S

2.4.4 Dot blot

Purified MBP tagged receptors were dotted on nitrocellulose membranes (2 μ l, 0.05-0.25 mg/ml) and the membrane was left to dry (10-15 minutes) before blocking for 1h at room temperature (5% BSA, 0.1% tween-20 in HEPES buffer (HBST+5%BSA)).

Membranes were then incubated with second purified protein for 2h at room temperature, and then washed 3x5 minutes with HBST before incubating with primary antibody for 2h at room temperature. Membranes were then washed 3x5 minutes with HBST before adding secondary antibody. Before detection membranes were washed 3x5 minutes with HBST and finally ECL was added. The blots were detected using Syngene G:box, an imager for chemiluminescent blots.

2.5 Mammalian cell culture

2.5.1 Cell lines and maintenance

Human cell lines (Table 6) were maintained in Dulbecco's modified Eagle's high-glucose medium (DMEM), supplemented with 1% Penicillin/Streptomycin (ThermoFisher Gibco™, 10378016) and 10% v/v Gibco® foetal bovine serum (FBS, Life Technologies™). All cells were kept in in a humidified incubator at 37 °C with 5% CO₂. Cells were passaged twice per week at 1:10.

Table 6 Cell lines used in mammalian cell culture

Cell line	Growth medium	Comments
HEK 293T	DMEM + 10% FBS + 1% Pen/Strep	
SkBr3	DMEM + 10% FBS + 1% Pen/Strep	
MCF7	DMEM + 10% FBS + 1% Pen/Strep	
SH-SY5Y	DMEM + 10% FBS + 1% Pen/Strep	
HEK 293 gRNA2	DMEM + 10% FBS + 1% Pen/Strep	GRB2 knockdown, Amy Stainthorp, University of Leeds
HEK 293 scr	DMEM + 10% FBS + 1% Pen/Strep	Scramble knockdown, Amy Stainthorp, University of Leeds
HeLa	DMEM + 10% FBS + 1% Pen/Strep	

2.5.2 Transient transfections

Cells were seeded to 6-well plates (250 000 cells) or 10 cm² tissue culture dishes (500 000 cells) and incubated until 80% confluency. Plasmid DNA (Table 7) (2-15 µg) was diluted in 50-200 µL optimem and incubated with Lipofectamine2000 (1:1 ratio DNA to volume Lipofectamine) for 15-20 minutes before adding the DNA:Lipofectamine complex drop-wise to cells. The transfection medium was replaced with fresh media after 12 hours incubation.

Table 7 Plasmids for mammalian transfection

Plasmid	Encoded gene	Selection	Origin	Tag
perbB2-EGFP	ErbB2	Ampicillin	AddGene Plasmid #39321	GFP
FGFR2-GFP	FGFR2	Kanamycin	(Ahmed et al., 2010)	GFP
EGFP-FGFR2 Δ25	FGFR2 Δ25, deletion of last 25 amino acids	Kanamycin	Chi-Chuan Lin, University of Leeds	GFP
mCherry-Lasp1- N-10	LASP1	Kanamycin	AddGene Plasmid #55071	mCherry (N- terminal)

pcDNA3-MTS-WT-c-Src-FLAG	SRC	Ampicillin	AddGene Plasmid #44652	Flag
pcDNA3-MTS-KD-c-Src-FLAG	SRC K298M, kinase dead mutant	Ampicillin	AddGene Plasmid #44653	Flag
pcDNA3-MTS-CA-c-Src-FLAG	SRC Y530F, open conformation mutant	Ampicillin	AddGene Plasmid #44654	Flag
NS5A	NS5A	Kanamycin	Andrew Macdonald, University of Leeds	GFP
RFP	RFP	Ampicillin	Chi-Chuan Lin, University of Leeds	RFP
GFP	GFP	Kanamycin	Chi-Chuan Lin, University of Leeds	GFP
mCardinal-N2	mCardinal	Kanamycin	AddGene Plasmid #54590	mCardinal

2.5.3 Cell lysis

Cells were seeded out in 10 cm² culture dishes and at 80% confluency starved overnight. Cells were then either stimulated with FBS (15 min), EGF (100 nM, 5 min) or kept as starved. Medium was removed and cells were washed with cold PBS and placed on ice. Cells were then scraped into an Eppendorf tube and cell lysis buffer was added (150 mM NaCl, 50 mM Tris-HCl pH 7.4, 1% Nonidet P-40, 0.25% Sodium Deoxycholate, 1 mM EGTA, 1mM PMSF, Protease inhibitor cocktail, 1 mM activated Na₃VO₄ and 1mM NaF). Tubes were incubated for 15 minutes on ice before spinning down cell debris. Supernatant was transferred to a fresh tube.

2.6 Immunocytochemistry

2.6.1 Growing cells on coverslips and fixation

Glass coverslips were washed in 70% ethanol and treated with poly-L-lysine (5 minutes). Cells in suspension were seeded on top of the coverslips, and medium was added (2 ml/well). Cells were transfected at 40% confluency and any further treatments performed (e.g. serum starvation) undertaken when cells were at 50% confluency. Treated cells were fixed to the coverslips by treatment with 4% paraformaldehyde, for 10 minutes at room temperature. Paraformaldehyde was removed and coverslips were washed 3x with PBS. Samples were then analysed by proximity ligation assay (PLA) or immuno-cytochemistry (ICC).

2.6.2 Proximity ligation assay and ICC

Fixed cells on coverslips were permeabilised (0.01% BSA, 1% NP-40 in PBS) for 10 minute at room temperature. Cells were blocked (0.01% BSA, 1% NP-40, 5% NGS (normal goat serum) in PBS) for 1h at room temperature. Primary antibodies were added at 1:100 dilution in 0.01% BSA, 5% NGS in PBS for 1h room temperature. Coverslips were washed 3x5 minutes with PBS before either adding the PLA minus and plus probes (Sigma, Duo92004). Probes were incubated for 1h at 37°C, and washed off 3x5 minutes using Wash buffer A from PLA kit (Sigma, DUO82049-4L). The ligation step was performed using ligase and ligase buffer and was incubated at 37°C for 30 minutes. Coverslips were then washed 3x5 minutes with wash buffer A and the amplification of the signal was achieved by adding polymerase and polymerase buffer at 37°C for 100 minutes. Coverslips were then washed 2x5 minutes with wash buffer B and 1x5 minutes 0.01% wash buffer B. Coverslips were

added inverted to glass-slides containing a drop of DAPI solution and then imaged by confocal microscopy.

2.6.3 Microscopy

Cells from PLA and ICC was images using Zeiss LSM700 confocal microscope at the Bioimaging and Flow Cytometry facilities at University of Leeds.

2.6.4 Statistics for PLA

Statistics for PLA signals were done in ImageJ, two different methods were used in the analysis, which was either whole images imaged by confocal microscopy or individual cells. For whole images channels were split and the channel containing the PLA signal was taken forward. The channel was changed to RBG colour and colour threshold was changed. Signals were analysed by analyse particles and the parameters were selected as following; 0.1-5 μM size and 0-1 circularity. Number of particles counted were summarised. For each condition this was repeated for 8 or more images and graphically represented. Signal from individual cells were used to analyse PLA signal from transfected cells. Channels were split, then merged. Selection tool was used to draw around individual cells. Right click inside the cell and select duplicate. Channels were again split and the PLA signal channel was selected. Colour was changed to RGB and colour threshold was changed before analysing particles using the same parameters as for whole images. 15 or more cells were analysed and graphically represented. To test statistical significance unpaired standard t-test was used. Statistically significant differences were indicated by *($P \leq 0.05$), **($P \leq 0.01$) or ***($P \leq 0.001$).

2.7 Immunoprecipitation and pull downs

2.7.1 Sample preparation for Mass Spectrometry

Biotinylated peptides was incubated with cell lysate (500 µg total protein concentration) and streptavidin beads (New England Biolabs, S1420S). The mixture was incubated overnight at 4°C rotating. Beads were then washed with cold PBS twice and sample buffer were added. Samples were then sent for mass spectrometry analysis to FingerPrints Proteomics, University of Dundee

2.7.2 Co-IP

Cell lysate (500-2000 µg total protein concentration) was added to 5 µl Protein A/G PLUS-Agarose (Santa Cruz, sc-2003) beads to remove any proteins that interacts non-specifically with the beads. The beads and cell lysate mixture were incubated for 1 hour at 4°C, rotating. Supernatant was collected by centrifugation and appropriate antibody was added (1-2 µg). Pre-cleared cell lysate and antibodies were incubated overnight at 4°C rotating. Agarose beads (20 µl per sample) were prepared by one wash with PBS and then added to the cell lysate/antibody mixture and incubated for a further 2 hours at room temperature or overnight at 4°C rotating. Beads were then washed two times with cell lysis buffer (1 ml) and one wash PBS (1 ml). 4X sample buffer containing β-mercaptoethanol was added (25 µl) to the beads and the mixture was boiled at 95°C for 5-7 minutes. Eluted proteins were analysed by SDS-PAGE and western blotting.

2.7.3 GFP/RFP pull down

Magnetic GFP- or RFP-trap beads (ChromoTek, gtma or rtma) were used in with cell lysate for pull downs. For each reaction 25 µl bead slurry was added to a clean

microcentrifuge tube. Ice-cold dilution buffer (10 mM Tris/Cl, pH: 7.5, 150 mM NaCl, 0.5 mM EDTA) (500 μ l) containing 1x phosphatase inhibitor cocktail was added to the beads, and the beads were washed with this solution three times using a magnetic rack. Cell lysates were diluted in dilution buffer to a total volume of 1 mL, and beads were added. Beads and cell lysates were either incubated for 1 hour at room temperature or overnight at 4°C rotating. Beads were then magnetically separated and the supernatant was discarded. Beads were then washed 3-5 times with ice-cold dilution buffer (500 μ l). Beads were then resuspended in 25 μ l 4X sample buffer containing β -mercaptoethanol. Immunocomplexes were dissociated from beads by boiling at 95°C for 5-10 minutes before SDS-PAGE gel separation of supernatant.

2.7.4 GST/MBP pull down

Glutathione or amylose agarose beads (5-10 μ l) with either GST or MBP tagged expressed and purified proteins were washed with Tris (GST) or HEPES (MBP) buffer before being incubated with cell lysate (0.5-1 mg). Beads were incubated overnight at 4°C rotating before being washed 3x Tris/HEPES buffer. After removing the last wash 25 μ l of 4x sample buffer was added and samples were boiled before running SDS-PAGE and Western blot analysis.

2.8 Microscale thermophoresis (MST)

2.8.1 Protein labelling

Purified proteins were concentrated to 100 μ M using appropriately sized columns for protein of interest (Merck Amicon Ultra Centrifugal Filters, 10 kDa (UFC501024), 3 kDa (UFC500324), and 30 kDa (UFC503024)). Concentrated protein (10 μ l at 100

μM) was mixed with labelling buffer (0.1 M sodium bicarbonate pH: 8.3) and Atto488 NHS ester (Sigma-Aldrich, catalogue number 41698). The solution was incubated for 1 hour in the dark before separation of labelled protein and free dye on gel filtration column.

2.8.2 Microscale thermophoresis

A dilution of the unlabelled protein was made in a 16 times² dilution series, starting concentration varied from 100 μM to 1 mM depending on protein or peptide used. Labelled protein was added to all 16 samples at a final concentration of 50-100 nM. Solution containing labelled and unlabelled protein was transferred to capillaries (Monolith, MO-K022) by capillary action and inserted into MST equipment (Monolith™ NT.115). LED colour was set to green and power was selected so that the maximum fluorescence from the capillaries was between 300-1200 counts. Other parameters included MST power and repeats, a view of a typical set up with parameters can be seen in Figure 2.1.

File Settings Capillaries Temperature Control Tools Expert

LED Settings

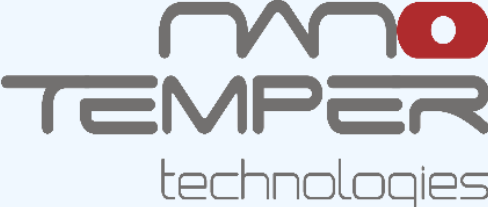
Blue-Green Type
LED Color Blue

Table of Runs

No	LED Power [%]	MST Power [%]	Fluo. Before [s]	MST On [s]	Fluo. After [s]	Delay [s]	Name
01	20	20	5	30	5	25	
02	20	20	5	30	5	25	
03	20	20	5	30	5	25	
04	20	40	5	30	5	25	
05	20	40	5	30	5	25	
06	20	40	5	30	5	25	
07	20	60	5	30	5	25	
08	20	60	5	30	5	25	
09	20	60	5	30	5	25	

Temperature Loop

No	Temp. [°C]	Delay [s]



Manual Temperature Control

Manual Target Temp

Actual Temperature 28.4

Connected ✔

Start Cap Scan Start CapScan + MST Measurement Actual Experiment's Name

Capillary Scanning

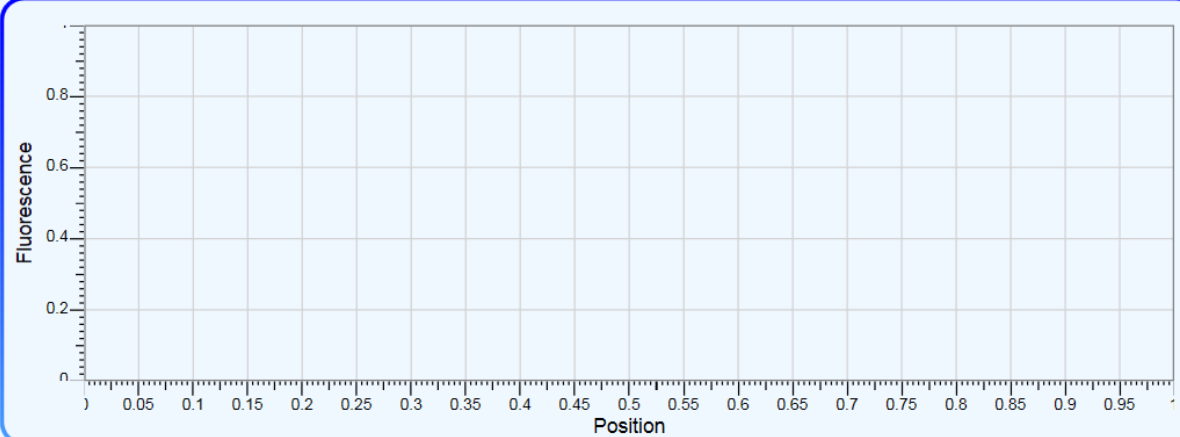
From Cap No To Cap No LED Power [%]

Project File:

Start MST Measurement Concentration Fluor. Mol.

Dilution 1:1

Graphic



Ready

Position 0.01 mm Temperature 28.4°C Temperature Control Off LED Off MST Power Off

Table of Capillaries

No	Concentration	Position	Name	Used
01	1000000.0000			<input type="checkbox"/>
02	500000.0000			<input type="checkbox"/>
03	250000.0000			<input type="checkbox"/>
04	125000.0000			<input type="checkbox"/>
05	62500.0000			<input type="checkbox"/>
06	31250.0000			<input type="checkbox"/>
07	15625.0000			<input type="checkbox"/>
08	7812.5000			<input type="checkbox"/>
09	3906.2500			<input type="checkbox"/>
10	1953.1250			<input type="checkbox"/>
11	976.5625			<input type="checkbox"/>
12	488.2813			<input type="checkbox"/>
13	244.1406			<input type="checkbox"/>
14	122.0703			<input type="checkbox"/>
15	61.0352			<input type="checkbox"/>
16	30.5176			<input type="checkbox"/>

Figure 2-1 A typical experimental setup of Microscale Thermophoresis interface.

2.9 Growth and migration assays

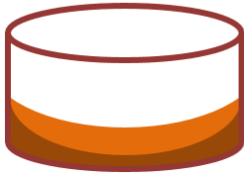
2.9.1 Growth assays

For both soft agar and colony formation assays cells were seeded out in 6-well plates for transfection. HEK293T (gRNA or scr) were seeded at 100 000 cells/well. HeLa cells were seeded at 150 000 cells/well. Cells were transfected the following day and medium with DNA:Lipofectamine complex was removed after 12 hours. Cells were resuspended 48 hours after transfection and taken forward to either soft agar or colony formation assay.

2.9.1.1 Anchorage-independent (Soft agar) assay

1% agarose was melted and cooled to 40°C in a water bath (TopVision Low Melting Point Agarose. Cat No. – R0801). 2X DMEM (Merck; Cat No. SLM-202-B) with 2X FBS and 2X antibiotics was warmed to 37°C. Equal volumes of 1% agarose and 2X DMEM was mixed and 1 mL was added to wells in a 6-well plate. The plates were left to set at 4°C. Before use the plates were brought to room temperature.

0.7% agarose was made and melted, and cooled to 40°C, then mixed with prewarmed 2X DMEM with FBS and antibiotics. Transfected cells were trypsinized and 500-1000 (HeLa and HEK293 respectively) cells were resuspended in 1.5 mL 0.7% agarose and 1.5 mL 2X DMEM (Figure 2.2). 1 mL from this mixture was added to the base layer of agarose. Plates were left to set for an hour at 4°C before normal DMEM was added on top. Plates were left at 37°C in humidified incubator for 10 to 30 days, until visible colonies were formed.



0.7% agarose + 2x DMEM + cells

1% agarose + 2x DMEM

Figure 2-2 Soft agar assay illustration. A typical well for Soft agar assay consisted of a base layer of 1% agarose mixed with 2X DMEM. Cells were mixed with a top layer of 0.7% agarose and 2X DMEM.

2.9.1.2 Anchorage-dependent (colony formation) assay

Transfected cells were trypsinized and 500-1000/well (HeLa and HEK293 respectively) were seeded to a 6-well plate. 2 mL DMEM was added to each well. Plates were left at 37°C in humidified incubator for 10 to 30 days and medium replaced every two days. When visible colonies were formed the medium was removed and wells were washed with PBS. 1 mL crystal violet solution was added (1% crystal violet stain, 25% methanol in water). Plates were left to incubate at room temperature for 15 minutes before removing the crystal violet solution. Plates were washed thoroughly and left to dry before colonies were counted.

2.9.2 Scratch wound assay

HEK293T (gRNA or scr) were seeded at 250 000 cells/well in a 6-well plate. Cells were transfected the following day and medium with DNA:Lipofectamine complex was removed after 12 hours. After 48 hours a scratch wound was made using a pipette tip and wells were imaged using fluorescent microscope (EVOS FL, Life Technologies). Cells were left at 37°C in humidified incubator and imaged again after 24 hours.

Chapter 3: High-throughput analysis to detect SH3 containing proteins which interact with the proline-rich motifs of receptor tyrosine kinases

An important mechanism for receptor activation under non-stimulated conditions was discovered for FGFR2 and could be a previously undiscovered regulation of RTKs. This chapter focuses on discovering novel interactions which can play a role in this potential “second tier” signalling, using high-throughput techniques.

Published data provides precedent for a critical role of SH3 domain interactions with a proline-rich motif in the carboxyl terminus of the RTK FGFR2 (Ahmed et al., 2010; Timsah et al., 2014). This interaction could result in an inhibition of downstream signalling, as seen with the GRB2 dimer interaction with a proline-rich motif on the C-terminal tail of FGFR2 (Ahmed et al., 2010; Lin et al., 2012) or alternatively could result in activation of downstream signalling, as observed for the interaction between PLC1 and the same proline-rich motif of FGFR2, which stimulates downstream signalling in a PLC γ 1 concentration dependent manner (Timsah et al., 2014). There are 58 RTKs in the human proteome and most of them contain one or more proline-rich motifs in their C-terminal tail. Moreover, there are approximately 300 SH3 domains found in proteins, most of which can be found in the cytoplasm which can potentially interact with these proline-rich motifs. These interactions could potentially have diverse effects on receptor mediated signalling. Canonical RTK activation and consequently downstream signalling is through extracellular ligand binding which causes receptor dimerization and trans-autophosphorylation of specific tyrosine residues in the cytoplasmic domains of the RTK. Activation of these receptors through interactions between SH3 domains and proline-rich motifs has the potential

to serve as a “second tier” form of RTK-mediated signalling. Discovering novel interactions between SH3 domains and the proline-rich motifs of RTKs is thus important and might uncover previously unrecognised signalling. To begin to investigate this potential form of interaction, a preliminary screen was performed in which purified recombinant SH3 or WW (an alternative small protein domain capable of interacting with proline-rich motifs) domains were arrayed on a nitrocellulose coated glass slide and then incubated with fluorophore tagged peptides containing the proline-rich sequences from the RTKs ALK, ErbB2, FGFR1, FGFR2, INSR, PDGFRB and IGFR (Figure 3.1). Detection of a fluorescent signal would be indicative of a potential interaction between the proline-rich peptide and the recombinant SH3 or WW domain. This high-throughput assay which is able to identify novel protein-protein interactions has previously been described (Espejo et al., 2002). Results from the screen indicate that a number of SH3 domains from various proteins can interact with the RTK peptides (Figure 3.1) (screen performed by Prof. M. Bedford (MD Anderson Cancer Centre), unpublished). The top five SH3 domain hits from each receptor is summarised in Table 8. These interactions can be taken further to validate and characterise the interaction. The screen consisted of 40 different purified SH3 domains and is therefore limited, as other proteins in the cell can also potentially interact with the proline-rich motifs and as such will remain undiscovered.

Based on previous publications and preliminary data it is interesting to investigate a potential new role for SH3 domains as regulators of RTKs. This chapter will focus on the different high throughput techniques that have been applied to identify proteins with the potential to interact with RTK proline-rich motifs via their SH3 domains. This will include techniques such as mass spectrometry (MS) with proline-rich peptides in

order to uncover other SH3 domain containing proteins interacting with RTKs.

Following this approach, a dot blot method will be described that looks specifically at an interesting protein containing an SH3 domain and its interaction with RTKs.

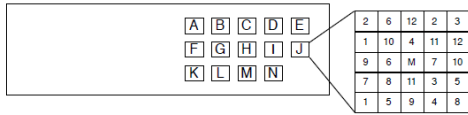
Finally, approaches and various techniques will be described that have been used to validate the interactions uncovered by the dot blot.

Table 8 High-throughput screen of C-terminal tails and SH3 domains done by Prof. M. Bedford. Relative fluorescence for each SH3 domain was measured and here are the top five hits presented.

Receptor C-terminal	Top 5 SH3 domains measured by fluorescence
ALK	SH3PXD2B FYN Shank1 SPTAN1 NCK1
FGFR1	SH3PXD2B ARHGEF7-1 ARHGAP12 FYN ARHGEF16
FGFR2	Shank1 SH3PXD2B ARHGAP12 VAV3 ARHGEF7-1
PDGFRB	Shank1 ARHGAP12 SH3PXD2B MPP2

	ARHGEF7-1
ErbB2-1	LYN FYN PLCG2 PLCG1 Shank1
ErbB2-2	SH3PXD2B FYN LASP1 NEB NCK1
IGFR	FYN LASP1 SH3PXD2B YES1 NEB
INSR	FYN PIK3R1 YES1 SH3PXD2B LYN

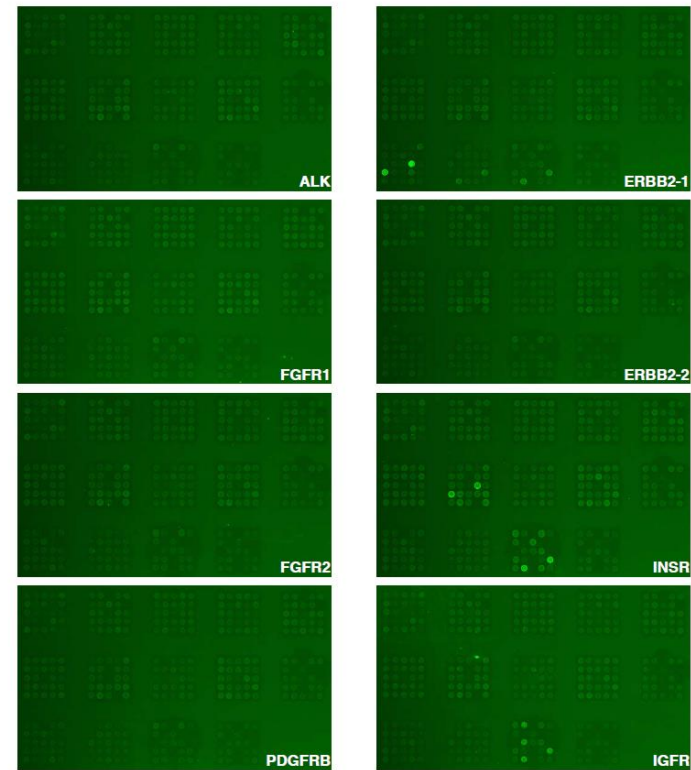
a) WW/SH3 Array



WW	WW	WW	WW	WW
A 1) ESS1 YEAST A 2) PRP40-1 YEAST A 3) PRP40-2 YEAST A 4) RSP5-1 YEAST A 5) RSP5-2 YEAST A 6) RSP5-3 YEAST A 7) SET2 YEAST A 8) URN1 YEAST A 9) YFB0 YEAST A 10) AUS1 YEAST A 11) VID30 YEAST A 12) SSN4 YEAST	B 1) ALG9 YEAST B 2) NEDD4L-1 B 3) NEDD4L-2 B 4) NEDD4L-3 B 5) NEDD4L-4 B 6) NEDD4-1 B 7) NEDD4-2 B 8) NEDD4-3 B 9) NEDD4-4 B 10) PIN1 B 11) PIN1L	C 1) WWP1-1 C 2) WWP1-2 C 3) WWP1-3 C 4) WWP1-4 C 5) WWP2-1 C 6) WWP2-2 C 7) WWP2-3 C 8) WWP2-4 C 9) ITCH-1 C 10) ITCH-2 C 11) ITCH-3 C 12) ITCH-4	D 1) SMURF1-1 D 2) SMURF1-2 D 3) SMURF2-1 D 4) SMURF2-2 D 5) SMURF2-3 D 6) SAV1-1 D 7) SAV1-2 D 8) TCERG1-1 D 9) TCERG1-2 D 10) TCERG1-3 D 11) TCERG1L-2 D 12) TCERG1LorH2-1	E 1) YAP1-1 E 2) YAP1-2 E 3) YAP-WW1* E 4) KIBRA-1 E 5) KIBRA-2 E 6) HYPC-1 E 7) HYPC-2 E 8) FNBP3-1 E 9) FNBP3-2 E 10) WWOX-2 E 11) WWOX-2
WW F 1) MAG11-1 F 2) MAG11-2 F 3) HECW2-1 F 4) HECW2-2 F 5) HECW1-1 F 6) HECW1-2 F 7) MAG12-1 F 8) MAG12-2 F 9) MAG13-1 F 10) MAG13-2 F 11) WBP4-1 F 12) WBP4-2	WW G 1) APBB2 G 2) PLEKHA5-1 G 3) PLEKHA5-2 G 4) GAS7 G 5) WWTR1 G 6) APBB3 G 7) FNBP4-1 G 8) FNBP4-2 G 9) STXBPA G 10) BAG3 G 11) HYPB G 12) DYSTROPHIN	WW H 1) DRP2 H 2) APBB1 H 3) WAC H 4) C20orf67 H 5) UTROPHIN H 6) CEP164(1) H 7) CEP164(2) H 8) KIAA1688-1 H 9) KIAA1688-2 H 10) IQGAP1 H 11) IQGAP2 H 12) IQGAP3	WW I 1) ARHGAP12-1 I 2) ARHGAP12-2 I 3) ARHGAP27-1 I 4) ARHGAP27-2 I 5) ARHGAP27-3 I 6) PDDX10 I 7) ARHGAP9 I 8) PQBP1 I 9) KIAA0082 I 10) MLK3 I 11) KIAA0055 I 12) DiGeorge	WW J 1) PLEKHA2-1 J 2) PLEKHA2-2 J 3) HLA-DQA2 J 4) HOMER3 J 5) genomicseq/YAP1 J 6) esPLEKHA5 J 7) est+1readingframe/MAG11 J 8) FLJ22029-1/WWC2 J 9) FLJ22029-2/WWC2
SH3 K 1) MYO7A K 2) MYO7B K 3) PLCG2 K 4) Shank1 K 5) SKAP1 K 6) ABL2 K 7) LYN K 8) GRB2(1) K 9) GRB2(2) K 10) CRK K 11) WISP K 12) SLA	SH3 L 1) TJP2 L 2) TJP1 L 3) BCR-ABL1 L 4) CSK L 5) PLCG1 L 6) GRB2-like L 7) ITSN1 L 8) RASA1 L 9) VAV3 L 10) MPP2 L 11) GRAP2(1) L 12) GRAP2(2)	SH3 M 1) NEB M 2) SH3PX2D2B M 3) NCK1 M 4) LASP1 M 5) FYN M 6) PIK3R1 M 7) YES1 M 8) SPTAN1	SH3 N 1) ARHGEF7(1) N 2) ARHGEF7(2) N 3) ARHGEF5 N 4) ARHGEF37 N 5) ARHGEF16 N 6) ARHGAP10 N 7) ARHGAP32 N 8) ARHGAP12	

WW Domains provided by: Dr. Marius Sudol and Dr. Sachdev Sidhu

b)



Preserved Middle Intensity
PMT Gain: 360
Power: 16

Figure 3-1 Fluorescent screen with purified SH3 and WW domains incubated with peptides containing proline-rich motifs from various RTKs. (a) The purified domains are arrayed in a specific order onto a glass slide and then incubated with fluorophore tagged peptides from ALK, ErbB2, FGFR1, FGFR2, INSR, PDGFRB and IGFR. (b) If there is an interaction between the peptide and a specific domain it will give a fluorescent signal upon laser scanning

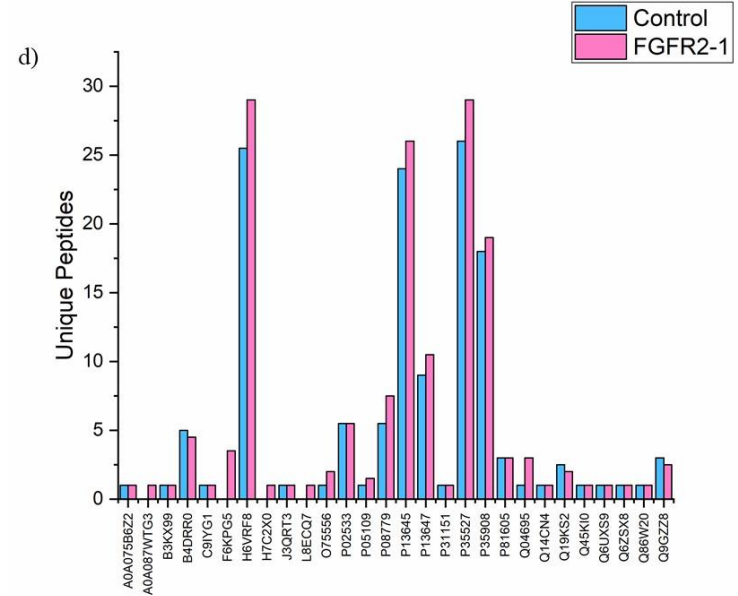
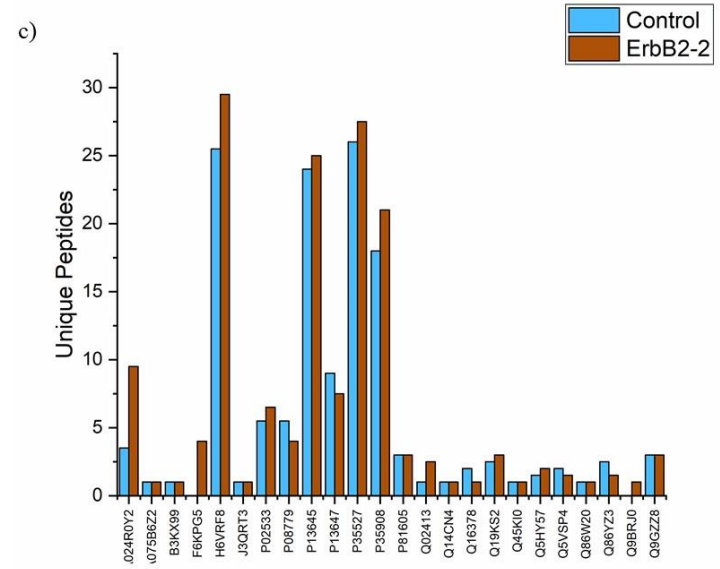
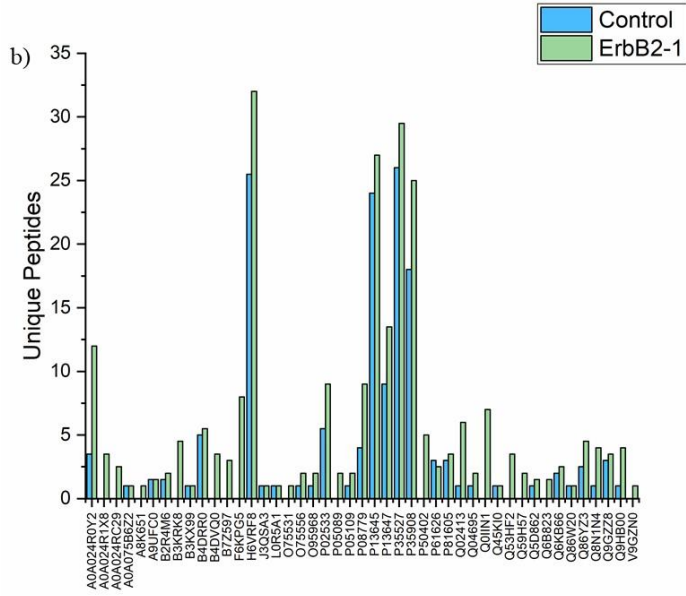
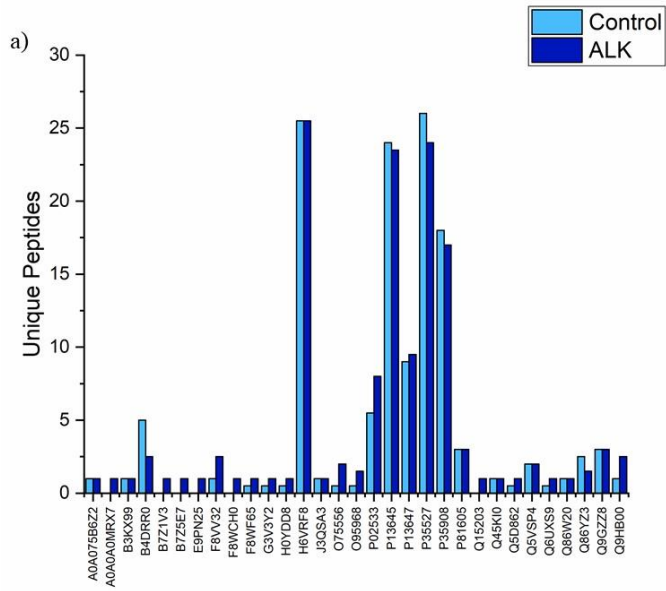
3.1.1 The use of mass spectrometry to detect SH3 domain containing proteins

The proline-rich sequences from the C-terminal tails of a number of RTKs were generated as biotinylated peptides. These peptides were coupled to Streptavidin beads and then incubated with lysates from the human HEK293T cell line overnight. The identification of any bound protein was next determined by MS analysis (FingerPrints Proteomics, University of Dundee). The full dataset from the analysis can be found in Appendix A. Pull-down experiments were performed in duplicate and bound proteins were then determined from unique peptides detected by the mass spectrometer. Only proteins that were identified in both duplicates from the pull-down screens were taken forward for further analysis (Appendix B). These proteins were then compared to a control peptide. The control peptide was a randomised peptide containing no prolines and was used to eliminate proteins that bind non-specifically. Many proteins that were detected by the peptides containing proline-rich motifs were also detected with the control peptide, suggesting a non-specific binding. To avoid missing true interactions with peptides containing proline-rich motifs the number of unique peptides for each protein was compared to unique peptides from the same protein for the control peptide. If the number of unique peptides from proteins detected from peptides containing proline-rich motifs were higher compared to the control peptide, or if they were only detected for the proline-rich peptides the proteins could be considered as specific interactions. Next, the accession numbers from protein hits were used to verify that the protein target contained a known SH3 domain. Finally, cell atlas was used to check if the proteins in question are expressed in HEK293T cells or if they were contaminants from the procedure such

as trypsin or human contaminants from handling the samples such as keratin. This step was critical as a number of contaminating proteins were detected, which were both detected in the control peptide samples as well as in the RTK peptide samples. Strikingly, bioinformatic analysis demonstrated that none of the proteins found in the mass spec analysis contained SH3 domains. In contrast, one protein detected, MAGI-1, did contain a WW domain, which can also bind proline-rich motifs. Despite the lack of canonical proline-rich motif interaction domains in the interaction partners identified, the data pulldown may have revealed a potential novel interaction partner that interacted with the proline-rich peptides by an unknown mechanism. As such, a closer look at the integrity of the datasets was carried out. Datasets from each peptide were compared to the control peptide to check which proteins could be classed as a true interacting partners with the proline-rich motif. Each protein as a measurement of unique peptides was then plotted for both the receptor peptide and control peptide. For example, analysis revealed that most of the proteins precipitated by the ALK RTK peptide could also be precipitated by the control peptide (Figure 3.2 a). Indeed, the highest number of unique peptides from both precipitations originated from keratin proteins, which are known contaminants. Disappointingly, there were no proteins that were pulled down with the ALK peptide that resulted in a larger number of unique peptides, suggesting that none of them bind specifically to the ALK peptide. Similarly, many of the peptides identified from the first ErbB2 peptide could also be found in the control peptide samples (Figure 3.2 b). However, there were also two interesting proteins detected that showed a higher number of unique peptides compared to the control. These are entry A0A024R0Y2 which is the protein HCG30204, isoform CRA_a. This protein is highly similar to Acetyl-CoA carboxylase 1 which utilises as a cofactor for biotin. The protein does not have an SH3 domain

and could possibly have been interacting with the biotin part of the peptide, and potentially the ErbB2-1 peptide has strengthened the interaction. The second is entry P50402 which is emerlin. Emerlin is a nuclear membrane protein and anchors the cytoskeleton to the membrane, and is also involved in actin polymerisation amongst other functions (Berk et al., 2013). ErbB2 has previously been shown to phosphorylate emerlin on an unknown tyrosine (Tiffet et al., 2009). ErbB2 contains several proline-rich motifs in the C-terminal tail, and for this screen two peptides were generated based on two different motifs. The second peptide containing proline-rich motif from ErbB2 (Figure 3.2 c) shows no real differences in the number of unique peptides compared to control apart from entry F6KPG5. This is albumin, which comes up in several screens, and is a contaminant. FGFR2 also has several proline-rich motifs in the C-terminal tail, and two peptides based on two proline-rich motifs were generated and used in the mass spec screen. The first FGFR2 peptide shows no interesting differences compared to the control (Figure 3.2 d). Whilst the second peptide interacts with entry P31151 (Figure 3.2 e). This is protein S100-A7, also known as psoriasin as it is upregulated in the skin of psoriasis patients (Madsen et al., 1991). Psoriasin contains two EF-hand domains, and is part of the S100 family of proteins which bind calcium ions, via their EF-hand domains. The S100 family is involved in many biological processes including cellular differentiation, proliferation and migration and members are implicated in many cancers, either as a promoter of growth and metastasis or even as tumour suppressors (L. Geczy et al., 2012; Bresnick et al., 2015a). Extracellular S100A13 has been shown to interact with FGF1 (LaVallee et al., 2002). S100-A7 is overexpressed in breast cancer but no expression is detected in normal breast epithelial cells. S100-A7 can either activate pro-survival pathways in ER α -negative breast cancer cells but inhibit proliferation in

ER α -positive breast cancer cells (Bresnick et al., 2015b). The question remains what part of S100-A7 interacts with the FGFR2 peptide and what is the biological impact of this interaction. For the PDGFRB peptide no significant differences between the proline-rich peptide and the control peptide was observed (Figure 3.2 f). The IGFR peptide generated a small number of entries that could be of potential interest (Figure 3.2 g). This was the only peptide that pulled out a protein containing a domain which can bind specifically to proline-rich motifs. Entry A0A087WXD2 is membrane-associated guanylate kinase, WW and PDZ domain-containing protein 1 (MAGI-1). As its name suggests, it contains two WW domains and five PDZ domains. It is part of the superfamily membrane-associated guanylate kinases (MAGUK), which can contain PDZ, SH3 and GUK domains (Godreau et al., 2004). This interaction was also picked up in the fluorescent screen from Prof M. Bedford, where two WW domains from MAGI was used. A fluorescent signal can be detected for both WW domains for all the tested RTK peptides. The next entry of interest is Q53HF2 which is Heat shock 70 kDa protein 8 isoform 2 variant. Interestingly this entry also showed up for the first ErbB2 peptide in a 3:1 ratio compared to control peptide. The heat shock protein 70kDa family of proteins are involved in protein folding (Mayer and Bukau, 2005).



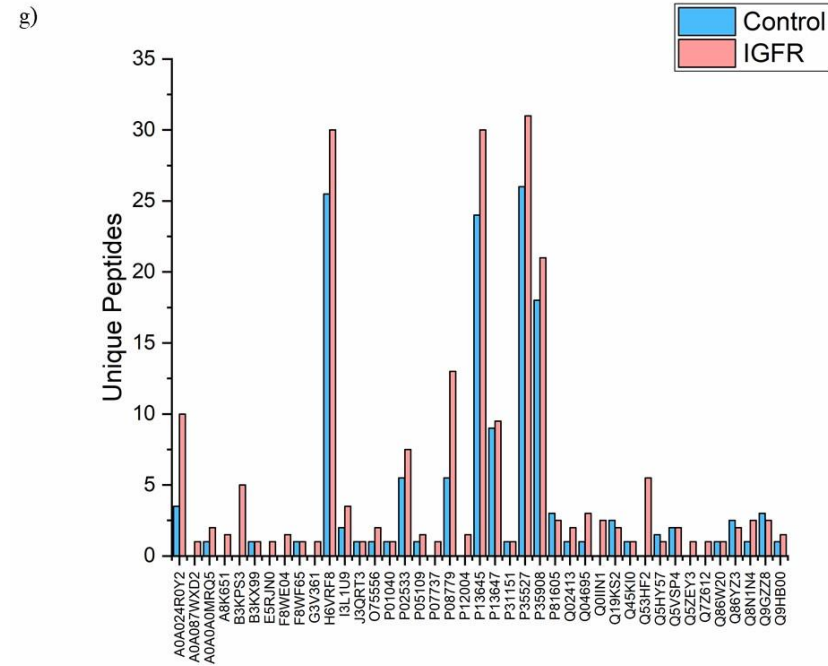
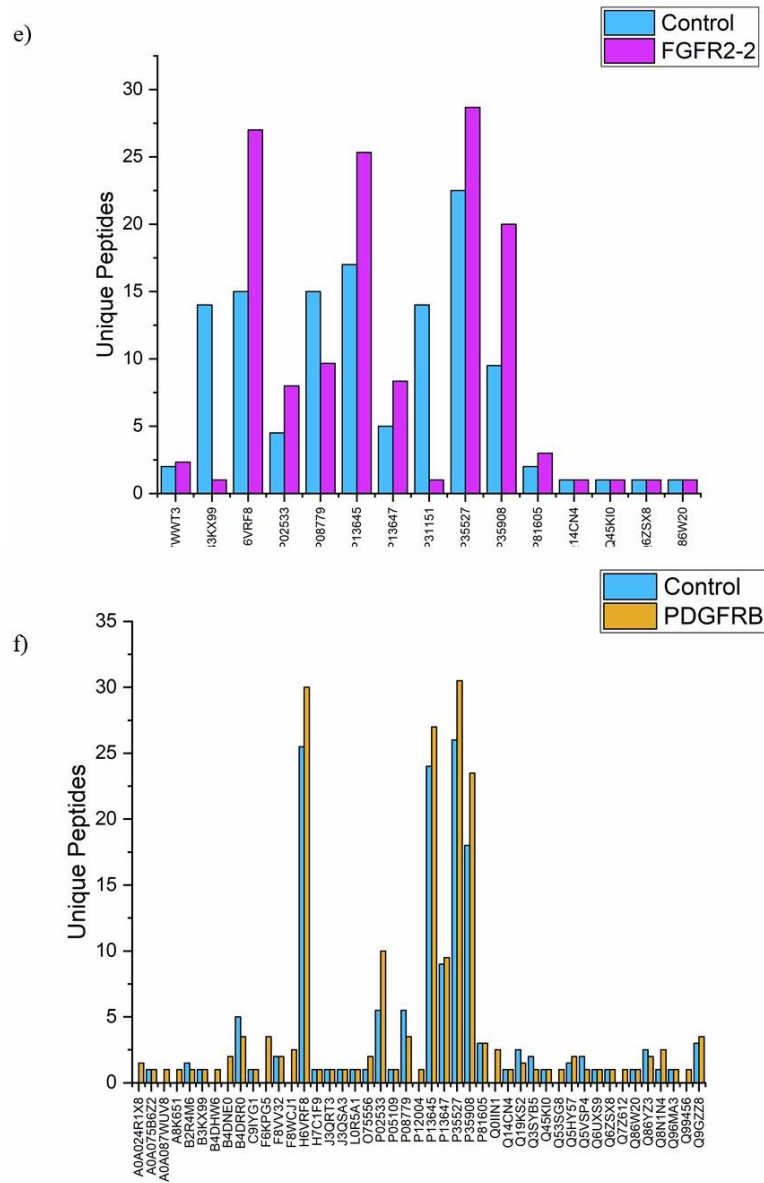


Figure 3-2 Number of unique peptides from each protein that were pulled down by proline-rich peptides from receptors

ALK (a), ErbB2-1 (b), ErbB2-2 (c), FGFR2-1 (d), FGFR2-2 (e), PDGFRB (f) and IGFR (g) plotted together with control peptide containing no prolines.

3.1.2 Using purified peptides of the C-terminal tails of RTKs in a dot blot

The MS screen yielded no novel interactions between SH3 domains and proline-rich motifs from RTKs, suggesting that the screen must undergo various steps of optimisation, or further exploration of techniques which are able to detect these weak interactions. To further test the hypothesis that proline-rich motifs can interact with SH3 domains, a screen using purified peptides from the C-terminal tail of RTKs and purified LASP1 was performed. LASP1 is a cytoplasmic protein that contains an SH3 domain. The SH3 domain has been shown to interact with proline-rich motifs of a range of different proteins (Orth et al., 2014). Additionally the screen from Prof M. Bedford showed that the SH3 domain from LASP1 might directly interact with several of the RTK proline-rich motifs (Figure 3.1). The accessibility to LASP1 with and without the SH3 domain, the ease of purifying it and the stability of the protein provided a good starting point for evaluating the dot blot as a technique, but is not limited to LASP1.

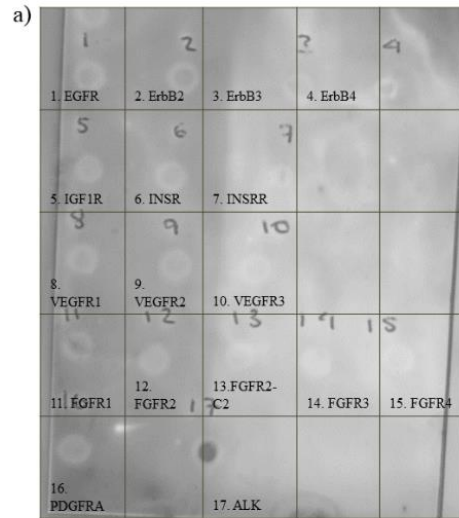
The C-terminal tails of a range of RTKs were cloned into vectors containing maltose binding protein (MBP) tag (work by Dr. Chi-Chuan Lin, University of Leeds). After bacterial expression and purification the MBP tagged C-terminal peptides were arrayed onto a nitrocellulose membrane and incubated with recombinant GST-tagged LASP1 (Figure 3.3 a) or a mutant LASP-1 lacking the SH3 domain (LASP1 Δ SH3, (Figure 3.3 b). Blotting was then performed with an antibody raised against GST. Any GST signal was indicative of an interaction between LASP1 and the MBP tagged RTK peptide. Both the wild type and Δ SH3 mutant LASP1 appeared to interact with the C-terminal tails of several RTKs, with the most intense signal originating from the ALK fusion. Signals were also detected from C-terminal tails of EGFR, ErbB2 and FGFR1, and even weaker signals detected from other receptor

tails. The interactions are summarised in a graph showing relative intensity and summarised in Table 9 (Figure 3.3 c and Table 9). The membrane was also probed for MBP to confirm the presence of the C-terminal peptide fusions on the dot blot (Figure 3.3 d). Another membrane was dotted with LASP1 wild type and Δ SH3 mutant and analysed for GST (Figure 3.3 e). Additionally, an SDS PAGE gel was run to confirm the molecular weight of the various C-terminal tail fusions (Figure 3.3 f, Table 10). According to the molecular weight of the C-terminal tails some of the receptors possibly only contain the MBP tag (42 kDa), such as ErbB3, ErbB4, VEGFR3 and ALK. This is quite surprising as ALK gave the strongest signal in the dot blot. A closer look at the western blot reveals that for ErbB3, ErbB4 and ALK two bands with similar molecular weight is detected. Additionally, the ErbB4 lane also shows a faint band at a higher molecular weight which corresponds to full length MBP-ErbB4. Some run lower than they were predicted to such as VEGFR1 and VEGFR2. The disparity of the predicted molecular weights and how the proteins run on the gel could be the way the samples are prepared, denaturing by boiling. The MBP tag can in some cases be cleaved off, as a result of proteolytic cleavage, and in the case of ErbB3, ErbB4 and ALK would leave two species at 42 kDa (MBP) and 41/36.6/30 kDa. This could explain the double bands at similar molecular weights that are seen on the western blot. INSRR runs higher than the predicted molecular weight which could be the result of a dimerization which was not lost in the preparation of the samples. Insulin receptors exist at the cell membrane as dimers stabilised by disulphide bonds. With ligand binding they undergo conformational changes which activates the receptor and consequently downstream signalling (Maruyama, 2014). The pre-existing INSRR dimer does not explain the results from the western blot as only the INSRR C-terminal tail was used in these experiments.

The dot blot method can detect interactions between the C-terminal tails of several RTKs and LASP1. Some of the RTKs interact with the SH3 mutant differently to wild type LASP1. The dot blot method can be further used with other proteins containing an SH3 domain, or even just the SH3 domains from various proteins on its own. Having to express and purify proteins or domains of proteins can be limiting, and the dot blot as a method overall is limited as interactions might still remain uncovered based on the fact that purified proteins or domains are used.

Table 9 Interactions between RTK C-terminal tail and LASP1 with and without the SH3 domain based on relative intensity from dot blot (Figure 3.3)

C-terminal tail	LASP1 WT	LASP1 Δ SH3
EGFR	++++	+++
ErbB2	++++	+++
ErbB3	++	+++
ErbB4	++	
IGFR1	++++	++
INSR	+++	++
INSRR	+	++
VEGFR1	++++	+
VEGFR2	+++	+
VEGFR3		+
FGFR1	+++++	++
FGFR2	++++	+
FGFR2-C2	+	++
FGFR3		+++++
FGFR4		+++++
PDGFRA	+++++	++
ALK	+++++	+++++



LASP1 WT
IB: α -GST



LASP1 Δ SH3
IB: α -GST

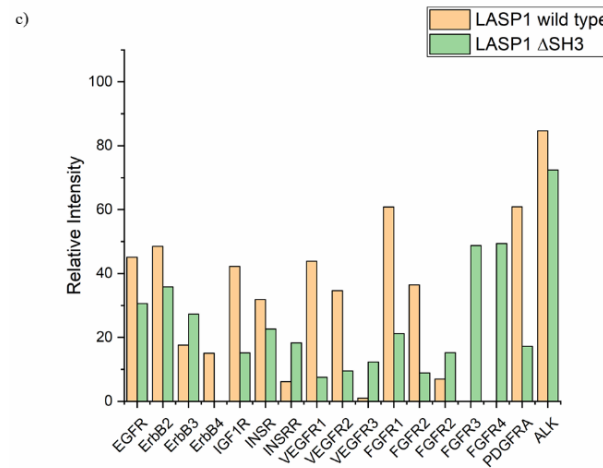


Figure 3-3 Dot blot with purified MBP-tagged C-terminal tails of RTKs.

Nitrocellulose membranes were incubated with purified GST-tagged LASP1 wild type (a) or LASP1 Δ SH3 (b). The intensity of each dot was quantified using ImageJ and normalised to the background. The relative intensity was summarised in a graph showing the differences between wild type and Δ SH3 mutant (c). The dot blot was also incubated with antibody raised against MBP (d) and GST (e). MBP-tagged receptor tails were also run on a gel to separate them and confirm molecular weights (f)

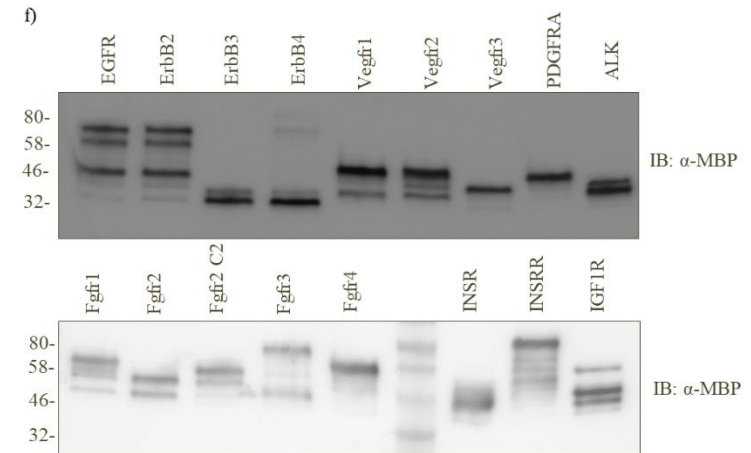
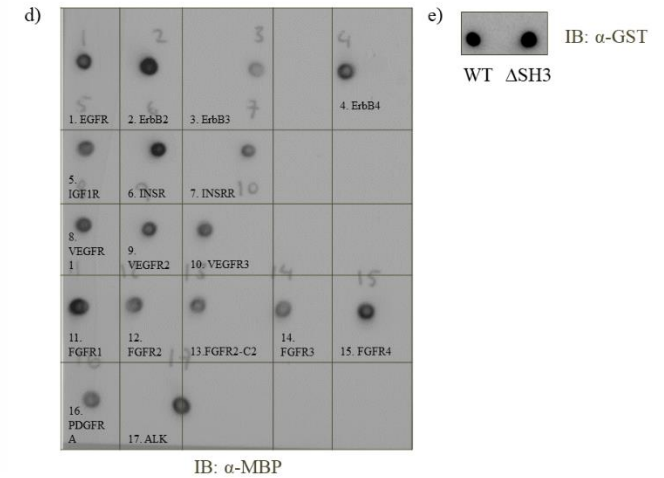


Table 10 List of C-terminal tail peptides and molecular weight used in dot blot

C-terminal tail	Molecular weight (with MBP tag) (kDa)
EGFR	25.6 (67.6)
ErbB2	28.3 (70.3)
ErbB3	41.0 (83.0)
ErbB4	36.6 (78.6)
IGF1R	10.7 (52.7)
INSR	9.2 (51.2)
INSRR	4.6 (46.6)
VEGFR1	20.0 (62.0)
VEGFR2	21.2 (63.2)
VEGFR3	21.1 (63.1)
FGFR1	7.2 (49.2)
FGFR2	6.8 (48.8)
FGFR2-C2	2.8 (44.8)
FGFR3	4.5 (46.5)
FGFR4	4.7 (46.7)
PDGFRA	16.0 (58.0)
ALK	30.0 (72.3)

3.1.3 Verifying LASP1 binding to selected receptors from the dot blot

Some of the putative interactions identified from the dot blot were taken forward for validation in a cellular environment. Recombinant GST-LASP1, GST-LASP-1 Δ SH3 and GST-LASP1 Δ LIM fusion proteins were generated in *E. coli* and used in pull down experiments. According to the dot blot the C-terminal tail of ALK can interact with LASP1 regardless of whether the SH3 domain is present, suggesting a role for other domains and regions of LASP1. For this reason a mutant lacking the LIM-

domain was used in order to evaluate whether the ALK interaction was with this domain. The GST pull down experiments were performed with lysates from SH SY5Y cells. SH SY5Y is a human neuroblastoma cell line derived from a biopsy of a metastatic bone marrow tumour and further subcloned. They have a neuronal like phenotype and are often used in research on amyloid proteins (Kovalevich and Langford, 2013). Based on data from cell atlas SH SY5Y cells highly express ALK and were considered a good source for the GST pull down. As seen from the cell lysates, ALK could be detected in two forms, a full length protein (220 kDa), and also a cleaved form of 140 kDa form, the cleaved form lacks the extracellular domains (Figure 3.4 a) (Moog-Lutz et al., 2005; Mazot et al., 2012). Because the cleavage of ALK affects the extracellular domains it is thought not to interfere with the potential interaction with LASP-1, which would most likely happen in the cytoplasm. Indeed, both forms of ALK were pulled down with all three recombinant LASP1 proteins, but not with GST alone (Figure 3.4 a). This suggests that ALK can interact with LASP-1 via another region of the LASP-1 protein, such as the nebulin repeats. Based on these findings, purified GST-LASP1 and MBP-ALK C-terminal receptor were taken forward to determine binding affinity using microscale thermophoresis (MST). MST is a biophysical method and a powerful tool which can be used to determine binding affinity between two molecules. A concentration dilution series is incubated with a fluorescently labelled protein at a constant concentration. An IR-laser focused on the capillary containing the solution generates a temperature gradient. Molecules move either away from, or towards the laser point to lower temperature regions until an equal distribution is created. Because a protein in a complex moves with a reduced velocity compared to when it is isolated, the measured fluorescence is distributed differentially across the protein concentration gradient, based on the concentration

titration of the unlabelled protein. A sigmoidal binding curve can be created as a function of changes of temperature, fluorescence and concentration, and the dissociation constant K_D can be determined from the curve. The K_D between C-terminal tail of ALK and LASP1 was determined to 365 μM (Figure 3.4 b). The binding curve determined by MST is not a true sigmoidal curve fit as the concentration of the ALK peptide was not high enough to reach complete binding of LASP1 WT, so some caution should be taken with the K_D determined. Nevertheless, taken together the data suggests that LASP-1 directly interacts with ALK in the C-terminal tail part of the receptor and that this interaction is independent of either SH3 or LIM domain.

According to the dot blot, the C-terminal tail of ErbB2 also interacts with LASP-1. SkBr3 cell lysates were used in a GST pull down experiment. SkBr3 cells is a breast cancer cell line which overexpress ErbB2. Wild type LASP1, LASP1 ΔSH3 and LASP1 ΔLIM could all pull down ErbB2. The ΔSH3 mutant appeared to pull down 3-fold the amount of ErbB2 relative to wild type and the ΔLIM mutant (Figure 3.4 c). A proximity ligation assay (PLA) was performed to verify the ErbB2 and LASP1 interaction. Furthermore, in addition to verify the interaction, PLA can show that this interaction can happen endogenously and that it could be physiologically important. PLA uses antibodies that are specific to the two proteins of interest, but originate from different species. Two probes acting as a secondary antibody detects the primary antibody, one for each species the primary antibody was raised in. A DNA probe attached to the secondary antibody serves as a template for oligonucleotide amplification if the probes are in close proximity of each other. The DNA probes can undergo rolling circle DNA synthesis in a ligation step which can then be amplified. Fluorescently tagged oligonucleotides in the amplification step binds and this allows

for fluorescently visualisation. A signal indicates that the proteins are in close proximity to each other. Data from the PLA suggests that endogenous LASP1 and ErbB2 interact in SkBr3 cells (Figure 3.4 d). Taken together these data suggest that LASP1 and ErbB2 interact endogenously in the breast cancer cell line SkBr3 and this interaction is not through either the SH3 domain or LIM domain. In fact, the LASP-1 mutant lacking the SH3 domain appeared to pull down 3-fold more ErbB2 compared to wild type and Δ LIM mutant. Possibly the full length LASP1 could be sterically hindering ErbB2 access to the binding site of LASP1 and removing the SH3 domain changes the conformation of LASP-1 in such a way as to allow for tighter binding, by for example having more of the surface area that interacts with ErbB2 exposed. It would be interesting to compare MST analysis with and without the SH3 domain to see if a higher affinity could be obtained. Regardless, LASP1 can interact with ErbB2 in a breast cancer cell line.

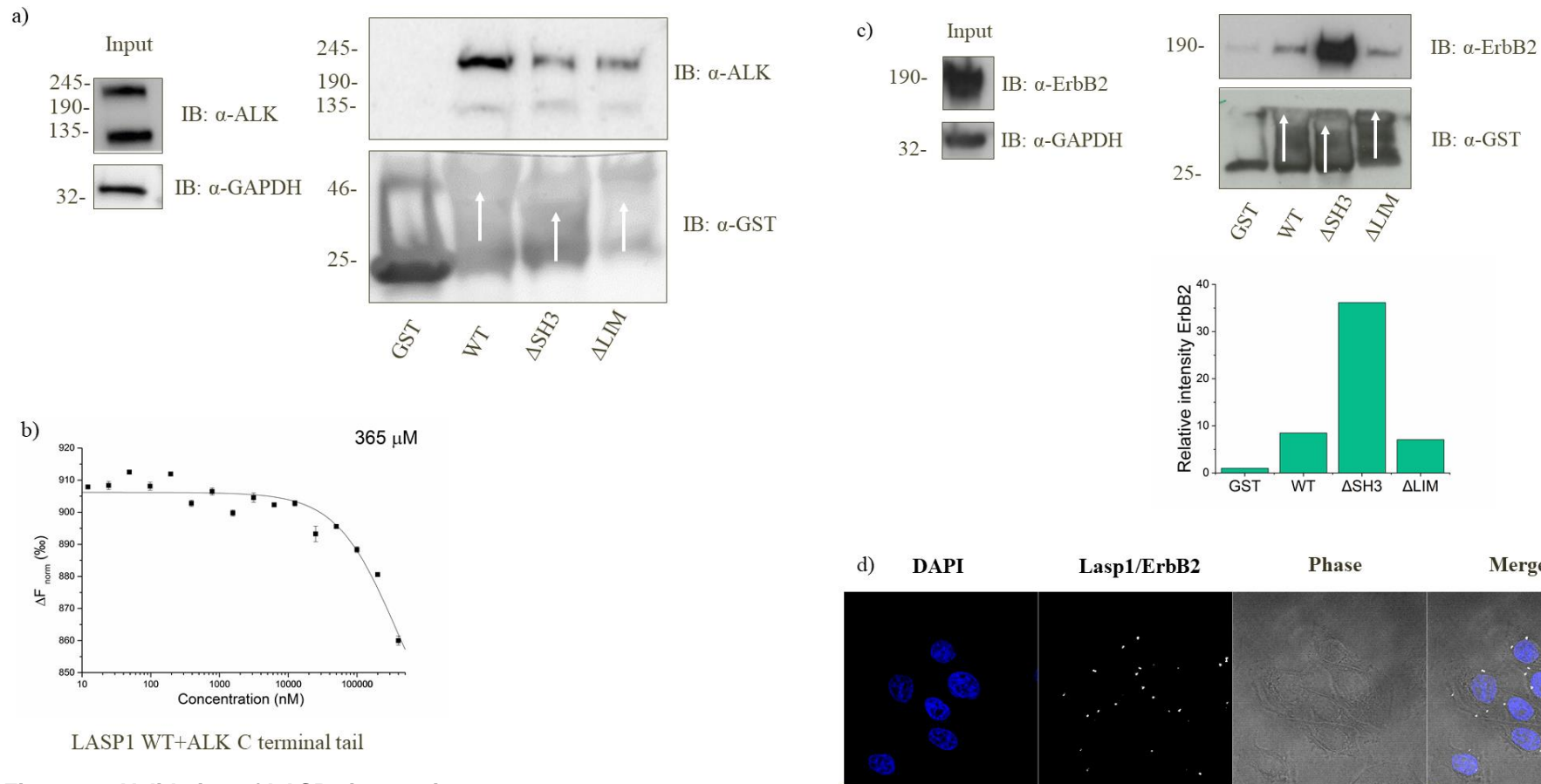


Figure 3-4 Validation of LASP1 interactions.

a) GST pull down using wild type LASP1, Δ SH3 and Δ LIM mutant with cell lysate from SH SY5Y cells. Both wild type and the mutant LASP1 was able to pull down ALKs. b) MST determined a K_D of 365 μ M between wild type LASP1 and the C-terminal tail of ALK. Experiment was done at pH 7.5 in HEPES buffer. c) GST pull down using cell lysate from SkBr3 cells shows that wild type LASP1 can pull down ErbB2, as can the Δ LIM and Δ SH3 mutants. White arrows show the molecular weights of GST-LASP1 WT, GST-LASP1 Δ SH3 and LASP1 Δ LIM. Graph illustrates the relative intensity of the ErbB2 bands. d) PLA using SkBr3 cells shows that LASP1 and ErbB2 interact endogenously in the cells.

3.1.4 Discussion

This chapter focusses on two different methods to discover previously unknown interactions between SH3 domains and proline-rich motifs. MS is a very sensitive method for analysing unknown proteins and is often used for that reason in high throughput screens. Theoretically, it would be a powerful technique to identify novel interactions but in reality yielded few hits, suggesting that experimental set up and/or conditions would have to be optimised. The majority of the unique peptides identified stem from various contaminants, and none of the proteins identified had a *bona fide* SH3 domain. Interestingly, one protein did contain a WW domain which are also able to bind proline-rich sequences and further verification and characterisation of this interaction would be interesting. Interactions between SH3 domains and proline-rich motifs are weak interactions and therefore inherently difficult to discover or capture. Different approaches could have been taken to ensure a better and larger dataset containing SH3 domain containing proteins would be discovered such as using additional cell lines to ensure fuller coverage from that perspective. The biotin-streptavidin interaction is a strong interaction but the wash steps of the streptavidin beads might have been too harsh for proteins bound to the peptide, and buffer content could be further explored to ensure the stability of binding. In addition the length of the linker between the peptide and biotin could be further optimised, where a longer peptide could potentially increase the interaction potential. Furthermore the streptavidin beads can also play a role in restricting interactions as they come in different sizes (1-10 μm), so bead sizes used in the experiments could be explored. Using the MS service was not very cost effective so exploration of the protocol contents such as buffer content could end up costing a lot of money. Other approaches could be using bioID where not the peptide itself is biotinylated but

rather the peptide is fused to a biotin ligase and upon expression in cells it can biotinylate proteins in close proximity (Roux et al., 2013). There are some interesting proteins that came from the MS screen which could be followed up on but as none contained SH3 domains they fell short of the scope of this project. The focus then shifted to a semi high throughput approach for looking specifically at the SH3 domain containing protein LASP1 and its interaction with the C-terminal tail of several RTKs. The SH3 domain of LASP1 was previously demonstrated by Prof M. Bedford to interact with several C-terminal tails from RTKs, as demonstrated by fluorescent signal where LASP1 SH3 domain was immobilised and incubated with fluorescently labelled RTK peptides (Figure 3.1 and Table 8). The dot blot method is limited to discovering novel proteins interacting through the SH3 domain, but can be applied to many proteins or protein domains given that they can be expressed and purified. Using the dot blot with purified LASP1 and LASP1 Δ SH3 gave an opportunity to see if there was a difference in receptor tail interacting with either protein and suggestive of it being through the SH3 domain. A strong signal was detected for both wild type and mutant with ALK and a pull down experiment and binding study confirmed that this was indeed a real interaction and K_D was determined to be 365 μ M. Another confirmation of interaction was with ErbB2. This interaction also came up as one of the top hits from the preliminary fluorescent screen done by Prof. M. Bedford (Figure 3.1 and Table 8). Results presented here demonstrates using both GST pull down and PLA that LASP1 and ErbB2 interacts, but again this was not through the SH3 domain. Intriguingly the interaction between LASP1 and ErbB2 was shown endogenously in a breast cancer cell line. LASP1 was originally discovered in metastatic breast cancer tissue and is reported to be overexpressed in 8% of breast carcinomas (Tomasetto, Régnier, et al., 1995; Tomasetto, Moog-Lutz, et al., 1995;

Bièche et al., 1996). Further work would have to be done to identify how ALK and ErbB2 interact with LASP1, and which regions of the proteins are necessary for mediating the interaction. A crystal structure trial could be set up with wild type LASP1 and the C-terminal tails of ALK and ErbB2. Cloning the nebulin repeats into a GST construct to see if they are the only parts of LASP1 needed to pull down ALK or ErbB2 could be an alternative approach. Once the interaction site has been identified it would be even more interesting to see if the interactions have any impact physiologically on the cells. All three proteins are oncoproteins and implicated in a wide range of cancers. It would be interesting to see if the LASP1-ErbB2 interaction has any impact on breast cancer cell phenotypes. One potential way of analysing the phenotype would be knocking down LASP1 and determining if this impacts cell growth and migration. ALK is normally found to be oncogenic as a fusion protein that makes the kinase region of ALK constitutively active (Chiarle et al., 2008). These data suggest that LASP1 interacts with full length ALK, and it would be interesting to further investigate what this interaction means for the cell. One potential way to study this would be to observe the signalling events downstream of ALK in the presence or absence of LASP1. Furthermore this illustrates that the dot blot has provided preliminary data for an interaction, and that this has been confirmed in cells. Additionally, the relative intensity for IGF1R, VEGFR1, VEGFR2, FGFR1, FGFR2 and PDGFRB all showed a more intense dot for wild type LASP1 compared to the SH3 mutant, and would all be interesting to further verify and investigate.

Chapter 4: Interaction between LASP1 and FGFR2 proline-rich motif and physiological significance of the interaction in cells

Preliminary data suggest that FGFR2 can interact with the SH3 domain of LASP1.

This chapter focuses on characterising the interaction, as well as establishing it in a cellular context. Demonstrating that the LASP1 SH3 domain can interact with a proline-rich motif on FGFR2 adds value to a possible “second tier” RTK regulation and signalling.

FGFR2 has been previously demonstrated to be important in the “second tier” RTK regulation. A proline-rich motif in the FGFR2 C-terminal tail has been shown to interact with both GRB2 and PLC1 in a concentration dependent matter (Timsah et al., 2014). While a dimeric GRB2 holds two receptor molecules in close proximity to each other, the receptor itself is not activated (Lin et al., 2012). PLC γ 1 competes for binding to the same proline-rich motif and GRB2 depleted cells have been shown to have increased migration and growth potential as a result of phospholipase activity from the PLC γ 1 interaction with FGFR2 (Timsah et al., 2014; Timsah et al., 2015). This was the first demonstration of a non-stimulated RTK activation from protein concentration alone, i.e. where a higher PLC γ 1 concentration compared to GRB2 leads to activation. Some evidence suggests that the SH3 domain from LASP1 can interact with a peptide containing the proline-rich motif from FGFR2. SH3 domains from various proteins were arrayed on a nitrocellulose coated glass slide and then incubated with fluorophore tagged FGFR2 peptide (Figure 4.1 a). A weak signal was detected from the LASP1 SH3 domain (blue circles), suggesting that the SH3 domain interacts with FGFR2 peptide (screen performed by Prof. M. Bedford (MD Anderson Cancer Centre), unpublished). In addition a weak signal was detected

when LASP1 was incubated with the dot blot containing MBP-tagged FGFR2 C-terminal tail (Chapter 3, Figure 3.3 and Table 9). When the dot blot was incubated with the mutant LASP1 lacking the SH3 domain, the detected signal was 3-fold weaker suggesting that the interaction is primarily mediated by SH3 domains and the C-terminal tail of FGFR2. LASP1 is a ubiquitously expressed protein containing a LIM domain, two nebulin repeats (R1 and R2) and an SH3 domain (Figure 4.1 b). After first being discovered in metastatic lymph nodes originating from breast cancer, LASP1 has since been shown to be overexpressed in many cancers (Butt and Raman, 2018). This chapter focuses on characterisation of the LASP1 interaction with FGFR2, and some preliminary work has been undertaken to study the physiological outcome of this interaction.

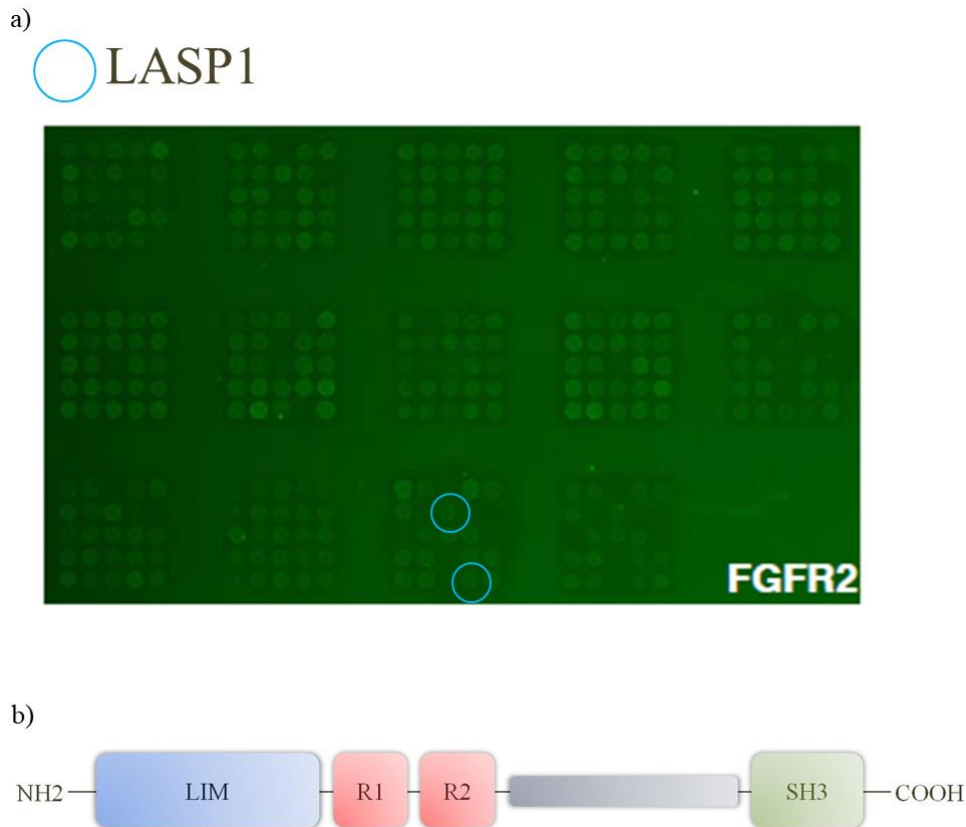


Figure 4-1 Preliminary fluorescent screen with FGFR2 peptide

a) Screen using purified SH3 domains arrayed onto a glass slide and incubated with fluorophore tagged FGFR2 peptide containing proline-rich motifs shows a weak signal for LASP1 SH3 domain suggesting an interaction. b) LASP1 contains a LIM domain, two nebulin repeats (R1 and R2) and a SH3 domain.

4.1.1 FGFR2 C-terminal tail interacts with LASP1 SH3 domain in cells

To validate the data from the fluorescent screen and the dot blot, and to determine whether the interaction occurs in cells, GST pull downs and PLA were performed. GST-tagged LASP1 and two mutants lacking either the SH3 or LIM domains (Δ SH3 and Δ LIM respectively) were expressed in *E. coli* and purified prior to incubation with cell lysates from HEK293T cells. The lysates were from cells that had been transfected with FGFR2. Cells were also starved overnight to ensure that the potential interaction was with a non-activated receptor. LASP1 effectively pulled

down FGFR2 while the Δ SH3 mutant was unable to (Figure 4.2 a). Interestingly, the Δ LIM mutant appeared to pull down 3-fold more FGFR2 compared to wild type. Taken together the data suggests that LASP1 and FGFR2 interact and that it is mediated by the LASP1 SH3 domain. As there is currently no structure of full length LASP1, only speculations can be made as to why the LIM domain is potentially restricting FGFR2 binding. The domain could potentially be a steric hindrance from how the protein is folded, there could be interactions between the SH3 and LIM domain. A repeat experiment was performed to include controls for the GST and GFP tags. Cell lysate from starved HEK293T cells that had been transfected with GFP-FGFR2 and also a GFP-FGFR2 construct lacking the last 25 amino acids of the C-terminal tail of FGFR2 (FGFR2 Δ 25) was incubated with GST, GST-LASP1 or GST- Δ SH3. Again wild type LASP1 pulled down FGFR2 but not the Δ SH3 mutant (Figure 4.2 b). Interestingly FGFR2 Δ 25 mutant was not pulled down with wild type LASP1 to the same extent as wild type FGFR2 suggesting that the interaction lies within the C-terminal tail of FGFR2. Additionally, the C-terminal tail of FGFR2 was able to pull down LASP1 in a GST-pull down experiment. A GST-tagged construct consisting of 58 amino acids from the C-terminal tail of FGFR2 (C58) was incubated with lysates from starved HEK 293T, which had been transfected with LASP1. GST-C58 was able to pull down LASP1 but not GST alone (Figure 4.2 c), further confirming that this interaction is through the FGFR2 C-terminal tail.

Further confirmation of the interaction between LASP1 and FGFR2 was observed by PLA in HEK293T cells that had been transfected with either GFP-FGFR2 or GFP-FGFR2 Δ 25. Cells were serum starved overnight and then either stimulated with FBS and taken forward to PLA analysis, or taken directly to PLA analysis. PLA signal was detected for GFP/LASP1 in both serum starved (Figure 4.3 a) and stimulated

(Figure 4.3 b) cells when cells were transfected with FGFR2. Less or no signal was detected when cells were transfected with the $\Delta 25$ mutant. A quantification of the PLA signal in individual cells was undertaken by analysing particles in ImageJ (Figure 4.3 c-e) and showed a significant difference between cells transfected with wild type FGFR2 and the FGFR2 $\Delta 25$ mutant, further confirming that LASP1 interact with the C-terminal tail of FGFR2. The interaction happened irrespective of whether the receptor was activated.

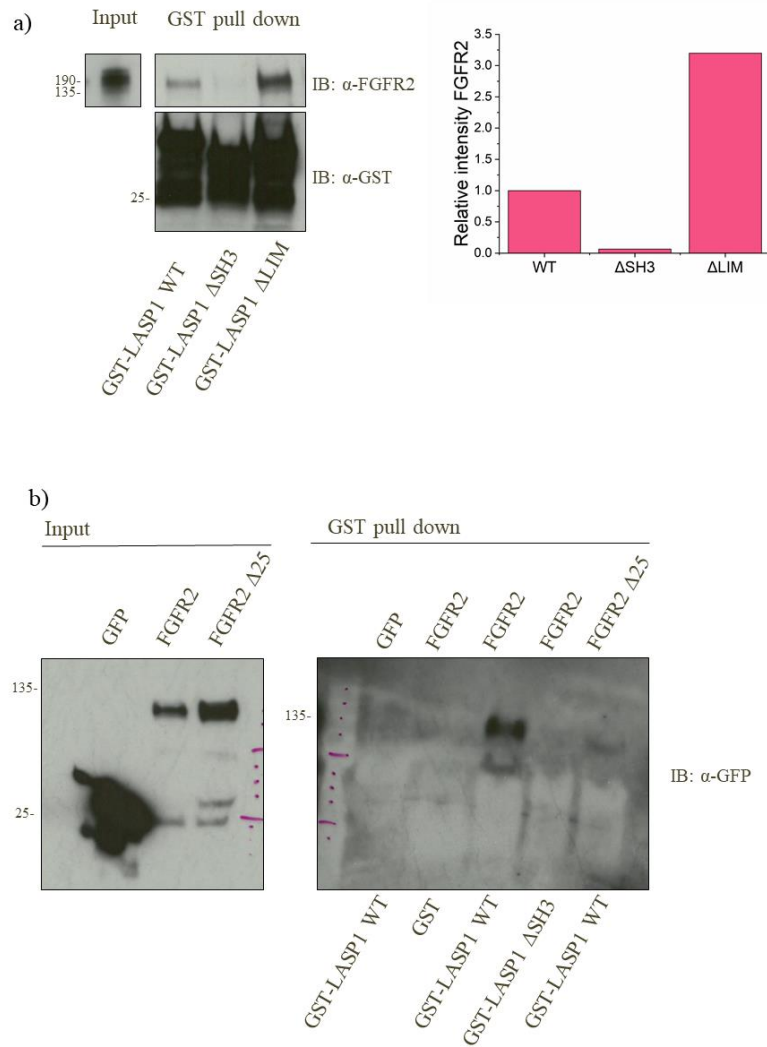


Figure 4-2 GST pull downs shows LASP1 interaction with FGFR2

a) Purified GST tagged LASP1, and mutants lacking the SH3 and LIM domains (Δ SH3 and Δ LIM) were incubated with cell lysate from starved HEK 293T cells overexpressing FGFR2. Both LASP1 and Δ LIM can pull

down FGFR2 but not the Δ SH3 mutant suggesting an interaction between FGFR2 and LASP1 SH3 domain. Graph shows relative intensity of FGFR2 being pulled down b) A repeat experiment incorporating controls such as GST only and GFP transfected cells again shows that LASP1 can pull down FGFR2 but not the Δ SH3 domain. Another construct of FGFR2 lacking the last 25 amino acids in the C-terminus (FGFR2 Δ 25) was also transfected into cells and incubated with GST-LASP1. Less FGFR2 Δ 25 was pulled down by LASP1 suggesting that the interaction is in the C-terminal region of FGFR2. c) GST-tagged C-terminal tail of FGFR2 consisting of 58 amino acids (C58) was incubated with starved HEK293T cell lysate overexpressing LASP1. LASP1 was pulled down by GST-C58 but not GST alone

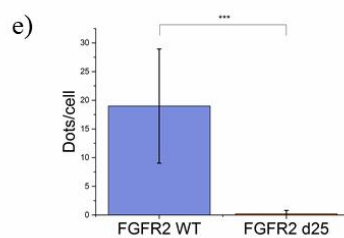
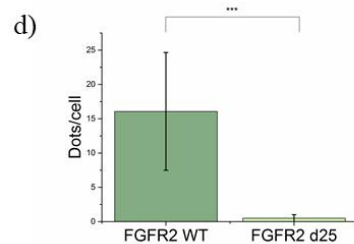
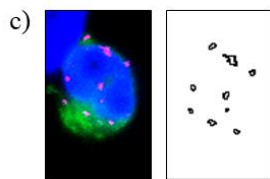
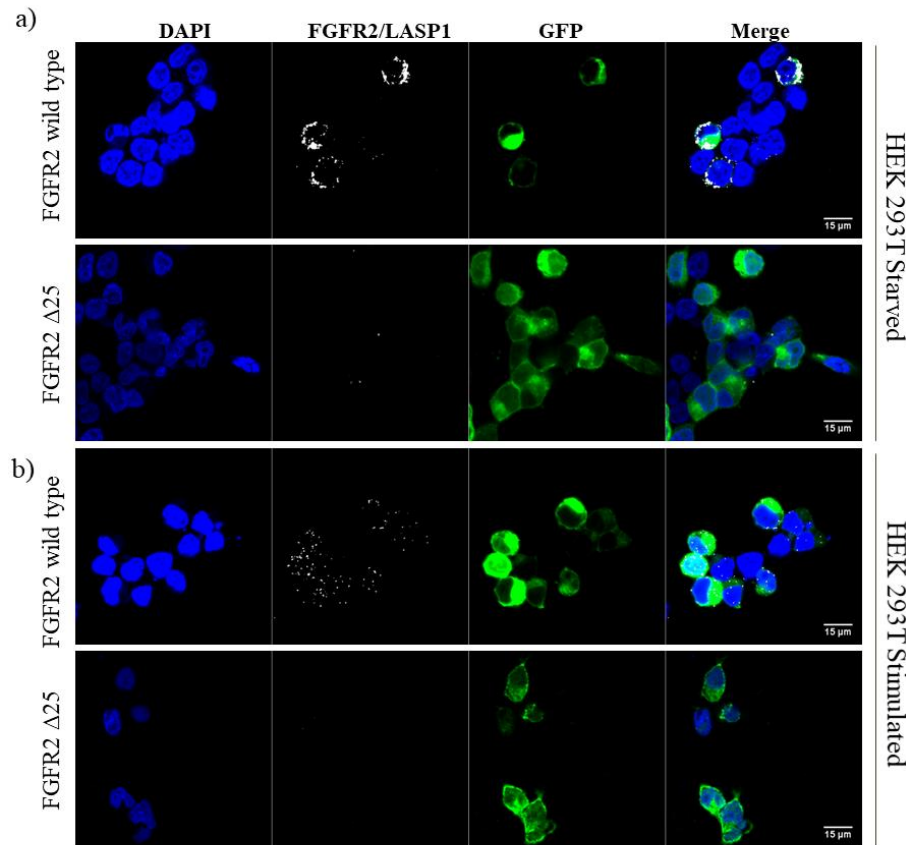


Figure 4-3 PLA demonstrated that FGFR2 and LASP1 interacts in HEK293T cells and that it is through the C-terminal tail

PLA shows that FGFR2 and LASP1 can interact in HEK293T cells transfected with FGFR2-GFP in both starved (a) and FBS stimulated cells (b). When cells are transfected with FGFR2 Δ25 the signal is lost suggesting that LASP1 interacts with FGFR2 in the C-terminal tail. This is true for both starved (a) and stimulated (b) cells. Analysis of signal per cell was performed using ImageJ and analyse particles (c) and a graphic representation of the difference between FGFR2 and FGFR2 Δ25 for starved (d) and FBS stimulated cells (e) is statistically significant. Serum (FBS) stimulation of cells was done for 15 minutes. DAPI was used to visualise the cell nucleus. Scale bar 15 μm. Mean values and standard errors are represented. Using standard t-test the statistically significant differences are indicated by * (P ≤ 0.05), ** (P ≤ 0.01) or *** (P ≤ 0.001).

4.1.2 Further characterisation of the FGFR2 and LASP1 interaction using MST and mutants

Most SH3 interactions with proline-rich motifs are weak and can therefore be difficult to discover. Having demonstrated the binding between LASP1 and FGFR2 in cells it was of interest to determine how strong the affinity is. Towards this, MST studies were used to determine binding affinities *in vitro*. LASP1 was labelled with Atto488 at the N-terminal amine. Unlabelled FGFR2 C58 was titrated from 1 mM to 30 nM. A binding curve was obtained (Figure 4.5 a) and a K_D was determined to be $37.2 \pm 4.7 \mu\text{M}$. This is a similar affinity to that seen for PLC γ 1 binding FGFR2 proline-rich motif, which is $40 \mu\text{M}$ (Timsah et al., 2014). Initially an experiment using labelled LASP1 Δ SH3 and C58 gave a binding curve showing no binding (Figure 4.5 b, left), suggesting that the interaction is through the SH3 domain from LASP1. However the concentration of C58 was from $125 \mu\text{M}$ to 1.9 nM , lower when compared to LASP1 WT, suggesting that the concentration was not high enough to be able to determine the K_D . The experiment was repeated using C58 at a concentration range from 1 mM as highest concentration which gave a binding curve and a K_D between C58 and LASP1 Δ SH3 was determined to $62.2 \pm 4.8 \mu\text{M}$ (Figure 4.5 b, right). Together these data suggest that LASP1 interacts with the C-terminal tail of FGFR2, irrespective of the SH3 domain. Further investigations of the interaction focused on which parts of C58 interact with LASP1. Constructs of C58 where prolines were mutated to alanines and deletion constructs of C58 were utilised (Figure 4.4, see Appendix C for full amino acid sequences). The prolines were mutated to alanines individually and included prolines that were already established as interaction partners of GRB2 and PLC γ 1 (P810 and P813). Additionally, P800, P802, P804 and P807 were also included in the analysis (Figure 4.5 c-h). In some cases mutating individual prolines

(P802, P804 and P813) increased the affinity of the C58 – LASP1 interaction (see Table 11). Mutating P800 and P807 decreased the binding affinity. The binding affinities obtained from MST for the point mutated C58 constructs and LASP1 interaction vary over two orders of magnitude, ranging from ~1-100 μM . One proline, P810, seemed to be particularly important for the C58 interaction as no K_D could be obtained for this particular alanine mutant. Comparing the graph for P810A shows a similar binding curve to, for example P807A and P800A, suggesting that some optimisation such as increasing the C58 concentration could potentially produce a graph where K_D can be determined. Deletion mutants of C58, six in total, between the final 3 amino acids of C58 and the final 23 amino acids ($\Delta 3$, $\Delta 6$, $\Delta 9$, $\Delta 12$, $\Delta 15$ and $\Delta 23$) were employed in order to further investigate which region of C58 interacts with LASP1 (Figure 4.5 i-n). Deleting the 6 last amino acids from C58 increased the affinity for LASP1 as both C58 $\Delta 3$ and $\Delta 6$ with LASP1 produced a binding curve giving a K_D of ~1 μM and 234 nM respectively (Table 11). The more amino acids removed the lower the C58 affinity to LASP1 becomes, from 149 and 117 μM for $\Delta 9$ and $\Delta 15$ respectively, to no binding curve for $\Delta 12$ and $\Delta 23$. This does to some extent follow the binding affinities from the point mutations, as $\Delta 12$, $\Delta 15$ and $\Delta 23$ has had P810 removed.

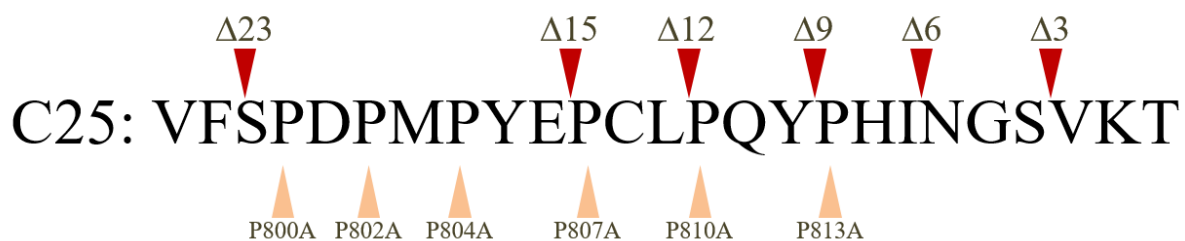


Figure 4-4 Mutations in the C58 construct. The last 25 amino acids are used here to highlight the different deletion mutants and point mutations used in the MST experiments.

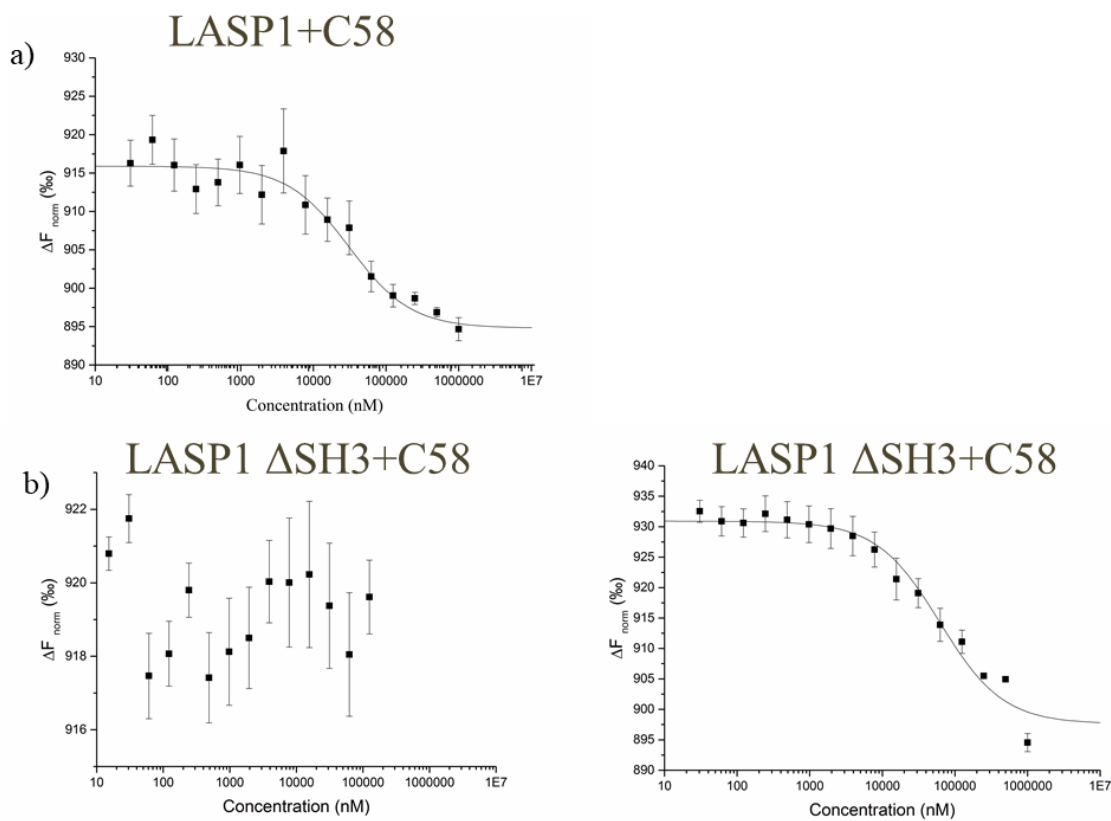


Figure 4-5 Binding affinities determined by MST

a) Labelled LASP1 was at a constant concentration of 100 nM while C58 was titrated into the capillaries at starting concentration 1 mM. K_D was determined to be 37.2 μM . b) C58 was titrated into labelled LASP1 Δ SH3 at 100 nM. Two different experiments were run with variable starting concentrations for C58. The first shows no binding curve when the highest C58 concentration was 125 μM . A repeat experiment increasing the highest C58 concentration to 1 mM gave a K_D of 62.2 μM . **Next page:** c-h) Constructs with point mutations changing prolines to alanines in C58 were expressed and purified for MST, and titrated into labelled LASP1 at fixed concentration of 100 nM. K_D for LASP1 and C58 P800A were determined to be 126 μM (c), C58 P802A was 4.3 μM (d), C58 P804A was 11.7 μM (e), C58 P807A was 108 μM (f), No K_D could be measured for LASP1 and C58 P810A (g) and finally LASP1 and C58 P813A had a K_D determined to be 1.35 μM . i-n) Constructs of C58 having amino acids deleted from 3-23 final amino acids were expressed and purified for MST, and titrated into labelled LASP1 at fixed concentration of 100 nM. C58 Δ 3 and LASP1 produced a binding curve which gave a K_D of 1.05 μM (i), C58 Δ 6 and LASP1 produced a K_D at 0.234 μM (j), C58 Δ 9 and LASP1 K_D was determined to 149 μM (k), C58 Δ 12 and LASP1 did not produce a binding curve (l), C58 Δ 15 and LASP1 K_D was determined to 117 μM (m) and finally a binding curve for C58 Δ 23 and LASP1 could not be determined (n). All experiments was performed in HEPES buffer at pH 7.5

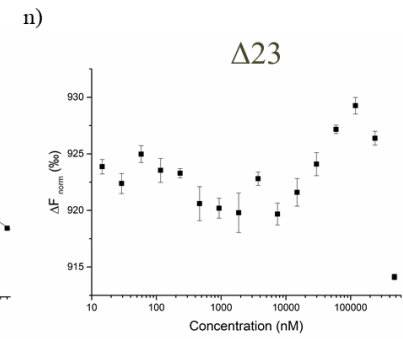
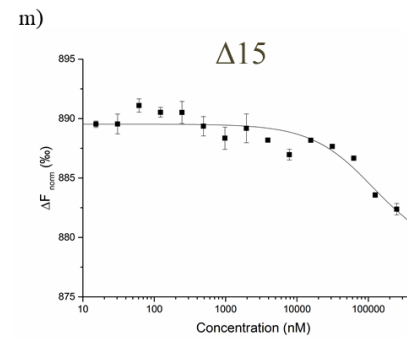
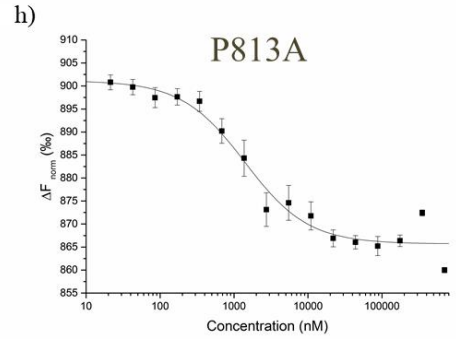
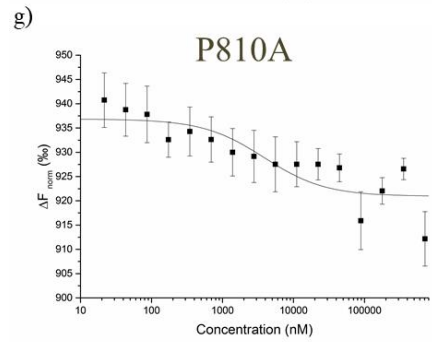
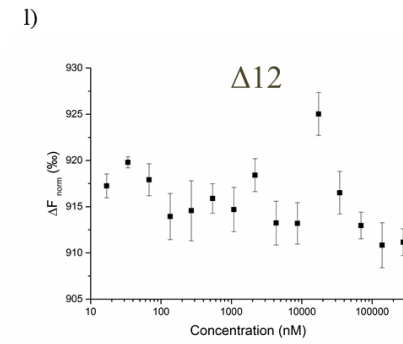
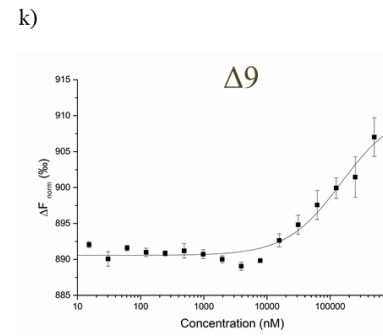
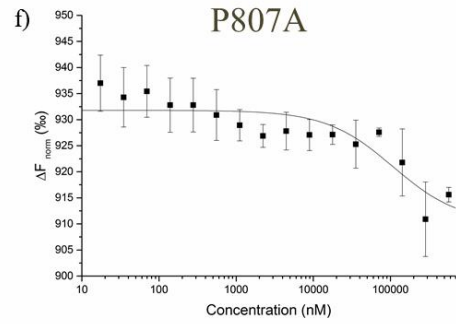
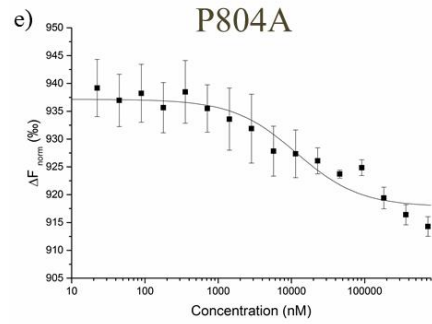
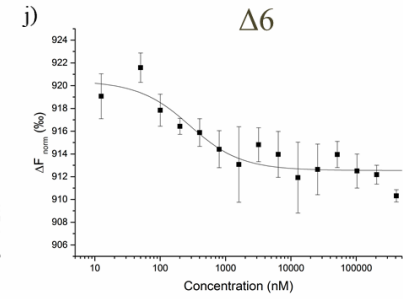
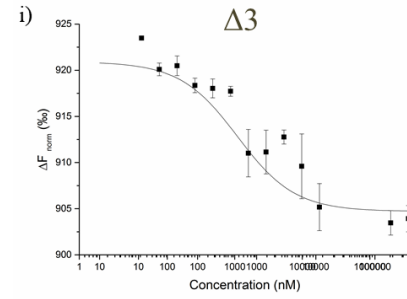
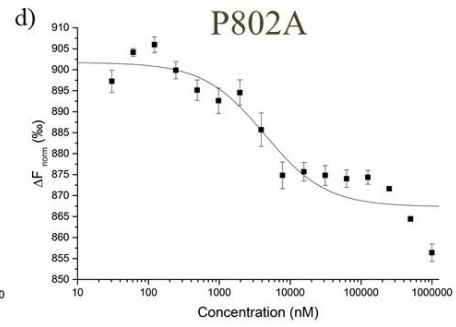
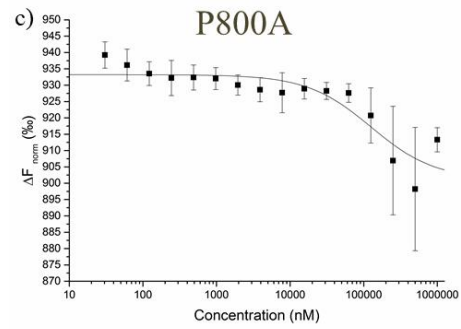


Table 11 MST binding affinities. Labelled proteins are listed first and always at a concentration of 100 nM

Protein	Binding affinity (μM)
LASP1 + C58	37.2 ± 4.7
LASP1 ΔSH3 + C58	62.2 ± 4.8
LASP1 + C58 P800A	126 ± 35.2
LASP1 + C58 P802A	4.3 ± 0.6
LASP1 + C58 P804A	11.7 ± 2.4
LASP1 + C58 P807A	108 ± 25
LASP1 + C58 P810A	-
LASP1 + C58 P813A	1.35 ± 0.1
LASP1 + C58 Δ3	1.05 ± 0.17
LASP1 + C58 Δ6	0.234 ± 0.05
LASP1 + C58 Δ9	149 ± 13.2
LASP1 + C58 Δ12	-
LASP1 + C58 Δ15	117 ± 8.6
LASP1 + C58 Δ23	-

4.1.3 Physiological relevance of the LASP1 and FGFR2 interaction

The data previously presented in this chapter established an interaction between LASP1 and the C-terminal tail of FGFR2, and demonstrated that this is not mediated by the LASP1 SH3 domain. No previous reports have shown this interaction.

Importantly, as both LASP1 and FGFR2 are considered oncoproteins it is vital to see what impact the interaction has in cells. While the interactions were previously demonstrated in HEK 293T cells, further work was carried out in HEK293 gRNA (gRNA) which had the *GRB2* gene removed by CRISPR/Cas9 technology (work by Amy Stainthorpe, University of Leeds). From the MST data it is likely that LASP1

binds to the same region of FGFR2 as GRB2, and GRB2 binding to FGFR2 could potentially disrupt LASP1 access to FGFR2. As a control, HEK293 scrambled (scr) were used. These cells contain a scramble RNA construct with Cas9 to ensure that any cellular changes seen in gRNA are not from the CRISPR/Cas9 process (work by Amy Stainthorpe, University of Leeds). In addition to the two HEK293 cell lines, HeLa cells were used as a more relevant to disease cell line. All three cell lines were co-transfected with either RFP/FGFR2, GFP/LASP1 or LASP1/FGFR2. It has also been established that the interaction between the FGFR2 C-terminal tail and LASP1 happens irrespective of receptor activation so cells were not starved before any of the further analysis. Changes in key components of the cell cycle were analysed by western blot (Figure 4.6 a). For both gRNA and scr no apparent changes could be detected in expression of Cyclin B1 and E1 when FGFR2 and LASP1 were expressed on their own compared to co-expression, suggesting that the FGFR2/LASP1 interaction has no impact on these particular components of the cell cycle machinery. Cyclin B1 expression increases when the cells go from the G₂-Phase to Mitosis. Cyclin E1 expression begins at the end of the G₁-Phase and carries on into S-Phase. In HeLa cells, Cyclin B1 seems to decrease with LASP1 expression, while Cyclin E1 goes up, as quantified by ImageJ (Figure 4.6 b-c). This suggests that LASP1 could potentially affect the cell cycle and drive the cells into S-Phase, but this is independent on the interaction with FGFR2. Cyclin D1 is required for the progression into G₁-Phase and it is degraded in S-Phase. No Cyclin D1 was detected for any of the cells. Further western blot analysis shows the expected difference in GRB2 expression for gRNA compared to scr and HeLa cells. As these cells are grown under serum containing conditions FGFR2 is activated. FRS2 can then bind to a phosphorylated tyrosine on the receptor, SOS and GRB2 are recruited

to form a complex which can activate MAPK pathway. In gRNA cells no GRB2 expression is detected and consequently phosphorylated ERK (pERK, p42/44) as a readout of activation of the MAPK pathway is not detected in gRNA cells.

Interestingly in scr cells co-transfected with FGFR2 and LASP1 pERK was higher compared to FGFR2 or LASP1 on their own, as quantified by ImageJ (Figure 4.6 d).

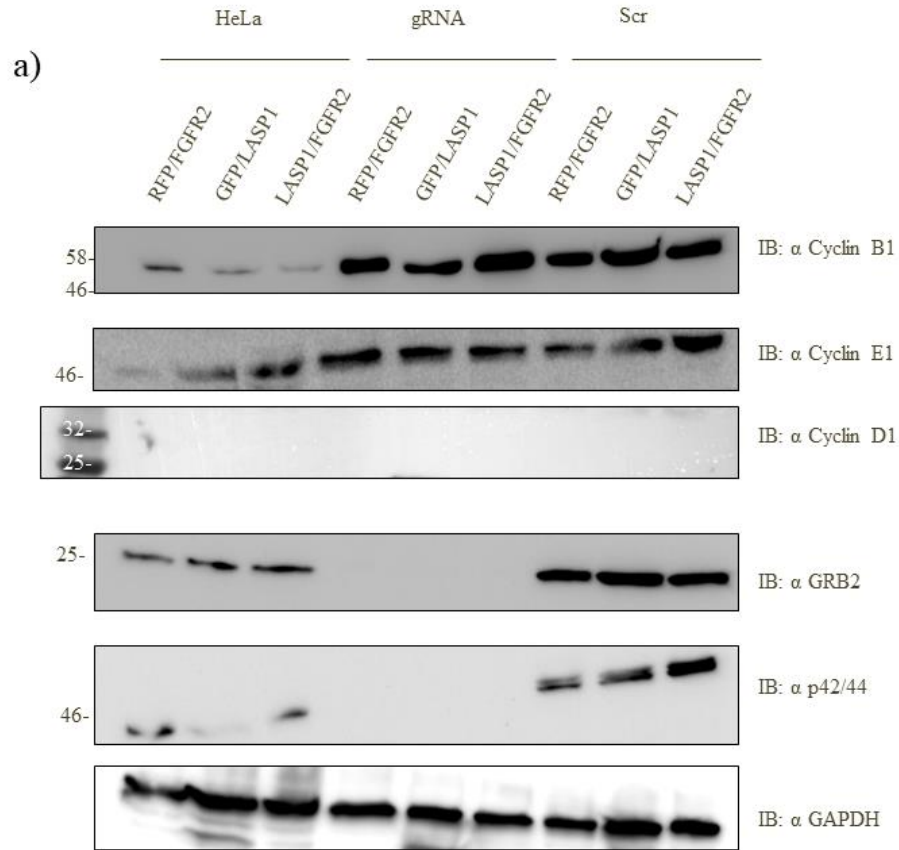
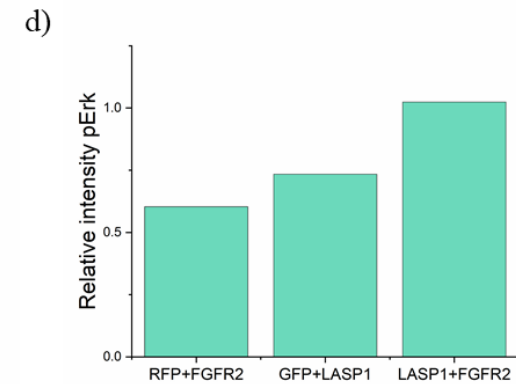
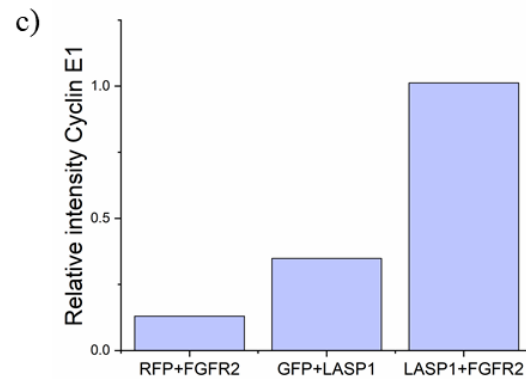
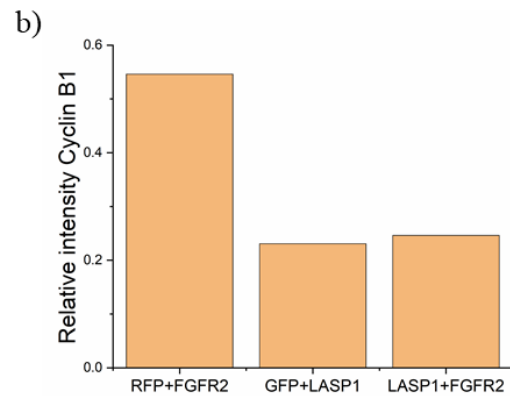


Figure 4-6 Western blot analysis of protein changes under LASP1 and FGFR2 overexpression

a) Western blot analysis was performed to establish expression in the three cell lines used. HeLa, HEK 293 gRNA and HEK 293 Scr was transfected with RFP and FGFR2, GFP and LASP1 and finally LASP1 and FGFR2. Expression of Cyclins B1, E1 and D1, GRB2 and pERK was evaluated. GAPDH was used as loading control. b) Quantification of Cyclin B1 expression in HeLa. c) Quantification of Cyclin E1 in HeLa. d) Quantification of pErk in scr.



To assess cells survival and proliferative capacity a number of techniques can be used. Commonly used are colony formation assay and soft agar assay. Soft agar assays are anchorage independent. A low number of cells were seeded into agar containing medium. When the agar was set the plates were left with feeding medium and growth was monitored until colonies were visible (Figure 4.7 a). Colonies were counted for each treatment and a graphic representation shows that in scr and HeLa cells anchorage dependent growth increases when LASP1 is transfected, and when FGFR2 is co-transfected with LASP1 growth further increases (Figure 4.7 b). For gRNA growth is increased when FGFR2 is transfected on its own. Co-transfection with LASP1 decreases growth compared to FGFR2 on its own. To look at anchorage-dependent growth, colony formation assay was performed. A low number of cells were seeded directly to plates and growth was monitored until colonies were visible. Colonies were then visualised using crystal violet solution (Figure 4.7 c), counted and graphically represented (Figure 4.7 d). gRNA cells show similar anchorage dependent and independent growth. FGFR2 promotes more growth than LASP1, and when LASP1 is co-transfected with FGFR2 growth decreases. Moderate growth differences are seen for transfected scr in the colony formation assay. Colonies formed by transfected HeLa cells shows similarities with the soft agar assay, LASP1 on its own increases growth and expression of both LASP1 and FGFR2 further increases growth.

LASP1 is thought to have a structural role in cytoskeletal organisation and stabilisation of the actin network. LASP1 can interact with filamentous actin via the nebulin repeats, and are also found accumulated in focal adhesions (Schreiber et al., 1998; Chew, 2002). Both filamentous actin and focal adhesions plays a central role

in cell migration, so it would be interesting to elucidate whether the interaction between FGFR2 and LASP1 has an impact on cell migration. gRNA and scr cells were transfected with RFP/FGFR2, GFP/LASP1 or LASP1/FGFR2. A scratch wound was generated and cells were imaged at 0h and 24h (Figure 4.8). For both gRNA and scr it appears that when LASP1 is transfected on its own cells migrate further compared to FGFR2 on its own. However when both FGFR2 and LASP1 are overexpressed together the cells migrate less compared to LASP1 on its own, and this is comparable to cell migration affected by FGFR2 on its own.

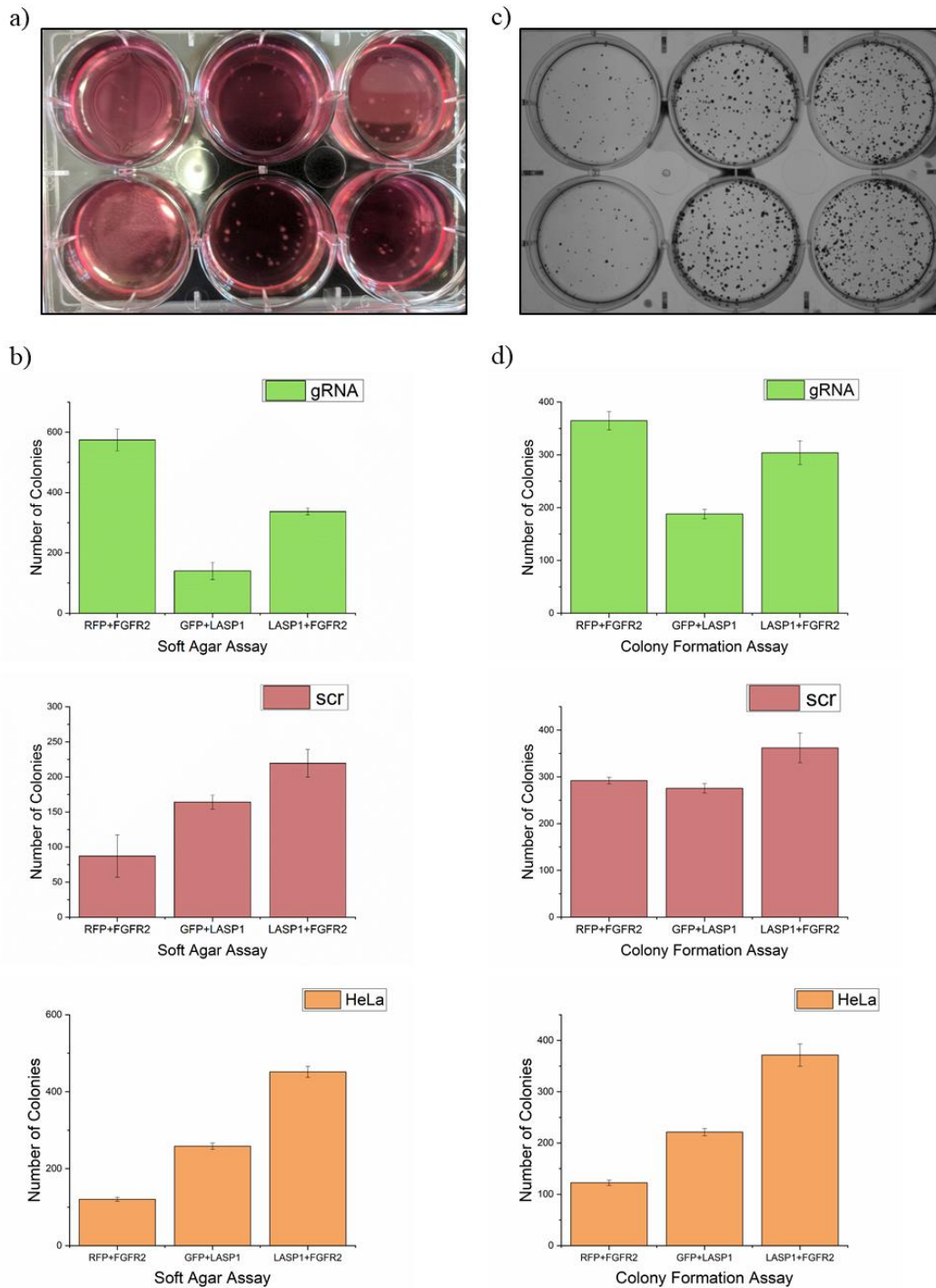


Figure 4-7. Growth assays for FGFR2 and LASP1 interaction

a) Soft agar assay was used to determine anchorage independent growth of cells, this is an example of what to expect to see after 2-3 weeks of growth. b) Graphical representation of transfected cells growing in a soft agar plate. N=3 for each transfection. c) Colony formation assay was used to determine growth in an anchorage dependent way. Crystal violet was used to visualise colonies. d) Graphical representation of colonies counted for cells that were transfected and seeded for colony formation assay. N=3 for each transfection.

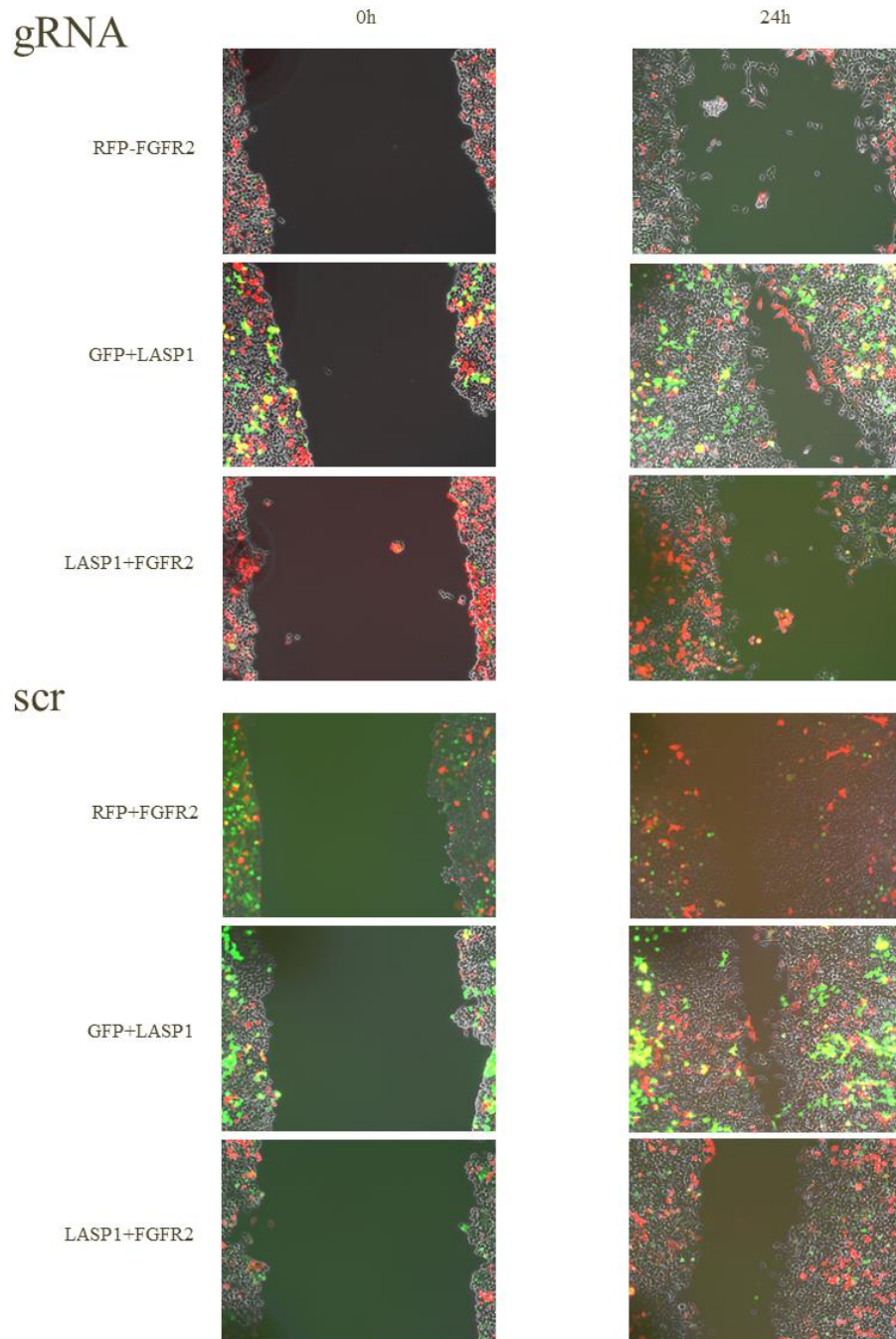


Figure 4-8 Migration assay for LASP1 and FGFR2 interaction.

gRNA and scr cells were transfected with RFP/FGFR2, GFP/LASP1 or LASP1/FGFR2. At 100% confluency a scratch wound was produced and cells were imaged at 0h and 24h to track cell migration.

4.1.4 Discussion

Several experiments have been performed to show that FGFR2 and LASP1 interact. GST-pull downs and PLA showed that this interaction is mediated by the C-terminal tail of FGFR2. Some evidence suggests that in cells it is the SH3 domain of LASP1 that interacts with FGFR2, although *in vitro* assays using MST demonstrate lower dependence on the SH3 domain. Data from MST suggests that both wild type and Δ SH3 mutant interact with FGFR2 with similar affinities at $\sim 40 \mu\text{M}$ and $\sim 60 \mu\text{M}$, suggesting that there is a different region of LASP1 that interacts with the C-terminal tail of FGFR2. It would be interesting to see whether the LASP1 Δ LIM mutant could increase affinity compared to wild type as in the GST-pull down more FGFR2 was pulled down with this mutant. Unfortunately, after purification the protein was not stable being suspended in MST buffer for long enough to carry out the experiment. Many proteins have been shown to interact with LASP1 in the cell (Orth et al., 2014). This includes filamentous actin which interacts with the nebulin repeats, and the chemokine receptor CXCR2 which interacts with the LASP1 LIM domain. Removing the SH3 domain could mean easier access for other binding partners of other domains in LASP1, and with a higher affinity compared to FGFR2. For example would removing the SH3 domain mean easier access to the filamentous actin network, and in this way affect cell motility? In a GST-pull down these interacting partners could preferably bind LASP1 Δ SH3 instead of FGFR2. Interestingly the LASP1/FGFR2 interaction occurs irrespectively of the cells being starved or serum stimulated.

Further characterisation of the interaction focused on the C-terminal tail of FGFR2. Point mutations of prolines and deletion mutants of C58 were used in MST with labelled LASP1 to determine binding curves. Several of the point mutations

increased the affinity of the interaction. Proline has a distinctive structure compared to other amino acids and are often found in turns, a protein secondary structure. By mutating prolines to alanines in C58 the peptide might be found in a different secondary conformation that favours binding to LASP1. Consequently when prolines in other positions of the peptide are mutated the change in conformation can reduce affinity. In the case of P810A the K_D could not be determined, although the graph forms a shape similar to sigmoidal, and it is possible that with optimisation a binding curve can be formed. Deleting the 6 final amino acids of the C58 peptide increased affinity. The length of the peptide could potentially have a role in the interaction, and a shorter peptide can in some cases decrease affinity. Deleting a range from 9-23 amino acids in C58 reduces affinity and in some cases abolishes the peptides ability to interact. This does follow to some degree what was seen with the point mutations as P810 was deemed to be important for binding and deletion mutant $\Delta 12$, $\Delta 15$ and $\Delta 23$ does not include this particular proline. Some buffer optimisation could also be carried out to expand on what effect pH and buffer composition has on binding. HEPES was used in all the MST experiments, and the chemical structure of HEPES show some similarity to prolines, would this have an impact on the mutants interacting with LASP1. Conclusively this data supports that C58 interacts with LASP1, and P810 is important in this interaction. Using a mammalian plasmid containing FGFR2 with the P810A mutation could be used to further investigate the interaction in cells, and if the mutation is also important in a cellular environment. Further investigations were performed to look at what effect the interaction has in cells. MST data suggests that LASP1 binds FGFR2 in the same region as GRB2, so experiments were also undertaken in cells where the *GRB2* gene had been removed by CRISPR/Cas9. A control cell line expressing a scramble guide RNA in

CRISPR/Cas9 was used to ensure that any effects seen were not as a result of the CRISPR/Cas9 methodology. Additionally HeLa cells were utilised as a cell line with relevance to cancer. While establishing the interaction is important, determining whether it has any physiological relevance in cells, especially cancerous cells as both LASP1 and FGFR2 are oncoproteins. As the interaction between FGFR2 and LASP1 has not been established in HeLa cells, caution must be taken concluding anything from cell cycle and growth results in HeLa cells. Different cyclins are expressed at various stages of the cell cycle and the analysis of expression of the different cyclins is a suitable method for determining cell cycle progression (K. A. Schafer, 1998). Certain treatments and proteins can trap the cells in a specific phase of the cell cycle. In HeLa cells Cyclin B1 expression was reduced when LASP1 was overexpressed while Cyclin E1 expression was increased, suggesting that overexpression of LASP1 potentially can keep HeLa cells in a G₁/S-Phase. This is independent of FGFR2 expression. Further work needs to be carried out to elucidate what impact LASP1 and FGFR2 have on the cell cycle, such as knocking down LASP1 and/or FGFR2 expression.

In both anchorage dependent and independent colony formation assays expression of LASP1 increased growth. FGFR2 co-expression with LASP1 seemed to have more impact on cell growth compared to LASP1 alone. One can only speculate whether this is linked to a possible FGFR2 interaction with LASP1 at this stage. In gRNA and scr no apparent difference in any of the cyclins were detected. More interestingly in the presence of GRB2 a difference in pERK was detected when LASP1 and FGFR2 were co-overexpressed. LASP1 has been shown to have a role in MAPK signalling before. miR-133a has been shown to target and suppress LASP1 expression. miR-133a also inactivates MAPK pathway by dephosphorylation of ERK.

This suggests a potential role for LASP1 in the MAPK pathway where overexpression of LASP1 causes miR-133a to suppress LASP1 translation rather than MAPK pathway inactivation (Xu et al., 2014). So whether the increase in pERK is from overexpressing two proteins known to be involved in the MAPK pathway individually or if it is a result of an interaction is not clear at this point. Expression of LASP1 and FGFR2 either individually or together had different impacts on growth, and whether GRB2 is expressed or not. In gRNA cells LASP1 expression reduced growth in both anchorage dependent and independent assays. FGFR2 growth is also reduced when co-expressed with LASP1. In scr cells anchorage-independent growth increased with LASP1 expression and co-expression of LASP1 and FGFR2 further increased the growth. This effect could again originate from roles of FGFR2 and LASP1 that are independent of each other. Interestingly, no apparent difference was seen in anchorage-dependent growth. Taken together it suggests that when GRB2 is absent LASP1 suppress growth, but this is not necessarily dependent on an interaction with FGFR2 as growth increases when LASP1 and FGFR2 are both overexpressed. Scratch wound healing assays demonstrated that when LASP1 was expressed cells migrated further compared to when FGFR2 is overexpressed alone or with LASP1. This is independent of GRB2 expression. It is possible that the LASP1 interaction with FGFR2 C-terminal tail might be inhibitory of LASP1 impact on cell migration. Taken together there is evidence that LASP1 interacts in the C-terminal tail of FGFR at an affinity of $\sim 40 \mu\text{M}$. Some data suggest that this interaction can potentially have an impact on growth and migration, but further work would need to be carried out in order to establish specifically what these events are.

Chapter 5: ErbB2 and SRC interact in starved conditions in a breast cancer cell line

The “second tier” RTK regulation has been demonstrated with FGFR2. The possibility that this regulation can be found across RTKs remains to be answered. Demonstrating that other RTKs can interact with and be regulated by SH3 domains in proteins would add value to what would be a paradigm shift in RTK signalling biology. In this chapter the results demonstrates an interaction between ErbB2 and SRC, and some data indicates that this is through the SRC SH3 domain and ErbB2 proline rich motif.

The C-terminal tail of ErbB2 is rich in proline residues (Figure 5.1 a), and several of them in the typical canonical proline rich motif PXXP (underlined). Previous published reports demonstrated that a proline-rich motif from ErbB2 bound directly to the SH3 domain from the SRC family non-receptor kinase FYN (Bornet et al., 2014). In this chapter an investigation of the interaction of the proline-rich motif of this receptor with the proto oncogene SRC was carried out. A sequence alignment of the SH3 domains from FYN and SRC shows a 76% sequence homology (Figure 5.1 b). The residues marked in green for FYN SH3 were found to be important in the ErbB2 proline-rich motif interaction from the Bornet paper, and the residues marked in orange for SRC SH3 domain are the ones that differ from the FYN residues. SRC kinases consist of an SH2, SH3 and a kinase domain (Figure 5.1 c). At the N-terminal end there is a myristoylation site (Myr) allowing SRC to be associated with the cell membrane. There is a proline-rich motif in the linker region between the SH2 domain and kinase domain which interacts with the SH3 domain when SRC is in its inactive form. Prior to this research a screen of SH3 domains from a broad range of

proteins was performed to determine whether any were ligands for a selected proline-rich sequence from ErbB2. A preliminary screen used to identify proteins with SH3 domains which interact with a peptide corresponding to the proline-rich sequence from ErbB2 has been carried out (Figure 5.1 d) (screen performed by Prof. M. Bedford (MD Anderson Cancer Centre), unpublished). A glass slide with 40 SH3 domains from different proteins immobilized in discrete spots on its surface was incubated with a two peptides peptide containing proline-rich motifs from ErbB2 fused to a green fluorescent protein tag. The cognate SH3 domain can be identified from the position of the spot. Several proteins containing SH3 domains directly interact with the ErbB2 peptide. These preliminary data shows that the proline-rich sequence from the ErbB2 interacts with several members of the SRC family of kinases including LYN, YES and FYN (Figure 5.1 d, circles). The intensity showed that they were part of the top hits for the ErbB2 proline-rich peptides in this particular screen (Chapter 4, Table 8). This screen further supports the previously reported interaction between the proline-rich motif on ErbB2 and FYN and suggests that investigation of interactions between the SH3 domains of other SRC family kinases could prevail. Indeed alignment of the SH3 domain from FYN and SRC show 76% sequence identity (Figure 5.1 b). The preliminary screens and published data suggest that several of the Src family members interact with ErbB2 via the SH3 domain, but does not provide evidence for an endogenous interaction. Additionally there is some evidence suggesting that the SRC family kinase SRC interacts with ErbB2 in breast cancer cell lines, but this interaction was not detected in the breast cancer cell line SkBr3. Preliminary results suggest a role for SRC family kinase SH3 domains and proline-rich motifs from ErbB2. These are weak interactions and would not necessarily been picked up by previous studies looking at SRC interaction with

ErbB2. The following chapter investigates the interaction between ErbB2 and the SRC family kinase, SRC and whether it interacts endogenously in SkBr3 cells and if it is via the SH3 domain and proline-rich motif.

a)

ErbB2 C-terminal tail:

VIQNEDLGPASPLDSTFYRSLL~~EDDD~~MGDLVDAEEYLVPQQGFFCPDPAPGAGGMV
 HHRHRSSSTRSGGGDLTLGLEPSEEEAPRSPLAPSEGAGSDVFDGDLGMGAAKGL
 QSLPTHDPSPLQRYSEDPTVPLSETDGYVAPLTCSPQPEYVNQPDVRPQPPSPRE
 GPLPAARPAGATLERPKTLSPGKNGVVKDVFAGGAVENPEYLTPQGGAAPQPHPP
PAFSPAFDNLYYWDQDPPERGAPPSTFKGTPTAENPEYLGLDVPV

b)

FYN GVTLFVALYDYEARTEDDL~~S~~FHKGEKFQILNSSEGDWWEARSLTTGETGYIPSNYVAP
 SRC GVTTFVALYDYESRTEIDL~~S~~FKKGERLQIVNNT~~E~~GDWWLAHSLSTGQTGYIPSNYVAP

c)



d)

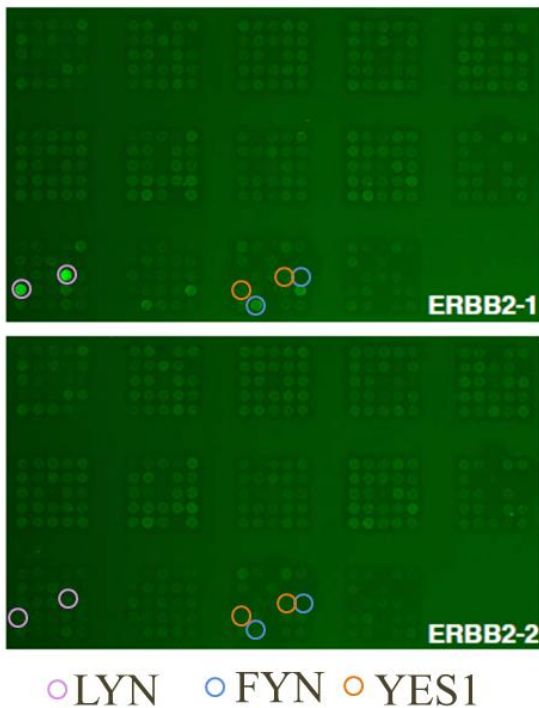


Figure 5-1 ErbB2 proline-rich motifs and Src/Fyn homology

a) ErbB2 C-terminal tail contains 16% prolines (in red) and several proline-rich motifs (underlined). b) An amino acid alignment of the SH3 domain of FYN and SRC highlights the similarity. The residues important for FYN SH3 interaction with ErbB2 proline-rich peptide is highlighted in green and in orange is the residues that are different in the SH3 domain of SRC. c) SRC family kinases are structurally similar having an SH2 and SH3 domain, a kinase domain and a myristoylation site (Myr) in the unique region (U). d) A high throughput assay using proteins containing SH3 domains arrayed on a glass plate highlights how various SRC family kinases LYN, FYN and YES1 can interact with ErbB2 peptides demonstrated by fluorescence.

5.1.1 SRC and ErbB2 interact in the breast cancer cell line SkBr3 under starved conditions

To investigate whether SRC and ErbB2 interact endogenously, the cancer cell line SkBr3 was used. SkBr3 is a breast cancer cell line that overexpresses ErbB2. Initial work was carried out looking at ErbB2 expression in SkBr3 cells by immunofluorescence (Figure 5.2 a). Cells were fixed on a glass slide and incubated with an antibody specific for ErbB2, and then a secondary antibody which was conjugated with a fluorescent tag for visualisation by confocal microscopy. In cells that were starved for 12 hours ErbB2 are found in clusters at what appeared to be the plasma membrane. Despite ErbB2 being an orphan receptor, EGF enhances the accumulation of ErbB2 on the membrane of SkBr3 cells. ErbB2 is known to form heterodimers with EGFR (see Introduction Chapter). EGF is a known ligand for EGFR and on binding is known to promote a conformational change to the extracellular region of the receptor which is recognized by the ligand-free ErbB2. Stimulation of SkBr3 cells with EGF resulted in an increase in population of heterodimers consisting of EGFR and ErbB2. The reduction in the fluorescent signal suggests that this complex is subsequently internalised and degraded. In further experiments EGF was used along with serum stimulation to differentiate SRC and ErbB2 interaction under starved and stimulated conditions. To investigate whether SRC and ErbB2 interact endogenously, a co-immunoprecipitation using cell lysate from SkBr3 cells and antibodies against SRC was used. SRC co-precipitated with ErbB2 under starved and serum stimulated conditions, but not when cells are stimulated with EGF (Figure 5.2 b). However, the experiment revealed that ErbB2 is phosphorylated in starved conditions. As a result our data cannot confirm the SH3 domain-proline-rich motif because an interaction between the SH2 of SRC and a

pTyr on the receptor cannot be ruled out. It is interesting to speculate at this point whether recruitment of SRC via its SH3 domain could activate the SRC kinase domain through a conformational change similar to that experienced on binding of the SH2 domain (see Introduction Chapter). This could then be responsible for phosphorylation of pTyr on ErbB2. To further validate the interaction a PLA was performed in starved and stimulated SkBr3 cells. ErbB2 and SRC are shown to be in close proximity to each other under starved conditions, serum stimulation and EGF stimulation (Figure 5.3 a), suggesting an interaction between SRC and ErbB2. PLA signal was quantified and compared to control PLA images where no primary antibodies against SRC and ErbB2 were used (Figure 5.3 b).

Upon stimulation there is a possibility that the signal comes from a heterodimer between EGFR and ErbB2 as EGFR is a known interacting partner of SRC (McCarley et al., 2006). Additionally SRC can interact with pTyr on either receptor via the SH2 domain. To address this PLA was next performed in MCF7 cells that lack endogenous EGFR expression (Figure 5.4 a) Expression of ErbB2 was also lower compared to SkBr3 cells and hence the appearance of pTyr is reduced. PLA signal is maintained in both starved and EGF-stimulated conditions, suggesting that the interaction is not from a EGFR/ErbB2 heterocomplex or SH2/pTyr interaction (Figure 5.4 b). Together these data suggest an interaction between endogenously expressed SRC and ErbB2 in both the breast cancer cell lines SkBr3 and MCF7.

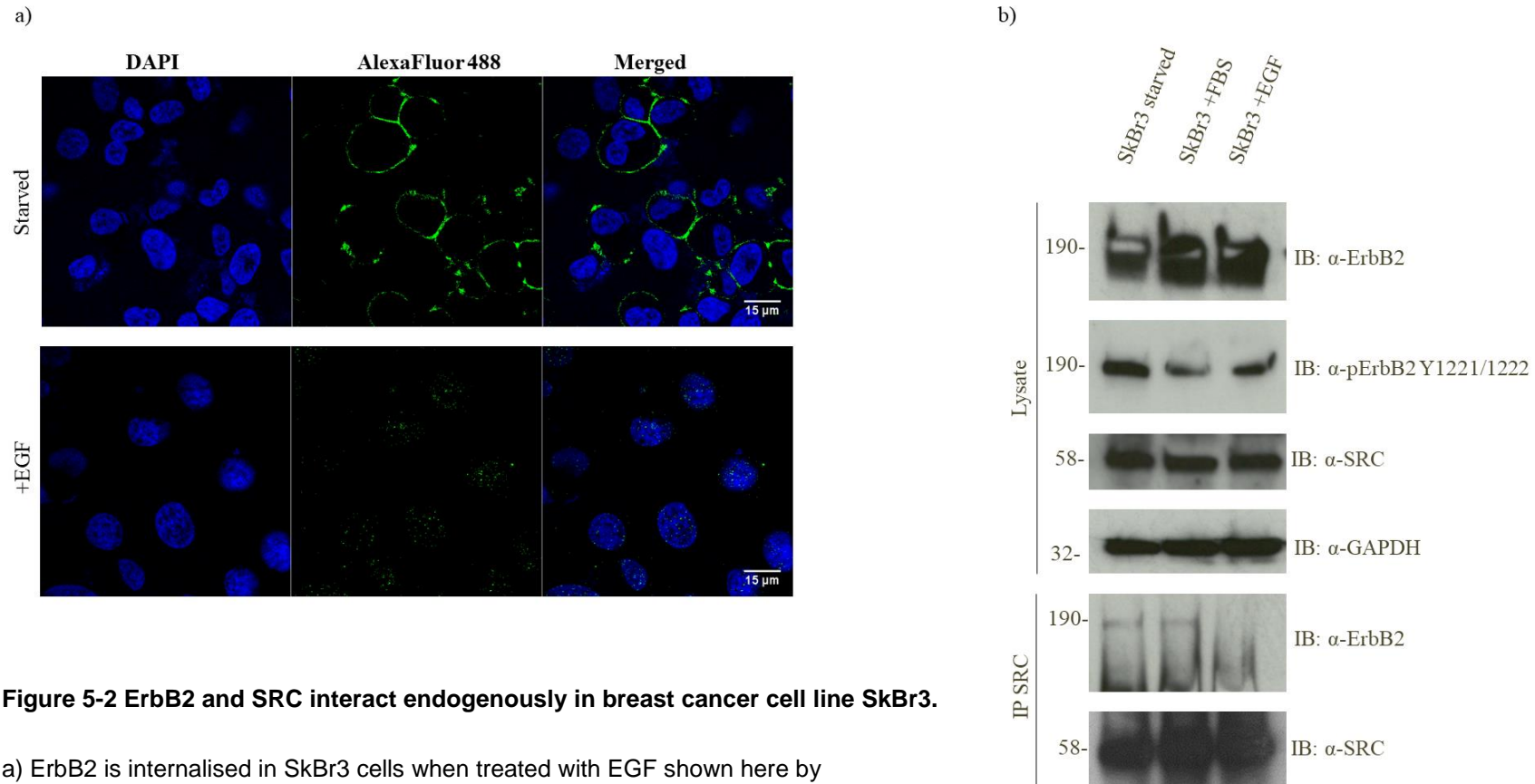


Figure 5-2 ErbB2 and SRC interact endogenously in breast cancer cell line SkBr3.

a) ErbB2 is internalised in SkBr3 cells when treated with EGF shown here by immunofluorescence. Using antibody specific for ErbB2 (1:100) shows that under starved conditions the receptor remains at the cell membrane while upon stimulation it is internalised. DAPI was used to visualise the cell nucleus. Scale bar 15 μ m.

b) Co-immunoprecipitation was performed using antibody specific for SRC, and SRC is able to pull down ErbB2 in starved and serum stimulated conditions in SkBr3 cells, but not in EGF stimulated cells. Total protein concentration of cell lysate was determined to be 1 mg. SkBr3 cells were starved for 24 hour before stimulation. EGF stimulation of starved cells were done at 100 ng/mL for 5 minutes, and serum (FBS) stimulation was done for 15 minutes.

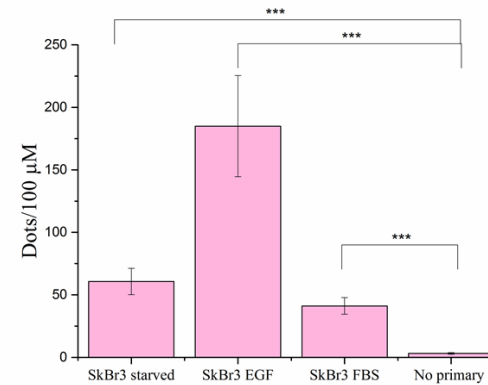
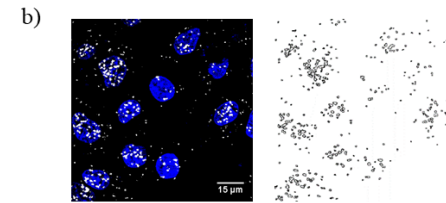
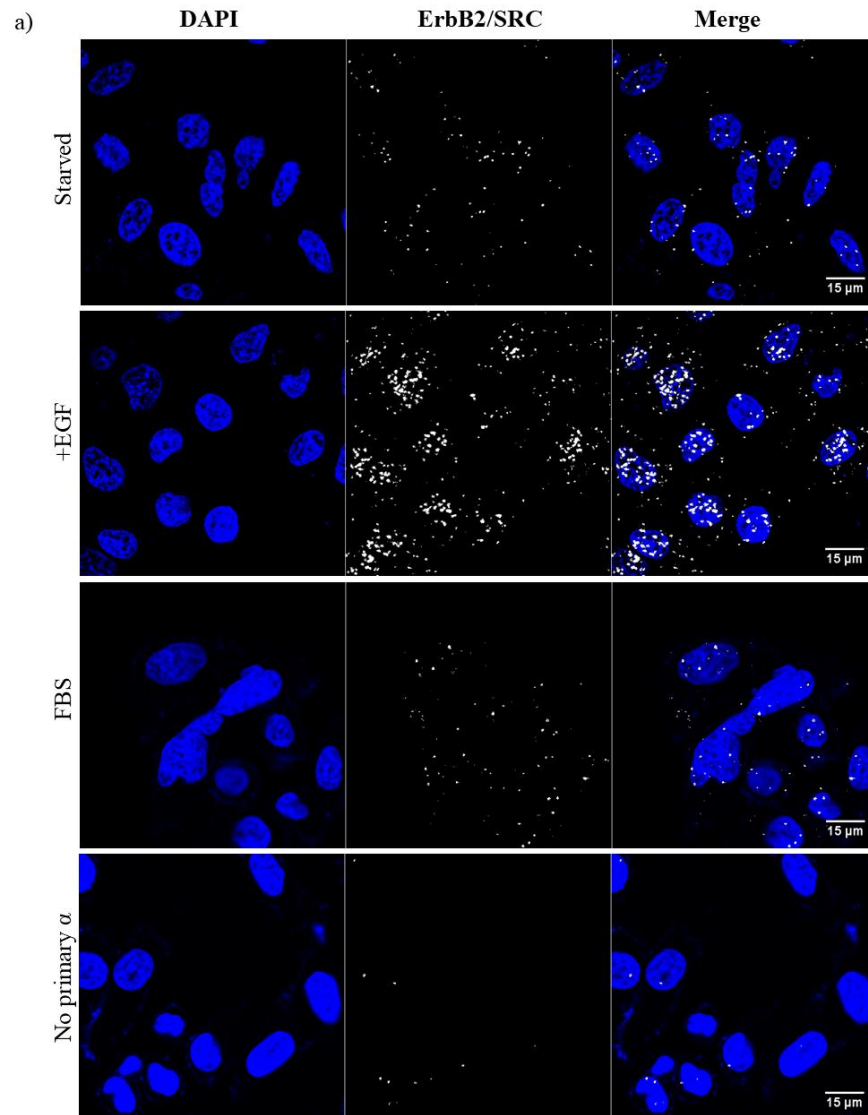


Figure 5-3 ErbB2 and SRC interact endogenously in breast cancer cell line SkBr3

a) Proximity ligation assay shows that ErbB2 and SRC interact endogenously in SkBr3 cells under starved conditions, EGF stimulation and serum stimulation. There is no signal when no primary antibodies for SRC and ErbB2 was used. Scale bar 15 μ m. b)

To determine the difference in PLA signal between starved, serum stimulated and EGF stimulated cells compared to signal from no primary antibody ImageJ was used to quantify the signal. Images with similar cell average per image was selected and PLA signal was quantified by using analyse particles. A minimum of 5 images per condition was used. All conditions shows a significant difference compared to the no primary antibody sample. Mean values and standard errors are represented. Using standard t-test the statistically significant differences are indicated by * (P \leq 0.05), ** (P \leq 0.01) or *** (P \leq 0.001). Scale bar 15 μ m.

DAPI was used for nucleus visualisation. SkBr3 cells were starved for 24 hour before stimulation. EGF stimulation of starved cells were done at 100 ng/mL for 5 minutes, and serum (FBS) stimulation was done for 15 minutes.

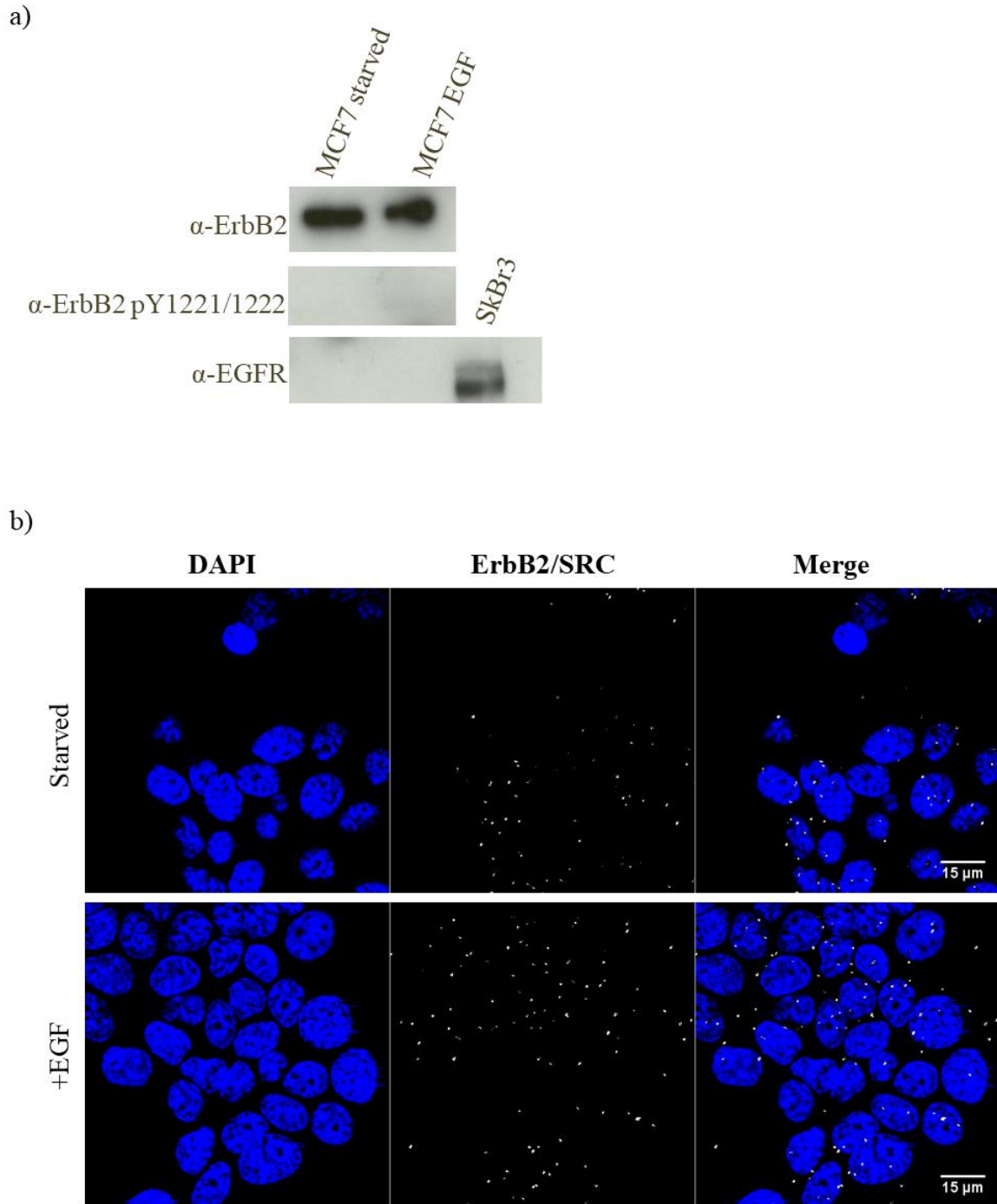


Figure 5-4 ErbB2 and SRC interact in absence of EGFR

a) Western blot comparing EGFR expression between MCF7 and SkBr3 cells, ErbB2 expression and tyrosine phosphorylation of Y1221/1222 in ErbB2. b) PLA signal between ErbB2 and SRC is maintained under starved and EGF stimulated conditions in MCF7. Scale bar 15 μ m. MCF7 cells were starved for 24 hour before stimulation. EGF stimulation of starved cells were done at 100 ng/mL for 5 minutes, and serum (FBS) stimulation was done for 15 minutes. DAPI was used to visualise cells.

5.1.2 ErbB2 interacts with the SH3 domain of SRC and FYN

The SH3 domains of SRC and FYN were expressed and purified from *E. coli* and used in a pull down with SkBr3 cell lysate. Both SH3 domains were able to pull down ErbB2 in serum stimulated conditions (Figure 5.5). These results confirm the interaction between FYN SH3 domain and ErbB2 from Bornet et al, but additionally demonstrates the interaction in a cellular lysate context (Bornet et al., 2014). SRC SH3 was also able to pull down ErbB2 from the lysates of serum starved cells. Stimulation of the receptor should presumably not have any impact on SH3 interacting with ErbB2, although these results demonstrates that the SRC SH3 domain pulls down 5-fold the amount of ErbB2 from lysates of stimulated cells compared to starved cells. This could potentially come from a complex formation around the SRC SH3 domain. In some cases phosphorylated tyrosines can strengthen an interaction between proline-rich motifs and SH3 domains. Based on the paper suggesting an interaction between FYN SH3 domain and ErbB2 peptide several tyrosines are involved in the interaction interface (Figure 5.1 b, (Bornet et al., 2014)). Additionally there is evidence that some RTKs C-terminal tail can bind itself in the kinase-domain when it is inactive (Lemmon and Schlessinger, 2010). If this is the case for ErbB2 activating the receptor might mean better access for SRC SH3 domain to interact when the cells are serum stimulated.

In the cell SRC switches between open and closed conformations (Figure 5.6 a).

Phosphorylation of Y530 allows the tyrosine to form an intramolecular interaction with the SH2 domain and the constrict the kinase is in its inactive form.

Dephosphorylation of Y530 causes a conformational change to an active state. This leads to a conformational change which opens up the structure making the kinase domain accessible resulting in auto-phosphorylation of Y416 in the active site, which

in turn increases SRC kinase activity (Xu, Wenqing, 1997; Xu et al., 1999). When SRC is in its open conformation, all of the domains – including the SH3 domain - are more easily accessible. Using a constitutively active and kinase dead form of the kinase SRC mutants were used to determine whether the specific conformation of SRC plays a role in mediating the interaction with ErbB2. Substitution of the tyrosine in the 530 position by phenylalanine prevents phosphorylation of the tyrosine making it permanently constitutively active SRC (Y530F). In addition the lysine residue in the 298 position was substituted by a methionine (K298M). Lysines are positively charged and essential for turnover of ATP by the kinase. Therefore, substitution with the neutral methionine renders the protein kinase dead. HEK 293T cells were transfected with ErbB2 and either FLAG epitope tagged wild type SRC, constitutively active SRC mutant (Y530F) or kinase-dead SRC (298M) (Figure 5.6 b). A FLAG-pull down using anti-FLAG beads was performed. In serum starved cells the constitutive active mutant, which should be conformationally open was able to pull down 3-fold the amount of ErbB2 relative to wild type and kinase dead SRC (Figure 5.6 c). This could potentially suggest that the receptor has easier access to binding with an open conformation SRC. In serum stimulated cells the kinase dead SRC mutant precipitated 2-fold less ErbB2 compared to either the wild type or constitutively active mutant, suggesting that phosphorylated Y416 could potentially have an impact on the interaction. It has been shown that auto-phosphorylation at Y416 reduces the ability of SRC to bind pTyr via its SH2 domain (Sun et al., 2001).

Overexpressing ErbB2 in cells causes receptor activation as evidenced by the pTyr and pErk blots in both starved and stimulated cells (Harari and Yarden, 2000). To overcome the problem of artificially overexpressing ErbB2 and subsequently activating the receptor, SkBr3 cells were used which endogenously express a lower

level of ErbB2. In these cells less pTyr was seen in the starved cells compared to stimulated cells (Figure 5.6 c). In starved SkBr3 cells wild type SRC was able to pull down 2-fold more the amount of ErbB2 compared to the mutants (Figure 5.6 e). In stimulated cells the kinase dead mutant was able to pull down 2-fold more ErbB2 relative to the wild type or Y530F mutant. Taken together the results from the flag pull down are inconclusive regarding the importance of SRC conformation and interaction with ErbB2. The different cell types might play a role, SkBr3 cells express more endogenous SRC compared to HEK293T which can compete for binding (Sam et al., 2007). In all the pull downs ErbB2 was pulled down to various levels further supporting an interaction between SRC and ErbB2. The phosphorylated state of ErbB2 throughout means that a pTyr/SH2 domain interaction cannot be ruled out in these experiments. Mutating the SH2 domain to prevent pTyr interaction would help elucidate whether the interaction is SH2 dependent. ErbB2 pTyr was still detected in cells that were transfected with the kinase dead SRC, suggesting that SRC is not responsible for phosphorylation of ErbB2.

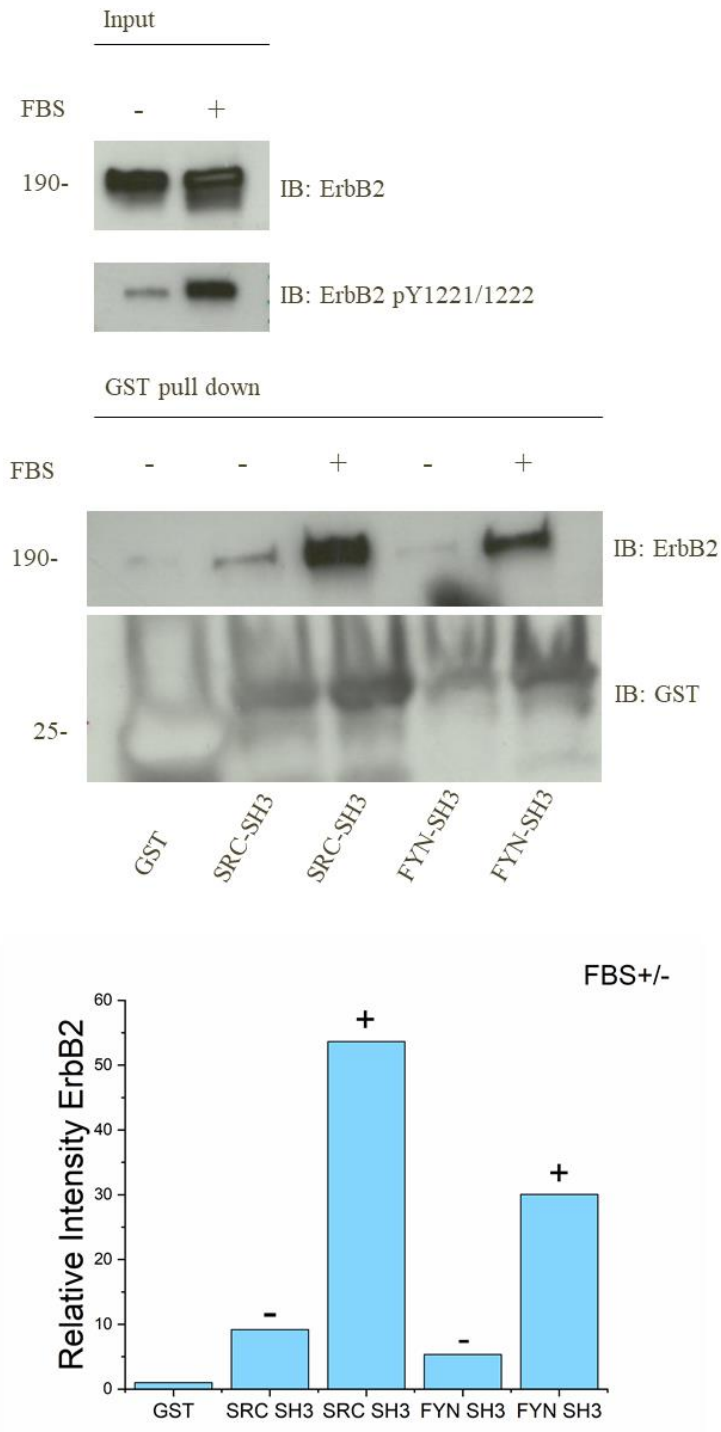


Figure 5-5 The SH3 domain of SRC is interacting with ErbB2.

A GST-pull down experiment using GST tagged SH3 domains of SRC and FYN can pull down ErbB2 in serum stimulated conditions. SRC SH3 domain can also pull down ErbB2 under starved conditions. SkBr3 cell lysate was used at 1 mg/ml.

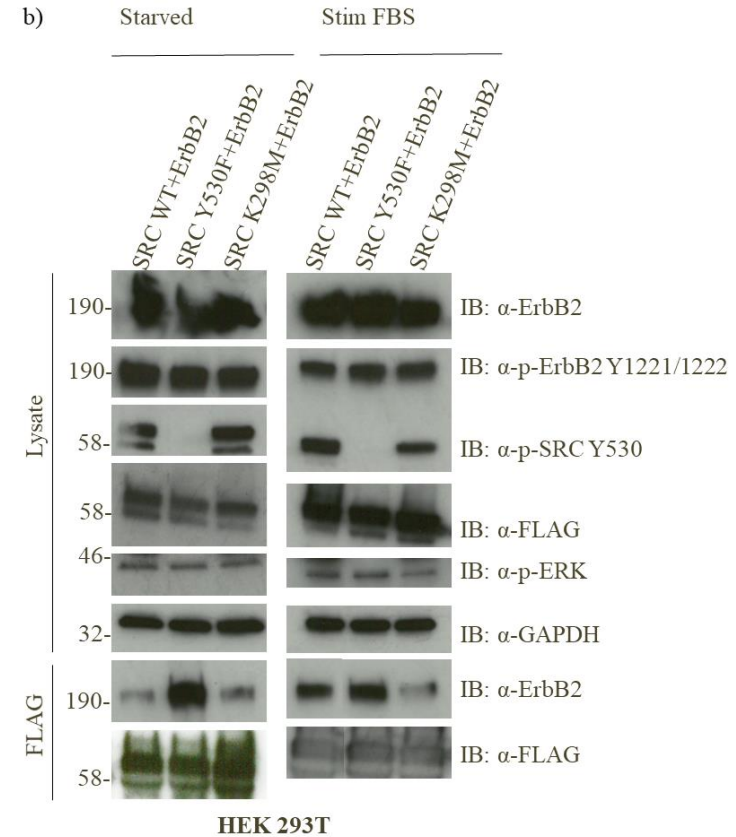
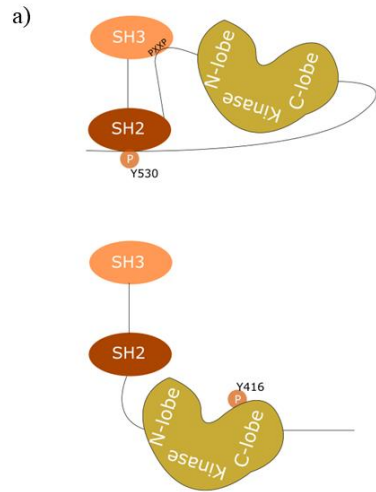
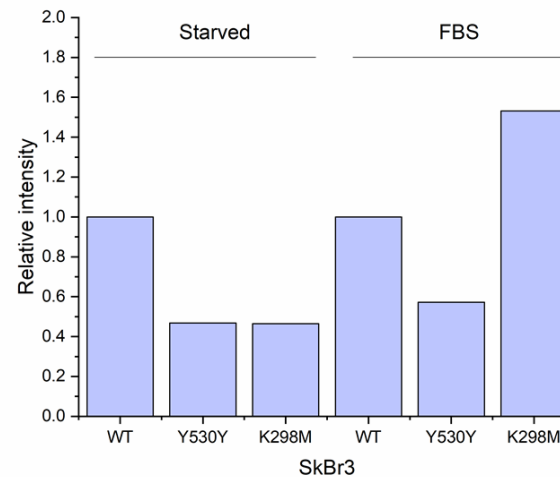
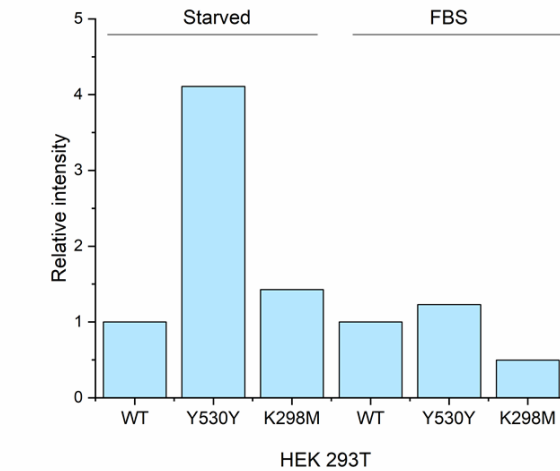
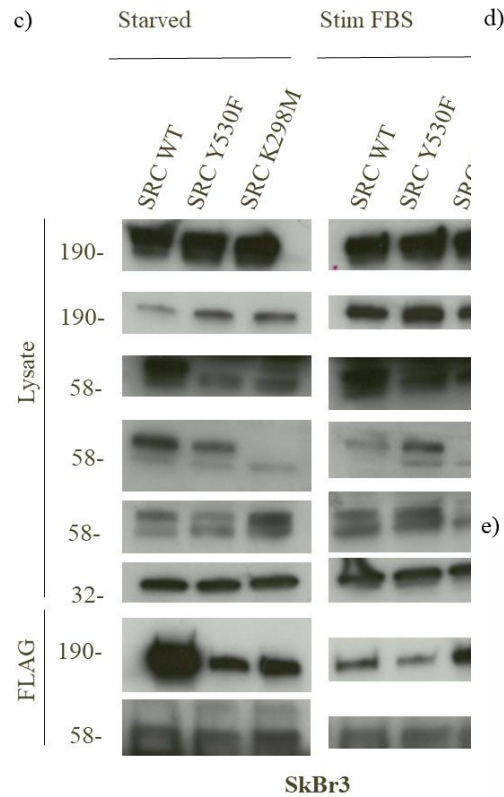


Figure 5-6 SRC interaction with ErbB2 could be dependent on SRC conformation.

a) SRC family kinases are found both in open and active conformation, and a closed inactive conformation in the cell. The conformation is determined by a deactivating phosphorylation of Tyr530. Auto-phosphorylation of Tyr416 renders a hyperactive enzyme. b) HEK293T cells were transfected with ErbB2 and either wild type SRC, SRC Y530F or SRC K298M. Cells were then serum-starved and then either taken forward to a FLAG-pull down or serum stimulated before used in a FLAG-pull down (cont)



c) SkBr3 cell were transfected with either wild type SRC, Y530F or K298M and serum-starved or serum-stimulated lysates was used in a FLAG-pull down. d) Relative intensity of ErbB2 being pulled down by wild type and mutant SRC in HEK293T. In cells that was starved the Y530F mutant was able to pull down 4-fold the amount of ErbB2 relative to wild type and K298M. In cells that had been stimulated with FBS both wild type and Y530F was able to pull down two-fold ErbB2 compared to K298M e) Relative intensity of ErbB2 being pulled down by wild type and mutant SRC in SkBr3. In starved SkBr3 wild type SRC was able to pull down two-fold more ErbB2 in a flag pull down than the mutants. In FBS stimulated cells the kinase dead mutant K298M was able to pull down 1.5-fold more ErbB2 relative to wild type SRC, and 2-fold the amount of ErbB2 compared to Y530F

5.1.3 A proline-rich motif in ErbB2 C-terminal tail interacts SRC

To further investigate the interaction between ErbB2 and SRC, cells that express lower levels of ErbB2 were used. HeLa cells express 27-fold lower levels of ErbB2 compared to SkBr3 cells and, as expected, a lower level of signal was detected in the PLA assay (Figure 5.7 a and b). ImageJ was used to quantify PLA signals in both SkBr3 and HeLa cells and the difference between them are shown. These data reveal a statistical difference between the different cell types in both starved and EGF stimulated cells (Figure 5.7 c). These results demonstrated that HeLa cells were useful for further studies of the interaction by transfecting in the ErbB2 receptor. To assess the interaction of the receptor with SRC, the proline-rich motif which has been shown to bind SRC family kinases was corrupted by three mutations, i.e. arginine in the 1146 position, proline 1149 and proline 1152 were mutated to alanine (R1146A/P1149A/P1152A). HeLa cells were then transfected with either GFP-tagged wild type ErbB2 or the triple mutant. PLA signal was observed in HeLa cells transfected with wild type ErbB2 in both starved and stimulated cells (Figure 5.7 d and e). Interestingly, in cells transfected with the triple mutant ErbB2 plasmid the PLA signal was not rescued in starved cells. Stimulation of the cells however resulted in rescue of the signal. This further supports the idea that SRC and ErbB2 interact under both starved and stimulated conditions, but strongly suggest that this interaction occurs through distinct mechanisms. In EGF stimulated conditions heterocomplex formation between EGFR/ErbB2 could lead to a SRC interaction with pTyr residues in the receptors. Importantly, these results also support that in starved conditions this interaction might instead occur via the proline-rich motif found in the C-terminal tail of ErbB2.

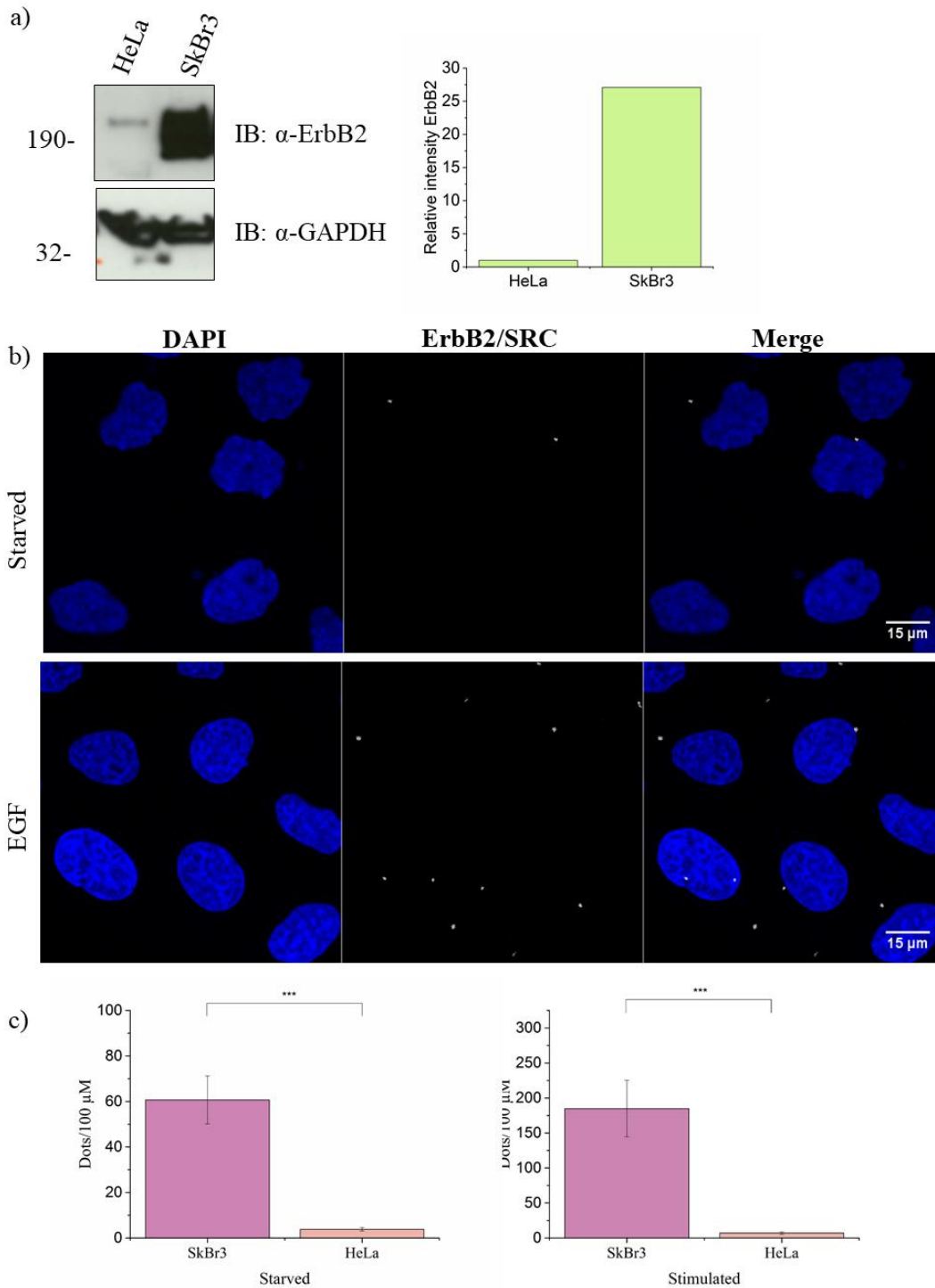
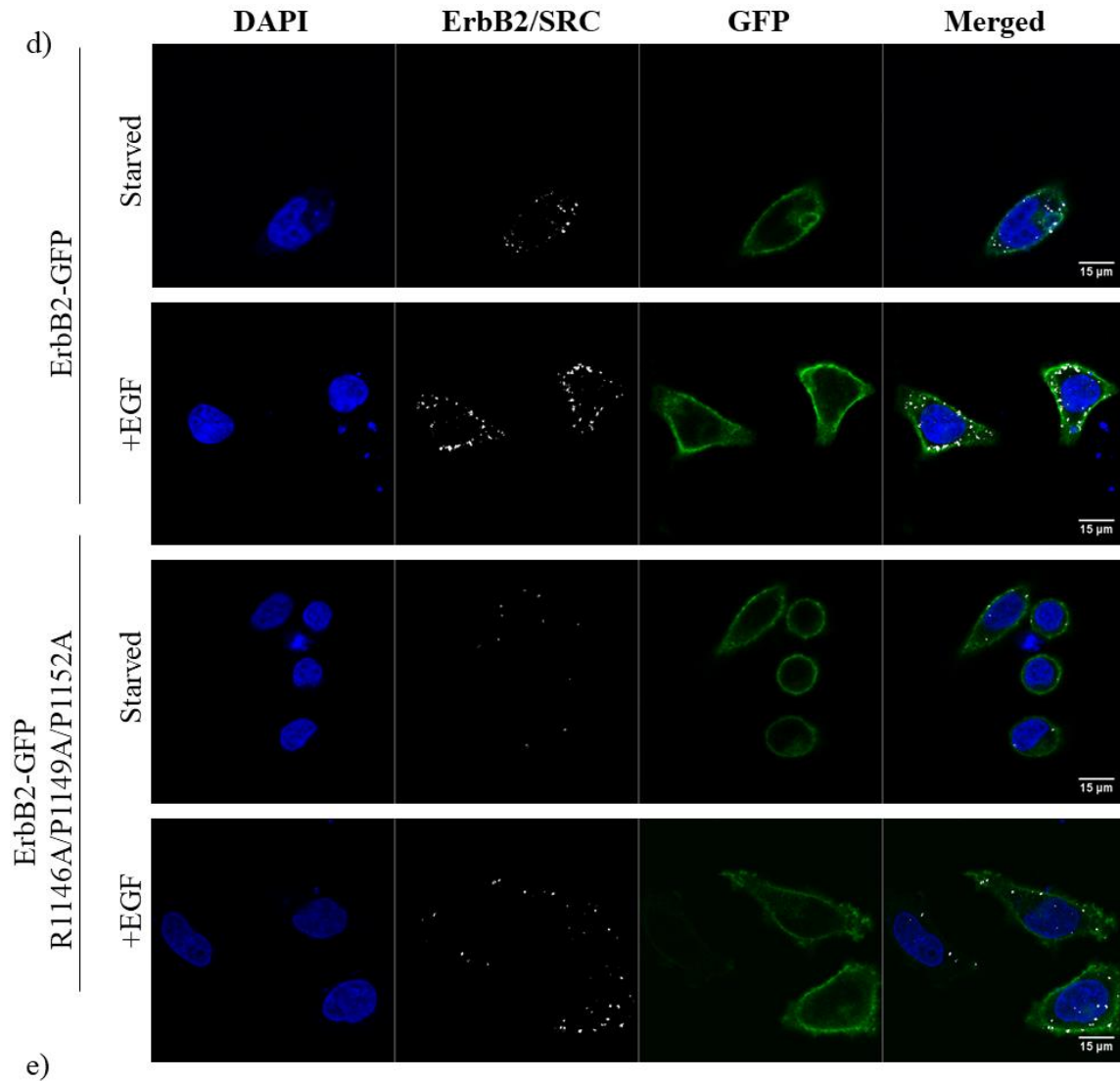


Figure 5-7 The C-terminal tail of ErbB2 is interacting with SRC.

a) Western blot and relative intensity graph shows that HeLa cells express 27-fold lower levels of ErbB2 compared SkBr3 b) PLA signal is detected for SRC and ErbB2 interaction in both starved and stimulated conditions in HeLa c) To look at the difference in PLA signal between HeLa and SkBr3 cells ImageJ was used to quantify the signal. Images with similar cell average per image was selected and PLA signal was quantified by using analyse particles. A minimum of 8 images per condition was used. In both starved and EGF stimulated cells SkBr3 has a significant higher signal compared to HeLa (continues next page)



d-e) HeLa cells were transfected with ErbB2 and mutant ErbB2 (R1146A/P1149A/P1152A) where a proline-rich motif in the C-terminal tail was mutated. With wild type ErbB2 PLA signal was rescued in both starved and EGF stimulated cells. With mutant ErbB2 signal was rescued only in EGF stimulated cells and not starved cells. Scale bar 15 μ m. DAPI was used to visualise the nucleus. Mean values and standard errors are represented. Using standard t-test the statistically significant differences are indicated by * ($P \leq 0.05$), ** ($P \leq 0.01$) or *** ($P \leq 0.001$).

5.1.4 Binding affinities between ErbB2 peptides and SRC SH3 domain suggest a weak interaction

ErbB2 has six canonical PXXP proline-rich motifs in the cytoplasmic region. To explore their potential contribution to the interaction with SRC, six peptides were created and used for binding measurements by MST measurements to determine binding affinity between the proline-rich motifs and the SH3 domain of SRC. Peptide 1 is based on the same amino acid sequence as previously reported to interact with FYN SH3 domain (Bornet et al., 2014). The binding affinity (expressed at the dissociation constant, K_D) between peptide 1 and FYN SH3 domain was found to be 1.4 mM in the MST experiments. This was similar to the K_D reported by Bornet et al (Table 12 and Figure 5.8 a) which was 0.9 mM. The affinity of the interaction between SRC SH3 domain and the same peptide was slightly weaker ($K_D = 7.1$ mM)(Figure 5.8 b). The same order of affinity was recorded for several of the other peptides (Figure 5.8 c-g and Table 12). Peptide 5 shows a non-traditional binding curve, but it could be that two events are happening here. The first event where the peptide concentration is between 0.1-100 μ M (potential binding affinity at 10 μ M) and the next event happens when the peptide concentration reaches 1 mM. Further exploration of this peptide should be done by for example using a lower peptide concentration to obtain the possible binding affinity of the first event. The obtained affinities for peptide 1, 2, 4 and 8 are extremely low and do not represent the affinities that would be expected for the full length intact proteins in the cell. Interactions between SH3 domains and proline-rich motifs are normally quite weak (Ladbury and Arold, 2000). For example the SH3 domain from FYN

could interact with peptides containing proline-rich motifs from known interacting proteins with a K_D ranging from 16-2002 μ M. The SH3 domain from GRB2 was shown to interact with two peptides based on proline-rich motifs from SOS at 5 and 21 μ M. A control peptide was used based on a reported interaction between NS5A and SRC family kinase SH3 domains, and a K_D was measured to 258 μ M, a magnitude lower than for the ErbB2 peptides (Figure 5.8 h) (Macdonald et al., 2005).

Table 12 Peptides containing proline-rich motifs from ErbB2 C-terminal tail and NS5A.

MST was used to determine binding affinity between the peptides and SH3 domains from SRC and FYN

Peptide	Sequence	SH3 domain	Binding affinity
ErbB2 peptide 1*	NQPDV <u>RPQPPSP</u> REGPL	SRC	7.1 mM
ErbB2 peptide 1	NQPDV <u>RPQPPSP</u> REGPL	FYN	1.4 mM
ErbB2 peptide 2	LEKGERL <u>PQPPICT</u> ID	SRC	6.4 mM
ErbB2 peptide 3	VIQNE <u>DLGPAS</u> PLDSTFYR	SRC	-
ErbB2 peptide 4	GLEPSEEE <u>APRSPLA</u> SEG	SRC	3.7 mM
ErbB2 peptide 5	LQRYSE <u>DPTVPLP</u> SETDGY	SRC	-
ErbB2 peptide 6	GGA <u>APQPHPPA</u> FSPAFD	SRC	6.7 mM
NS5A peptide PP2.1/PP2.2†	GS <u>LPPAKAPP</u> IPPRRKRTV	SRC	258 μ M

* Sequence is based on data from Bornet et al., 2014

† Sequence is based on data Macdonald et al., 2004

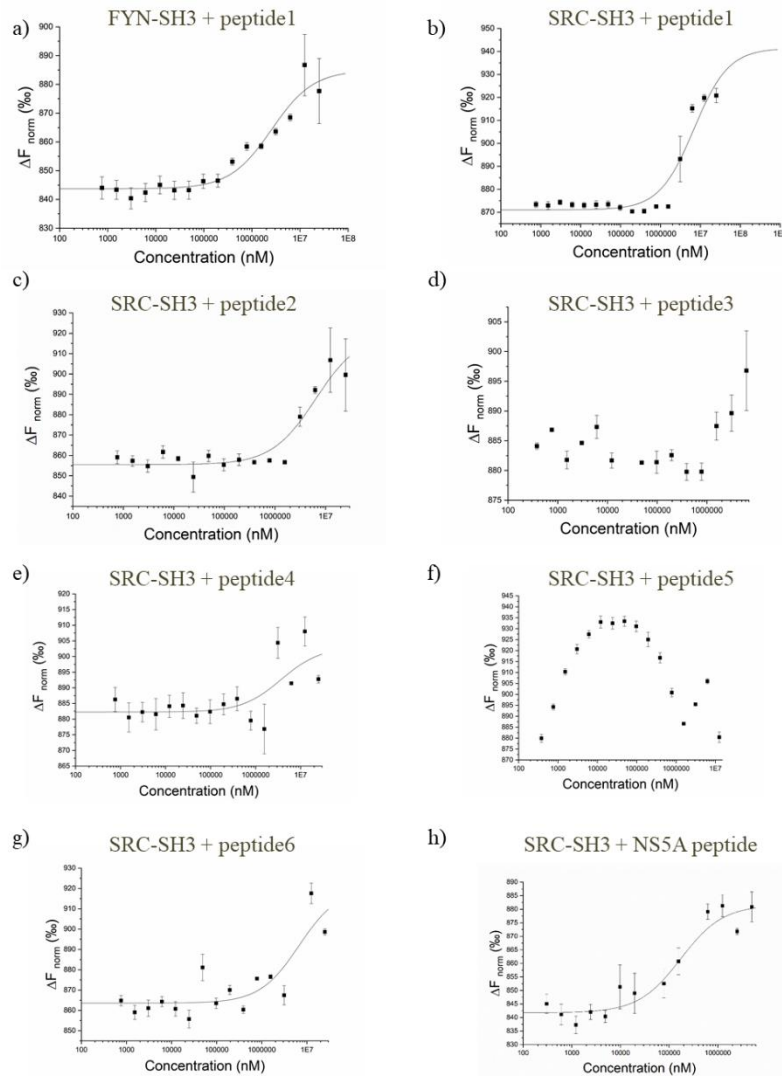


Figure 5-8 MST was used to determine binding affinities between peptides based on sequences in the C-terminal tail of ErbB2 containing proline-rich motifs and the SH3 domains of either SRC or FYN.

Peptides, the amino acid sequence and binding affinity obtained from MST measurements are summarised in Table 122. a) FYN SH3 domain was labelled and a peptide (ErbB2 peptide 1) containing a proline-rich motif previously reported to interact with FYN SH3 domain (Bornet et al., 2014) was used in a dilution series to determine binding affinity between FYN SH3 and peptide 1. The affinity was determined to be 1.4 mM. b) ErbB2 peptide 1 was added in a dilution series to labelled SRC SH3 domain and MST measurements was used to determine the binding affinity, 7.1 mM. c-g) Labelled SRC SH3 was used in MST measurements with peptides based on proline-rich motifs in the C-terminal tail of ErbB2, peptide 2-6. Binding affinities was obtained for some of the peptides. h) Additionally a peptide based on a previously reported binding partner of SRC kinases SH3 domain, NS5A was used (Macdonald et al., 2004). A binding affinity of 258 μM was measured with labelled SRC SH3 and the control peptide

All experiments was performed in HEPES buffer at pH 7.5

5.1.5 Discussion

There is previously reported evidence of a direct interaction between SRC and ErbB2. This has been shown *in vitro* to be through the SH2 domain of SRC and pTyr residues of ErbB2 (Muthuswamy et al., 1994), or through a combination of SH2/SH3 domains where SH2/SH3 complex was able to pull down more ErbB2 than the SH2 domain on its own (Luttrell et al., 1994).

The data in this chapter demonstrate that SRC and ErbB2 interact endogenously, and that this interaction can also be measured when the cells are starved. One of the key questions is whether this interaction is through the SH2 domain and pTyr of ErbB2, since phosphorylation of the receptor can prevail in starved cells as observed in SkBr3. Using a different cell line, MCF7 in which phosphorylation of tyrosine residues on ErbB2 was negligible the SRC/ErbB2 interaction was still visible suggesting that this interaction is not mediated by the SRC SH2 and ErbB2 pTyr. The PLA study using MCF7 cells also shows that the interaction is unlikely to be between a pTyr on ErbB2 which has been phosphorylated in the context of a heterodimer with EGFR, because MCF7 cells do not express EGFR. The PLA signal is observed for the interaction of SRC and ErbB2 in these cells. Combined with our *ex vivo* evidence that suggests that the association with SRC and ErbB2 is through the SRC SH3 domain and a proline-rich motif in the C-terminal tail of ErbB2 *in vitro* assays using MST show direct binding. The K_D values for interactions between peptides containing proline-rich motifs derived from the C-terminus of ErbB2 and the SRC SH3 domain suggest that the binding affinity is in the mM range. This provides evidence of an interaction, although it would be interesting whether using full length proteins could yield an

increased affinity. It is also possible that the interaction with the receptor could require a combination of the SH2 and SH3 domains of SRC interacting with pTyr and a proline-rich motif. Another example of a SRC interaction that requires both the SH2 and SH3 domains is with the SRC substrate Sam68 (Src-associated in mitosis). A higher affinity interaction is obtained when both domains are involved (Taylor and Shalloway, 1994; Fumagalli et al., 1994). An association of ErbB2 with both SH2 and SH3 domains of SRC could potentially stabilise the open conformation of SRC and allow a prolonged SRC activity (Figure 5.9). The flag pull down in starved HEK293T supports this observation as the Y530F mutant pulled down more ErbB2. SRC conformation has previously been shown to be important when SRC interacts with ErbB2 (Marcotte et al., 2009). An open conformation of SRC can interact with the kinase domain of ErbB2 and this interaction is not dependent on SH2 or SH3 domains, and only the kinase domain of SRC is required for interaction but independently of kinase activity. Both SH2/pTyr and SH3/PXXP interactions are transient interactions as the cell needs to be able to switch on and off signalling in a quick manner and a prolonged interaction can be achieved by having both SH2 and SH3 domains interact with the receptor. Whether a prolonged interaction can have any impact on SRC and ErbB2 activity and downstream signalling remains to be elucidated.

Evidence presented here suggest an interaction between SRC and ErbB2 in breast cancer cell line SkBr3, most importantly when the cells are starved. Some evidence suggest that this is partially or fully through the SH3 domain. This further demonstrates that there is interactions happening between RTKs C-terminal tail and cytoplasmic SH3 domains, and could potentially

have a massive impact on how RTK signalling is regulated. More intriguingly this is the first demonstration of these interactions in a different RTK, and not just FGFR2.

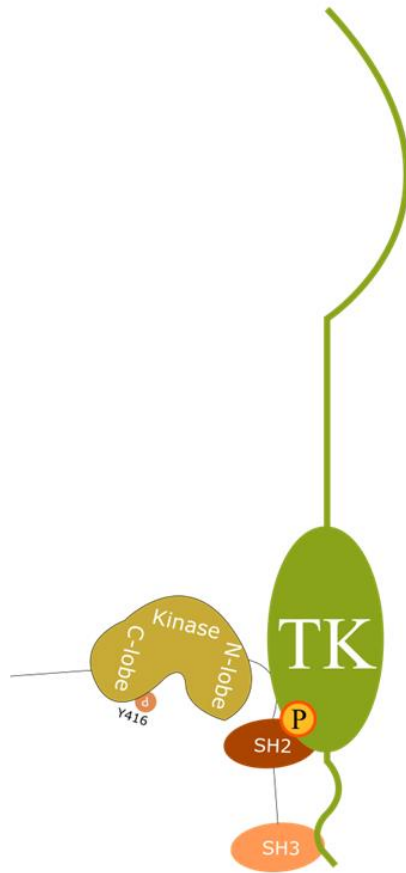


Figure 5-9 Proposed model for SRC and ErbB2 interaction. Both SH2 and SH3 can interact with the receptor, either with pTyr or a PXXP motif on the C-terminal tail of ErbB2.

Chapter 6: Discussion

The discovery of a “second tier” RTK regulation should lead to a paradigm shift in cell signalling, and there might be a whole network of signalling that is waiting to be uncovered. Data presented here further adds to this previously under-investigated field.

PLC γ 1 has been shown to interact with FGFR2, resulting in PLC γ 1 pathway activation (Timsah et al., 2014; Timsah et al., 2015). The interaction is mediated by SH3 domain and proline-rich motifs. RTKs contain one or several proline-rich motifs in the C-terminal tail and SH3 domains are abundant in the cell. SH3 interactions with proline-rich motifs are considered weak interactions in the cell and for this reason difficult to demonstrate. Therefore it is interesting to question the potential of a new and possible “second tier” of signalling from RTKs, which have largely remained undiscovered in the complexity that is cell signalling.

Several approaches were used to identify new interactions between SH3 domains and proline-rich motifs in the C-terminal tail of a range of RTKs. Peptides containing proline-rich motifs from 5 RTKs were used in a high-throughput MS screen. The results yielded a substantial number of proteins. After a rigorous comparison system using a control peptide to reveal specific hits, the list was narrowed down. Comparing the number of unique peptides from the RTK peptides to the control peptide demonstrated that most of the remaining hits were largely non-specific and the high scoring proteins were contaminants such as keratin. Keratin is not expressed in HEK293T which was used as the default cell line to test the MS approach, suggesting that any keratin found must be from the handling of samples before MS.

Altogether the results from the MS suggest that further optimisation would have to be carried out such as optimising the peptide lengths to ensure binding, buffer conditions and a way to remove human contaminants. Using MS is not very cost-effective and it would therefore be useful to look at other approaches rather than optimising the conditions. BioID would be a useful approach to explore. Plasmids containing the peptides with proline-rich motifs together with the gene for biotin ligase can be transfected into the cell line of choice, and in this way will ensure that proteins in close proximity to the peptide will be biotinylated and can be pulled out and sent for MS. This avoids the intermediate and possible weak interaction between the peptide and the protein of interest, and instead directly biotinylates the protein of interest, resulting in a stronger interaction that can be pulled out by streptavidin. Although none of the proteins contained an SH3 domain, some proteins that were discovered in the screen could be of interest for further characterisation, although not within the scope of this project.

Further work was carried out focusing on the LASP1 SH3 domain using a dot blot with the C-terminal tails of several RTKs. This approach yielded several hits, and some were further demonstrated in cells, although none of the characterised interactions were SH3 domain specific. Other RTKs can be taken further to characterise the LASP1 interaction and demonstrate a specific SH3 domain interaction. Unfortunately due to time constraints it was not carried out. Since some of the hits in the dot blot also occur in cells suggests that this method could also be applied to other proteins with SH3 domains as well. Compared to MS-based analysis, the dot blot is more constrained as a method to detect novel interactions. The proteins that are used must be expressed and purified and it is currently constrained to one

protein. Further approaches in making a library of SH3 domains from several proteins could be carried out to create a high throughput screen. This could potentially be a better method of discovering interactions between SH3 domains and proline-rich motifs. The SH3 domain-proline-rich interactions are inherently low affinity and there is the potential that the use of small peptides and cell lysate, in a MS-based analysis might not be capable of identifying the proteins. Both methods requires optimisation and using the dot blot could potentially serve as a more cost-effective path. Regardless of method, interactions should be further characterised. In addition the interactions should be demonstrated to occur in the cell as a proof of principle.

LASP1 was shown to interact with both RTKs ALK and ErbB2. These data further support the importance of RTK C-terminal tails, despite the lack of a SH3 domain specific binding to the receptors. The genes encoding LASP1 and ErbB2 are found in close proximity on the chromosome and have been demonstrated to be co-overexpressed in breast cancers. Results presented here suggest a direct role for LASP1 and ErbB2, and they were shown to interact endogenously in the breast cancer cell line SkBr3. LASP1 does not contain any SH2 domains to bind pTyr in ErbB2 C-terminal tail. The direct interaction between the ErbB2 C-terminal tail and LASP1 suggest therefore another mechanism for protein-protein interactions in the RTK C-terminal tail. Further work would have to be carried out to demonstrate the physiological relevance of this interaction.

A preliminary method from Prof. Bedford's group at the MD Anderson Cancer Center, TX, USA showed that LASP1 SH3 could also interact with

FGFR2. Some evidence of this interaction was recapitulated with the dot blot, but this approach suggested that it is a low affinity interaction, i.e. the intensity of the dot was low, but there was a 3-fold difference in binding FGFR2 between wild type LASP1 and the mutant LASP1 lacking the SH3 domain. Further work with FGFR2 and LASP1 demonstrated that the interaction can occur in cells, and that it involves the C-terminal tail of FGFR2. This is consistent with the dot blot analysis which is based on an immobilised C-terminal tail of FGFR2. Binding affinities were obtained and LASP1 Δ SH3 was also able to bind the FGFR2 C-terminal tail with slightly lower affinity compared to wild type LASP1, suggesting that the SH3 domain could potentially be important in stabilising the interaction but is not critical. Conclusively LASP1 interacts with FGFR2 but not via the SH3 domain. Crystallising either full length LASP or the SH3 on its own with the C58 peptide could further elucidate how C58 interacts with LASP1, and how important the SH3 domain is for this interaction. Further binding studies, based on site-specific mutations, suggested that P810 is important for this interaction. Because the SH3 domain was shown to only strengthen the interaction rather than being essential, it was interesting to see that prolines are still important for the interaction. Prolines have unique roles in protein structure and folding, and can be viewed as a structural disruptor of proteins. Removing the prolines can therefore have a detrimental effect on the overall structure of the C58 peptide and result in no binding with LASP1.

The physiological effect of the LASP1 interaction with the FGFR2 C-terminal tail suggests that it can affect cell growth and migration. In cells that are depleted for GRB2, cell growth is higher when FGFR2 is overexpressed on its own. This is potentially a result of FGFR2 interacting with PLC γ 1, with

LASP1 and PLC γ 1 competing for binding. When LASP1 and FGFR2 are co-overexpressed cell growth decreased. The K_D determined for FGFR2/LASP1 and FGFR2/PLC γ 1 are both $\sim 40 \mu\text{M}$. In the GRB2-depleted cells, LASP1 and PLC γ 1 can compete for binding to the C-terminal tail of FGFR2 and LASP1. In this way LASP1 could inhibit PLC γ 1 activation. Further work needs to be carried out, such as MST competition studies to elucidate whether LASP1 and PLC γ 1 actually compete for binding. For the growth and migration assays the cells were not starved but grown in serum-containing medium. It is therefore also a possibility that other pathways might be activated by phosphorylated tyrosines. This could also be the reason why the effects of overexpression in either scr or HeLa cells are different to the GRB2-depleted cells. Both FGFR2 and LASP1 can contribute to cell growth on their own, through other mechanisms such as FRS2/GRB2 activation. The increased growth when LASP1 and FGFR2 are co-overexpressed could be the result of individual effects. The most intriguing result is the effect that FGFR2/LASP1 has on cell migration. LASP1 is known to interact with the cytoskeleton and is involved in cell migration. Co-overexpressing LASP1 with FGFR2 decrease of migration, suggesting an inhibitory role for FGFR2 on LASP1-mediated cell migration. These initial observations of a physiological effect from a LASP1 and FGFR2 interaction on both growth and migration serves as an interesting starting point.

The preliminary screen from Prof. Bedford's group also identified a number of SRC family kinase members with the potential to interact with ErbB2. In addition it has been demonstrated that the FYN SH3 domain can specifically interact with a proline-rich motif in the ErbB2 C-terminal tail (Bornet et al., 2014). These preliminary results suggest that several SRC kinases are able

to interact but this has not been shown in cells. The members of the SRC family are homologues, suggesting that an interaction between SRC and ErbB2 is also possible. Both SRC and ErbB2 are oncogenes that are upregulated in breast cancers (Sheffield, 1998). Although an interaction between SRC and ErbB2 has been demonstrated in breast cancer cell lines, this is driven through interaction with the SRC SH2 domain and phosphorylated tyrosine of ErbB2. However, this interaction was not been demonstrated in the breast cancer cell line SkBr3, but in the UACC-812, MDA-MB-361 and MDA-MB-453 cell lines (Muthuswamy and Muller, 1995; Belsches-Jablonski et al., 2001; Kim et al., 2005). Breast cancer cell lines are heterogeneous and have different features. The genetic make-up that leads to tumour formation varies between them (Riaz et al., 2013). MDA-MB-361 and MDA-MB-453 belong to the “MDA” series (Cailleau et al., 1978). Between them they show heterogeneity, as MDA-MB361 is positive for the breast cancer markers ErbB2, Estrogen receptor (ER) and progesterone receptor (PR) while MDA-MB453 is only ErbB2 positive. UAC-812 is also positive for ErbB2, ER and PR (Dai et al., 2017). SkBr3 cells overexpress ErbB2, but is not positive for either ER or PR. An interaction between SRC and ErbB2 has been demonstrated here in both SkBr3 and MCF7 breast cancer cell lines. The breast cancer cell line MCF7 is positive for both ER and PR markers, but ErbB2 is not overexpressed. Some ErbB2 expression is detected but no tyrosine phosphorylation which is seen in SkBr3 cells where ErbB2 is overexpressed. This suggests that in MCF7 cells the interaction with SRC is not through the SH2 domain which was demonstrated in the other breast cancer cell lines.

Some evidence indicates that the SH3 domain is important for the interaction with ErbB2 in SkBr3 cells. However *in vitro* assays suggest that this is a weak interaction and physiologically unlikely to happen endogenously in the cell. The GST-pull downs shows that SH3 domains from both FYN and SRC are able to interact with ErbB2 directly. Using high concentrations of cell lysates with ErbB2 overexpressed could potentially overcome the low affinity which was demonstrated between the SRC SH3 domain and an ErbB2 peptide using MST and artificially force the interaction using high levels of receptor. This leads to a proposed model that SRC can potentially interact with ErbB2 via both the SH2 and SH3 domains in SkBr3 cells. Such an interaction can stabilise the interaction and keep SRC in an open conformation, allowing the kinase domain to remain functional for a prolonged period. Further work needs to be carried out to demonstrate and validate the proposed model. If this model is true for SkBr3 cells, is there a possibility that this can also happen in the other breast cancer cell lines where an interaction between SRC and ErbB2 was demonstrated?

Another question that remains unanswered is by what mechanism does SRC interact with ErbB2 in MCF7 cells? A PLA signal was detected in both serum-starved and stimulated cells for SRC and ErbB2. In accordance with previous results the SH3 domain was not solely responsible for this interaction. In the MCF7 cells, phosphorylation of tyrosines 1221/1222 were used as a readout of receptor activation, but could other tyrosines in ErbB2 be phosphorylated? A scenario could be that ErbB2 has some background phosphorylation, but with the receptor not fully activated, and this allows SRC to interact via the SH2 domain. Another explanation could be complex formation at the receptor. PLA detects signal from antibodies that are in

close proximity to each other within 40 nm. SRC has been suggested to also have a role downstream of ErbB2, therefore the PLA signal could be the result of complex formation between SRC, ErbB2 and an unknown adaptor/scaffold protein.

The C-terminal tail of ErbB2 is important for SRC binding. A proline-rich motif in the C-terminal tail of ErbB2 was demonstrated to bind FYN SH3 at low affinity in NMR and SPR experiments (Bornet et al., 2014). When the proline-rich motif was mutated it abolished binding between SRC and mutant ErbB2 in transfected, and serum-starved HeLa cells. In HeLa cells that have been stimulated the interaction still occurred, suggesting different mechanisms for SRC and ErbB2 interaction in serum-starved and stimulated HeLa cells. One can speculate whether the interaction in starved cells is mediated via the SH3 domain, despite being a rejected theory based on biophysical data.

Chapter 7: Conclusions and further directions

Several novel interactions have been demonstrated between RTKs and either LASP1 or SRC. Some of these interactions provide further examples of how important the RTK C-terminal tail is. More importantly this work shows several RTKs other than FGFR2 interacting with SH3 domains and under serum-starved conditions, an important requisite for “second-tier” signalling. This lays down some of the groundwork which can ultimately lead to a paradigm shift in RTK regulation.

Two different approaches were taken to discover novel interactions between proline-rich motifs from RTKs and SH3 domains. Neither provided a straight forward technique to use and both require further optimisation, to accommodate the difficulties of identifying weak interactions. Further work could also look into using BioID as an approach, which would potentially overcome the difficulties of weak interactions at the same time as being an unbiased approach.

The dot blot uncovered new interactions and further verification showed that the oncogenic protein LASP1 can interact with both ALK and ErbB2. Both receptors are known oncogenes, and these data shows that the C-terminal tail is important in binding LASP1. These are both novel interactions, and further exploration can unravel the importance of them.

An interaction between LASP1 and the C-terminal tail of FGFR2 was also demonstrated, and some preliminary data suggested that it can have an effect on cell growth and cell migration. Further work looking into effects of knocking out LASP1 and FGFR2 expression using siRNA can be carried out, and would hopefully demonstrate that the effects seen are indeed

specifically from an interaction between FGFR2 and LASP1. The effects of FGFR2 on LASP1-mediated cell migration is an intriguing preliminary result. It would be interesting to see whether FGFR2 expression varies in tumours that overexpress LASP1 and if FGFR2 expression can determine tumour aggressiveness.

There are many questions remaining to elucidate the interaction between SRC and ErbB2. One thing is clear is that breast cancer cell lines are heterogeneous, and do not retain the same biological responses and processes. A model is proposed where SRC is in a stabilised interaction with ErbB2 via both the SH2 and SH3 domains. Further work will have to be carried out to strengthen this theory. Mutant SRC lacking the ability to bind phosphorylated tyrosines can be utilised to demonstrate a difference in PLA signal or in IP experiments, compared to wild type SRC. A GST-pull down experiment using the SRC SH2 domain can be performed to show this interaction. Further biophysical analysis using the C-terminal tail of ErbB2 (phosphorylated and unphosphorylated) and individual domains of SRC can be used to determine binding affinities. If these further experiments support the proposed model it would be very interesting to see what effects it would have physiologically. If both the SH2 and SH3 domains interact with ErbB2, SRC is held in an open conformation. SRC kinase can then have prolonged activity and activate downstream effectors, which can have a detrimental effect on the cell.

Bibliography

- Adnane, J., Gaudray, P., Dionne, C.A., Crumley, G., Jaye, M., Schlessinger, J., Jeanteur, P., Birnbaum, D. and Theillet, C. 1991. BEK and FLG, two receptors to members of the FGF family, are amplified in subsets of human breast cancers. *Oncogene*. **6**(4), pp.659–63.
- Ahmed, Z., George, R., Lin, C.-C., Suen, K.M., Levitt, J.A., Suhling, K. and Ladbury, J.E. 2010. Direct binding of Grb2 SH3 domain to FGFR2 regulates SHP2 function. *Cellular Signalling*. **22**(1), pp.23–33.
- Ahmed, Z., Lin, C.C., Suen, K.M., Melo, F. a., Levitt, J. a., Suhling, K. and Ladbury, J.E. 2013. Grb2 controls phosphorylation of FGFR2 by inhibiting receptor kinase and Shp2 phosphatase activity. *Journal of Cell Biology*. **200**(4), pp.493–504.
- Ahmed, Z., Schüller, A.C., Suhling, K., Tregidgo, C. and Ladbury, J.E. 2008. Extracellular point mutations in FGFR2 elicit unexpected changes in intracellular signalling. *The Biochemical journal*. **413**(1), pp.37–49.
- Bach, I. 2000. The LIM domain: regulation by association. *Mechanisms of development*. **91**(1–2), pp.5–17.
- Bange, J., Zwick, E. and Ullrich, A. 2001. Molecular targets for breast cancer therapy and prevention. *NATURE MEDICINE* • **7**(5).
- Baselga, J. and Swain, S.M. 2009. Novel anticancer targets: Revisiting ERBB2 and discovering ERBB3. *Nature Reviews Cancer*. **9**(7), pp.463–475.
- Belsches-Jablonski, A.P., Biscardi, J.S., Peavy, D.R., Tice, D.A., Romney, D.A. and Parsons, S.J. 2001. Src family kinases and HER2 interactions

in human breast cancer cell growth and survival. *Oncogene*. **20**(12), pp.1465–1475.

Ben-Levy, R., Paterson, H.F., Marshall, C.J. and Yarden, Y. 2018. A single autophosphorylation site confers oncogenicity to the Neu/ErbB-2 receptor and enables coupling to the MAP kinase pathway. *The EMBO Journal*. **13**(14), pp.3302–3311.

Berk, J.M., Tiffit, K.E. and Wilson, K.L. 2013. The nuclear envelope LEM-domain protein emerin. *Nucleus (United States)*. **4**(4), pp.298–314.

Berman, J., Crosby, R.M., Jung, K.D., Willard, D., Lee, A., Gilmer, T.M., Luther, M., Lansing, T.J., Luttrell, D.K. and Rodriguez, M. 2006. Involvement of pp60c-src with two major signaling pathways in human breast cancer. *Proceedings of the National Academy of Sciences*. **91**(1), pp.83–87.

Bièche, I., Tomasetto, C., Régnier, C.H., Moog-Lutz, C., Rio, M.C. and Lidereau, R. 1996. Two distinct amplified regions at 17q11-q21 involved in human primary breast cancer. *Cancer research*. **56**(17), pp.3886–90.

Birrer, M.J., Johnson, M.E., Hao, K., Wong, K.-K., Park, D.-C., Bell, A., Welch, W.R., Berkowitz, R.S. and Mok, S.C. 2007. Whole genome oligonucleotide-based array comparative genomic hybridization analysis identified fibroblast growth factor 1 as a prognostic marker for advanced-stage serous ovarian adenocarcinomas. *Journal of clinical oncology : official journal of the American Society of Clinical Oncology*. **25**(16), pp.2281–7.

Bjorge, J.D., Pang, A. and Fujita, D.J. 2000. Identification of protein-tyrosine phosphatase 1B as the major tyrosine phosphatase activity capable of

- dephosphorylating and activating c-Src in several human breast cancer cell lines. *The Journal of biological chemistry*. **275**(52), pp.41439–46.
- Bornet, O., Nouailler, M., Feracci, M., Sebban-Kreuzer, C., Byrne, D., Halimi, H., Morelli, X., Badache, A. and Guerlesquin, F. 2014. Identification of a Src kinase SH3 binding site in the C-terminal domain of the human ErbB2 receptor tyrosine kinase. *FEBS Letters*. **588**(12), pp.2031–2036.
- Bresnick, A.R., Weber, D.J. and Zimmer, D.B. 2015a. S100 proteins in cancer HHS Public Access. *Nat Rev Cancer*. **15**(2), pp.96–109.
- Bresnick, A.R., Weber, D.J. and Zimmer, D.B. 2015b. S100 proteins in cancer HHS Public Access. *Nat Rev Cancer*. **15**(2), pp.96–109.
- Brooks, a. N., Kilgour, E. and Smith, P.D. 2012. Molecular pathways: Fibroblast growth factor signaling: A new therapeutic opportunity in cancer. *Clinical Cancer Research*. **18**(7), pp.1855–1862.
- Burgess, A.W., Cho, H.S., Eigenbrot, C., Ferguson, K.M., Garrett, T.P.J., Leahy, D.J., Lemmon, M.A., Sliwkowski, M.X., Ward, C.W. and Yokoyama, S. 2003. An open-and-shut case? Recent insights into the activation of EGF/ErbB receptors. *Molecular Cell*. **12**(3), pp.541–552.
- Butt, E. and Raman, D. 2018. New Frontiers for the Cytoskeletal Protein LASP1. *Frontiers in Oncology*. **8**, p.391.
- Cailleau, R., Olivé, M. and Cruciger, Q.V.J. 1978. Long-term human breast carcinoma cell lines of metastatic origin: Preliminary characterization. *In Vitro*. **14**(11), pp.911–915.
- Campbell, K.S., Ogris, E., Burke, B., Su, W., Auger, K.R., Druker, B.J., Schaffhausen, B.S., Roberts, T.M. and Pallas, D.C. 1994. Polyoma

middle tumor antigen interacts with SHC protein via the NPTY (Asn-Pro-Thr-Tyr) motif in middle tumor antigen. *Proceedings of the National Academy of Sciences of the United States of America*. **91**(14), pp.6344–8.

Campbell, R.B., Liu, F. and Ross, A.H. 2003. Allosteric Activation of PTEN Phosphatase by Phosphatidylinositol 4,5-Bisphosphate. *Journal of Biological Chemistry*. **278**(36), pp.33617–33620.

Chew, C.S. 2002. Lasp-1 binds to non-muscle F-actin in vitro and is localized within multiple sites of dynamic actin assembly in vivo. *Journal of Cell Science*.

Chiarle, R., Voena, C., Ambrogio, C., Piva, R. and Inghirami, G. 2008. The anaplastic lymphoma kinase in the pathogenesis of cancer. *Nature Reviews Cancer*.

Courjal, F., Cuny, M., Simony-Lafontaine, J., Louason, G., Speiser, P., Zeillinger, R., Rodriguez, C. and Theillet, C. 1997. Mapping of DNA amplifications at 15 chromosomal localizations in 1875 breast tumors: definition of phenotypic groups. *Cancer research*. **57**(19), pp.4360–7.

Dai, X., Cheng, H., Bai, Z. and Li, J. 2017. Breast Cancer Cell Line Classification and Its Relevance with Breast Tumor Subtyping. *Journal of Cancer*. **8**(16), pp.3131–3141.

Davies, H., Hunter, C., Smith, R., Stephens, P., Greenman, C., Bignell, G., Teague, J., Butler, A., Edkins, S., Stevens, C., Parker, A., O'Meara, S., Avis, T., Barthorpe, S., Brackenbury, L., Buck, G., Clements, J., Cole, J., Dicks, E., Edwards, K., Forbes, S., Gorton, M., Gray, K., Halliday, K., Harrison, R., Hills, K., Hinton, J., Jones, D., Kosmidou, V., Laman, R.,

Lugg, R., Menzies, A., Perry, J., Petty, R., Raine, K., Shepherd, R., Small, A., Solomon, H., Stephens, Y., Tofts, C., Varian, J., Webb, A., West, S., Widaa, S., Yates, A., Brasseur, F., Cooper, C.S., Flanagan, A.M., Green, A., Knowles, M., Leung, S.Y., Looijenga, L.H.J., Malkowicz, B., Pierotti, M.A., Teh, B.T., Yuen, S.T., Lakhani, S.R., Easton, D.F., Weber, B.L., Goldstraw, P., Nicholson, A.G., Wooster, R., Stratton, M.R. and Futreal, P.A. 2005. Somatic Mutations of the Protein Kinase Gene Family in Human Lung Cancer. *Cancer Research*. **65**(17), pp.7591–7595.

Engelman, J.A., Luo, J. and Cantley, L.C. 2006. The evolution of phosphatidylinositol 3-kinases as regulators of growth and metabolism. *Nature reviews. Genetics*. **7**(8), pp.606–19.

Espejo, A., Côté, J., Bednarek, A., Richard, S. and Bedford, M.T. 2002. A protein-domain microarray identifies novel protein-protein interactions. *The Biochemical journal*. **367**(Pt 3), pp.697–702.

Frame, M.C. 2002. Src in cancer: Deregulation and consequences for cell behaviour. *Biochimica et Biophysica Acta - Reviews on Cancer*. **1602**(2), pp.114–130.

Franke, T.F., Kaplan, D.R., Cantley, L.C. and Toker, A. 1997. Direct regulation of the Akt proto-oncogene product by phosphatidylinositol-3,4-bisphosphate. *Science (New York, N.Y.)*. **275**(5300), pp.665–8.

Frietsch, J.J., Grunewald, T.G.P., Jasper, S., Kammerer, U., Herterich, S., Kapp, M., Honig, A. and Butt, E. 2010. Nuclear localisation of LASP-1 correlates with poor long-term survival in female breast cancer. *British journal of cancer*. **102**(11), pp.1645–53.

- Frietsch, J.J., Kastner, C., Grunewald, T.G.P., Schweigel, H., Nollau, P., Ziermann, J., Clement, J.H., La Rosée, P., Hochhaus, A. and Butt, E. 2014. LASP1 is a novel BCR-ABL substrate and a phosphorylation-dependent binding partner of CRKL in chronic myeloid leukemia. *Oncotarget*. **5**(14), pp.5257–71.
- Fumagalli, S., Totty, N.F., Hsuan, J.J. and Courtneidge, S.A. 1994. A target for Src in mitosis. *Nature*. **368**(6474), pp.871–874.
- Garrett, T.P.J., McKern, N.M., Lou, M., Elleman, T.C., Adams, T.E., Lovrecz, G.O., Kofler, M., Jorissen, R.N., Nice, E.C., Burgess, A.W. and Ward, C.W. 2003. The crystal structure of a truncated ErbB2 ectodomain reveals an active conformation, poised to interact with other ErbB receptors. *Molecular cell*. **11**(2), pp.495–505.
- Gartside, M.G., Chen, H., Ibrahimi, O.A., Byron, S.A., Curtis, A. V., Wellens, C.L., Bengston, A., Yudt, L.M., Eliseenkova, A. V., Ma, J., Curtin, J.A., Hyder, P., Harper, U.L., Riedesel, E., Mann, G.J., Trent, J.M., Bastian, B.C., Meltzer, P.S., Mohammadi, M. and Pollock, P.M. 2009. Loss-of-Function Fibroblast Growth Factor Receptor-2 Mutations in Melanoma. *Molecular Cancer Research*. **7**(1), pp.41–54.
- Glynn, R.W., Miller, N., Mahon, S. and Kerin, M.J. 2012. Expression levels of HER2/neu and those of collocated genes at 17q12-21, in breast cancer. *Oncology Reports*. **28**(1), pp.365–369.
- Godreau, D., Neyroud, N., Vranckx, R. and Hatem, S. 2004. Les MAGUK : au-delà de l'accrochage des canaux ioniques. *MEDECINE/SCIENCES*. **20**, pp.84–92.
- Graus-Porta, D., Beerli, R.R., Daly, J.M. and Hynes, N.E. 1997. ErbB-2, the

preferred heterodimerization partner of all ErbB receptors, is a mediator of lateral signaling. *EMBO Journal*. **16**(7), pp.1647–1655.

Grunewald, T.G., Pasedag, S.M. and Butt, E. 2009. Cell Adhesion and Transcriptional Activity - Defining the Role of the Novel Protooncogene LPP. *Translational oncology*. **2**(3), pp.107–16.

Grunewald, T.G.P., Kammerer, U., Kapp, M., Eck, M., Dietl, J., Butt, E. and Honig, A. 2007. Nuclear localization and cytosolic overexpression of LASP-1 correlates with tumor size and nodal-positivity of human breast carcinoma. *BMC cancer*. **7**, p.198.

Grunewald, T.G.P., Kammerer, U., Schulze, E., Schindler, D., Honig, A., Zimmer, M. and Butt, E. 2006. Silencing of LASP-1 influences zyxin localization, inhibits proliferation and reduces migration in breast cancer cells. *Experimental cell research*. **312**(7), pp.974–82.

Harari, D. and Yarden, Y. 2000. Molecular mechanisms underlying ErbB2/HER2 action in breast cancer. *Oncogene*. **19**(53), pp.6102–6114.

Harmer, S.L. and DeFranco, A.L. 1997. Shc contains two Grb2 binding sites needed for efficient formation of complexes with SOS in B lymphocytes. *Molecular and cellular biology*. **17**(7), pp.4087–95.

Hart, K.C., Robertson, S.C., Kanemitsu, M.Y., Meyer, A.N., Tynan, J.A. and Donoghue, D.J. 2000. Transformation and Stat activation by derivatives of FGFR1, FGFR3, and FGFR4. *Oncogene*. **19**(29), pp.3309–20.

Holbro, T., Beerli, R.R., Maurer, F., Koziczak, M., Barbás, C.F., Hynes, N.E. and Hynes, N.E. 2003. The ErbB2/ErbB3 heterodimer functions as an oncogenic unit: ErbB2 requires ErbB3 to drive breast tumor cell

proliferation. *Proceedings of the National Academy of Sciences of the United States of America*. **100**(15), pp.8933–8.

Holbro, T., Civenni, G. and Hynes, N.E. 2003. The ErbB receptors and their role in cancer progression. *The EGF Receptor Family: Biologic Mechanisms and Role in Cancer*. **284**(1), pp.103–114.

Ishizawar, R.C., Miyake, T. and Parsons, S.J. 2007. c-Src modulates ErbB2 and ErbB3 heterocomplex formation and function. *Oncogene*. **26**(24), pp.3503–3510.

Jacquemier, J., Adelaide, J., Parc, P., Penault-Llorca, F., Planche, J., Delapeyriere, O. and Birnbaum, D. 1994. Expression of the FGFR1 gene in human breast-carcinoma cells. *International Journal of Cancer*. **59**(3), pp.373–378.

Jang, J.H., Shin, K.H., Park, J.G., Hatch, H., Yashiro, M., Bacco, A. Di, Elbi, C. and Lutterbach, B. 2001. Mutations in fibroblast growth factor receptor 2 and fibroblast growth factor receptor 3 genes associated with human gastric and colorectal cancers. *Cancer research*. **61**(9), pp.3541–3.

Janni, W., Sarosiek, T., Karaszewska, B., Pikiel, J., Staroslawska, E., Potemski, P., Salat, C., Brain, E., Caglevic, C., Briggs, K., Mahood, K., DeSilvio, M., Marini, L. and Papadimitriou, C. 2015. Final overall survival analysis of a phase II trial evaluating vinorelbine and lapatinib in women with ErbB2 overexpressing metastatic breast cancer. *The Breast*. **24**(6), pp.769–773.

Jura, N., Endres, N.F., Engel, K., Deindl, S., Das, R., Lamers, M.H., Wemmer, D.E., Zhang, X. and Kuriyan, J. 2009. Mechanism for

activation of the EGF receptor catalytic domain by the juxtamembrane segment. *Cell*. **137**(7), pp.1293–307.

K. A. Schafer 1998. The Cell Cycle: A review. *Veterinary Pathology*. **35**, pp.461–478.

Katoh, M. 1992. Cancer genomics and genetics of FGFR2 (Review). *International Journal of Oncology*. **33**(2), pp.233–237.

Katoh, M. 2009. FGFR2 Abnormalities Underlie a Spectrum of Bone, Skin, and Cancer Pathologies. *Journal of Investigative Dermatology*. **129**(8), pp.1861–1867.

Keicher, C., Gambaryan, S., Schulze, E., Marcus, K., Meyer, H.E. and Butt, E. 2004. Phosphorylation of mouse LASP-1 on threonine 156 by cAMP- and cGMP-dependent protein kinase. *Biochemical and Biophysical Research Communications*. **324**(1), pp.308–316.

Kim, H., Chan, R., Dankort, D.L., Zuo, D., Najoukas, M., Park, M. and Muller, W.J. 2005. The c-Src tyrosine kinase associates with the catalytic domain of ErbB-2: implications for ErbB-2 mediated signaling and transformation. *Oncogene*. **24**, pp.7599–7607.

Knighton, D.R., Zheng, J.H., Ten Eyck, L.F., Ashford, V.A., Xuong, N.H., Taylor, S.S. and Sowadski, J.M. 1991. Crystal structure of the catalytic subunit of cyclic adenosine monophosphate-dependent protein kinase. *Science (New York, N.Y.)*. **253**(5018), pp.407–14.

Kohda, D., Hatanaka, H., Odaka, M., Mandiyan, V., Ullrich, a, Schlessinger, J. and Inagaki, F. 1993. Solution structure of the SH3 domain of phospholipase C-gamma. *Cell*. **72**(6), pp.953–960.

- Kouhara, H., Hadari, Y.R., Spivak-Kroizman, T., Schilling, J., Bar-Sagi, D., Lax, I. and Schlessinger, J. 1997. A lipid-anchored Grb2-binding protein that links FGF-receptor activation to the Ras/MAPK signaling pathway. *Cell*. **89**(5), pp.693–702.
- Kovalevich, J. and Langford, D. 2013. Considerations for the use of SH-SY5Y neuroblastoma cells in neurobiology. *Methods in molecular biology (Clifton, N.J.)*. **1078**, pp.9–21.
- Kunii, K., Davis, L., Gorenstein, J., Hatch, H., Yashiro, M., Di Bacco, A., Elbi, C. and Lutterbach, B. 2008. FGFR2-amplified gastric cancer cell lines require FGFR2 and Erbb3 signaling for growth and survival. *Cancer Research*. **68**(7), pp.2340–2348.
- Kurochkina, N. and Guha, U. 2013. SH3 domains: modules of protein-protein interactions. *Biophysical reviews*. **5**(1), pp.29–39.
- Kwiatkowski, A. V, Gertler, F.B. and Loureiro, J.J. 2003. Function and regulation of Ena/VASP proteins. *Trends in cell biology*. **13**(7), pp.386–92.
- L. Geczy, C., Hsu, K., Sorci, G., Riuzzi, F., R. Cannon, B., J. Weber, D. and Donato, R. 2012. Functions of S100 Proteins. *Current Molecular Medicine*. **13**(1), pp.24–57.
- Ladbury, J.E. and Arold, S. 2000. Searching for specificity in SH domains. *Chemistry and Biology*. **7**(1), pp.3–8.
- LaVallee, T.M., Maciag, T., Burgess, W.H., Jackson, A., Tarantini, F., Hampton, B., Carreira, C.M. and Lathrop, J.T. 2002. S100A13 Is Involved in the Regulation of Fibroblast Growth Factor-1 and p40

- Synaptotagmin-1 Release in Vitro. *Journal of Biological Chemistry*. **273**(35), pp.22224–22231.
- Lemmon, M.A. and Schlessinger, J. 2010. Cell signaling by receptor-tyrosine kinases. *Cell*. **141**(7), pp.1117–1134.
- Leung, H.Y. and Neal, D.E. 1997. Fibroblast Growth Factor Receptor (FGFR). *Emerging Therapeutic Targets*. **1**(1), pp.173–175.
- Li, B., Zhuang, L. and Trueb, B. 2004. Zyxin Interacts with the SH3 Domains of the Cytoskeletal Proteins LIM-nebulette and Lasp-1. *Journal of Biological Chemistry*. **279**(19), pp.20401–20410.
- Lin, C.C., Melo, F. a., Ghosh, R., Suen, K.M., Stagg, L.J., Kirkpatrick, J., Arold, S.T., Ahmed, Z. and Ladbury, J.E. 2012. Inhibition of basal FGF receptor signaling by dimeric Grb2. *Cell*. **149**(7), pp.1514–1524.
- Lin, Y.H., Park, Z.-Y., Lin, D., Brahmbhatt, A.A., Rio, M.-C., Yates, J.R., Klemke, R.L. and Klemke, R.L. 2004. Regulation of cell migration and survival by focal adhesion targeting of Lasp-1. *The Journal of cell biology*. **165**(3), pp.421–32.
- Linggi, B. and Carpenter, G. 2006. ErbB receptors: new insights on mechanisms and biology. *Trends in Cell Biology*. **16**(12), pp.649–656.
- Macdonald, A., Crowder, K., Street, A., McCormick, C. and Harris, M. 2004. The hepatitis C virus NS5A protein binds to members of the Src family of tyrosine kinases and regulates kinase activity. *The Journal of general virology*. **85**(2004), pp.721–729.
- Macdonald, A., Mazaleyrat, S., McCormick, C., Street, A., Burgoyne, N.J., Jackson, R.M., Cazeaux, V., Shelton, H., Saksela, K. and Harris, M.

2005. Further studies on hepatitis C virus NS5A-SH3 domain interactions: Identification of residues critical for binding and implications for viral RNA replication and modulation of cell signalling. *Journal of General Virology*. **86**(4), pp.1035–1044.

Madsen, P., Rasmussen, H.H., Leffers, H., Honoré, B., Dejgaard, K., Olsen, E., Kiil, J., Walbum, E., Andersen, A.H. and Basse, B. 1991. Molecular cloning, occurrence, and expression of a novel partially secreted protein "psoriasin" that is highly up-regulated in psoriatic skin. *The Journal of investigative dermatology*. **97**(4), pp.701–12.

Marcotte, R., Zhou, L., Kim, H., Roskelly, C.D. and Muller, W.J. 2009. c-Src Associates with ErbB2 through an Interaction between Catalytic Domains and Confers Enhanced Transforming Potential. *MOLECULAR AND CELLULAR BIOLOGY*. **29**(21), pp.5858–5871.

di Martino, E., L'Hôte, C.G., Kennedy, W., Tomlinson, D.C. and Knowles, M.A. 2009. Mutant fibroblast growth factor receptor 3 induces intracellular signaling and cellular transformation in a cell type- and mutation-specific manner. *Oncogene*. **28**(48), pp.4306–16.

Maruyama, I.N. 2014. Mechanisms of activation of receptor tyrosine kinases: monomers or dimers. *Cells*. **3**(2), pp.304–30.

Masaki, T., Okada, M., Tokuda, M., Shiratori, Y., Hatase, O., Shirai, M., Nishioka, M. and Omata, M. 1999. Reduced C-terminal Src kinase (Csk) activities in hepatocellular carcinoma. *Hepatology*. **29**(2), pp.379–384.

Mayer, B.J. 2001. SH3 domains: complexity in moderation. *Journal of cell science*. **114**(Pt 7), pp.1253–1263.

- Mayer, M.P. and Bukau, B. 2005. Hsp70 chaperones: Cellular functions and molecular mechanism. *Cellular and Molecular Life Sciences*. **62**(6), pp.670–684.
- McCarley, D.J., Schatzman, R.C., Maa, M.C., Leu, T.H. and Parsons, S.J. 2006. Potentiation of epidermal growth factor receptor-mediated oncogenesis by c-Src: implications for the etiology of multiple human cancers. *Proceedings of the National Academy of Sciences*. **92**(15), pp.6981–6985.
- Miao, G.G., Curran, T., Chew, C.S., Carragher, N.O., Scott-Carragher, L.A., Yuan, Z., Croft, D.R., Olson, M.F., Frame, M. and Ozanne, B.W. 1994. Cell transformation by c-fos requires an extended period of expression and is independent of the cell cycle. *Molecular and cellular biology*. **14**(6), pp.4295–310.
- Mihlan, S., Reiß, C., Thalheimer, P., Herterich, S., Gaetzner, S., Kremerskothen, J., Pavenstädt, H.J., Lewandrowski, U., Sickmann, A. and Butt, E. 2013. Nuclear import of LASP-1 is regulated by phosphorylation and dynamic protein-protein interactions. *Oncogene*. **32**(16), pp.2107–2113.
- Miki, T., Bottaro, D.P., Fleming, T.P., Smith, C.L., Burgess, W.H., Chan, A.M. and Aaronson, S.A. 1992. Determination of ligand-binding specificity by alternative splicing: two distinct growth factor receptors encoded by a single gene. *Proceedings of the National Academy of Sciences of the United States of America*. **89**(1), pp.246–50.
- Moasser, M.M. 2007. The oncogene HER2: Its signaling and transforming functions and its role in human cancer pathogenesis. *Oncogene*. **26**(45),

pp.6469–6487.

Muthuswamy, S.K., Li, D., Lelievre, S., Bissell, M.J. and Brugge, J.S. 2001.

ErbB2, but not ErbB1, reinitiates proliferation and induces luminal repopulation in epithelial acini. *Nature cell biology*. **3**(9), pp.785–92.

Muthuswamy, S.K. and Muller, W.J. 1995. Direct and specific interaction of

c-Src with Neu is involved in signaling by the epidermal growth factor receptor. *Oncogene*. **11**(2), pp.271–9.

Muthuswamy, S.K., Siegel, P.M., Dankort, D.L., Webster, M.A. and Muller,

W.J. 1994. Mammary Tumors Expressing the neu Proto-oncogene Possess Elevated c-Src Tyrosine Kinase Activity. *Molecular and Cellular Biology*. **14**(1), pp.735–743.

Nakatani, H., Sakamoto, H., Yoshida, T., Yokota, J., Tahara, E., Sugimura,

T. and Terada, M. 1990. Isolation of an amplified DNA sequence in stomach cancer. *Japanese journal of cancer research : Gann*. **81**(8), pp.707–10.

Nolen, B., Taylor, S. and Ghosh, G. 2004. Regulation of Protein Kinases:

Controlling Activity through Activation Segment Conformation. *Molecular Cell*. **15**(5), pp.661–675.

Okamoto, C.T., Li, R., Zhang, Z., Jeng, Y.Y. and Chew, C.S. 2002.

Regulation of protein and vesicle trafficking at the apical membrane of epithelial cells. *Journal of controlled release : official journal of the Controlled Release Society*. **78**(1–3), pp.35–41.

Ong, S.H., Guy, G.R., Hadari, Y.R., Laks, S., Gotoh, N., Schlessinger, J. and

Lax, I. 2000a. FRS2 proteins recruit intracellular signaling pathways by

binding to diverse targets on fibroblast growth factor and nerve growth factor receptors. *Molecular and cellular biology*. **20**(3), pp.979–89.

Ong, S.H., Guy, G.R., Hadari, Y.R., Laks, S., Gotoh, N., Schlessinger, J. and Lax, I. 2000b. FRS2 proteins recruit intracellular signaling pathways by binding to diverse targets on fibroblast growth factor and nerve growth factor receptors. *Molecular and cellular biology*. **20**(3), pp.979–89.

Ornitz, D.M. and Itoh, N. 2001. Fibroblast growth factors. *Genome*. **2**(3), pp.1–12.

Ornitz, D.M. and Itoh, N. 2015. The Fibroblast Growth Factor signaling pathway. *Wiley Interdisciplinary Reviews: Developmental Biology*. **4**(3), pp.215–266.

Orth, M.F., Cazes, A., Butt, E. and Grunewald, T.G.P. 2014. An update on the LIM and SH3 domain protein 1 (LASP1): a versatile structural , signaling , and biomarker protein. . **6**(1).

Parsons, S.J. and Parsons, J.T. 2004. Src family kinases, key regulators of signal transduction. *Oncogene*. **23**(48), pp.7906–7909.

Peters, K.G., Marie, J., Wilson, E., Ives, H.E., Escobedo, J., Rosario, M. Del, Mirda, D. and Williams, L.T. 1992. Point mutation of an FGF receptor abolishes phosphatidylinositol turnover and Ca²⁺ flux but not mitogenesis. *Nature*. **358**(6388), pp.678–681.

Pohlmann, P.R., Mayer, I.A. and Mernaugh, R. 2009. Resistance to Trastuzumab in Breast Cancer. *Clinical cancer research : an official journal of the American Association for Cancer Research*. **15**(24), pp.7479–7491.

- Rachlin, A.S. and Otey, C.A. 2006. Identification of palladin isoforms and characterization of an isoform-specific interaction between Lasp-1 and palladin. *Journal of Cell Science*. **119**(6), pp.995–1004.
- Ram, T.G. and Ethier, S.P. 1996. Phosphatidylinositol 3-kinase recruitment by p185erbB-2 and erbB-3 is potently induced by neu differentiation factor/hereregulin during mitogenesis and is constitutively elevated in growth factor-independent breast carcinoma cells with c-erbB-2 gene amplification. *Cell growth & differentiation : the molecular biology journal of the American Association for Cancer Research*. **7**(5), pp.551–61.
- Raman, D., Sai, J., Neel, N.F., Chew, C.S. and Richmond, A. 2010. LIM and SH3 Protein -1 Modulates CXCR2-Mediated Cell Migration. *PLoS ONE*. **5**(4).
- Red Brewer, M., Choi, S.H., Alvarado, D., Moravcevic, K., Pozzi, A., Lemmon, M.A. and Carpenter, G. 2009. The juxtamembrane region of the EGF receptor functions as an activation domain. *Molecular cell*. **34**(6), pp.641–51.
- Redfern, R.E., Redfern, D., Furgason, M.L.M., Munson, M., Ross, A.H. and Gericke, A. 2008. PTEN phosphatase selectively binds phosphoinositides and undergoes structural changes. *Biochemistry*. **47**(7), pp.2162–71.
- Riaz, M., van Jaarsveld, M.T.M., Hollestelle, A., Prager-van der Smissen, W.J.C., Heine, A.A.J., Boersma, A.W.M., Liu, J., Helmijr, J., Ozturk, B., Smid, M., Wiemer, E.A., Foekens, J.A. and Martens, J.W.M. 2013. miRNA expression profiling of 51 human breast cancer cell lines reveals subtype and driver mutation-specific miRNAs. *Breast cancer research :*

BCR. **15**(2), p.R33.

Robinson, D.R., Wu, Y.-M. and Lin, S.-F. 2000. The protein tyrosine kinase family of the human genome. *Oncogene*. **19**(49), pp.5548–5557.

Roskoski, R. 2012. ERK1/2 MAP kinases: Structure, function, and regulation. *Pharmacological Research*. **66**(2), pp.105–143.

Roskoski, R. 2004. Src protein-tyrosine kinase structure and regulation. *Biochemical and Biophysical Research Communications*. **324**(4), pp.1155–1164.

Roumiantsev, S., Krause, D.S., Neumann, C.A., Dimitri, C.A., Asiedu, F., Cross, N.C.P. and Van Etten, R.A. 2004. Distinct stem cell myeloproliferative/T lymphoma syndromes induced by ZNF198-FGFR1 and BCR-FGFR1 fusion genes from 8p11 translocations. *Cancer cell*. **5**(3), pp.287–98.

Roux, K.J., Kim, D.I. and Burke, B. 2013. BioID: a screen for protein-protein interactions. *Current protocols in protein science*. **74**, Unit 19.23.

Sam, M.R., Elliott, B.E. and Mueller, C.R. 2007. A novel activating role of SRC and STAT3 on HGF transcription in human breast cancer cells. *Molecular cancer*. **6**, p.69.

Schlessinger, J. 1994. SH2/SH3 signaling proteins. *Current Opinion in Genetics and Development*. **4**(1), pp.25–30.

Schreiber, V., Moog-Lutz, C., Regnier, C.H., Chenard, M.-P., Boeuf, H., Vonesch, J.-L., Tomasetto, C. and Rio, M.-C. 1998. Lasp-I, a Novel Type of Actin-Binding Protein Accumulating in Cell Membrane Extensions. *Molecular Medicine*. **4**, pp.675–687.

- Schulze, W.X., Deng, L. and Mann, M. 2005. Phosphotyrosine interactome of the ErbB-receptor kinase family. *Molecular Systems Biology*. **25**.
- Sheffield, L.G. 1998. C-Src Activation by ErbB2 Leads to Attachment-Independent Growth of Human Breast Epithelial Cells. *Biochemical and Biophysical Research Communications*. **250**(1), pp.27–31.
- Slamon, D.J., Clark, G.M., Wong, S.G., Levin, W.J., Ullrich, A. and McGuire, W.L. n.d. Human Breast Cancer: Correlation of Relapse and Survival with Amplification of the HER-2/neu Oncogene.
- Sleeman, M., Fraser, J., McDonald, M., Yuan, S., White, D., Grandison, P., Kumble, K., Watson, J.D. and Murison, J.G. 2001. Identification of a new fibroblast growth factor receptor, FGFR5. *Gene*. **271**(2), pp.171–182.
- Stehelin, D., Fujita, D.J., Padgett, T., Varmus, H.E. and Bishop, J.M. 1977. Detection and enumeration of transformation-defective strains of avian sarcoma virus with molecular hybridization. *Virology*. **76**(2), pp.675–84.
- Stephens, P., Ekins, S., Davies, H., Greenman, C., Cox, C., Hunter, C., Bignell, G., Teague, J., Smith, R., Stevens, C., O'Meara, S., Parker, A., Tarpey, P., Avis, T., Barthorpe, A., Brackenbury, L., Buck, G., Butler, A., Clements, J., Cole, J., Dicks, E., Edwards, K., Forbes, S., Gorton, M., Gray, K., Halliday, K., Harrison, R., Hills, K., Hinton, J., Jones, D., Kosmidou, V., Laman, R., Lugg, R., Menzies, A., Perry, J., Petty, R., Raine, K., Shepherd, R., Small, A., Solomon, H., Stephens, Y., Tofts, C., Varian, J., Webb, A., West, S., Widaa, S., Yates, A., Brasseur, F., Cooper, C.S., Flanagan, A.M., Green, A., Knowles, M., Leung, S.Y., Looijenga, L.H.J., Malkowicz, B., Pierotti, M.A., Teh, B., Yuen, S.T.,

- Nicholson, A.G., Lakhani, S., Easton, D.F., Weber, B.L., Stratton, M.R., Futreal, P.A. and Wooster, R. 2005. A screen of the complete protein kinase gene family identifies diverse patterns of somatic mutations in human breast cancer. *Nature Genetics*. **37**(6), pp.590–592.
- Sun, G., Ramdas, L., Wang, W., Vinci, J., McMurray, J. and Budde, R.J.A. 2001. Effect of Autophosphorylation on the Catalytic and Regulatory Properties of Protein Tyrosine Kinase Src.
- Taylor, S.J. and Shalloway, D. 1994. An RNA-binding protein associated with Src through its SH2 and SH3 domains in mitosis. *Nature*. **368**(6474), pp.867–871.
- Teyra, J., Huang, H., Jain, S., Guan, X., Dong, A., Liu, Y., Tempel, W., Min, J., Tong, Y., Kim, P.M., Bader, G.D. and Sidhu, S.S. 2017. Comprehensive Analysis of the Human SH3 Domain Family Reveals a Wide Variety of Non-canonical Specificities. *Structure*.
- Tifft, K.E., Bradbury, K.A. and Wilson, K.L. 2009. Tyrosine phosphorylation of nuclear-membrane protein emerin by Src, Abl and other kinases. *Journal of Cell Science*. **122**(20), pp.3780–3790.
- Timsah, Z., Ahmed, Z., Ivan, C., Berrout, J., Gagea, M., Zhou, Y., Pena, G.N. a, Hu, X., Vallien, C., Kingsley, C. V, Lu, Y., Hancock, J.F., Liu, J., Gladden, a B., Mills, G.B., Lopez-Berestein, G., Hung, M.-C., Sood, a K., Bogdanov, M. and Ladbury, J.E. 2015. Grb2 depletion under non-stimulated conditions inhibits PTEN, promotes Akt-induced tumor formation and contributes to poor prognosis in ovarian cancer. *Oncogene*. (May), pp.1–11.
- Timsah, Z., Ahmed, Z., Lin, C.-C., Melo, F. a, Stagg, L.J., Leonard, P.G.,

- Jeyabal, P., Berrout, J., O'Neil, R.G., Bogdanov, M. and Ladbury, J.E. 2014. Competition between Grb2 and Plc γ 1 for FGFR2 regulates basal phospholipase activity and invasion. *Nature structural & molecular biology*. **21**(2), pp.180–8.
- Tomasetto, C., Moog-Lutz, C., Régnier, C.H., Schreiber, V., Basset, P. and Rio, M.C. 1995. Lasp-1 (MLN 50) defines a new LIM protein subfamily characterized by the association of LIM and SH3 domains. *FEBS letters*. **373**(3), pp.245–9.
- Tomasetto, C., Régnier, C., Moog-Lutz, C., Mattei, M.G., Chenard, M.P., Lidereau, R., Basset, P. and Rio, M.C. 1995. Identification of four novel human genes amplified and overexpressed in breast carcinoma and localized to the q11-q21.3 region of chromosome 17. *Genomics*. **28**(3), pp.367–376.
- Trzaskowski, B., Latek, D., Yuan, S., Ghoshdastider, U., Debinski, A. and Filipek, S. 2012. Action of Molecular Switches in GPCRs - Theoretical and Experimental Studies. *Current Medicinal Chemistry*. **19**(8), pp.1090–1109.
- Turner, N. and Grose, R. 2010. Fibroblast growth factor signalling: from development to cancer. *Nature reviews. Cancer*. **10**(2), pp.116–129.
- Tzahar, E., Waterman, H., Chen, X., Levkowitz, G., Karunagaran, D., Lavi, S., Ratzkin, B.J. and Yarden, Y. 1996. A hierarchical network of interreceptor interactions determines signal transduction by Neu differentiation factor/neuregulin and epidermal growth factor. *Molecular and Cellular Biology*. **16**(10), pp.5276–5287.
- Uings, I.J. and Farrow, S.N. 2000. Cell receptors and cell signalling.

Molecular pathology : MP. **53**(6), pp.295–9.

Vermeulen, K., Bockstaele, D.R. Van and Berneman, Z.N. 2003. The cell cycle: a review of regulation, deregulation and therapeutic targets in cancer. *Cell Prolif.* **36**, pp.131–149.

Vogel, C.L., Cobleigh, M.A., Tripathy, D., Gutheil, J.C., Harris, L.N., Fehrenbacher, L., Slamon, D.J., Murphy, M., Novotny, W.F., Burchmore, M., Shak, S., Stewart, S.J. and Press, M. 2002. Efficacy and safety of trastuzumab as a single agent in first-line treatment of HER2-overexpressing metastatic breast cancer. *Journal of clinical oncology : official journal of the American Society of Clinical Oncology.* **20**(3), pp.719–26.

Wang, Y. and Becker, D. 1997. Antisense targeting of basic fibroblast growth factor and fibroblast growth factor receptor-1 in human melanomas blocks intratumoral angiogenesis and tumor growth. *Nature medicine.* **3**(8), pp.887–93.

Wee, P. and Wang, Z. 2017. Epidermal growth factor receptor cell proliferation signaling pathways. *Cancers.* **9**(5), pp.1–45.

Wildenhain, Y., Pawson, T., Blackstein, M.E. and Andrulis, I.L. 1990. p185neu is phosphorylated on tyrosine in human primary breast tumors which overexpress neu/erbB-2. *Oncogene.* **5**(6), pp.879–83.

Wolfson, E., Goldenberg, M., Solomon, S., Frishberg, A. and Pinkas-Kramarski, R. 2016. Nucleolin-binding by ErbB2 enhances tumorigenicity of ErbB2-positive breast cancer. *Oncotarget.* **7**(40), pp.65320–65334.

- Xiao, S., Nalabolu, S.R., Aster, J.C., Ma, J., Abruzzo, L., Jaffe, E.S., Stone, R., Weissman, S.M., Hudson, T.J. and Fletcher, J.A. 1998. FGFR1 is fused with a novel zinc-finger gene, ZNF198, in the t(8;13) leukaemia/lymphoma syndrome. *Nature Genetics*. **18**(1), pp.84–87.
- Xu, Wenqing, S.C.H.& M.J.E. 1997. Three-dimensional structure of the tyrosine kinase C-Src. *Nature*. **385**, pp.595–602.
- Xu, L., Zhang, Y., Wang, H., Zhang, G., Ding, Y. and Zhao, L. 2014. Tumor suppressor miR-1 restrains epithelial-mesenchymal transition and metastasis of colorectal carcinoma via the MAPK and PI3K/AKT pathway. *Journal of Translational Medicine*. **12**(1).
- Xu, W., Doshi, A., Lei, M., Eck, M.J. and Harrison, S.C. 1999. Crystal structures of c-Src reveal features of its autoinhibitory mechanism. *Molecular Cell*. **3**(5), pp.629–638.
- Xu, W., Yuan, X., Beebe, K., Xiang, Z. and Neckers, L. 2007. Loss of Hsp90 Association Up-Regulates Src-Dependent ErbB2 Activity. *Molecular and Cellular Biology*. **27**(1), pp.220–228.
- Zhan, L., Xiang, B. and Muthuswamy, S.K. 2006. Controlled activation of ErbB1/ErbB2 heterodimers promote invasion of three-dimensional organized epithelia in an ErbB1-dependent manner: implications for progression of ErbB2-overexpressing tumors. *Cancer research*. **66**(10), pp.5201–8.
- Zhang W, L.H. 2002. MAPK signal pathways in the regulation of cell proliferation in mammalian cells. *Cell Res*. **12**, pp.9–18.
- Zheng, X.-M., Resnick, R.J. and Shalloway, D. 2000. A phosphotyrosine

displacement mechanism for activation of Src by PTP α . *The EMBO Journal*. **19**(5), pp.964–978.

Appendix A: All identified proteins from MS screen using peptides with proline-rich motifs from RTKs

ALK-1

Accession	Description	# Proteins	# Unique Peptides	# Peptides	# PSMs	# AAs	MW [kDa]	calc. pI
H6VRF8	Keratin 1 OS=Homo sapiens GN=KRT1 PE=3 SV=1 - [H6VRF8_HUMAN]	16	24	26	105	644	66.0	8.12
P35527	Keratin, type I cytoskeletal 9 OS=Homo sapiens GN=KRT9 PE=1 SV=3 - [K1C9_HUMAN]	2	24	24	100	623	62.0	5.24
P13645	Keratin, type I cytoskeletal 10 OS=Homo sapiens GN=KRT10 PE=1 SV=6 - [K1C10_HUMAN]	25	23	26	83	584	58.8	5.21
P35908	Keratin, type II cytoskeletal 2 epidermal OS=Homo sapiens GN=KRT2 PE=1 SV=2 - [K22E_HUMAN]	14	16	23	53	639	65.4	8.00
P02533	Keratin, type I cytoskeletal 14 OS=Homo sapiens GN=KRT14 PE=1 SV=4 - [K1C14_HUMAN]	41	9	12	46	472	51.5	5.16
P13647	Keratin, type II cytoskeletal 5 OS=Homo sapiens GN=KRT5 PE=1 SV=3 - [K2C5_HUMAN]	19	9	17	24	590	62.3	7.74
B4DRR0	cDNA FLJ53910, highly similar to Keratin, type II cytoskeletal 6A OS=Homo sapiens PE=2 SV=1 - [B4DRR0_HUMAN]	24	2	11	16	535	57.8	8.00
Q6UXS9	Inactive caspase-12 OS=Homo sapiens GN=CASP12 PE=2 SV=2 - [CASPC_HUMAN]	1	1	1	6	341	38.8	6.02
Q45K10	Trypsin I (Fragment) OS=Homo sapiens GN=PRSS1 PE=3 SV=1 - [Q45K10_HUMAN]	17	1	1	4	84	9.2	9.99
Q86YZ3	Hornerin OS=Homo sapiens GN=HRNR PE=1 SV=2 - [HORN_HUMAN]	1	2	2	4	2850	282.2	10.04
Q9GZ28	Extracellular glycoprotein lacritin OS=Homo sapiens GN=LACRT PE=1 SV=1 - [LACRT_HUMAN]	2	3	3	4	138	14.2	5.50
P81605	Dermcidin OS=Homo sapiens GN=DCD PE=1 SV=2 - [DCD_HUMAN]	1	3	3	3	110	11.3	6.54
A0A087WWT3	Serum albumin OS=Homo sapiens GN=ALB PE=1 SV=1 - [A0A087WWT3_HUMAN]	14	3	3	3	396	45.1	6.10
A0A075B6Z2	Protein TRAJ56 (Fragment) OS=Homo sapiens GN=TRAJ56 PE=4 SV=1 - [A0A075B6Z2_HUMAN]	2	1	1	10	21	2.2	10.29
O75556	Mammaglobin-B OS=Homo sapiens GN=SCGB2A1 PE=1 SV=1 - [SG2A1_HUMAN]	1	2	2	2	95	10.9	5.78
B3KX99	cDNA FLJ45019 fis, clone BRAWH3015825 OS=Homo sapiens PE=2 SV=1 - [B3KX99_HUMAN]	2	1	1	3	333	38.5	8.97

F8VV32	Lysozyme OS=Homo sapiens GN=LYZ PE=1 SV=1 - [F8VV32_HUMAN]	3	2	2	2	104	11.5	9.07
H3BUH7	Fructose-bisphosphate aldolase (Fragment) OS=Homo sapiens GN=ALDOA PE=1 SV=1 - [H3BUH7_HUMAN]	19	2	2	2	155	16.9	8.56
Q9HB00	Desmocollin 1, isoform CRA_b OS=Homo sapiens GN=DSC1 PE=4 SV=1 - [Q9HB00_HUMAN]	2	2	2	2	840	93.8	5.53
Q19KS2	Lactoferrin (Fragment) OS=Homo sapiens PE=2 SV=1 - [Q19KS2_HUMAN]	13	2	2	2	353	39.1	9.03
Q8WUW7	Pyruvate kinase (Fragment) OS=Homo sapiens GN=PKM2 PE=2 SV=2 - [Q8WUW7_HUMAN]	8	2	2	3	343	37.3	8.22
Q5VSP4	Putative lipocalin 1-like protein 1 OS=Homo sapiens GN=LCN1P1 PE=5 SV=1 - [LC1L1_HUMAN]	2	2	2	2	162	17.9	5.00
Q5TDG9	DnaJ (Hsp40) homolog, subfamily C, member 16, isoform CRA_a OS=Homo sapiens GN=DNAJC16 PE=1 SV=1 - [Q5TDG9_HUMAN]	4	1	1	2	595	69.3	7.15
F8WF65	Elongation factor 1-beta OS=Homo sapiens GN=EEF1B2 PE=1 SV=1 - [F8WF65_HUMAN]	4	1	1	1	29	3.1	4.46
F8VXZ7	Tubulin alpha-1A chain (Fragment) OS=Homo sapiens GN=TUBA1A PE=4 SV=1 - [F8VXZ7_HUMAN]	22	1	1	1	26	2.7	4.89
J3QSA3	Polyubiquitin-B (Fragment) OS=Homo sapiens GN=UBB PE=1 SV=1 - [J3QSA3_HUMAN]	37	1	1	1	43	4.9	5.19
O95968	Secretoglobin family 1D member 1 OS=Homo sapiens GN=SCGB1D1 PE=1 SV=1 - [SG1D1_HUMAN]	1	1	1	1	90	9.9	9.25
Q86W20	Protease serine 1 (Fragment) OS=Homo sapiens GN=PRSS1 PE=3 SV=1 - [Q86W20_HUMAN]	6	1	1	1	84	9.2	10.27
H0YDD8	60S acidic ribosomal protein P2 (Fragment) OS=Homo sapiens GN=RPLP2 PE=1 SV=1 - [H0YDD8_HUMAN]	2	1	1	1	92	9.1	4.46
B2R4M6	Protein S100 OS=Homo sapiens PE=2 SV=1 - [B2R4M6_HUMAN]	2	1	1	1	114	13.2	6.13
A0A0A0MRQ5	Peroxiredoxin-1 OS=Homo sapiens GN=PRDX1 PE=1 SV=1 - [A0A0A0MRQ5_HUMAN]	6	1	1	1	97	10.7	8.72
Q5D862	Filaggrin-2 OS=Homo sapiens GN=FLG2 PE=1 SV=1 - [FILA2_HUMAN]	1	1	1	1	2391	247.9	8.31
D6R9F0	Leucine-rich repeat-containing G-protein-coupled receptor 6 OS=Homo sapiens GN=LGR6 PE=1 SV=1 - [D6R9F0_HUMAN]	1	1	1	1	348	39.2	7.74
Q15203	Prothymosin alpha OS=Homo sapiens PE=4 SV=2 - [Q15203_HUMAN]	18	1	1	1	73	8.2	3.76
E9PN25	Heat shock cognate 71 kDa protein (Fragment) OS=Homo sapiens GN=HSPA8 PE=1 SV=1 - [E9PN25_HUMAN]	35	1	1	1	132	14.6	6.55
P04080	Cystatin-B OS=Homo sapiens GN=CSTB PE=1 SV=2 - [CYTB_HUMAN]	1	1	1	1	98	11.1	7.56
F8VVB8	Meiosis arrest female protein 1 OS=Homo sapiens GN=KIAA0430 PE=1 SV=1 - [F8VVB8_HUMAN]	2	1	1	1	1037	112.9	8.38
C9IYG1	BRCA1-associated RING domain protein 1 (Fragment) OS=Homo sapiens GN=BARD1 PE=1 SV=1 - [C9IYG1_HUMAN]	9	1	1	1	216	24.4	8.47
B7Z5E7	cDNA FLJ51046, highly similar to 60 kDa heat shock protein, mitochondrial OS=Homo sapiens PE=2 SV=1 - [B7Z5E7_HUMAN]	5	1	1	1	517	55.0	5.60
Q7R7Y7	Ovochymase-1 OS=Homo sapiens GN=OVCH1 PE=2 SV=2 - [OVCH1_HUMAN]	1	1	1	1	1134	125.0	8.32

C9JG98	Probable ATP-dependent RNA helicase DHX58 (Fragment) OS=Homo sapiens GN=DHX58 PE=1 SV=1 - [C9JG98_HUMAN]	5	1	1	1	302	34.0	6.71
A0A0A0MRX7	Transcription factor TFIIIB component B' homolog OS=Homo sapiens GN=BDP1 PE=1 SV=1 - [A0A0A0MRX7_HUMAN]	5	1	1	1	846	95.5	8.15
O00186	Syntaxin-binding protein 3 OS=Homo sapiens GN=STXB3 PE=1 SV=2 - [STXB3_HUMAN]	1	1	1	1	592	67.7	7.80
I3L1H9	Zymogen granule protein 16 homolog B (Fragment) OS=Homo sapiens GN=ZG16B PE=1 SV=1 - [I3L1H9_HUMAN]	5	1	1	1	69	7.5	9.32
H0YGI8	Stress-induced-phosphoprotein 1 (Fragment) OS=Homo sapiens GN=STIP1 PE=1 SV=1 - [H0YGI8_HUMAN]	3	1	1	1	137	15.9	6.19
B7Z1V3	cDNA FLJ54733, highly similar to General transcription factor 3C polypeptide 5 OS=Homo sapiens PE=2 SV=1 - [B7Z1V3_HUMAN]	1	1	1	1	412	45.6	9.45
B7Z5R3	Src family associated phosphoprotein 2, isoform CRA_c OS=Homo sapiens GN=SCAP2 PE=2 SV=1 - [B7Z5R3_HUMAN]	3	1	1	1	187	21.6	4.46
F8WCH0	Actin, gamma-enteric smooth muscle OS=Homo sapiens GN=ACTG2 PE=1 SV=1 - [F8WCH0_HUMAN]	43	1	1	1	52	5.6	6.49
B8ZZ51	Malate dehydrogenase, cytoplasmic OS=Homo sapiens GN=MDH1 PE=1 SV=1 - [B8ZZ51_HUMAN]	3	1	1	1	169	18.7	5.94
A0PJ54	PEX12 protein (Fragment) OS=Homo sapiens GN=PEX12 PE=2 SV=1 - [A0PJ54_HUMAN]	1	1	1	1	324	36.9	9.98
O14594	Neurocan core protein OS=Homo sapiens GN=NCAN PE=1 SV=3 - [NCAN_HUMAN]	2	1	1	1	1321	143.0	5.38
Q96MA3	cDNA FLJ32709 fis, clone TESTI2000695, weakly similar to KINESIN HEAVY CHAIN (Fragment) OS=Homo sapiens PE=2 SV=1 - [Q96MA3_HUMAN]	4	1	1	1	648	73.5	5.31
B4DIJ7	Histone-lysine N-methyltransferase OS=Homo sapiens PE=2 SV=1 - [B4DIJ7_HUMAN]	2	1	1	1	323	37.2	8.78
Q53RS3	Putative uncharacterized protein DDEF2 (Fragment) OS=Homo sapiens GN=DDEF2 PE=4 SV=1 - [Q53RS3_HUMAN]	2	1	1	1	635	69.2	5.74
L0R5A1	Alternative protein CSF2RB OS=Homo sapiens GN=CSF2RB PE=4 SV=1 - [L0R5A1_HUMAN]	1	1	1	1	108	11.6	11.30
Q59EC6	Ret finger protein isoform beta variant (Fragment) OS=Homo sapiens PE=2 SV=1 - [Q59EC6_HUMAN]	1	1	1	1	382	43.4	8.16
G3V3Y2	Fibulin-5 (Fragment) OS=Homo sapiens GN=FBLN5 PE=1 SV=1 - [G3V3Y2_HUMAN]	5	1	1	1	91	9.9	6.37
H0YJY2	Signal-induced proliferation-associated 1-like protein 1 (Fragment) OS=Homo sapiens GN=SIPA1L1 PE=1 SV=5 - [H0YJY2_HUMAN]	1	1	1	1	262	30.3	7.24
F5H6Q3	Ubiquitin carboxyl-terminal hydrolase 28 (Fragment) OS=Homo sapiens GN=USP28 PE=1 SV=1 - [F5H6Q3_HUMAN]	2	1	1	1	46	5.3	8.57
B3KQA6	cDNA FLJ90055 fis, clone HEMBA1003047, highly similar to Cubilin OS=Homo sapiens PE=2 SV=1 - [B3KQA6_HUMAN]	4	1	1	1	350	38.7	5.60
B4E0Q6	cDNA FLJ60209, highly similar to Transcriptional repressor p66 alpha OS=Homo sapiens PE=2 SV=1 - [B4E0Q6_HUMAN]	1	1	1	1	262	28.6	9.95
A0A0A0MTR7	E3 ubiquitin-protein ligase RNF213 OS=Homo sapiens GN=RNF213 PE=1 SV=1 - [A0A0A0MTR7_HUMAN]	3	1	1	1	5207	591.0	6.48

A0A0A7UX25	MHC class I antigen (Fragment) OS=Homo sapiens GN=HLA-C PE=3 SV=1 - [A0A0A7UX25_HUMAN]	1	1	1	1	91	10.6	5.01
------------	----------------------------------------------------------------------------------------	---	---	---	---	----	------	------

ALK-2

Accession	Description	# Proteins	# Unique Peptides	# Peptides	# PSMs	# AAs	MW [kDa]	calc . pI
P35527	Keratin, type I cytoskeletal 9 OS=Homo sapiens GN=KRT9 PE=1 SV=3 - [K1C9_HUMAN]	2	24	24	138	623	62.0	5.24
H6VRF8	Keratin 1 OS=Homo sapiens GN=KRT1 PE=3 SV=1 - [H6VRF8_HUMAN]	16	27	32	148	644	66.0	8.12
P13645	Keratin, type I cytoskeletal 10 OS=Homo sapiens GN=KRT10 PE=1 SV=6 - [K1C10_HUMAN]	22	24	27	106	584	58.8	5.21
P35908	Keratin, type II cytoskeletal 2 epidermal OS=Homo sapiens GN=KRT2 PE=1 SV=2 - [K22E_HUMAN]	7	18	26	68	639	65.4	8.00
P02533	Keratin, type I cytoskeletal 14 OS=Homo sapiens GN=KRT14 PE=1 SV=4 - [K1C14_HUMAN]	36	7	17	52	472	51.5	5.16
P08779	Keratin, type I cytoskeletal 16 OS=Homo sapiens GN=KRT16 PE=1 SV=4 - [K1C16_HUMAN]	32	6	14	50	473	51.2	5.05
P13647	Keratin, type II cytoskeletal 5 OS=Homo sapiens GN=KRT5 PE=1 SV=3 - [K2C5_HUMAN]	16	10	19	35	590	62.3	7.74
B4DRR0	cDNA FLJ53910, highly similar to Keratin, type II cytoskeletal 6A OS=Homo sapiens PE=2 SV=1 - [B4DRR0_HUMAN]	18	3	13	28	535	57.8	8.00
Q0IIN1	Keratin 77 OS=Homo sapiens GN=KRT77 PE=1 SV=1 - [Q0IIN1_HUMAN]	7	4	7	20	578	61.8	5.85
Q04695	Keratin, type I cytoskeletal 17 OS=Homo sapiens GN=KRT17 PE=1 SV=2 - [K1C17_HUMAN]	26	1	8	11	432	48.1	5.02
Q14CN4	Keratin, type II cytoskeletal 72 OS=Homo sapiens GN=KRT72 PE=1 SV=2 - [K2C72_HUMAN]	7	1	4	12	511	55.8	6.89
F6KPG5	Albumin (Fragment) OS=Homo sapiens PE=2 SV=1 - [F6KPG5_HUMAN]	14	7	7	9	585	66.5	6.04
Q6KB66	Keratin, type II cytoskeletal 80 OS=Homo sapiens GN=KRT80 PE=1 SV=2 - [K2C80_HUMAN]	9	1	2	5	452	50.5	5.67
O75556	Mammaglobin-B OS=Homo sapiens GN=SCGB2A1 PE=1 SV=1 - [SG2A1_HUMAN]	1	2	2	3	95	10.9	5.78

B2MV14	Truncated lactoferrin OS=Homo sapiens GN=LTF PE=3 SV=1 - [B2MV14_HUMAN]	16	6	6	7	585	64.2	8.0 7
Q45KI0	Trypsin I (Fragment) OS=Homo sapiens GN=PRSS1 PE=3 SV=1 - [Q45KI0_HUMAN]	17	1	1	3	84	9.2	9.9 9
Q8N1N4	Keratin, type II cytoskeletal 78 OS=Homo sapiens GN=KRT78 PE=2 SV=2 - [K2C78_HUMAN]	3	3	3	5	520	56.8	6.0 2
F8WF65	Elongation factor 1-beta OS=Homo sapiens GN=EEF1B2 PE=1 SV=1 - [F8WF65_HUMAN]	4	1	1	3	29	3.1	4.4 6
Q9HB00	Desmocollin 1, isoform CRA_b OS=Homo sapiens GN=DSC1 PE=4 SV=1 - [Q9HB00_HUMAN]	2	3	3	4	840	93.8	5.5 3
O95968	Secretoglobin family 1D member 1 OS=Homo sapiens GN=SCGB1D1 PE=1 SV=1 - [SG1D1_HUMAN]	1	2	2	4	90	9.9	9.2 5
Q9GZZ8	Extracellular glycoprotein lacritin OS=Homo sapiens GN=LACRT PE=1 SV=1 - [LACRT_HUMAN]	2	3	3	3	138	14.2	5.5 0
A0A0C4 DGN4	Zymogen granule protein 16 homolog B OS=Homo sapiens GN=ZG16B PE=1 SV=1 - [A0A0C4DGN4_HUMAN]	5	2	2	2	178	19.6	5.9 5
P81605	Dermcidin OS=Homo sapiens GN=DCD PE=1 SV=2 - [DCD_HUMAN]	1	3	3	3	110	11.3	6.5 4
J3QSA3	Polyubiquitin-B (Fragment) OS=Homo sapiens GN=UBB PE=1 SV=1 - [J3QSA3_HUMAN]	37	1	1	2	43	4.9	5.1 9
F8VV32	Lysozyme OS=Homo sapiens GN=LYZ PE=1 SV=1 - [F8VV32_HUMAN]	3	3	3	4	104	11.5	9.0 7
Q5VSP4	Putative lipocalin 1-like protein 1 OS=Homo sapiens GN=LCN1P1 PE=5 SV=1 - [LC1L1_HUMAN]	2	2	2	3	162	17.9	5.0 0
Q99456	Keratin, type I cytoskeletal 12 OS=Homo sapiens GN=KRT12 PE=1 SV=1 - [K1C12_HUMAN]	1	1	2	3	494	53.5	4.7 8
A0A0A0 MRX7	Transcription factor TFIIIB component B" homolog OS=Homo sapiens GN=BDP1 PE=1 SV=1 - [A0A0A0MRX7_HUMAN]	5	1	1	3	846	95.5	8.1 5
B3KX99	cDNA FLJ45019 fis, clone BRAWH3015825 OS=Homo sapiens PE=2 SV=1 - [B3KX99_HUMAN]	2	1	1	4	333	38.5	8.9 7
Q6UXS9	Inactive caspase-12 OS=Homo sapiens GN=CASP12 PE=2 SV=2 - [CASPC_HUMAN]	1	1	1	2	341	38.8	6.0 2
P25311	Zinc-alpha-2-glycoprotein OS=Homo sapiens GN=AZGP1 PE=1 SV=2 - [ZA2G_HUMAN]	3	2	2	2	298	34.2	6.0 5
A9UFC0	Caspase 14 OS=Homo sapiens GN=CASP14 PE=2 SV=1 - [A9UFC0_HUMAN]	2	2	2	2	242	27.6	5.3 4
A0A075 B6Z2	Protein TRAJ56 (Fragment) OS=Homo sapiens GN=TRAJ56 PE=4 SV=1 - [A0A075B6Z2_HUMAN]	2	1	1	1 0	21	2.2	10. 29
Q86YZ3	Hornerin OS=Homo sapiens GN=HRNR PE=1 SV=2 - [HORN_HUMAN]	1	1	1	1	2850	282. 2	10. 04

H0YDD8	60S acidic ribosomal protein P2 (Fragment) OS=Homo sapiens GN=RPLP2 PE=1 SV=1 - [H0YDD8_HUMAN]	2	1	1	1	92	9.1	4.4 6
J3KSP2	60S ribosomal protein L38 (Fragment) OS=Homo sapiens GN=RPL38 PE=1 SV=1 - [J3KSP2_HUMAN]	4	1	1	1	21	2.6	9.9 9
Q86W20	Protease serine 1 (Fragment) OS=Homo sapiens GN=PRSS1 PE=3 SV=1 - [Q86W20_HUMAN]	6	1	1	1	84	9.2	10. 27
P12273	Prolactin-inducible protein OS=Homo sapiens GN=PIP PE=1 SV=1 - [PIP_HUMAN]	1	1	1	1	146	16.6	8.0 5
E5RGE1	14-3-3 protein zeta/delta (Fragment) OS=Homo sapiens GN=YWHAZ PE=1 SV=5 - [E5RGE1_HUMAN]	8	1	1	1	52	5.9	4.7 8
Q5HY57	Emerin OS=Homo sapiens GN=EMD PE=1 SV=1 - [Q5HY57_HUMAN]	2	1	1	1	219	24.9	5.0 2
E7EN95	Filamin-B OS=Homo sapiens GN=FLNB PE=1 SV=1 - [E7EN95_HUMAN]	4	1	1	1	2409	256. 1	5.7 3
Q5D862	Filaggrin-2 OS=Homo sapiens GN=FLG2 PE=1 SV=1 - [FILA2_HUMAN]	1	1	1	1	2391	247. 9	8.3 1
Q8NFZ8	Cell adhesion molecule 4 OS=Homo sapiens GN=CADM4 PE=1 SV=1 - [CADM4_HUMAN]	1	1	1	1	388	42.8	6.3 0
L8ECQ7	Alternative protein C10orf112 OS=Homo sapiens GN=C10orf112 PE=4 SV=1 - [L8ECQ7_HUMAN]	1	1	1	1	130	14.3	10. 02
F8WCH0	Actin, gamma-enteric smooth muscle OS=Homo sapiens GN=ACTG2 PE=1 SV=1 - [F8WCH0_HUMAN]	43	1	1	1	52	5.6	6.4 9
G3V361	Calmodulin (Fragment) OS=Homo sapiens GN=CALM1 PE=1 SV=1 - [G3V361_HUMAN]	8	1	1	1	98	11.1	4.2 5
B7Z1V3	cDNA FLJ54733, highly similar to General transcription factor 3C polypeptide 5 OS=Homo sapiens PE=2 SV=1 - [B7Z1V3_HUMAN]	1	1	1	1	412	45.6	9.4 5
O43283	Mitogen-activated protein kinase kinase kinase 13 OS=Homo sapiens GN=MAP3K13 PE=1 SV=1 - [M3K13_HUMAN]	1	1	1	1	966	108. 2	6.4 9
S4R457	Heterogeneous nuclear ribonucleoprotein K OS=Homo sapiens GN=HNRNPK PE=1 SV=1 - [S4R457_HUMAN]	8	1	1	1	77	8.8	4.8 8
K7EMM8	Putative oxidoreductase GLYR1 (Fragment) OS=Homo sapiens GN=GLYR1 PE=1 SV=2 - [K7EMM8_HUMAN]	4	1	1	1	524	57.3	9.2 3
Q15203	Prothymosin alpha OS=Homo sapiens PE=4 SV=2 - [Q15203_HUMAN]	18	1	1	1	73	8.2	3.7 6
A0A0A0MRQ0	Tetratricopeptide repeat protein 39A OS=Homo sapiens GN=TTC39A PE=1 SV=1 - [A0A0A0MRQ0_HUMAN]	4	1	1	1	426	48.3	7.0 8
E9PN25	Heat shock cognate 71 kDa protein (Fragment) OS=Homo sapiens GN=HSPA8 PE=1 SV=1 - [E9PN25_HUMAN]	35	1	1	1	132	14.6	6.5 5
P31151	Protein S100-A7 OS=Homo sapiens GN=S100A7 PE=1 SV=4 - [S10A7_HUMAN]	1	1	1	1	101	11.5	6.7 7

B7Z5E7	cDNA FLJ51046, highly similar to 60 kDa heat shock protein, mitochondrial OS=Homo sapiens PE=2 SV=1 - [B7Z5E7_HUMAN]	5	1	1	1	517	55.0	5.6 0
Q15461	Pregnancy-specific beta-1 glycoprotein-11 (Fragment) OS=Homo sapiens GN=PSG11 PE=4 SV=1 - [Q15461_HUMAN]	10	1	1	1	236	26.8	7.4 4
P05109	Protein S100-A8 OS=Homo sapiens GN=S100A8 PE=1 SV=1 - [S100A8_HUMAN]	1	1	1	1	93	10.8	7.0 3
F8VRZ4	Tubulin alpha-1A chain (Fragment) OS=Homo sapiens GN=TUBA1A PE=4 SV=1 - [F8VRZ4_HUMAN]	15	1	1	1	112	12.2	5.7 7
C9JCF9	WD repeat-containing protein 81 (Fragment) OS=Homo sapiens GN=WDR81 PE=1 SV=1 - [C9JCF9_HUMAN]	2	1	1	1	172	18.7	9.6 3
A8KA05	Protein argonaute-3 OS=Homo sapiens GN=EIF2C3 PE=2 SV=1 - [A8KA05_HUMAN]	1	1	1	1	860	97.3	9.1 1
Q16478	Glutamate receptor ionotropic, kainate 5 OS=Homo sapiens GN=GRIK5 PE=2 SV=2 - [GRIK5_HUMAN]	1	1	1	1	980	109. 2	8.2 1
P12004	Proliferating cell nuclear antigen OS=Homo sapiens GN=PCNA PE=1 SV=1 - [PCNA_HUMAN]	3	1	1	1	261	28.8	4.6 9
H7C5S2	Sarcolemmal membrane-associated protein (Fragment) OS=Homo sapiens GN=SLMAP PE=1 SV=1 - [H7C5S2_HUMAN]	8	1	1	1	65	7.4	5.2 4
V9HWK3	Carboxylic ester hydrolase OS=Homo sapiens GN=HEL126 PE=2 SV=1 - [V9HWK3_HUMAN]	3	1	1	1	525	58.2	6.5 2
D6RF99	Synaptotagmin-15 (Fragment) OS=Homo sapiens GN=SYT15 PE=1 SV=1 - [D6RF99_HUMAN]	5	1	1	1	136	15.8	8.2 8
G3V3Y2	Fibulin-5 (Fragment) OS=Homo sapiens GN=FBLN5 PE=1 SV=1 - [G3V3Y2_HUMAN]	5	1	1	1	91	9.9	6.3 7
Q9H637	cDNA: FLJ22628 fis, clone HSI06177 OS=Homo sapiens PE=2 SV=1 - [Q9H637_HUMAN]	2	1	1	1	1133	131. 2	7.5 3
A0A075 B7G2	Zinc finger protein 208 OS=Homo sapiens GN=ZNF208 PE=4 SV=2 - [A0A075B7G2_HUMAN]	2	1	1	1	1167	134. 3	9.0 9
H0YHR3	Protein phosphatase Slingshot homolog 1 (Fragment) OS=Homo sapiens GN=SSH1 PE=1 SV=1 - [H0YHR3_HUMAN]	2	1	1	1	95	11.0	4.9 4
B7ZA99	cDNA, FLJ79113, highly similar to Zinc finger SWIM domain-containing protein 3 OS=Homo sapiens PE=2 SV=1 - [B7ZA99_HUMAN]	1	1	1	1	690	78.3	7.5 0
B4DMV5	cDNA FLJ51248, weakly similar to Melanoma-associated antigen C3 OS=Homo sapiens PE=2 SV=1 - [B4DMV5_HUMAN]	1	1	1	1	126	13.4	5.1 0
A8K651	cDNA FLJ75700, highly similar to Homo sapiens complement component 1, q subcomponent binding protein (C1QBP), nuclear gene encoding mitochondrial protein, mRNA OS=Homo sapiens PE=2 SV=1 - [A8K651_HUMAN]	2	1	1	1	282	31.4	4.8 4

ErbB2-1-1

Accession	Description	# Proteins	# Unique Peptides	# Peptides	# PSMs	# AAs	MW [kDa]	calc. pI
P35527	Keratin, type I cytoskeletal 9 OS=Homo sapiens GN=KRT9 PE=1 SV=3 - [K1C9_HUMAN]	2	31	32	325	623	62.0	5.24
H6VRF8	Keratin 1 OS=Homo sapiens GN=KRT1 PE=3 SV=1 - [H6VRF8_HUMAN]	14	33	39	277	644	66.0	8.12
P13645	Keratin, type I cytoskeletal 10 OS=Homo sapiens GN=KRT10 PE=1 SV=6 - [K1C10_HUMAN]	13	29	35	196	584	58.8	5.21
P35908	Keratin, type II cytoskeletal 2 epidermal OS=Homo sapiens GN=KRT2 PE=1 SV=2 - [K22E_HUMAN]	5	29	38	201	639	65.4	8.00
P02533	Keratin, type I cytoskeletal 14 OS=Homo sapiens GN=KRT14 PE=1 SV=4 - [K1C14_HUMAN]	25	10	29	114	472	51.5	5.16
P08779	Keratin, type I cytoskeletal 16 OS=Homo sapiens GN=KRT16 PE=1 SV=4 - [K1C16_HUMAN]	25	9	23	89	473	51.2	5.05
P04259	Keratin, type II cytoskeletal 6B OS=Homo sapiens GN=KRT6B PE=1 SV=5 - [K2C6B_HUMAN]	9	1	22	71	564	60.0	8.00
P13647	Keratin, type II cytoskeletal 5 OS=Homo sapiens GN=KRT5 PE=1 SV=3 - [K2C5_HUMAN]	14	17	29	64	590	62.3	7.74
B4DRR0	cDNA FLJ53910, highly similar to Keratin, type II cytoskeletal 6A OS=Homo sapiens PE=2 SV=1 - [B4DRR0_HUMAN]	16	4	27	55	535	57.8	8.00
Q0IIN1	Keratin 77 OS=Homo sapiens GN=KRT77 PE=1 SV=1 - [Q0IIN1_HUMAN]	5	12	15	41	578	61.8	5.85
Q04695	Keratin, type I cytoskeletal 17 OS=Homo sapiens GN=KRT17 PE=1 SV=2 - [K1C17_HUMAN]	17	2	16	34	432	48.1	5.02
Q02413	Desmoglein-1 OS=Homo sapiens GN=DSG1 PE=1 SV=2 - [DSG1_HUMAN]	1	10	10	21	1049	113.7	5.03
A0A024R0Y2	HCG30204, isoform CRA_a OS=Homo sapiens GN=hCG_30204 PE=4 SV=1 - [A0A024R0Y2_HUMAN]	18	16	16	20	2268	257.1	6.61
A1A4E9	Keratin 13 OS=Homo sapiens GN=KRT13 PE=1 SV=1 - [A1A4E9_HUMAN]	6	3	8	20	458	49.6	4.96
F6KPG5	Albumin (Fragment) OS=Homo sapiens PE=2 SV=1 - [F6KPG5_HUMAN]	14	12	12	20	585	66.5	6.04
E7EQB2	Lactotransferrin (Fragment) OS=Homo sapiens GN=LTF PE=1 SV=1 - [E7EQB2_HUMAN]	16	12	12	17	696	76.6	8.02
Q6KB66	Keratin, type II cytoskeletal 80 OS=Homo sapiens GN=KRT80 PE=1 SV=2 - [K2C80_HUMAN]	8	4	5	15	452	50.5	5.67
Q3SY84	Keratin, type II cytoskeletal 71 OS=Homo sapiens GN=KRT71 PE=1 SV=3 - [K2C71_HUMAN]	8	1	4	18	523	57.3	6.61
B3KPS3	cDNA FLJ32131 fis, clone PEBLM2000267, highly similar to Tubulin alpha-ubiquitous chain OS=Homo sapiens PE=2 SV=1 - [B3KPS3_HUMAN]	38	8	8	12	416	46.2	5.12
Q8N1N4	Keratin, type II cytoskeletal 78 OS=Homo sapiens GN=KRT78 PE=2 SV=2 - [K2C78_HUMAN]	4	7	9	11	520	56.8	6.02
P15924	Desmoplakin OS=Homo sapiens GN=DSP PE=1 SV=3 - [DESP_HUMAN]	7	9	9	11	2871	331.6	6.81
Q86YZ3	Hornerin OS=Homo sapiens GN=HRNR PE=1 SV=2 - [HORN_HUMAN]	1	5	5	7	2850	282.2	10.04

Q15323	Keratin, type I cuticular Ha1 OS=Homo sapiens GN=KRT31 PE=1 SV=3 - [K1H1_HUMAN]	19	2	6	9	416	47.2	4.88
A0A0C4DGN4	Zymogen granule protein 16 homolog B OS=Homo sapiens GN=ZG16B PE=1 SV=1 - [A0A0C4DGN4_HUMAN]	5	4	4	7	178	19.6	5.95
Q9HB00	Desmocollin 1, isoform CRA_b OS=Homo sapiens GN=DSC1 PE=4 SV=1 - [Q9HB00_HUMAN]	2	6	6	7	840	93.8	5.53
Q9GZZ8	Extracellular glycoprotein lacritin OS=Homo sapiens GN=LACRT PE=1 SV=1 - [LACRT_HUMAN]	2	4	4	7	138	14.2	5.50
P50402	Emerin OS=Homo sapiens GN=EMD PE=1 SV=1 - [EMD_HUMAN]	2	5	5	8	254	29.0	5.50
A0A0G2JMB2	Uncharacterized protein OS=Homo sapiens PE=4 SV=1 - [A0A0G2JMB2_HUMAN]	13	1	3	6	340	36.5	6.10
A0A087X2I6	Keratin, type I cuticular Ha3-II OS=Homo sapiens GN=KRT33B PE=1 SV=1 - [A0A087X2I6_HUMAN]	18	1	6	8	404	46.1	4.84
Q99456	Keratin, type I cytoskeletal 12 OS=Homo sapiens GN=KRT12 PE=1 SV=1 - [K1C12_HUMAN]	1	1	3	7	494	53.5	4.78
A0A024R1X8	Junction plakoglobin, isoform CRA_a OS=Homo sapiens GN=JUP PE=4 SV=1 - [A0A024R1X8_HUMAN]	12	6	6	7	745	81.7	6.14
O95968	Secretoglobin family 1D member 1 OS=Homo sapiens GN=SCGB1D1 PE=1 SV=1 - [SG1D1_HUMAN]	1	2	2	6	90	9.9	9.25
P01876	Ig alpha-1 chain C region OS=Homo sapiens GN=IGHA1 PE=1 SV=2 - [IGHA1_HUMAN]	10	1	3	5	353	37.6	6.51
Q9NSB2	Keratin, type II cuticular Hb4 OS=Homo sapiens GN=KRT84 PE=2 SV=2 - [KRT84_HUMAN]	4	1	4	11	600	64.8	7.56
Q53HF2	Heat shock 70kDa protein 8 isoform 2 variant (Fragment) OS=Homo sapiens PE=1 SV=1 - [Q53HF2_HUMAN]	33	5	6	6	493	53.5	5.86
Q45KI0	Trypsin I (Fragment) OS=Homo sapiens GN=PRSS1 PE=3 SV=1 - [Q45KI0_HUMAN]	17	1	1	3	84	9.2	9.99
P31025	Lipocalin-1 OS=Homo sapiens GN=LCN1 PE=1 SV=1 - [LCN1_HUMAN]	2	4	4	5	176	19.2	5.58
O75556	Mammaglobin-B OS=Homo sapiens GN=SCGB2A1 PE=1 SV=1 - [SG2A1_HUMAN]	1	3	3	5	95	10.9	5.78
B3KRK8	cDNA FLJ34494 fis, clone HLUNG2005030, highly similar to VIMENTIN OS=Homo sapiens PE=2 SV=1 - [B3KRK8_HUMAN]	29	6	6	7	407	46.9	5.00
B4DVQ0	cDNA FLJ58286, highly similar to Actin, cytoplasmic 2 OS=Homo sapiens PE=2 SV=1 - [B4DVQ0_HUMAN]	60	5	5	6	333	37.3	5.71
B7Z597	cDNA FLJ54373, highly similar to 60 kDa heat shock protein, mitochondrial OS=Homo sapiens PE=2 SV=1 - [B7Z597_HUMAN]	10	4	4	5	564	60.0	5.74
Q2VPJ6	HSP90AA1 protein (Fragment) OS=Homo sapiens GN=HSP90AA1 PE=1 SV=1 - [Q2VPJ6_HUMAN]	17	6	6	7	585	68.3	5.19
P05089	Arginase-1 OS=Homo sapiens GN=ARG1 PE=1 SV=2 - [ARGI1_HUMAN]	1	3	3	5	322	34.7	7.21
Q8TC04	Keratin 23 (Histone deacetylase inducible) OS=Homo sapiens GN=KRT23 PE=2 SV=1 - [Q8TC04_HUMAN]	1	1	1	7	422	48.1	6.54
P04040	Catalase OS=Homo sapiens GN=CAT PE=1 SV=3 - [CATA_HUMAN]	3	5	5	5	527	59.7	7.39
P81605	Dermcidin OS=Homo sapiens GN=DCD PE=1 SV=2 - [DCD_HUMAN]	1	4	4	4	110	11.3	6.54

B7Z1V7	cDNA FLJ51811, highly similar to Stress-70 protein, mitochondrial OS=Homo sapiens PE=2 SV=1 - [B7Z1V7_HUMAN]	7	2	2	4	437	47.3	6.61
O76011	Keratin, type I cuticular Ha4 OS=Homo sapiens GN=KRT34 PE=2 SV=2 - [KRT34_HUMAN]	6	1	4	5	436	49.4	5.06
B3KX99	cDNA FLJ45019 fis, clone BRAWH3015825 OS=Homo sapiens PE=2 SV=1 - [B3KX99_HUMAN]	2	1	1	5	333	38.5	8.97
Q9NP55	BPI fold-containing family A member 1 OS=Homo sapiens GN=BPIFA1 PE=1 SV=1 - [BPIA1_HUMAN]	1	3	3	3	256	26.7	5.76
A0A0A0MSI0	Peroxiredoxin-1 (Fragment) OS=Homo sapiens GN=PRDX1 PE=1 SV=1 - [A0A0A0MSI0_HUMAN]	4	3	4	4	171	19.0	6.92
B4E1T6	cDNA FLJ54342, highly similar to Heat shock 70 kDa protein 1 OS=Homo sapiens PE=2 SV=1 - [B4E1T6_HUMAN]	23	2	3	3	398	43.0	5.39
Q5D862	Filaggrin-2 OS=Homo sapiens GN=FLG2 PE=1 SV=1 - [FILA2_HUMAN]	1	2	2	3	2391	247.9	8.31
Q6B823	Histone H4 (Fragment) OS=Homo sapiens PE=3 SV=1 - [Q6B823_HUMAN]	3	2	2	3	43	4.9	10.92
B4DF70	cDNA FLJ60461, highly similar to Peroxiredoxin-2 (EC 1.11.1.15) OS=Homo sapiens PE=2 SV=1 - [B4DF70_HUMAN]	4	2	3	3	183	20.1	8.78
P61626	Lysozyme C OS=Homo sapiens GN=LYSC PE=1 SV=1 - [LYSC_HUMAN]	3	3	3	4	148	16.5	9.16
A0M8Q9	C1 segment protein (Fragment) OS=Homo sapiens GN=C1 segment PE=4 SV=1 - [A0M8Q9_HUMAN]	59	1	1	2	105	11.3	7.87
A0A024RC29	Desmocollin 3, isoform CRA_b OS=Homo sapiens GN=DSC3 PE=4 SV=1 - [A0A024RC29_HUMAN]	3	3	3	3	896	99.9	6.10
Q96C29	Putative uncharacterized protein (Fragment) OS=Homo sapiens PE=2 SV=1 - [Q96C29_HUMAN]	33	2	2	3	248	26.3	9.29
A0A075B6Z2	Protein TRAJ56 (Fragment) OS=Homo sapiens GN=TRAJ56 PE=4 SV=1 - [A0A075B6Z2_HUMAN]	2	1	1	14	21	2.2	10.29
H0YKZ7	Annexin (Fragment) OS=Homo sapiens GN=ANXA2 PE=1 SV=1 - [H0YKZ7_HUMAN]	18	2	2	3	119	13.0	8.13
B2R4M6	Protein S100 OS=Homo sapiens PE=2 SV=1 - [B2R4M6_HUMAN]	2	3	3	4	114	13.2	6.13
A0JNT2	KRT83 protein OS=Homo sapiens GN=KRT83 PE=2 SV=1 - [A0JNT2_HUMAN]	13	1	3	3	447	49.6	5.39
P12273	Prolactin-inducible protein OS=Homo sapiens GN=PIP PE=1 SV=1 - [PIP_HUMAN]	1	3	3	3	146	16.6	8.05
Q9UGM3	Deleted in malignant brain tumors 1 protein OS=Homo sapiens GN=DMBT1 PE=1 SV=2 - [DMBT1_HUMAN]	1	1	1	2	2413	260.6	5.44
Q0EFA5	S protein OS=Homo sapiens GN=S PE=4 SV=1 - [Q0EFA5_HUMAN]	7	1	1	2	512	49.9	8.13
P25311	Zinc-alpha-2-glycoprotein OS=Homo sapiens GN=AZGP1 PE=1 SV=2 - [ZA2G_HUMAN]	3	4	4	4	298	34.2	6.05
Q59H57	Fusion (Involved in t(12;16) in malignant liposarcoma) isoform a variant (Fragment) OS=Homo sapiens PE=2 SV=1 - [Q59H57_HUMAN]	8	2	2	2	300	32.0	9.52
M0R1I1	Tubulin beta-4A chain (Fragment) OS=Homo sapiens GN=TUBB4A PE=1 SV=1 - [M0R1I1_HUMAN]	27	1	1	1	74	7.8	4.94

Q53RR5	Putative uncharacterized protein YWHAQ (Fragment) OS=Homo sapiens GN=YWHAQ PE=4 SV=1 - [Q53RR5_HUMAN]	31	2	2	2	98	11.2	6.70
B2R7Z6	cDNA, FLJ93674 OS=Homo sapiens PE=2 SV=1 - [B2R7Z6_HUMAN]	2	2	2	2	484	52.5	7.55
P78386	Keratin, type II cuticular Hb5 OS=Homo sapiens GN=KRT85 PE=1 SV=1 - [KRT85_HUMAN]	5	1	3	3	507	55.8	6.55
J3KRG2	Gasdermin-A (Fragment) OS=Homo sapiens GN=GSDMA PE=1 SV=5 - [J3KRG2_HUMAN]	2	3	3	3	159	17.9	6.02
A9UFC0	Caspase 14 OS=Homo sapiens GN=CASP14 PE=2 SV=1 - [A9UFC0_HUMAN]	2	2	2	2	242	27.6	5.34
Q15203	Prothymosin alpha OS=Homo sapiens PE=4 SV=2 - [Q15203_HUMAN]	18	1	1	2	73	8.2	3.76
Q3SYB5	SERPINB12 protein OS=Homo sapiens GN=SERPINB12 PE=2 SV=1 - [Q3SYB5_HUMAN]	2	2	2	2	183	20.9	5.87
J3QSA3	Polyubiquitin-B (Fragment) OS=Homo sapiens GN=UBB PE=1 SV=1 - [J3QSA3_HUMAN]	37	1	1	1	43	4.9	5.19
P05109	Protein S100-A8 OS=Homo sapiens GN=S100A8 PE=1 SV=1 - [S10A8_HUMAN]	1	2	2	3	93	10.8	7.03
E7EUT5	Glyceraldehyde-3-phosphate dehydrogenase OS=Homo sapiens GN=GAPDH PE=1 SV=1 - [E7EUT5_HUMAN]	3	1	1	1	260	27.9	6.95
E5RJN0	Heparan-alpha-glucosaminide N-acetyltransferase OS=Homo sapiens GN=HGSNAT PE=1 SV=1 - [E5RJN0_HUMAN]	2	1	1	1	352	38.9	8.32
Q86W20	Protease serine 1 (Fragment) OS=Homo sapiens GN=PRSS1 PE=3 SV=1 - [Q86W20_HUMAN]	6	1	1	1	84	9.2	10.27
C9JZ65	Serpin B4 (Fragment) OS=Homo sapiens GN=SERPINB4 PE=1 SV=1 - [C9JZ65_HUMAN]	10	1	1	1	211	24.4	6.61
A0A087WUV8	Basigin OS=Homo sapiens GN=BSG PE=1 SV=1 - [A0A087WUV8_HUMAN]	6	1	1	1	189	20.5	6.68
M0QZK8	Uncharacterized protein OS=Homo sapiens PE=4 SV=1 - [M0QZK8_HUMAN]	4	1	1	1	103	11.6	4.92
J3KSP2	60S ribosomal protein L38 (Fragment) OS=Homo sapiens GN=RPL38 PE=1 SV=1 - [J3KSP2_HUMAN]	4	1	1	1	21	2.6	9.99
V9GZN0	Histone H2A gene (lambda-HHG55) (Fragment) OS=Homo sapiens PE=4 SV=1 - [V9GZN0_HUMAN]	19	1	1	1	47	5.0	11.90
Q8IWS0	PHD finger protein 6 OS=Homo sapiens GN=PHF6 PE=1 SV=1 - [PHF6_HUMAN]	1	1	1	1	365	41.3	8.68
P04080	Cystatin-B OS=Homo sapiens GN=CSTB PE=1 SV=2 - [CYTB_HUMAN]	1	1	1	1	98	11.1	7.56
O75531	Barrier-to-autointegration factor OS=Homo sapiens GN=BANF1 PE=1 SV=1 - [BAF_HUMAN]	1	1	1	1	89	10.1	6.09
C9IYG1	BRCA1-associated RING domain protein 1 (Fragment) OS=Homo sapiens GN=BARD1 PE=1 SV=1 - [C9IYG1_HUMAN]	9	1	1	1	216	24.4	8.47
P07737	Profilin-1 OS=Homo sapiens GN=PFN1 PE=1 SV=2 - [PROF1_HUMAN]	2	1	1	1	140	15.0	8.27
K7EJT5	60S ribosomal protein L22 (Fragment) OS=Homo sapiens GN=RPL22 PE=1 SV=1 - [K7EJT5_HUMAN]	8	1	1	1	47	5.1	9.42
Q5TIG5	Afadin OS=Homo sapiens GN=MLLT4 PE=1 SV=1 - [Q5TIG5_HUMAN]	5	1	1	1	1665	189.0	6.49

B4DL87	cDNA FLJ52243, highly similar to Heat-shock protein beta-1 OS=Homo sapiens PE=2 SV=1 - [B4DL87_HUMAN]	3	1	1	1	170	18.5	6.95
B7Z1V3	cDNA FLJ54733, highly similar to General transcription factor 3C polypeptide 5 OS=Homo sapiens PE=2 SV=1 - [B7Z1V3_HUMAN]	1	1	1	1	412	45.6	9.45
A0A075B6G4	Protein crumbs homolog 1 OS=Homo sapiens GN=CRB1 PE=4 SV=1 - [A0A075B6G4_HUMAN]	6	1	1	1	674	74.6	5.59
H0YH81	ATP synthase subunit beta (Fragment) OS=Homo sapiens GN=ATP5B PE=1 SV=1 - [H0YH81_HUMAN]	3	1	1	1	362	38.2	5.55
C9JM43	Zinc finger protein 621 (Fragment) OS=Homo sapiens GN=ZNF621 PE=4 SV=1 - [C9JM43_HUMAN]	2	1	1	1	152	17.3	5.29
H0YLF3	Beta-2-microglobulin (Fragment) OS=Homo sapiens GN=B2M PE=1 SV=1 - [H0YLF3_HUMAN]	7	1	1	1	71	8.5	5.15
A8K651	cDNA FLJ75700, highly similar to Homo sapiens complement component 1, q subcomponent binding protein (C1QBP), nuclear gene encoding mitochondrial protein, mRNA OS=Homo sapiens PE=2 SV=1 - [A8K651_HUMAN]	2	1	1	1	282	31.4	4.84
B4DSX3	cDNA FLJ58938, moderately similar to Syntaxin-1A OS=Homo sapiens PE=2 SV=1 - [B4DSX3_HUMAN]	8	1	1	1	171	19.4	4.96
Q59H71	Sodium channel protein type II alpha subunit variant (Fragment) OS=Homo sapiens PE=2 SV=1 - [Q59H71_HUMAN]	7	1	1	1	1315	149.2	5.49
K7EMV3	Histone H3 OS=Homo sapiens GN=H3F3B PE=1 SV=1 - [K7EMV3_HUMAN]	15	1	1	1	92	10.3	11.8 2
P31151	Protein S100-A7 OS=Homo sapiens GN=S100A7 PE=1 SV=4 - [S10A7_HUMAN]	1	1	1	1	101	11.5	6.77
P12004	Proliferating cell nuclear antigen OS=Homo sapiens GN=PCNA PE=1 SV=1 - [PCNA_HUMAN]	3	1	1	1	261	28.8	4.69
H7C1V0	Cathepsin D (Fragment) OS=Homo sapiens GN=CTSD PE=1 SV=1 - [H7C1V0_HUMAN]	2	1	1	1	189	20.4	8.44
E5RI98	Nucleophosmin (Fragment) OS=Homo sapiens GN=NPM1 PE=1 SV=1 - [E5RI98_HUMAN]	16	1	1	1	111	11.9	4.35
Q16378	Proline-rich protein 4 OS=Homo sapiens GN=PRR4 PE=1 SV=3 - [PROL4_HUMAN]	2	2	2	3	134	15.1	7.06
B4DHW6	cDNA FLJ54930, highly similar to Homo sapiens Dbf4-related factor 1 (DRF1), transcript variant 2, mRNA OS=Homo sapiens PE=2 SV=1 - [B4DHW6_HUMAN]	3	1	1	1	154	16.7	10.2 7
Q8NH58	Olfactory receptor OS=Homo sapiens PE=3 SV=1 - [Q8NH58_HUMAN]	1	1	1	1	276	30.4	7.71
L0R5A1	Alternative protein CSF2RB OS=Homo sapiens GN=CSF2RB PE=4 SV=1 - [L0R5A1_HUMAN]	1	1	1	1	108	11.6	11.3 0
Q9HA72	Calcium homeostasis modulator protein 2 OS=Homo sapiens GN=CALHM2 PE=2 SV=1 - [CAHM2_HUMAN]	1	1	1	1	323	36.2	7.69
Q96FX8	p53 apoptosis effector related to PMP-22 OS=Homo sapiens GN=PERP PE=2 SV=1 - [PERP_HUMAN]	1	1	1	1	193	21.4	7.03
O43915	Vascular endothelial growth factor D OS=Homo sapiens GN=FIGF PE=1 SV=1 - [VEGFD_HUMAN]	1	1	1	1	354	40.4	7.81
E5RGH4	Heterogeneous nuclear ribonucleoprotein H (Fragment) OS=Homo sapiens GN=HNRNPH1 PE=1 SV=1 - [E5RGH4_HUMAN]	17	1	1	1	100	11.2	6.79
B3KMI5	alpha-1,2-Mannosidase OS=Homo sapiens PE=2 SV=1 - [B3KMI5_HUMAN]	1	1	1	1	287	32.7	8.21

Q96QW8	DJ576K7.1 (FK506 binding protein 12-rapamycin associated protein 1) (Fragment) OS=Homo sapiens GN=FRAP1 PE=4 SV=1 - [Q96QW8_HUMAN]	3	1	1	1	895	102.9	7.28
F8WCJ1	Eukaryotic translation initiation factor 5A OS=Homo sapiens GN=EIF5A2 PE=1 SV=1 - [F8WCJ1_HUMAN]	8	1	1	1	105	11.7	9.14
G3V4X3	Protein NDRG2 OS=Homo sapiens GN=NDRG2 PE=1 SV=1 - [G3V4X3_HUMAN]	1	1	1	1	77	8.9	7.21
K7ENC2	Coiled-coil domain-containing protein 159 (Fragment) OS=Homo sapiens GN=CCDC159 PE=4 SV=5 - [K7ENC2_HUMAN]	5	1	1	1	110	12.7	5.96
H0Y9T2	Collagen alpha-5(VI) chain (Fragment) OS=Homo sapiens GN=COL6A5 PE=4 SV=1 - [H0Y9T2_HUMAN]	5	1	1	1	443	50.2	5.00
B4DXS1	Glycylpeptide N-tetradecanoyltransferase OS=Homo sapiens PE=2 SV=1 - [B4DXS1_HUMAN]	7	1	1	1	310	36.0	9.54
Q6ZSX8	cDNA FLJ45139 fis, clone BRAWH3039623 OS=Homo sapiens PE=2 SV=1 - [Q6ZSX8_HUMAN]	1	1	1	2	136	15.5	10.07
B3KQ62	cDNA FLJ32946 fis, clone TESTI2007872, weakly similar to INTRACELLULAR PROTEIN TRANSPORT PROTEIN USO1 OS=Homo sapiens PE=2 SV=1 - [B3KQ62_HUMAN]	4	1	1	1	405	47.2	6.90
B4DN11	cDNA FLJ54270 OS=Homo sapiens PE=2 SV=1 - [B4DN11_HUMAN]	4	1	1	1	140	16.1	6.42
B4DS32	cDNA FLJ56236, highly similar to Exportin-2 OS=Homo sapiens PE=2 SV=1 - [B4DS32_HUMAN]	5	1	1	1	569	64.3	5.69

ErbB2-1-2

Accession	Description	# Proteins	# Unique Peptides	# Peptides	# PSMs	# AAs	MW [kDa]	calc pI
P35527	Keratin, type I cytoskeletal 9 OS=Homo sapiens GN=KRT9 PE=1 SV=3 - [K1C9_HUMAN]	2	28	28	181	623	62.0	5.24
H6VRF8	Keratin 1 OS=Homo sapiens GN=KRT1 PE=3 SV=1 - [H6VRF8_HUMAN]	16	31	36	168	644	66.0	8.12
P13645	Keratin, type I cytoskeletal 10 OS=Homo sapiens GN=KRT10 PE=1 SV=6 - [K1C10_HUMAN]	23	25	28	109	584	58.8	5.21
P35908	Keratin, type II cytoskeletal 2 epidermal OS=Homo sapiens GN=KRT2 PE=1 SV=2 - [K22E_HUMAN]	8	21	29	74	639	65.4	8.00
P02533	Keratin, type I cytoskeletal 14 OS=Homo sapiens GN=KRT14 PE=1 SV=4 - [K1C14_HUMAN]	39	8	25	83	472	51.5	5.16
P08779	Keratin, type I cytoskeletal 16 OS=Homo sapiens GN=KRT16 PE=1 SV=4 - [K1C16_HUMAN]	40	9	21	69	473	51.2	5.05
P13647	Keratin, type II cytoskeletal 5 OS=Homo sapiens GN=KRT5 PE=1 SV=3 - [K2C5_HUMAN]	15	10	18	37	590	62.3	7.74

B4DRR0	cDNA FLJ53910, highly similar to Keratin, type II cytoskeletal 6A OS=Homo sapiens PE=2 SV=1 - [B4DRR0_HUMAN]	17	7	16	31	535	57.8	8.0 0
Q04695	Keratin, type I cytoskeletal 17 OS=Homo sapiens GN=KRT17 PE=1 SV=2 - [K1C17_HUMAN]	31	2	14	27	432	48.1	5.0 2
Q0IIN1	Keratin 77 OS=Homo sapiens GN=KRT77 PE=1 SV=1 - [Q0IIN1_HUMAN]	7	2	5	20	578	61.8	5.8 5
A0A024R0Y2	HCG30204, isoform CRA_a OS=Homo sapiens GN=hCG_30204 PE=4 SV=1 - [A0A024R0Y2_HUMAN]	13	8	8	10	2268	257.1	6.6 1
Q14CN4	Keratin, type II cytoskeletal 72 OS=Homo sapiens GN=KRT72 PE=1 SV=2 - [K2C72_HUMAN]	10	1	3	10	511	55.8	6.8 9
P50402	Emerin OS=Homo sapiens GN=EMD PE=1 SV=1 - [EMD_HUMAN]	2	5	5	10	254	29.0	5.5 0
Q86YZ3	Hornerin OS=Homo sapiens GN=HRNR PE=1 SV=2 - [HORN_HUMAN]	1	4	4	7	2850	282. 2	10. 04
Q45KI0	Trypsin I (Fragment) OS=Homo sapiens GN=PRSS1 PE=3 SV=1 - [Q45KI0_HUMAN]	17	1	1	4	84	9.2	9.9 9
Q6KB66	Keratin, type II cytoskeletal 80 OS=Homo sapiens GN=KRT80 PE=1 SV=2 - [K2C80_HUMAN]	9	1	2	5	452	50.5	5.6 7
P81605	Dermcidin OS=Homo sapiens GN=DCD PE=1 SV=2 - [DCD_HUMAN]	1	3	3	5	110	11.3	6.5 4
F6KPG5	Albumin (Fragment) OS=Homo sapiens PE=2 SV=1 - [F6KPG5_HUMAN]	14	4	4	5	585	66.5	6.0 4
Q9GZZ8	Extracellular glycoprotein lacritin OS=Homo sapiens GN=LACRT PE=1 SV=1 - [LACRT_HUMAN]	2	3	3	4	138	14.2	5.5 0
Q19KS2	Lactoferrin (Fragment) OS=Homo sapiens PE=2 SV=1 - [Q19KS2_HUMAN]	15	3	3	4	353	39.1	9.0 3
B3KRK8	cDNA FLJ34494 fis, clone HLUNG2005030, highly similar to VIMENTIN OS=Homo sapiens PE=2 SV=1 - [B3KRK8_HUMAN]	5	3	3	5	407	46.9	5.0 0
B3KX99	cDNA FLJ45019 fis, clone BRAWH3015825 OS=Homo sapiens PE=2 SV=1 - [B3KX99_HUMAN]	2	1	1	3	333	38.5	8.9 7
J3QSA3	Polyubiquitin-B (Fragment) OS=Homo sapiens GN=UBB PE=1 SV=1 - [J3QSA3_HUMAN]	37	1	1	2	43	4.9	5.1 9
Q53HF2	Heat shock 70kDa protein 8 isoform 2 variant (Fragment) OS=Homo sapiens PE=1 SV=1 - [Q53HF2_HUMAN]	37	2	2	3	493	53.5	5.8 6
C9K0U8	Single-stranded DNA-binding protein, mitochondrial (Fragment) OS=Homo sapiens GN=SSBP1 PE=1 SV=1 - [C9K0U8_HUMAN]	6	2	2	2	121	14.1	9.5 7
Q8N532	TUBA1C protein OS=Homo sapiens GN=TUBA1C PE=2 SV=1 - [Q8N532_HUMAN]	34	3	3	4	325	36.6	7.9 6
A0A024RC29	Desmocollin 3, isoform CRA_b OS=Homo sapiens GN=DSC3 PE=4 SV=1 - [A0A024RC29_HUMAN]	3	2	2	2	896	99.9	6.1 0
Q59H57	Fusion (Involved in t(12;16) in malignant liposarcoma) isoform a variant (Fragment) OS=Homo sapiens PE=2 SV=1 - [Q59H57_HUMAN]	8	2	2	3	300	32.0	9.5 2

B7Z597	cDNA FLJ54373, highly similar to 60 kDa heat shock protein, mitochondrial OS=Homo sapiens PE=2 SV=1 - [B7Z597_HUMAN]	9	2	2	2	564	60.0	5.7 4
Q9HB00	Desmocollin 1, isoform CRA_b OS=Homo sapiens GN=DSC1 PE=4 SV=1 - [Q9HB00_HUMAN]	2	2	2	2	840	93.8	5.5 3
O95968	Secretoglobin family 1D member 1 OS=Homo sapiens GN=SCGB1D1 PE=1 SV=1 - [SG1D1_HUMAN]	1	2	2	2	90	9.9	9.2 5
P61626	Lysozyme C OS=Homo sapiens GN=LYZ PE=1 SV=1 - [LYSC_HUMAN]	3	2	2	3	148	16.5	9.1 6
Q14568	Heat shock protein HSP 90-alpha A2 OS=Homo sapiens GN=HSP90AA2P PE=1 SV=2 - [HS902_HUMAN]	14	2	2	2	343	39.3	4.6 5
Q8N1N4	Keratin, type II cytoskeletal 78 OS=Homo sapiens GN=KRT78 PE=2 SV=2 - [K2C78_HUMAN]	1	1	1	2	520	56.8	6.0 2
O75556	Mammaglobin-B OS=Homo sapiens GN=SCGB2A1 PE=1 SV=1 - [SG2A1_HUMAN]	1	1	1	1	95	10.9	5.7 8
O75531	Barrier-to-autointegration factor OS=Homo sapiens GN=BANF1 PE=1 SV=1 - [BAF_HUMAN]	1	1	1	1	89	10.1	6.0 9
Q6B823	Histone H4 (Fragment) OS=Homo sapiens PE=3 SV=1 - [Q6B823_HUMAN]	3	1	1	1	43	4.9	10. 92
H0YDD8	60S acidic ribosomal protein P2 (Fragment) OS=Homo sapiens GN=RPLP2 PE=1 SV=1 - [H0YDD8_HUMAN]	2	1	1	1	92	9.1	4.4 6
Q86W20	Protease serine 1 (Fragment) OS=Homo sapiens GN=PRSS1 PE=3 SV=1 - [Q86W20_HUMAN]	6	1	1	1	84	9.2	10. 27
P05089	Arginase-1 OS=Homo sapiens GN=ARG1 PE=1 SV=2 - [ARGI1_HUMAN]	1	1	1	1	322	34.7	7.2 1
Q5VSP4	Putative lipocalin 1-like protein 1 OS=Homo sapiens GN=LCN1P1 PE=5 SV=1 - [LC1L1_HUMAN]	2	1	1	1	162	17.9	5.0 0
B4DVQ0	cDNA FLJ58286, highly similar to Actin, cytoplasmic 2 OS=Homo sapiens PE=2 SV=1 - [B4DVQ0_HUMAN]	50	2	2	2	333	37.3	5.7 1
Q02413	Desmoglein-1 OS=Homo sapiens GN=DSG1 PE=1 SV=2 - [DSG1_HUMAN]	1	2	2	2	1049	113. 7	5.0 3
V9GZN0	Histone H2A gene (lambda-HHG55) (Fragment) OS=Homo sapiens PE=4 SV=1 - [V9GZN0_HUMAN]	19	1	1	1	47	5.0	11. 90
H7BZV2	Cilia- and flagella-associated protein 69 (Fragment) OS=Homo sapiens GN=CFAP69 PE=4 SV=1 - [H7BZV2_HUMAN]	3	1	1	1	478	53.7	7.6 2
X6RKN2	Neurofascin (Fragment) OS=Homo sapiens GN=NFASC PE=1 SV=1 - [X6RKN2_HUMAN]	2	1	1	1	1165	131. 0	6.8 4
Q08ES8	Cell growth-inhibiting protein 34 OS=Homo sapiens PE=2 SV=1 - [Q08ES8_HUMAN]	2	1	1	1	177	20.1	9.6 0
A8MXP8	Reticulocalbin-2 OS=Homo sapiens GN=RCN2 PE=1 SV=1 - [A8MXP8_HUMAN]	2	1	1	1	216	24.8	4.4 2

O00186	Syntaxin-binding protein 3 OS=Homo sapiens GN=STXB3 PE=1 SV=2 - [STXB3_HUMAN]	1	1	1	1	592	67.7	7.8 0
B4DJC9	cDNA FLJ56952 OS=Homo sapiens PE=2 SV=1 - [B4DJC9_HUMAN]	1	1	1	1	130	13.9	11. 14
A0A024 R1X8	Junction plakoglobin, isoform CRA_a OS=Homo sapiens GN=JUP PE=4 SV=1 - [A0A024R1X8_HUMAN]	2	1	1	1	745	81.7	6.1 4
P05109	Protein S100-A8 OS=Homo sapiens GN=S100A8 PE=1 SV=1 - [S10A8_HUMAN]	1	2	2	2	93	10.8	7.0 3
Q5D862	Filaggrin-2 OS=Homo sapiens GN=FLG2 PE=1 SV=1 - [FILA2_HUMAN]	1	1	1	1	2391	247. 9	8.3 1
A1L378	STRC protein OS=Homo sapiens GN=STRC PE=2 SV=1 - [A1L378_HUMAN]	4	1	1	1	1002	110. 6	5.1 7
Q5JC44	KLHL9 protein OS=Homo sapiens PE=2 SV=1 - [Q5JC44_HUMAN]	2	1	1	2	617	69.4	6.3 5
A0A0C4 DGT3	IQ motif and SEC7 domain-containing protein 1 OS=Homo sapiens GN=IQSEC1 PE=1 SV=1 - [A0A0C4DGT3_HUMAN]	5	1	1	1	814	91.9	7.5 6
A8K651	cDNA FLJ75700, highly similar to Homo sapiens complement component 1, q subcomponent binding protein (C1QBP), nuclear gene encoding mitochondrial protein, mRNA OS=Homo sapiens PE=2 SV=1 - [A8K651_HUMAN]	2	1	1	1	282	31.4	4.8 4
A8MTF1	Phosphatidylinositol 4-kinase alpha (Fragment) OS=Homo sapiens GN=PI4KA PE=1 SV=2 - [A8MTF1_HUMAN]	8	1	1	1	435	49.6	5.8 2
Q5TDF0	Cancer-related nucleoside-triphosphatase OS=Homo sapiens GN=NTPCR PE=1 SV=1 - [Q5TDF0_HUMAN]	1	1	1	1	228	25.1	9.4 2
B3KRI8	cDNA FLJ34373 fis, clone FEBRA2017333, highly similar to Dual specificity protein kinase CLK3 (EC 2.7.12.1) OS=Homo sapiens PE=2 SV=1 - [B3KRI8_HUMAN]	2	1	1	1	638	73.5	9.9 5
A0A075 B6Z2	Protein TRAJ56 (Fragment) OS=Homo sapiens GN=TRAJ56 PE=4 SV=1 - [A0A075B6Z2_HUMAN]	2	1	1	3	21	2.2	10. 29
L0R5A1	Alternative protein CSF2RB OS=Homo sapiens GN=CSF2RB PE=4 SV=1 - [L0R5A1_HUMAN]	1	1	1	1	108	11.6	11. 30
B4DKX6	cDNA FLJ53584, highly similar to Desmoplakin (Fragment) OS=Homo sapiens PE=2 SV=1 - [B4DKX6_HUMAN]	4	1	1	1	954	112. 2	6.7 3
Q504Q3	PAB-dependent poly(A)-specific ribonuclease subunit PAN2 OS=Homo sapiens GN=PAN2 PE=1 SV=3 - [PAN2_HUMAN]	1	1	1	1	1202	135. 3	5.9 9
Q96NR3	Patched domain-containing protein 1 OS=Homo sapiens GN=PTCHD1 PE=2 SV=2 - [PTHD1_HUMAN]	1	1	1	1	888	101. 3	8.2 7
Q8VWZ7	E3 ubiquitin-protein ligase RNF133 OS=Homo sapiens GN=RNF133 PE=2 SV=1 - [RN133_HUMAN]	1	1	1	1	376	42.3	7.4 9
A0A024 R731	Uncharacterized protein OS=Homo sapiens GN=NAG6 PE=4 SV=1 - [A0A024R731_HUMAN]	4	1	1	1	957	111. 5	4.6 8
B4DKS8	cDNA FLJ57121, highly similar to Heterogeneous nuclear ribonucleoprotein F OS=Homo sapiens PE=2 SV=1 - [B4DKS8_HUMAN]	2	1	1	1	338	37.2	6.0 5

B2R4M6	Protein S100 OS=Homo sapiens PE=2 SV=1 - [B2R4M6_HUMAN]	2	1	1	1	114	13.2	6.1 3
H0Y908	Alpha-1,3-mannosyl-glycoprotein 4-beta-N-acetylglucosaminyltransferase-like protein MGAT4D (Fragment) OS=Homo sapiens GN=MGAT4D PE=4 SV=1 - [H0Y908_HUMAN]	1	1	1	1	91	11.3	9.9 4
A0JLQ0	AZGP1 protein (Fragment) OS=Homo sapiens GN=AZGP1 PE=2 SV=1 - [A0JLQ0_HUMAN]	3	1	1	1	159	18.7	8.9 7
H3BQL7	Paired amphipathic helix protein Sin3a OS=Homo sapiens GN=SIN3A PE=1 SV=1 - [H3BQL7_HUMAN]	1	1	1	1	156	17.1	9.9 2
E5RGW4	Nucleophosmin (Fragment) OS=Homo sapiens GN=NPM1 PE=1 SV=1 - [E5RGW4_HUMAN]	3	1	1	1	59	6.9	4.4 8
J3QLE0	E3 ubiquitin-protein ligase MIB2 (Fragment) OS=Homo sapiens GN=MIB2 PE=1 SV=1 - [J3QLE0_HUMAN]	6	1	1	1	57	6.7	11. 41
B4DX83	Sodium channel protein OS=Homo sapiens PE=2 SV=1 - [B4DX83_HUMAN]	3	1	1	1	483	54.7	5.4 1
H3BUZ5	Pseudopodium-enriched atypical kinase 1 (Fragment) OS=Homo sapiens GN=PEAK1 PE=1 SV=1 - [H3BUZ5_HUMAN]	3	1	1	1	656	71.9	6.5 5
Q5DTC5	Dendritic-cell specific protein CREA7-4 OS=Homo sapiens GN=CREA7-4 PE=2 SV=1 - [Q5DTC5_HUMAN]	6	1	1	1	215	24.8	6.8 4
B3KR56	cDNA FLJ33721 fis, clone BRAWH2016792, highly similar to Angiomotin-like protein 2 OS=Homo sapiens PE=2 SV=1 - [B3KR56_HUMAN]	2	1	1	1	405	44.6	7.5 0
A9UFC0	Caspase 14 OS=Homo sapiens GN=CASP14 PE=2 SV=1 - [A9UFC0_HUMAN]	2	1	1	1	242	27.6	5.3 4
H9KVB3	Otogelin OS=Homo sapiens GN=OTOG PE=4 SV=2 - [H9KVB3_HUMAN]	2	1	1	1	2913	313. 2	5.7 7

ErbB2-2-1

Accession	Description	# Proteins	# Unique Peptides	# Peptides	# PSMs	# AAs	MW [kDa]	calc . pI
P35527	Keratin, type I cytoskeletal 9 OS=Homo sapiens GN=KRT9 PE=1 SV=3 - [K1C9_HUMAN]	2	27	27	142	623	62.0	5.2 4
H6VRF8	Keratin 1 OS=Homo sapiens GN=KRT1 PE=3 SV=1 - [H6VRF8_HUMAN]	15	29	33	151	644	66.0	8.1 2
P13645	Keratin, type I cytoskeletal 10 OS=Homo sapiens GN=KRT10 PE=1 SV=6 - [K1C10_HUMAN]	25	22	26	98	584	58.8	5.2 1

P35908	Keratin, type II cytoskeletal 2 epidermal OS=Homo sapiens GN=KRT2 PE=1 SV=2 - [K22E_HUMAN]	12	19	27	68	639	65.4	8.0 0
P02533	Keratin, type I cytoskeletal 14 OS=Homo sapiens GN=KRT14 PE=1 SV=4 - [K1C14_HUMAN]	40	8	15	59	472	51.5	5.1 6
P08779	Keratin, type I cytoskeletal 16 OS=Homo sapiens GN=KRT16 PE=1 SV=4 - [K1C16_HUMAN]	36	5	12	51	473	51.2	5.0 5
P13647	Keratin, type II cytoskeletal 5 OS=Homo sapiens GN=KRT5 PE=1 SV=3 - [K2C5_HUMAN]	15	8	13	25	590	62.3	7.7 4
Q0IIN1	Keratin 77 OS=Homo sapiens GN=KRT77 PE=1 SV=1 - [Q0IIN1_HUMAN]	9	1	4	15	578	61.8	5.8 5
B4DRR0	cdNA FLJ53910, highly similar to Keratin, type II cytoskeletal 6A OS=Homo sapiens PE=2 SV=1 - [B4DRR0_HUMAN]	17	2	8	16	535	57.8	8.0 0
K7ERE3	Keratin, type I cytoskeletal 13 OS=Homo sapiens GN=KRT13 PE=1 SV=1 - [K7ERE3_HUMAN]	25	1	5	9	415	45.2	4.8 1
A0A024R0Y2	HCG30204, isoform CRA_a OS=Homo sapiens GN=hCG_30204 PE=4 SV=1 - [A0A024R0Y2_HUMAN]	13	5	5	7	2268	257.1	6.6 1
F6KPG5	Albumin (Fragment) OS=Homo sapiens PE=2 SV=1 - [F6KPG5_HUMAN]	14	5	5	6	585	66.5	6.0 4
Q14CN4	Keratin, type II cytoskeletal 72 OS=Homo sapiens GN=KRT72 PE=1 SV=2 - [K2C72_HUMAN]	12	1	3	6	511	55.8	6.8 9
Q6KB66	Keratin, type II cytoskeletal 80 OS=Homo sapiens GN=KRT80 PE=1 SV=2 - [K2C80_HUMAN]	10	1	2	5	452	50.5	5.6 7
Q45KI0	Trypsin I (Fragment) OS=Homo sapiens GN=PRSS1 PE=3 SV=1 - [Q45KI0_HUMAN]	17	1	1	3	84	9.2	9.9 9
Q9GZZ8	Extracellular glycoprotein lacritin OS=Homo sapiens GN=LACRT PE=1 SV=1 - [LACRT_HUMAN]	2	3	3	4	138	14.2	5.5 0
P81605	Dermcidin OS=Homo sapiens GN=DCD PE=1 SV=2 - [DCD_HUMAN]	1	3	3	4	110	11.3	6.5 4
B3KX99	cdNA FLJ45019 fis, clone BRAWH3015825 OS=Homo sapiens PE=2 SV=1 - [B3KX99_HUMAN]	2	1	1	4	333	38.5	8.9 7
Q02413	Desmoglein-1 OS=Homo sapiens GN=DSG1 PE=1 SV=2 - [DSG1_HUMAN]	1	3	3	3	1049	113. 7	5.0 3
Q19KS2	Lactoferrin (Fragment) OS=Homo sapiens PE=2 SV=1 - [Q19KS2_HUMAN]	15	3	3	4	353	39.1	9.0 3
Q86Y23	Hornerin OS=Homo sapiens GN=HRNR PE=1 SV=2 - [HORN_HUMAN]	1	2	2	2	2850	282. 2	10. 04
J3QSA3	Polyubiquitin-B (Fragment) OS=Homo sapiens GN=UBB PE=1 SV=1 - [J3QSA3_HUMAN]	37	1	1	2	43	4.9	5.1 9
Q5HY57	Emerin OS=Homo sapiens GN=EMD PE=1 SV=1 - [Q5HY57_HUMAN]	2	3	3	3	219	24.9	5.0 2
O95968	Secretoglobin family 1D member 1 OS=Homo sapiens GN=SCGB1D1 PE=1 SV=1 - [SG1D1_HUMAN]	1	2	2	2	90	9.9	9.2 5

Q6UXS9	Inactive caspase-12 OS=Homo sapiens GN=CASP12 PE=2 SV=2 - [CASPC_HUMAN]	1	1	1	2	341	38.8	6.0 2
P05109	Protein S100-A8 OS=Homo sapiens GN=S100A8 PE=1 SV=1 - [S10A8_HUMAN]	1	2	2	2	93	10.8	7.0 3
E9PN25	Heat shock cognate 71 kDa protein (Fragment) OS=Homo sapiens GN=HSPA8 PE=1 SV=1 - [E9PN25_HUMAN]	35	1	1	2	132	14.6	6.5 5
A0A075B6Z2	Protein TRAJ56 (Fragment) OS=Homo sapiens GN=TRAJ56 PE=4 SV=1 - [A0A075B6Z2_HUMAN]	2	1	1	8	21	2.2	10. 29
P61626	Lysozyme C OS=Homo sapiens GN=LYZ PE=1 SV=1 - [LYSC_HUMAN]	3	3	3	3	148	16.5	9.1 6
Q86W20	Protease serine 1 (Fragment) OS=Homo sapiens GN=PRSS1 PE=3 SV=1 - [Q86W20_HUMAN]	6	1	1	1	84	9.2	10. 27
P12273	Prolactin-inducible protein OS=Homo sapiens GN=PIP PE=1 SV=1 - [PIP_HUMAN]	1	1	1	1	146	16.6	8.0 5
Q53RR5	Putative uncharacterized protein YWHAQ (Fragment) OS=Homo sapiens GN=YWHAQ PE=4 SV=1 - [Q53RR5_HUMAN]	3	1	1	1	98	11.2	6.7 0
A0A0C4DGN4	Zymogen granule protein 16 homolog B OS=Homo sapiens GN=ZG16B PE=1 SV=1 - [A0A0C4DGN4_HUMAN]	3	1	1	1	178	19.6	5.9 5
Q9HB00	Desmocollin 1, isoform CRA_b OS=Homo sapiens GN=DSC1 PE=4 SV=1 - [Q9HB00_HUMAN]	2	1	1	1	840	93.8	5.5 3
J3QRT3	Uncharacterized protein KIAA0195 (Fragment) OS=Homo sapiens GN=KIAA0195 PE=1 SV=5 - [J3QRT3_HUMAN]	1	1	1	1	89	9.5	6.7 6
P31151	Protein S100-A7 OS=Homo sapiens GN=S100A7 PE=1 SV=4 - [S10A7_HUMAN]	1	1	1	1	101	11.5	6.7 7
G3V361	Calmodulin (Fragment) OS=Homo sapiens GN=CALM1 PE=1 SV=1 - [G3V361_HUMAN]	8	1	1	1	98	11.1	4.2 5
Q5VSP4	Putative lipocalin 1-like protein 1 OS=Homo sapiens GN=LCN1P1 PE=5 SV=1 - [LC1L1_HUMAN]	2	1	1	1	162	17.9	5.0 0
B7Z5E7	cDNA FLJ51046, highly similar to 60 kDa heat shock protein, mitochondrial OS=Homo sapiens PE=2 SV=1 - [B7Z5E7_HUMAN]	5	1	1	1	517	55.0	5.6 0
O14942	Heat shock protein beta (Fragment) OS=Homo sapiens PE=4 SV=1 - [O14942_HUMAN]	12	1	1	1	130	14.1	4.7 9
C9IYG1	BRCA1-associated RING domain protein 1 (Fragment) OS=Homo sapiens GN=BARD1 PE=1 SV=1 - [C9IYG1_HUMAN]	9	1	1	1	216	24.4	8.4 7
Q14222	EEF1A protein (Fragment) OS=Homo sapiens GN=EEF1A PE=2 SV=1 - [Q14222_HUMAN]	29	1	1	1	227	24.2	9.5 8
A0PJ54	PEX12 protein (Fragment) OS=Homo sapiens GN=PEX12 PE=2 SV=1 - [A0PJ54_HUMAN]	1	1	1	1	324	36.9	9.9 8
A0A087WUV8	Basigin OS=Homo sapiens GN=BSG PE=1 SV=1 - [A0A087WUV8_HUMAN]	6	1	1	1	189	20.5	6.6 8

H0YKZ7	Annexin (Fragment) OS=Homo sapiens GN=ANXA2 PE=1 SV=1 - [H0YKZ7_HUMAN]	16	1	1	1	119	13.0	8.1 3
E7EWK3	ATP-dependent RNA helicase DHX36 (Fragment) OS=Homo sapiens GN=DHX36 PE=1 SV=1 - [E7EWK3_HUMAN]	3	1	1	1	797	91.4	7.2 8
A9UFC0	Caspase 14 OS=Homo sapiens GN=CASP14 PE=2 SV=1 - [A9UFC0_HUMAN]	2	1	1	2	242	27.6	5.3 4
B4DKP2	cDNA FLJ54362, highly similar to Serine/threonine-protein kinase Duet (EC 2.7.11.1) OS=Homo sapiens PE=2 SV=1 - [B4DKP2_HUMAN]	4	1	1	1	489	55.7	6.3 8
P07737	Profilin-1 OS=Homo sapiens GN=PFN1 PE=1 SV=2 - [PROF1_HUMAN]	2	1	1	1	140	15.0	8.2 7
Q15203	Prothymosin alpha OS=Homo sapiens PE=4 SV=2 - [Q15203_HUMAN]	18	1	1	1	73	8.2	3.7 6
Q2Y0W8	Electroneutral sodium bicarbonate exchanger 1 OS=Homo sapiens GN=SLC4A8 PE=1 SV=1 - [S4A8_HUMAN]	1	1	1	1	1093	122. 9	6.6 8
I3L1U9	Actin, cytoplasmic 2 (Fragment) OS=Homo sapiens GN=ACTG1 PE=1 SV=1 - [I3L1U9_HUMAN]	16	1	1	1	214	23.8	5.4 4
H3BSE0	Ubiquitin-like protein 7 (Fragment) OS=Homo sapiens GN=UBL7 PE=1 SV=1 - [H3BSE0_HUMAN]	4	1	1	1	114	11.7	4.5 1
Q16378	Proline-rich protein 4 OS=Homo sapiens GN=PRR4 PE=1 SV=3 - [PROL4_HUMAN]	2	1	1	1	134	15.1	7.0 6
P81133	Single-minded homolog 1 OS=Homo sapiens GN=SIM1 PE=2 SV=2 - [SIM1_HUMAN]	1	1	1	1	766	85.5	7.4 3
Q96K75	Zinc finger protein 514 OS=Homo sapiens GN=ZNF514 PE=2 SV=1 - [ZN514_HUMAN]	1	1	1	1	400	45.9	8.8 7
B3KU25	Pyruvate dehydrogenase kinase, isozyme 4, isoform CRA_b OS=Homo sapiens GN=PKD4 PE=2 SV=1 - [B3KU25_HUMAN]	3	1	1	1	375	42.6	6.1 9
Q8IU77	Breast and ovarian cancer susceptibility protein (Fragment) OS=Homo sapiens GN=BRCA2 PE=4 SV=1 - [Q8IU77_HUMAN]	1	1	1	2	35	3.9	8.5 9
H3BV44	Unconventional myosin-IXa (Fragment) OS=Homo sapiens GN=MYO9A PE=1 SV=1 - [H3BV44_HUMAN]	3	1	1	1	1398	157. 9	7.8 7
A0JLQ0	AZGP1 protein (Fragment) OS=Homo sapiens GN=AZGP1 PE=2 SV=1 - [A0JLQ0_HUMAN]	3	1	1	1	159	18.7	8.9 7
B4DVL1	cDNA FLJ54179 OS=Homo sapiens PE=2 SV=1 - [B4DVL1_HUMAN]	1	1	1	1	159	16.0	11. 30
Q9BRJ0	HECTD1 protein (Fragment) OS=Homo sapiens GN=HECTD1 PE=2 SV=2 - [Q9BRJ0_HUMAN]	7	1	1	1	121	13.4	8.2 8
F8WF90	PRA1 family protein 3 OS=Homo sapiens GN=ARL6IP5 PE=1 SV=1 - [F8WF90_HUMAN]	7	1	1	1	59	6.9	6.6 0
Q0VAH5	Zinc finger protein 366 OS=Homo sapiens GN=ZNF366 PE=2 SV=1 - [Q0VAH5_HUMAN]	2	1	1	1	744	85.0	8.5 9

B4DS47	cDNA FLJ59745, highly similar to Trophinin OS=Homo sapiens PE=2 SV=1 - [B4DS47_HUMAN]	4	1	1	1	795	78.5	6.6 1
L8EAR9	Alternative protein ERP44 OS=Homo sapiens GN=ERP44 PE=4 SV=1 - [L8EAR9_HUMAN]	20	1	1	1	57	6.2	9.4 2
B4DYA3	cDNA FLJ52290, highly similar to F-box only protein 25 OS=Homo sapiens PE=2 SV=1 - [B4DYA3_HUMAN]	3	1	1	1	330	38.9	8.2 1
A8K651	cDNA FLJ75700, highly similar to Homo sapiens complement component 1, q subcomponent binding protein (C1QBP), nuclear gene encoding mitochondrial protein, mRNA OS=Homo sapiens PE=2 SV=1 - [A8K651_HUMAN]	2	1	1	1	282	31.4	4.8 4

ErbB2-2-2

Accession	Description	# Proteins	# Unique Peptides	# Peptides	# PSMs	# AAs	MW [kDa]	calc. pI
P13645	Keratin, type I cytoskeletal 10 OS=Homo sapiens GN=KRT10 PE=1 SV=6 - [K1C10_HUMAN]	25	28	32	148	584	58.8	5.21
P35527	Keratin, type I cytoskeletal 9 OS=Homo sapiens GN=KRT9 PE=1 SV=3 - [K1C9_HUMAN]	2	28	29	121	623	62.0	5.24
H6VRF8	Keratin 1 OS=Homo sapiens GN=KRT1 PE=3 SV=1 - [H6VRF8_HUMAN]	17	30	33	121	644	66.0	8.12
P35908	Keratin, type II cytoskeletal 2 epidermal OS=Homo sapiens GN=KRT2 PE=1 SV=2 - [K22E_HUMAN]	10	23	29	77	639	65.4	8.00
P02533	Keratin, type I cytoskeletal 14 OS=Homo sapiens GN=KRT14 PE=1 SV=4 - [K1C14_HUMAN]	42	5	15	44	472	51.5	5.16
P08779	Keratin, type I cytoskeletal 16 OS=Homo sapiens GN=KRT16 PE=1 SV=4 - [K1C16_HUMAN]	37	3	13	39	473	51.2	5.05
P13647	Keratin, type II cytoskeletal 5 OS=Homo sapiens GN=KRT5 PE=1 SV=3 - [K2C5_HUMAN]	16	7	13	23	590	62.3	7.74
A0A024R0Y2	HCG30204, isoform CRA_a OS=Homo sapiens GN=hCG_30204 PE=4 SV=1 - [A0A024R0Y2_HUMAN]	17	14	14	17	2268	257.1	6.61
F6KPG5	Albumin (Fragment) OS=Homo sapiens PE=2 SV=1 - [F6KPG5_HUMAN]	14	3	3	6	585	66.5	6.04
Q45KI0	Trypsin I (Fragment) OS=Homo sapiens GN=PRSS1 PE=3 SV=1 - [Q45KI0_HUMAN]	17	1	1	3	84	9.2	9.99
Q9GZZ8	Extracellular glycoprotein lacritin OS=Homo sapiens GN=LACRT PE=1 SV=1 - [LACRT_HUMAN]	2	3	3	5	138	14.2	5.50
Q14CN4	Keratin, type II cytoskeletal 72 OS=Homo sapiens GN=KRT72 PE=1 SV=2 - [K2C72_HUMAN]	11	1	4	7	511	55.8	6.89
P81605	Dermcidin OS=Homo sapiens GN=DCD PE=1 SV=2 - [DCD_HUMAN]	1	3	3	5	110	11.3	6.54

Q53HF2	Heat shock 70kDa protein 8 isoform 2 variant (Fragment) OS=Homo sapiens PE=1 SV=1 - [Q53HF2_HUMAN]	39	3	3	4	493	53.5	5.86
J3QRT3	Uncharacterized protein KIAA0195 (Fragment) OS=Homo sapiens GN=KIAA0195 PE=1 SV=5 - [J3QRT3_HUMAN]	1	1	1	3	89	9.5	6.76
B3KPS3	cDNA FLJ32131 fis, clone PEBLM2000267, highly similar to Tubulin alpha-ubiquitous chain OS=Homo sapiens PE=2 SV=1 - [B3KPS3_HUMAN]	35	4	4	4	416	46.2	5.12
Q19KS2	Lactoferrin (Fragment) OS=Homo sapiens PE=2 SV=1 - [Q19KS2_HUMAN]	15	3	3	3	353	39.1	9.03
B3KX99	cDNA FLJ45019 fis, clone BRAWH3015825 OS=Homo sapiens PE=2 SV=1 - [B3KX99_HUMAN]	2	1	1	3	333	38.5	8.97
Q86YZ3	Hornerin OS=Homo sapiens GN=HRNR PE=1 SV=2 - [HORN_HUMAN]	1	1	1	1	2850	282.2	10.04
Q8TC04	Keratin 23 (Histone deacetylase inducible) OS=Homo sapiens GN=KRT23 PE=2 SV=1 - [Q8TC04_HUMAN]	1	1	1	3	422	48.1	6.54
F8WCHO	Actin, gamma-enteric smooth muscle OS=Homo sapiens GN=ACTG2 PE=1 SV=1 - [F8WCHO_HUMAN]	43	1	1	2	52	5.6	6.49
M0R1V7	Ubiquitin-60S ribosomal protein L40 (Fragment) OS=Homo sapiens GN=UBA52 PE=1 SV=1 - [M0R1V7_HUMAN]	40	2	2	2	63	7.1	5.36
A0A075B6Z2	Protein TRAJ56 (Fragment) OS=Homo sapiens GN=TRAJ56 PE=4 SV=1 - [A0A075B6Z2_HUMAN]	2	1	1	10	21	2.2	10.29
Q5VSP4	Putative lipocalin 1-like protein 1 OS=Homo sapiens GN=LCN1P1 PE=5 SV=1 - [LC1L1_HUMAN]	2	2	2	2	162	17.9	5.00
O75556	Mammaglobin-B OS=Homo sapiens GN=SCGB2A1 PE=1 SV=1 - [SG2A1_HUMAN]	1	1	1	1	95	10.9	5.78
L0R5A1	Alternative protein CSF2RB OS=Homo sapiens GN=CSF2RB PE=4 SV=1 - [L0R5A1_HUMAN]	1	1	1	2	108	11.6	11.30
Q86W20	Protease serine 1 (Fragment) OS=Homo sapiens GN=PRSS1 PE=3 SV=1 - [Q86W20_HUMAN]	6	1	1	1	84	9.2	10.27
A0A087WYX2	Histone lysine demethylase PHF8 OS=Homo sapiens GN=PHF8 PE=1 SV=1 - [A0A087WYX2_HUMAN]	2	1	1	1	303	33.8	10.08
E9PMG1	RalBP1-associated Eps domain-containing protein 1 OS=Homo sapiens GN=REPS1 PE=1 SV=1 - [E9PMG1_HUMAN]	2	1	1	1	737	80.4	5.87
B4DPU1	cDNA FLJ60776 OS=Homo sapiens PE=2 SV=1 - [B4DPU1_HUMAN]	3	1	1	1	181	21.0	9.41
Q02413	Desmoglein-1 OS=Homo sapiens GN=DSG1 PE=1 SV=2 - [DSG1_HUMAN]	1	2	2	2	1049	113.7	5.03
A8K2T2	cDNA FLJ75519 (Fragment) OS=Homo sapiens PE=2 SV=1 - [A8K2T2_HUMAN]	4	1	1	1	1173	130.7	9.01
F8WCJ1	Eukaryotic translation initiation factor 5A OS=Homo sapiens GN=EIF5A2 PE=1 SV=1 - [F8WCJ1_HUMAN]	8	1	1	1	105	11.7	9.14
Q5HY57	Emerin OS=Homo sapiens GN=EMD PE=1 SV=1 - [Q5HY57_HUMAN]	2	1	1	1	219	24.9	5.02
Q5TDG9	DnaJ (Hsp40) homolog, subfamily C, member 16, isoform CRA_a OS=Homo sapiens GN=DNAJC16 PE=1 SV=1 - [Q5TDG9_HUMAN]	4	1	1	1	595	69.3	7.15

V9GZN0	Histone H2A gene (lambda-HHG55) (Fragment) OS=Homo sapiens PE=4 SV=1 - [V9GZN0_HUMAN]	19	1	1	1	47	5.0	11.90
Q9BRJ0	HECTD1 protein (Fragment) OS=Homo sapiens GN=HECTD1 PE=2 SV=2 - [Q9BRJ0_HUMAN]	7	1	1	1	121	13.4	8.28
J3KP89	Adenylate kinase 9 OS=Homo sapiens GN=AK9 PE=1 SV=1 - [J3KP89_HUMAN]	2	1	1	1	736	84.8	5.02
B2R4M6	Protein S100 OS=Homo sapiens PE=2 SV=1 - [B2R4M6_HUMAN]	2	1	1	2	114	13.2	6.13
B4DKX6	cDNA FLJ53584, highly similar to Desmoplakin (Fragment) OS=Homo sapiens PE=2 SV=1 - [B4DKX6_HUMAN]	4	1	1	1	954	112.2	6.73
Q86XH1	IQ and AAA domain-containing protein 1 OS=Homo sapiens GN=IQCA1 PE=2 SV=1 - [IQCA1_HUMAN]	3	1	1	3	822	95.3	9.47
Q16378	Proline-rich protein 4 OS=Homo sapiens GN=PRR4 PE=1 SV=3 - [PROL4_HUMAN]	2	1	1	1	134	15.1	7.06
Q9UHP3	Ubiquitin carboxyl-terminal hydrolase 25 OS=Homo sapiens GN=USP25 PE=1 SV=4 - [UBP25_HUMAN]	1	1	1	1	1055	122.1	5.34
G3V3Y2	Fibulin-5 (Fragment) OS=Homo sapiens GN=FBLN5 PE=1 SV=1 - [G3V3Y2_HUMAN]	5	1	1	1	91	9.9	6.37
Q6ZSX8	cDNA FLJ45139 fis, clone BRAWH3039623 OS=Homo sapiens PE=2 SV=1 - [Q6ZSX8_HUMAN]	1	1	1	1	136	15.5	10.07

FGFR1-1

Accession	Description	# Proteins	# Unique Peptides	# Peptides	# PSMs	# AAs	MW [kDa]	calc. pI
P35527	Keratin, type I cytoskeletal 9 OS=Homo sapiens GN=KRT9 PE=1 SV=3 - [K1C9_HUMAN]	2	28	29	121	623	62.0	5.24
P13645	Keratin, type I cytoskeletal 10 OS=Homo sapiens GN=KRT10 PE=1 SV=6 - [K1C10_HUMAN]	23	24	28	115	584	58.8	5.21
H6VRF8	Keratin 1 OS=Homo sapiens GN=KRT1 PE=3 SV=1 - [H6VRF8_HUMAN]	14	29	31	115	644	66.0	8.12
P35908	Keratin, type II cytoskeletal 2 epidermal OS=Homo sapiens GN=KRT2 PE=1 SV=2 - [K22E_HUMAN]	14	17	25	70	639	65.4	8.00
P02533	Keratin, type I cytoskeletal 14 OS=Homo sapiens GN=KRT14 PE=1 SV=4 - [K1C14_HUMAN]	35	5	19	50	472	51.5	5.16
P08779	Keratin, type I cytoskeletal 16 OS=Homo sapiens GN=KRT16 PE=1 SV=4 - [K1C16_HUMAN]	33	5	16	44	473	51.2	5.05
P13647	Keratin, type II cytoskeletal 5 OS=Homo sapiens GN=KRT5 PE=1 SV=3 - [K2C5_HUMAN]	19	10	19	37	590	62.3	7.74
B4DRR0	cDNA FLJ53910, highly similar to Keratin, type II cytoskeletal 6A OS=Homo sapiens PE=2 SV=1 - [B4DRR0_HUMAN]	23	6	16	30	535	57.8	8.00

Q04695	Keratin, type I cytoskeletal 17 OS=Homo sapiens GN=KRT17 PE=1 SV=2 - [K1C17_HUMAN]	27	2	13	21	432	48.1	5.02
Q0IIN1	Keratin 77 OS=Homo sapiens GN=KRT77 PE=1 SV=1 - [Q0IIN1_HUMAN]	9	1	4	11	578	61.8	5.85
F6KPG5	Albumin (Fragment) OS=Homo sapiens PE=2 SV=1 - [F6KPG5_HUMAN]	14	3	3	7	585	66.5	6.04
Q14CN4	Keratin, type II cytoskeletal 72 OS=Homo sapiens GN=KRT72 PE=1 SV=2 - [K2C72_HUMAN]	10	1	4	8	511	55.8	6.89
O75556	Mammaglobin-B OS=Homo sapiens GN=SCGB2A1 PE=1 SV=1 - [SG2A1_HUMAN]	1	3	3	5	95	10.9	5.78
P81605	Dermcidin OS=Homo sapiens GN=DCD PE=1 SV=2 - [DCD_HUMAN]	1	3	3	5	110	11.3	6.54
A0A075B6Z2	Protein TRAJ56 (Fragment) OS=Homo sapiens GN=TRAJ56 PE=4 SV=1 - [A0A075B6Z2_HUMAN]	2	1	1	35	21	2.2	10.29
Q45KI0	Trypsin I (Fragment) OS=Homo sapiens GN=PRSS1 PE=3 SV=1 - [Q45KI0_HUMAN]	17	1	1	3	84	9.2	9.99
J3QRT3	Uncharacterized protein KIAA0195 (Fragment) OS=Homo sapiens GN=KIAA0195 PE=1 SV=5 - [J3QRT3_HUMAN]	1	1	1	4	89	9.5	6.76
Q9GZZ8	Extracellular glycoprotein lacritin OS=Homo sapiens GN=LACRT PE=1 SV=1 - [LACRT_HUMAN]	2	3	3	4	138	14.2	5.50
Q86YZ3	Hornerin OS=Homo sapiens GN=HRNR PE=1 SV=2 - [HORN_HUMAN]	1	1	1	2	2850	282.2	10.04
Q86W20	Protease serine 1 (Fragment) OS=Homo sapiens GN=PRSS1 PE=3 SV=1 - [Q86W20_HUMAN]	6	1	1	3	84	9.2	10.27
Q19KS2	Lactoferrin (Fragment) OS=Homo sapiens PE=2 SV=1 - [Q19KS2_HUMAN]	15	2	2	4	353	39.1	9.03
A0A087W TG3	Cullin-3 OS=Homo sapiens GN=CUL3 PE=1 SV=1 - [A0A087W TG3_HUMAN]	1	1	1	2	342	39.1	9.48
H7C2X0	Translation initiation factor eIF-2B subunit epsilon (Fragment) OS=Homo sapiens GN=EIF2B5 PE=1 SV=1 - [H7C2X0_HUMAN]	4	1	1	2	92	9.4	9.41
F8WCJ1	Eukaryotic translation initiation factor 5A OS=Homo sapiens GN=EIF5A2 PE=1 SV=1 - [F8WCJ1_HUMAN]	8	1	1	2	105	11.7	9.14
Q6UXS9	Inactive caspase-12 OS=Homo sapiens GN=CASP12 PE=2 SV=2 - [CASPC_HUMAN]	1	1	1	1	341	38.8	6.02
B3KX99	cDNA FLJ45019 fis, clone BRAWH3015825 OS=Homo sapiens PE=2 SV=1 - [B3KX99_HUMAN]	2	1	1	2	333	38.5	8.97
L0R5A1	Alternative protein CSF2RB OS=Homo sapiens GN=CSF2RB PE=4 SV=1 - [L0R5A1_HUMAN]	1	1	1	3	108	11.6	11.30
Q9NR48	Histone-lysine N-methyltransferase ASH1L OS=Homo sapiens GN=ASH1L PE=1 SV=2 - [ASH1L_HUMAN]	1	1	1	1	2969	332.6	9.39
F8WCHO	Actin, gamma-enteric smooth muscle OS=Homo sapiens GN=ACTG2 PE=1 SV=1 - [F8WCHO_HUMAN]	43	1	1	1	52	5.6	6.49
D6R9F0	Leucine-rich repeat-containing G-protein-coupled receptor 6 OS=Homo sapiens GN=LGR6 PE=1 SV=1 - [D6R9F0_HUMAN]	1	1	1	1	348	39.2	7.74
M0QZJ2	Cytochrome P450 2B6 OS=Homo sapiens GN=CYP2B6 PE=1 SV=1 - [M0QZJ2_HUMAN]	4	1	1	1	255	29.1	7.15

Q5VSP4	Putative lipocalin 1-like protein 1 OS=Homo sapiens GN=LCN1P1 PE=5 SV=1 - [LC1L1_HUMAN]	2	2	2	2	162	17.9	5.00
P31151	Protein S100-A7 OS=Homo sapiens GN=S100A7 PE=1 SV=4 - [S10A7_HUMAN]	1	1	1	1	101	11.5	6.77
E7ERU0	Dystonin OS=Homo sapiens GN=DST PE=1 SV=1 - [E7ERU0_HUMAN]	6	1	1	1	5375	615.3	5.74
P05109	Protein S100-A8 OS=Homo sapiens GN=S100A8 PE=1 SV=1 - [S10A8_HUMAN]	4	2	2	2	93	10.8	7.03
Q8WXG9	G-protein coupled receptor 98 OS=Homo sapiens GN=GPR98 PE=1 SV=2 - [GPR98_HUMAN]	1	1	1	1	6306	692.6	4.64
B2R4M6	Protein S100 OS=Homo sapiens PE=2 SV=1 - [B2R4M6_HUMAN]	2	1	1	1	114	13.2	6.13
L8ECQ7	Alternative protein C10orf112 OS=Homo sapiens GN=C10orf112 PE=4 SV=1 - [L8ECQ7_HUMAN]	1	1	1	1	130	14.3	10.0 2
A0A024RC53	Phosphodiesterase 8A, isoform CRA_a OS=Homo sapiens GN=PDE8A PE=4 SV=1 - [A0A024RC53_HUMAN]	2	1	1	1	582	66.0	6.02
C9IYG1	BRCA1-associated RING domain protein 1 (Fragment) OS=Homo sapiens GN=BARD1 PE=1 SV=1 - [C9IYG1_HUMAN]	9	1	1	1	216	24.4	8.47
A0A087WYX2	Histone lysine demethylase PHF8 OS=Homo sapiens GN=PHF8 PE=1 SV=1 - [A0A087WYX2_HUMAN]	2	1	1	1	303	33.8	10.0 8
B4DPU1	cDNA FLJ60776 OS=Homo sapiens PE=2 SV=1 - [B4DPU1_HUMAN]	3	1	1	1	181	21.0	9.41
Q5HY57	Emerin OS=Homo sapiens GN=EMD PE=1 SV=1 - [Q5HY57_HUMAN]	2	1	1	1	219	24.9	5.02
Q6ZRA8	cDNA FLJ46514 fis, clone THYMU3032798, highly similar to Focal adhesion kinase 2 (EC 2.7.1.112) OS=Homo sapiens PE=2 SV=1 - [Q6ZRA8_HUMAN]	1	1	1	1	596	68.0	5.60
C9JG98	Probable ATP-dependent RNA helicase DHX58 (Fragment) OS=Homo sapiens GN=DHX58 PE=1 SV=1 - [C9JG98_HUMAN]	5	1	1	1	302	34.0	6.71
P46019	Phosphorylase b kinase regulatory subunit alpha, liver isoform OS=Homo sapiens GN=PHKA2 PE=1 SV=1 - [KPB2_HUMAN]	1	1	1	1	1235	138.3	6.44
K7EMZ7	Uncharacterized protein C19orf57 OS=Homo sapiens GN=C19orf57 PE=1 SV=1 - [K7EMZ7_HUMAN]	2	1	1	1	243	26.5	9.51
B4DK31	cDNA FLJ54634, highly similar to Acetyl-CoA carboxylase 1 (EC 6.4.1.2) OS=Homo sapiens PE=2 SV=1 - [B4DK31_HUMAN]	9	1	1	1	306	35.6	6.38
Q6ZSX8	cDNA FLJ45139 fis, clone BRAWH3039623 OS=Homo sapiens PE=2 SV=1 - [Q6ZSX8_HUMAN]	1	1	1	2	136	15.5	10.0 7
O95968	Secretoglobin family 1D member 1 OS=Homo sapiens GN=SCGB1D1 PE=1 SV=1 - [SG1D1_HUMAN]	1	1	1	1	90	9.9	9.25
B2RU33	POTE ankyrin domain family member C OS=Homo sapiens GN=POTEC PE=2 SV=2 - [POTEC_HUMAN]	7	1	1	1	542	61.1	6.76
Q9ULV8	E3 ubiquitin-protein ligase CBL-C OS=Homo sapiens GN=CBLC PE=1 SV=3 - [CBLC_HUMAN]	1	1	1	1	474	52.4	7.69
Q9NY74	Ewing's tumor-associated antigen 1 OS=Homo sapiens GN=ETAA1 PE=1 SV=2 - [ETAA1_HUMAN]	1	1	1	1	926	103.4	7.62
P80108	Phosphatidylinositol-glycan-specific phospholipase D OS=Homo sapiens GN=GPLD1 PE=1 SV=3 - [PHLD_HUMAN]	1	1	1	1	840	92.3	6.37

H7C0N5	Engulfment and cell motility protein 1 (Fragment) OS=Homo sapiens GN=ELMO1 PE=1 SV=1 - [H7C0N5_HUMAN]	3	1	1	1	124	14.1	9.14
A0A087WUV8	Basigin OS=Homo sapiens GN=BSG PE=1 SV=1 - [A0A087WUV8_HUMAN]	6	1	1	1	189	20.5	6.68
G3V3Y2	Fibulin-5 (Fragment) OS=Homo sapiens GN=FBLN5 PE=1 SV=1 - [G3V3Y2_HUMAN]	5	1	1	1	91	9.9	6.37
A0A087X099	Protocadherin-17 (Fragment) OS=Homo sapiens GN=PCDH17 PE=1 SV=1 - [A0A087X099_HUMAN]	2	1	1	1	184	20.2	5.06
I3L1H9	Zymogen granule protein 16 homolog B (Fragment) OS=Homo sapiens GN=ZG16B PE=1 SV=1 - [I3L1H9_HUMAN]	5	1	1	1	69	7.5	9.32

FGFR1-2

Accession	Description	# Proteins	# Unique Peptides	# Peptides	# PSMs	# AAs	MW [kDa]	calc . pI
P35527	Keratin, type I cytoskeletal 9 OS=Homo sapiens GN=KRT9 PE=1 SV=3 - [K1C9_HUMAN]	2	30	31	199	623	62.0	5.24
H6VRF8	Keratin 1 OS=Homo sapiens GN=KRT1 PE=3 SV=1 - [H6VRF8_HUMAN]	14	29	34	188	644	66.0	8.12
P13645	Keratin, type I cytoskeletal 10 OS=Homo sapiens GN=KRT10 PE=1 SV=6 - [K1C10_HUMAN]	23	28	32	128	584	58.8	5.21
P35908	Keratin, type II cytoskeletal 2 epidermal OS=Homo sapiens GN=KRT2 PE=1 SV=2 - [K22E_HUMAN]	11	21	29	99	639	65.4	8.00
P08779	Keratin, type I cytoskeletal 16 OS=Homo sapiens GN=KRT16 PE=1 SV=4 - [K1C16_HUMAN]	32	10	21	58	473	51.2	5.05
P02533	Keratin, type I cytoskeletal 14 OS=Homo sapiens GN=KRT14 PE=1 SV=4 - [K1C14_HUMAN]	31	6	21	56	472	51.5	5.16
P04259	Keratin, type II cytoskeletal 6B OS=Homo sapiens GN=KRT6B PE=1 SV=5 - [K2C6B_HUMAN]	12	2	21	54	564	60.0	8.00
P13647	Keratin, type II cytoskeletal 5 OS=Homo sapiens GN=KRT5 PE=1 SV=3 - [K2C5_HUMAN]	18	11	23	41	590	62.3	7.74
B4DRR0	cDNA FLJ53910, highly similar to Keratin, type II cytoskeletal 6A OS=Homo sapiens PE=2 SV=1 - [B4DRR0_HUMAN]	20	3	23	41	535	57.8	8.00
Q04695	Keratin, type I cytoskeletal 17 OS=Homo sapiens GN=KRT17 PE=1 SV=2 - [K1C17_HUMAN]	27	4	16	25	432	48.1	5.02
Q14CN4	Keratin, type II cytoskeletal 72 OS=Homo sapiens GN=KRT72 PE=1 SV=2 - [K2C72_HUMAN]	8	1	4	11	511	55.8	6.89

Q53HF2	Heat shock 70kDa protein 8 isoform 2 variant (Fragment) OS=Homo sapiens PE=1 SV=1 - [Q53HF2_HUMAN]	32	5	7	10	493	53.5	5.8 6
F6KPG5	Albumin (Fragment) OS=Homo sapiens PE=2 SV=1 - [F6KPG5_HUMAN]	14	4	4	7	585	66.5	6.0 4
Q45KI0	Trypsin I (Fragment) OS=Homo sapiens GN=PRSS1 PE=3 SV=1 - [Q45KI0_HUMAN]	17	1	1	4	84	9.2	9.9 9
B3KY79	cDNA FLJ46620 fis, clone TLUNG2000654, highly similar to Keratin, type II cytoskeletal 7 OS=Homo sapiens PE=2 SV=1 - [B3KY79_HUMAN]	15	1	4	8	445	49.0	5.4 8
B4E1T6	cDNA FLJ54342, highly similar to Heat shock 70 kDa protein 1 OS=Homo sapiens PE=2 SV=1 - [B4E1T6_HUMAN]	27	1	3	6	398	43.0	5.3 9
P15924	Desmoplakin OS=Homo sapiens GN=DSP PE=1 SV=3 - [DESP_HUMAN]	6	5	5	6	2871	331. 6	6.8 1
Q8N1N4	Keratin, type II cytoskeletal 78 OS=Homo sapiens GN=KRT78 PE=2 SV=2 - [K2C78_HUMAN]	4	3	4	5	520	56.8	6.0 2
A0A024 R0Y2	HCG30204, isoform CRA_a OS=Homo sapiens GN=hCG_30204 PE=4 SV=1 - [A0A024R0Y2_HUMAN]	10	4	4	5	2268	257. 1	6.6 1
Q6KB66	Keratin, type II cytoskeletal 80 OS=Homo sapiens GN=KRT80 PE=1 SV=2 - [K2C80_HUMAN]	8	1	2	4	452	50.5	5.6 7
B7Z597	cDNA FLJ54373, highly similar to 60 kDa heat shock protein, mitochondrial OS=Homo sapiens PE=2 SV=1 - [B7Z597_HUMAN]	11	3	3	3	564	60.0	5.7 4
F8VVB9	Tubulin alpha-1B chain (Fragment) OS=Homo sapiens GN=TUBA1B PE=1 SV=5 - [F8VVB9_HUMAN]	33	4	4	5	247	27.5	5.2 0
Q19KS2	Lactoferrin (Fragment) OS=Homo sapiens PE=2 SV=1 - [Q19KS2_HUMAN]	15	2	2	4	353	39.1	9.0 3
O75556	Mammaglobin-B OS=Homo sapiens GN=SCGB2A1 PE=1 SV=1 - [SG2A1_HUMAN]	1	1	1	2	95	10.9	5.7 8
P81605	Dermcidin OS=Homo sapiens GN=DCD PE=1 SV=2 - [DCD_HUMAN]	1	3	3	4	110	11.3	6.5 4
B3KX99	cDNA FLJ45019 fis, clone BRAWH3015825 OS=Homo sapiens PE=2 SV=1 - [B3KX99_HUMAN]	2	1	1	4	333	38.5	8.9 7
J3QSA3	Polyubiquitin-B (Fragment) OS=Homo sapiens GN=UBB PE=1 SV=1 - [J3QSA3_HUMAN]	37	1	1	2	43	4.9	5.1 9
Q86W20	Protease serine 1 (Fragment) OS=Homo sapiens GN=PRSS1 PE=3 SV=1 - [Q86W20_HUMAN]	6	1	1	2	84	9.2	10. 27
E5RGE1	14-3-3 protein zeta/delta (Fragment) OS=Homo sapiens GN=YWHAZ PE=1 SV=5 - [E5RGE1_HUMAN]	31	2	2	2	52	5.9	4.7 8
Q2VPJ6	HSP90AA1 protein (Fragment) OS=Homo sapiens GN=HSP90AA1 PE=1 SV=1 - [Q2VPJ6_HUMAN]	15	4	4	4	585	68.3	5.1 9
Q9GZZ8	Extracellular glycoprotein lacritin OS=Homo sapiens GN=LACRT PE=1 SV=1 - [LACRT_HUMAN]	2	2	2	2	138	14.2	5.5 0

E5RJN0	Heparan-alpha-glucosaminide N-acetyltransferase OS=Homo sapiens GN=HGSNAT PE=1 SV=1 - [E5RJN0_HUMAN]	2	1	1	2	352	38.9	8.3 2
H7C2X0	Translation initiation factor eIF-2B subunit epsilon (Fragment) OS=Homo sapiens GN=EIF2B5 PE=1 SV=1 - [H7C2X0_HUMAN]	4	1	1	2	92	9.4	9.4 1
Q6UXS9	Inactive caspase-12 OS=Homo sapiens GN=CASP12 PE=2 SV=2 - [CASPC_HUMAN]	1	1	1	2	341	38.8	6.0 2
J3QRT3	Uncharacterized protein KIAA0195 (Fragment) OS=Homo sapiens GN=KIAA0195 PE=1 SV=5 - [J3QRT3_HUMAN]	1	1	1	2	89	9.5	6.7 6
I3L1U9	Actin, cytoplasmic 2 (Fragment) OS=Homo sapiens GN=ACTG1 PE=1 SV=1 - [I3L1U9_HUMAN]	47	2	2	2	214	23.8	5.4 4
A0A0C4DFV9	Protein SET OS=Homo sapiens GN=SET PE=1 SV=1 - [A0A0C4DFV9_HUMAN]	6	1	1	2	266	31.1	4.2 3
A0A087WTG3	Cullin-3 OS=Homo sapiens GN=CUL3 PE=1 SV=1 - [A0A087WTG3_HUMAN]	1	1	1	3	342	39.1	9.4 8
P25311	Zinc-alpha-2-glycoprotein OS=Homo sapiens GN=AZGP1 PE=1 SV=2 - [ZA2G_HUMAN]	1	1	1	2	298	34.2	6.0 5
B4DEF7	cDNA FLJ60062, highly similar to 78 kDa glucose-regulated protein OS=Homo sapiens PE=2 SV=1 - [B4DEF7_HUMAN]	2	1	2	2	278	30.4	6.0 5
F8VV32	Lysozyme OS=Homo sapiens GN=LYZ PE=1 SV=1 - [F8VV32_HUMAN]	3	2	2	2	104	11.5	9.0 7
Q6ZSX8	cDNA FLJ45139 fis, clone BRAWH3039623 OS=Homo sapiens PE=2 SV=1 - [Q6ZSX8_HUMAN]	1	1	1	7	136	15.5	10. 07
Q86Y65	KIAA1529 protein (Fragment) OS=Homo sapiens GN=KIAA1529 PE=2 SV=2 - [Q86Y65_HUMAN]	4	1	1	1	900	104. 4	5.2 4
C9JD91	Tyrosine-protein phosphatase non-receptor type 23 (Fragment) OS=Homo sapiens GN=PTPN23 PE=1 SV=5 - [C9JD91_HUMAN]	5	1	1	1	170	19.2	7.4 2
Q6ICA1	DJ402G11.9 protein OS=Homo sapiens GN=dJ402G11.9 PE=2 SV=1 - [Q6ICA1_HUMAN]	3	1	1	1	543	59.5	8.7 2
A0A087WXD2	Membrane-associated guanylate kinase, WW and PDZ domain-containing protein 1 OS=Homo sapiens GN=MAGI1 PE=1 SV=1 - [A0A087WXD2_HUMAN]	7	1	1	1	980	106. 8	6.4 6
H0YKZ7	Annexin (Fragment) OS=Homo sapiens GN=ANXA2 PE=1 SV=1 - [H0YKZ7_HUMAN]	16	1	1	1	119	13.0	8.1 3
Q8NGY2	Olfactory receptor 6K2 OS=Homo sapiens GN=OR6K2 PE=2 SV=1 - [OR6K2_HUMAN]	1	1	1	1	324	36.5	7.9 3
B7Z1V7	cDNA FLJ51811, highly similar to Stress-70 protein, mitochondrial OS=Homo sapiens PE=2 SV=1 - [B7Z1V7_HUMAN]	6	1	1	1	437	47.3	6.6 1
P05109	Protein S100-A8 OS=Homo sapiens GN=S100A8 PE=1 SV=1 - [S10A8_HUMAN]	1	1	1	2	93	10.8	7.0 3
D3DS15	Uncharacterized protein OS=Homo sapiens GN=FLJ10357 PE=4 SV=1 - [D3DS15_HUMAN]	3	1	1	1	1498	162. 7	6.4 7

Q14222	EEF1A protein (Fragment) OS=Homo sapiens GN=EEF1A PE=2 SV=1 - [Q14222_HUMAN]	29	1	1	1	227	24.2	9.58
Q5ZEY3	Glyceraldehyde-3-phosphate dehydrogenase (Fragment) OS=Homo sapiens GN=GAPD PE=2 SV=1 - [Q5ZEY3_HUMAN]	6	1	1	1	86	9.2	9.72
H0YB22	40S ribosomal protein S14 (Fragment) OS=Homo sapiens GN=RPS14 PE=1 SV=1 - [H0YB22_HUMAN]	3	1	1	1	120	12.9	9.85
C9IYG1	BRCA1-associated RING domain protein 1 (Fragment) OS=Homo sapiens GN=BARD1 PE=1 SV=1 - [C9IYG1_HUMAN]	9	1	1	1	216	24.4	8.47
B4DHR1	cDNA FLJ53009, highly similar to Calreticulin OS=Homo sapiens PE=2 SV=1 - [B4DHR1_HUMAN]	5	1	1	1	212	24.3	5.11
A0A0A0MRQ5	Peroxiredoxin-1 OS=Homo sapiens GN=PRDX1 PE=1 SV=1 - [A0A0A0MRQ5_HUMAN]	6	1	1	1	97	10.7	8.72
P07737	Profilin-1 OS=Homo sapiens GN=PFN1 PE=1 SV=2 - [PROF1_HUMAN]	2	1	1	1	140	15.0	8.27
Q5BQ95	Kallikrein 13 splice variant 7 OS=Homo sapiens GN=KLK13 PE=2 SV=1 - [Q5BQ95_HUMAN]	1	1	1	1	98	10.7	9.69
A0A0A0MTR7	E3 ubiquitin-protein ligase RNF213 OS=Homo sapiens GN=RNF213 PE=1 SV=1 - [A0A0A0MTR7_HUMAN]	3	1	1	1	5207	591.0	6.48
Q7Z5L4	Spermatogenesis-associated protein 19, mitochondrial OS=Homo sapiens GN=SPATA19 PE=2 SV=2 - [SPT19_HUMAN]	1	1	1	1	167	19.2	6.96
B4DWS6	cDNA FLJ61181, highly similar to Homo sapiens hydroxysteroid (17-beta) dehydrogenase 12 (HSD17B12), mRNA OS=Homo sapiens PE=2 SV=1 - [B4DWS6_HUMAN]	4	1	1	1	304	33.5	9.39
L8ECQ7	Alternative protein C10orf112 OS=Homo sapiens GN=C10orf112 PE=4 SV=1 - [L8ECQ7_HUMAN]	1	1	1	1	130	14.3	10.02
Q9HB00	Desmocollin 1, isoform CRA_b OS=Homo sapiens GN=DSC1 PE=4 SV=1 - [Q9HB00_HUMAN]	2	1	1	1	840	93.8	5.53
A0PJ54	PEX12 protein (Fragment) OS=Homo sapiens GN=PEX12 PE=2 SV=1 - [A0PJ54_HUMAN]	1	1	1	1	324	36.9	9.98
Q15203	Prothymosin alpha OS=Homo sapiens PE=4 SV=2 - [Q15203_HUMAN]	18	1	1	1	73	8.2	3.76
A0A024R3V9	HCG37498, isoform CRA_b OS=Homo sapiens GN=hCG_37498 PE=4 SV=1 - [A0A024R3V9_HUMAN]	5	1	1	1	92	11.0	9.74
P31151	Protein S100-A7 OS=Homo sapiens GN=S100A7 PE=1 SV=4 - [S10A7_HUMAN]	1	1	1	1	101	11.5	6.77
K7ESD3	Zinc finger and SCAN domain-containing protein 5B (Fragment) OS=Homo sapiens GN=ZSCAN5B PE=4 SV=2 - [K7ESD3_HUMAN]	1	1	1	1	137	15.8	6.52
A0A024R1X8	Junction plakoglobin, isoform CRA_a OS=Homo sapiens GN=JUP PE=4 SV=1 - [A0A024R1X8_HUMAN]	2	1	1	1	745	81.7	6.14
Q3SYB5	SERPINB12 protein OS=Homo sapiens GN=SERPINB12 PE=2 SV=1 - [Q3SYB5_HUMAN]	2	1	1	1	183	20.9	5.87

B4DHW6	cDNA FLJ54930, highly similar to Homo sapiens Dbf4-related factor 1 (DRF1), transcript variant 2, mRNA OS=Homo sapiens PE=2 SV=1 - [B4DHW6_HUMAN]	3	1	1	1	154	16.7	10.27
Q9H700	cDNA: FLJ21617 fis, clone COL07481 OS=Homo sapiens PE=2 SV=1 - [Q9H700_HUMAN]	1	1	1	1	244	27.6	9.22
Q8TC57	Meiosis 1 arrest protein OS=Homo sapiens GN=M1AP PE=1 SV=1 - [M1AP_HUMAN]	1	1	1	1	530	59.3	6.87
Q562R1	Beta-actin-like protein 2 OS=Homo sapiens GN=ACTBL2 PE=1 SV=2 - [ACTBL_HUMAN]	1	1	1	1	376	42.0	5.59
Q8WVV4	Protein POF1B OS=Homo sapiens GN=POF1B PE=1 SV=3 - [POF1B_HUMAN]	1	1	1	1	589	68.0	6.32
F5GXD8	Stress-induced-phosphoprotein 1 OS=Homo sapiens GN=STIP1 PE=1 SV=1 - [F5GXD8_HUMAN]	4	1	1	1	138	15.6	8.25
D6RJF7	Serine/threonine-protein kinase Nek11 OS=Homo sapiens GN=NEK11 PE=4 SV=1 - [D6RJF7_HUMAN]	6	1	1	1	212	24.2	9.22
A0A087WU05	C-Maf-inducing protein OS=Homo sapiens GN=CMIP PE=1 SV=1 - [A0A087WU05_HUMAN]	4	1	1	1	586	65.2	5.94
A0A075B6Z2	Protein TRAJ56 (Fragment) OS=Homo sapiens GN=TRAJ56 PE=4 SV=1 - [A0A075B6Z2_HUMAN]	2	1	1	14	21	2.2	10.29
F8WE65	Peptidyl-prolyl cis-trans isomerase OS=Homo sapiens GN=PPIA PE=1 SV=1 - [F8WE65_HUMAN]	6	1	1	1	120	13.0	6.77
Q96HI1	Similar to plastin 3 (T isoform) (Fragment) OS=Homo sapiens PE=2 SV=1 - [Q96HI1_HUMAN]	5	1	1	1	409	46.0	6.67
F6KRJ2	MHC class I antigen (Fragment) OS=Homo sapiens GN=HLA-A PE=3 SV=1 - [F6KRJ2_HUMAN]	1	1	1	1	181	21.2	7.50
H0YJ59	Tyrosine-protein phosphatase non-receptor type 21 (Fragment) OS=Homo sapiens GN=PTPN21 PE=1 SV=1 - [H0YJ59_HUMAN]	3	1	1	1	128	14.0	6.28
Q8TC04	Keratin 23 (Histone deacetylase inducible) OS=Homo sapiens GN=KRT23 PE=2 SV=1 - [Q8TC04_HUMAN]	1	1	1	2	422	48.1	6.54
Q7Z5Z5	NPC-A-12 OS=Homo sapiens PE=2 SV=1 - [Q7Z5Z5_HUMAN]	1	1	1	1	103	11.8	9.86
A8K651	cDNA FLJ75700, highly similar to Homo sapiens complement component 1, q subcomponent binding protein (C1QBP), nuclear gene encoding mitochondrial protein, mRNA OS=Homo sapiens PE=2 SV=1 - [A8K651_HUMAN]	2	1	1	1	282	31.4	4.84
A0A096LP30	Hemicentin-2 OS=Homo sapiens GN=HMCN2 PE=1 SV=1 - [A0A096LP30_HUMAN]	2	1	1	1	5059	541.6	5.87

FGFR2-1

Accession	Description	# Proteins	# Unique Peptides	# Peptides	# PSMs	# AAs	MW [kDa]	calc. pI
P35527	Keratin, type I cytoskeletal 9 OS=Homo sapiens GN=KRT9 PE=1 SV=3 - [K1C9_HUMAN]	2	30	31	254	623	62.0	5.24
H6VRF8	Keratin 1 OS=Homo sapiens GN=KRT1 PE=3 SV=1 - [H6VRF8_HUMAN]	16	29	35	218	644	66.0	8.12
P13645	Keratin, type I cytoskeletal 10 OS=Homo sapiens GN=KRT10 PE=1 SV=6 - [K1C10_HUMAN]	22	29	33	146	584	58.8	5.21
P35908	Keratin, type II cytoskeletal 2 epidermal OS=Homo sapiens GN=KRT2 PE=1 SV=2 - [K22E_HUMAN]	7	26	34	127	639	65.4	8.00
P02533	Keratin, type I cytoskeletal 14 OS=Homo sapiens GN=KRT14 PE=1 SV=4 - [K1C14_HUMAN]	35	11	28	73	472	51.5	5.16
P08779	Keratin, type I cytoskeletal 16 OS=Homo sapiens GN=KRT16 PE=1 SV=4 - [K1C16_HUMAN]	36	13	26	67	473	51.2	5.05
P04259	Keratin, type II cytoskeletal 6B OS=Homo sapiens GN=KRT6B PE=1 SV=5 - [K2C6B_HUMAN]	9	2	19	59	564	60.0	8.00
P13647	Keratin, type II cytoskeletal 5 OS=Homo sapiens GN=KRT5 PE=1 SV=3 - [K2C5_HUMAN]	16	13	24	49	590	62.3	7.74
B4DRR0	cDNA FLJ53910, highly similar to Keratin, type II cytoskeletal 6A OS=Homo sapiens PE=2 SV=1 - [B4DRR0_HUMAN]	17	3	21	45	535	57.8	8.00
Q04695	Keratin, type I cytoskeletal 17 OS=Homo sapiens GN=KRT17 PE=1 SV=2 - [K1C17_HUMAN]	28	9	21	33	432	48.1	5.02
Q0IIN1	Keratin 77 OS=Homo sapiens GN=KRT77 PE=1 SV=1 - [Q0IIN1_HUMAN]	7	4	7	24	578	61.8	5.85
Q14CN4	Keratin, type II cytoskeletal 72 OS=Homo sapiens GN=KRT72 PE=1 SV=2 - [K2C72_HUMAN]	11	1	4	15	511	55.8	6.89
P15924	Desmoplakin OS=Homo sapiens GN=DSP PE=1 SV=3 - [DESP_HUMAN]	6	10	10	14	2871	331.6	6.81
Q6KB66	Keratin, type II cytoskeletal 80 OS=Homo sapiens GN=KRT80 PE=1 SV=2 - [K2C80_HUMAN]	9	3	4	10	452	50.5	5.67
Q86YZ3	Hornerin OS=Homo sapiens GN=HRNR PE=1 SV=2 - [HORN_HUMAN]	1	1	1	5	2850	282.2	10.04
B2R4M6	Protein S100 OS=Homo sapiens PE=2 SV=1 - [B2R4M6_HUMAN]	2	4	4	7	114	13.2	6.13
Q02413	Desmoglein-1 OS=Homo sapiens GN=DSG1 PE=1 SV=2 - [DSG1_HUMAN]	1	3	3	5	1049	113.7	5.03
A0A087WWT3	Serum albumin OS=Homo sapiens GN=ALB PE=1 SV=1 - [A0A087WWT3_HUMAN]	14	2	2	5	396	45.1	6.10
P81605	Dermcidin OS=Homo sapiens GN=DCD PE=1 SV=2 - [DCD_HUMAN]	1	3	3	4	110	11.3	6.54
Q99456	Keratin, type I cytoskeletal 12 OS=Homo sapiens GN=KRT12 PE=1 SV=1 - [K1C12_HUMAN]	1	1	3	5	494	53.5	4.78
B2MV14	Truncated lactoferrin OS=Homo sapiens GN=LTF PE=3 SV=1 - [B2MV14_HUMAN]	16	4	4	5	585	64.2	8.07
Q8N1N4	Keratin, type II cytoskeletal 78 OS=Homo sapiens GN=KRT78 PE=2 SV=2 - [K2C78_HUMAN]	3	4	4	4	520	56.8	6.02

O75556	Mammaglobin-B OS=Homo sapiens GN=SCGB2A1 PE=1 SV=1 - [SG2A1_HUMAN]	1	3	3	3	95	10.9	5.78
Q45KI0	Trypsin I (Fragment) OS=Homo sapiens GN=PRSS1 PE=3 SV=1 - [Q45KI0_HUMAN]	17	1	1	2	84	9.2	9.99
A0A024R1X8	Junction plakoglobin, isoform CRA_a OS=Homo sapiens GN=JUP PE=4 SV=1 - [A0A024R1X8_HUMAN]	2	3	3	4	745	81.7	6.14
I3L1U9	Actin, cytoplasmic 2 (Fragment) OS=Homo sapiens GN=ACTG1 PE=1 SV=1 - [I3L1U9_HUMAN]	48	3	3	3	214	23.8	5.44
M0R1V7	Ubiquitin-60S ribosomal protein L40 (Fragment) OS=Homo sapiens GN=UBA52 PE=1 SV=1 - [M0R1V7_HUMAN]	40	2	2	2	63	7.1	5.36
B3KX99	cDNA FLJ45019 fis, clone BRAWH3015825 OS=Homo sapiens PE=2 SV=1 - [B3KX99_HUMAN]	2	1	1	3	333	38.5	8.97
Q9GZZ8	Extracellular glycoprotein lacritin OS=Homo sapiens GN=LACRT PE=1 SV=1 - [LACRT_HUMAN]	2	2	2	2	138	14.2	5.50
O95968	Secretoglobin family 1D member 1 OS=Homo sapiens GN=SCGB1D1 PE=1 SV=1 - [SG1D1_HUMAN]	1	2	2	2	90	9.9	9.25
Q9HB00	Desmocollin 1, isoform CRA_b OS=Homo sapiens GN=DSC1 PE=4 SV=1 - [Q9HB00_HUMAN]	2	2	2	3	840	93.8	5.53
A0A0A0MRQ5	Peroxiredoxin-1 OS=Homo sapiens GN=PRDX1 PE=1 SV=1 - [A0A0A0MRQ5_HUMAN]	6	2	2	2	97	10.7	8.72
P05109	Protein S100-A8 OS=Homo sapiens GN=S100A8 PE=1 SV=1 - [S10A8_HUMAN]	4	3	3	4	93	10.8	7.03
P25311	Zinc-alpha-2-glycoprotein OS=Homo sapiens GN=AZGP1 PE=1 SV=2 - [ZA2G_HUMAN]	3	2	2	3	298	34.2	6.05
Q86W20	Protease serine 1 (Fragment) OS=Homo sapiens GN=PRSS1 PE=3 SV=1 - [Q86W20_HUMAN]	6	1	1	1	84	9.2	10.27
A0A024RC29	Desmocollin 3, isoform CRA_b OS=Homo sapiens GN=DSC3 PE=4 SV=1 - [A0A024RC29_HUMAN]	3	1	1	1	896	99.9	6.10
P47929	Galectin-7 OS=Homo sapiens GN=LGALS7 PE=1 SV=2 - [LEG7_HUMAN]	1	1	1	1	136	15.1	7.62
V9H0H9	Uncharacterized protein OS=Homo sapiens PE=2 SV=1 - [V9H0H9_HUMAN]	1	1	1	1	246	29.2	9.79
Q0EFA5	S protein OS=Homo sapiens GN=S PE=4 SV=1 - [Q0EFA5_HUMAN]	7	1	1	1	512	49.9	8.13
P31151	Protein S100-A7 OS=Homo sapiens GN=S100A7 PE=1 SV=4 - [S10A7_HUMAN]	1	1	1	1	101	11.5	6.77
Q5VSP4	Putative lipocalin 1-like protein 1 OS=Homo sapiens GN=LCN1P1 PE=5 SV=1 - [LC1L1_HUMAN]	2	1	1	1	162	17.9	5.00
E9PN51	NADH dehydrogenase [ubiquinone] iron-sulfur protein 8, mitochondrial (Fragment) OS=Homo sapiens GN=NDUFS8 PE=1 SV=1 - [E9PN51_HUMAN]	6	1	1	1	110	12.4	9.98
Q5ZEY3	Glyceraldehyde-3-phosphate dehydrogenase (Fragment) OS=Homo sapiens GN=GAPD PE=2 SV=1 - [Q5ZEY3_HUMAN]	6	1	1	1	86	9.2	9.72
H0YKZ7	Annexin (Fragment) OS=Homo sapiens GN=ANXA2 PE=1 SV=1 - [H0YKZ7_HUMAN]	16	1	1	1	119	13.0	8.13
A0A087WYX2	Histone lysine demethylase PHF8 OS=Homo sapiens GN=PHF8 PE=1 SV=1 - [A0A087WYX2_HUMAN]	2	1	1	1	303	33.8	10.08
C9J2I1	Armadillo repeat-containing protein 8 (Fragment) OS=Homo sapiens GN=ARMC8 PE=1 SV=1 - [C9J2I1_HUMAN]	1	1	1	1	352	39.9	7.85

B4DFN7	cDNA FLJ59676, highly similar to Myosin-18A OS=Homo sapiens PE=2 SV=1 - [B4DFN7_HUMAN]	7	1	1	1	320	36.8	4.81
E9PML7	Deoxyribose-phosphate aldolase (Fragment) OS=Homo sapiens GN=DERA PE=1 SV=1 - [E9PML7_HUMAN]	3	1	1	1	236	26.0	9.04
J3KSP2	60S ribosomal protein L38 (Fragment) OS=Homo sapiens GN=RPL38 PE=1 SV=1 - [J3KSP2_HUMAN]	4	1	1	1	21	2.6	9.99
A1L378	STRC protein OS=Homo sapiens GN=STRC PE=2 SV=1 - [A1L378_HUMAN]	4	1	1	1	1002	110.6	5.17
B4DK31	cDNA FLJ54634, highly similar to Acetyl-CoA carboxylase 1 (EC 6.4.1.2) OS=Homo sapiens PE=2 SV=1 - [B4DK31_HUMAN]	8	1	1	1	306	35.6	6.38
B4DUR8	T-complex protein 1 subunit gamma OS=Homo sapiens GN=CCT3 PE=1 SV=1 - [B4DUR8_HUMAN]	5	1	1	1	500	55.6	5.64
A0A0A0M RX7	Transcription factor TFIIB component B" homolog OS=Homo sapiens GN=BDP1 PE=1 SV=1 - [A0A0A0MRX7_HUMAN]	5	1	1	1	846	95.5	8.15
Q3SYB5	SERPINB12 protein OS=Homo sapiens GN=SERPINB12 PE=2 SV=1 - [Q3SYB5_HUMAN]	2	2	2	2	183	20.9	5.87
F8WBR5	Calmodulin OS=Homo sapiens GN=CALM2 PE=1 SV=1 - [F8WBR5_HUMAN]	10	1	1	1	65	7.4	4.01
A0PJ54	PEX12 protein (Fragment) OS=Homo sapiens GN=PEX12 PE=2 SV=1 - [A0PJ54_HUMAN]	1	1	1	1	324	36.9	9.98
B7Z5R3	Src family associated phosphoprotein 2, isoform CRA_c OS=Homo sapiens GN=SCAP2 PE=2 SV=1 - [B7Z5R3_HUMAN]	3	1	1	1	187	21.6	4.46
B4DHW6	cDNA FLJ54930, highly similar to Homo sapiens Dbf4-related factor 1 (DRF1), transcript variant 2, mRNA OS=Homo sapiens PE=2 SV=1 - [B4DHW6_HUMAN]	3	1	1	1	154	16.7	10.2 7
I3L234	Ribosomal L1 domain-containing protein 1 (Fragment) OS=Homo sapiens GN=RSL1D1 PE=1 SV=1 - [I3L234_HUMAN]	1	1	1	1	98	11.6	9.74
H7C1F9	Ral GTPase-activating protein subunit alpha-2 (Fragment) OS=Homo sapiens GN=RALGAPA2 PE=1 SV=1 - [H7C1F9_HUMAN]	2	1	1	2	1740	194.9	5.90
Q9NVE4	Coiled-coil domain-containing protein 87 OS=Homo sapiens GN=CCDC87 PE=1 SV=2 - [CCD87_HUMAN]	1	1	1	1	849	96.3	8.59
A8K5M9	Uncharacterized protein C15orf62, mitochondrial OS=Homo sapiens GN=C15orf62 PE=2 SV=1 - [CO062_HUMAN]	1	1	1	1	175	19.7	8.50
P08F94	Fibrocystin OS=Homo sapiens GN=PKHD1 PE=1 SV=1 - [PKHD1_HUMAN]	1	1	1	1	4074	446.4	6.57
A0A075B6 Z2	Protein TRAJ56 (Fragment) OS=Homo sapiens GN=TRAJ56 PE=4 SV=1 - [A0A075B6Z2_HUMAN]	2	1	1	1	21	2.2	10.2 9
F4MH53	Ubiquitously transcribed tetratricopeptide repeat protein Y-linked transcript variant 39 OS=Homo sapiens GN=UTY PE=2 SV=1 - [F4MH53_HUMAN]	1	1	1	1	1285	142.0	7.94
Q7Z4M2	RASA1 protein (Fragment) OS=Homo sapiens GN=RASA1 PE=1 SV=1 - [Q7Z4M2_HUMAN]	8	1	1	1	313	36.5	8.78
K7ERN1	E3 ubiquitin-protein ligase NEDD4-like (Fragment) OS=Homo sapiens GN=NEDD4L PE=1 SV=1 - [K7ERN1_HUMAN]	6	1	1	1	639	74.1	5.16
B4DWH5	cDNA FLJ53224, highly similar to Calpain-1 catalytic subunit (EC 3.4.22.52) OS=Homo sapiens PE=2 SV=1 - [B4DWH5_HUMAN]	5	1	1	1	660	75.8	6.29
I3L1H9	Zymogen granule protein 16 homolog B (Fragment) OS=Homo sapiens GN=ZG16B PE=1 SV=1 - [I3L1H9_HUMAN]	5	1	1	1	69	7.5	9.32

H7C0V3	Beta-chimaerin (Fragment) OS=Homo sapiens GN=CHN2 PE=1 SV=1 - [H7C0V3_HUMAN]	5	1	1	1	180	20.6	8.24
Q6ZSX8	cDNA FLJ45139 fis, clone BRAWH3039623 OS=Homo sapiens PE=2 SV=1 - [Q6ZSX8_HUMAN]	1	1	1	2	136	15.5	10.07
B4DL87	cDNA FLJ52243, highly similar to Heat-shock protein beta-1 OS=Homo sapiens PE=2 SV=1 - [B4DL87_HUMAN]	3	1	1	1	170	18.5	6.95
D9ZHQ0	Neuregulin 3 variant 6 OS=Homo sapiens GN=NRG3 PE=2 SV=1 - [D9ZHQ0_HUMAN]	1	1	1	1	239	27.2	7.44
B2RBY7	cDNA, FLJ95770 OS=Homo sapiens PE=2 SV=1 - [B2RBY7_HUMAN]	3	1	1	1	380	41.6	5.27

FGFR2-2

Accession	Description	# Proteins	# Unique Peptides	# Peptides	# PSMs	# AAs	MW [kDa]	calc . pI
P35527	Keratin, type I cytoskeletal 9 OS=Homo sapiens GN=KRT9 PE=1 SV=3 - [K1C9_HUMAN]	4	26	27	134	623	62.0	5.24
H6VRF8	Keratin 1 OS=Homo sapiens GN=KRT1 PE=3 SV=1 - [H6VRF8_HUMAN]	16	25	28	94	644	66.0	8.12
P13645	Keratin, type I cytoskeletal 10 OS=Homo sapiens GN=KRT10 PE=1 SV=6 - [K1C10_HUMAN]	25	22	25	91	584	58.8	5.21
P08779	Keratin, type I cytoskeletal 16 OS=Homo sapiens GN=KRT16 PE=1 SV=4 - [K1C16_HUMAN]	40	7	15	49	473	51.2	5.05
P35908	Keratin, type II cytoskeletal 2 epidermal OS=Homo sapiens GN=KRT2 PE=1 SV=2 - [K22E_HUMAN]	13	12	19	44	639	65.4	8.00
P02533	Keratin, type I cytoskeletal 14 OS=Homo sapiens GN=KRT14 PE=1 SV=4 - [K1C14_HUMAN]	44	7	15	48	472	51.5	5.16
A0A024R0Y2	HCG30204, isoform CRA_a OS=Homo sapiens GN=hCG_30204 PE=4 SV=1 - [A0A024R0Y2_HUMAN]	17	14	14	22	2268	257.1	6.61
P13647	Keratin, type II cytoskeletal 5 OS=Homo sapiens GN=KRT5 PE=1 SV=3 - [K2C5_HUMAN]	14	4	10	15	590	62.3	7.74
B4DRR0	cDNA FLJ53910, highly similar to Keratin, type II cytoskeletal 6A OS=Homo sapiens PE=2 SV=1 - [B4DRR0_HUMAN]	17	2	9	11	535	57.8	8.00
F8VVB9	Tubulin alpha-1B chain (Fragment) OS=Homo sapiens GN=TUBA1B PE=1 SV=5 - [F8VVB9_HUMAN]	36	4	4	5	247	27.5	5.20
P81605	Dermcidin OS=Homo sapiens GN=DCD PE=1 SV=2 - [DCD_HUMAN]	1	3	3	6	110	11.3	6.54
Q86W20	Protease serine 1 (Fragment) OS=Homo sapiens GN=PRSS1 PE=3 SV=1 - [Q86W20_HUMAN]	6	1	1	4	84	9.2	10.27

A0A087W WT3	Serum albumin OS=Homo sapiens GN=ALB PE=1 SV=1 - [A0A087WWT3_HUMAN]	14	2	2	4	396	45.1	6.1 0
Q53HF2	Heat shock 70kDa protein 8 isoform 2 variant (Fragment) OS=Homo sapiens PE=1 SV=1 - [Q53HF2_HUMAN]	39	3	3	5	493	53.5	5.8 6
Q45KI0	Trypsin I (Fragment) OS=Homo sapiens GN=PRSS1 PE=3 SV=1 - [Q45KI0_HUMAN]	17	1	1	2	84	9.2	9.9 9
Q14CN4	Keratin, type II cytoskeletal 72 OS=Homo sapiens GN=KRT72 PE=1 SV=2 - [K2C72_HUMAN]	12	1	3	3	511	55.8	6.8 9
F8VV32	Lysozyme OS=Homo sapiens GN=LYZ PE=1 SV=1 - [F8VV32_HUMAN]	3	2	2	3	104	11.5	9.0 7
J3QRT3	Uncharacterized protein KIAA0195 (Fragment) OS=Homo sapiens GN=KIAA0195 PE=1 SV=5 - [J3QRT3_HUMAN]	1	1	1	2	89	9.5	6.7 6
B3KX99	cDNA FLJ45019 fis, clone BRAWH3015825 OS=Homo sapiens PE=2 SV=1 - [B3KX99_HUMAN]	2	1	1	2	333	38.5	8.9 7
P11498	Pyruvate carboxylase, mitochondrial OS=Homo sapiens GN=PC PE=1 SV=2 - [PYC_HUMAN]	3	2	2	2	1178	129. 6	6.8 4
C9JL25	60 kDa heat shock protein, mitochondrial (Fragment) OS=Homo sapiens GN=HSPD1 PE=1 SV=1 - [C9JL25_HUMAN]	7	1	1	1	175	19.2	9.7 3
O14942	Heat shock protein beta (Fragment) OS=Homo sapiens PE=4 SV=1 - [O14942_HUMAN]	12	1	1	1	130	14.1	4.7 9
A1XP52	Catecholamine-regulated protein 40 OS=Homo sapiens PE=2 SV=1 - [A1XP52_HUMAN]	7	1	1	1	350	38.1	5.3 9
Q5HY57	Emerin OS=Homo sapiens GN=EMD PE=1 SV=1 - [Q5HY57_HUMAN]	2	1	1	1	219	24.9	5.0 2
P31151	Protein S100-A7 OS=Homo sapiens GN=S100A7 PE=1 SV=4 - [S10A7_HUMAN]	1	1	1	1	101	11.5	6.7 7
C9IYG1	BRCA1-associated RING domain protein 1 (Fragment) OS=Homo sapiens GN=BARD1 PE=1 SV=1 - [C9IYG1_HUMAN]	9	1	1	1	216	24.4	8.4 7
A8K651	cDNA FLJ75700, highly similar to Homo sapiens complement component 1, q subcomponent binding protein (C1QBP), nuclear gene encoding mitochondrial protein, mRNA OS=Homo sapiens PE=2 SV=1 - [A8K651_HUMAN]	2	1	1	1	282	31.4	4.8 4
P05109	Protein S100-A8 OS=Homo sapiens GN=S100A8 PE=1 SV=1 - [S10A8_HUMAN]	1	1	1	1	93	10.8	7.0 3
B4E1L2	cDNA FLJ59602, highly similar to Lactotransferrin (EC 3.4.21.-) OS=Homo sapiens PE=2 SV=1 - [B4E1L2_HUMAN]	15	1	1	1	151	16.5	9.9 4
Q9H8G4	cDNA FLJ13649 fis, clone PLACE1011399, weakly similar to Homo sapiens CGI-72 protein mRNA OS=Homo sapiens PE=2 SV=1 - [Q9H8G4_HUMAN]	3	1	1	1	150	16.5	9.1 0
P12004	Proliferating cell nuclear antigen OS=Homo sapiens GN=PCNA PE=1 SV=1 - [PCNA_HUMAN]	3	1	1	1	261	28.8	4.6 9
A8K0C1	Threonine synthase-like 2 OS=Homo sapiens GN=THNSL2 PE=1 SV=1 - [A8K0C1_HUMAN]	3	1	1	1	226	25.0	6.9 9

Q6ZSX8	cDNA FLJ45139 fis, clone BRAWH3039623 OS=Homo sapiens PE=2 SV=1 - [Q6ZSX8_HUMAN]	1	1	1	2	136	15.5	10.07
Q9NY61	Protein AATF OS=Homo sapiens GN=AATF PE=1 SV=1 - [AATF_HUMAN]	1	1	1	1	560	63.1	4.94
Q8NEG4	Protein FAM83F OS=Homo sapiens GN=FAM83F PE=1 SV=1 - [FA83F_HUMAN]	1	1	1	1	500	55.5	8.19
P58294	Prokineticin-1 OS=Homo sapiens GN=PROK1 PE=1 SV=1 - [PROK1_HUMAN]	1	1	1	1	105	11.7	8.59
I3L379	Active breakpoint cluster region-related protein (Fragment) OS=Homo sapiens GN=ABR PE=1 SV=1 - [I3L379_HUMAN]	6	1	1	1	117	13.6	7.14
A8K383	cDNA FLJ75428, highly similar to Homo sapiens activating transcription factor 6 (ATF6), mRNA OS=Homo sapiens PE=2 SV=1 - [A8K383_HUMAN]	2	1	1	1	670	74.5	8.22

FGFR2-3

Accession	Description	# Proteins	# Unique Peptides	# Peptides	# PSMs	# AAs	MW [kDa]	calc pI
P35527	Keratin, type I cytoskeletal 9 OS=Homo sapiens GN=KRT9 PE=1 SV=3 - [K1C9_HUMAN]	2	30	30	165	623	62.0	5.24
H6VRF8	Keratin 1 OS=Homo sapiens GN=KRT1 PE=3 SV=1 - [H6VRF8_HUMAN]	15	27	32	131	644	66.0	8.12
P13645	Keratin, type I cytoskeletal 10 OS=Homo sapiens GN=KRT10 PE=1 SV=6 - [K1C10_HUMAN]	23	25	28	116	584	58.8	5.21
P35908	Keratin, type II cytoskeletal 2 epidermal OS=Homo sapiens GN=KRT2 PE=1 SV=2 - [K22E_HUMAN]	8	22	30	73	639	65.4	8.00
P08779	Keratin, type I cytoskeletal 16 OS=Homo sapiens GN=KRT16 PE=1 SV=4 - [K1C16_HUMAN]	32	9	18	56	473	51.2	5.05
P02533	Keratin, type I cytoskeletal 14 OS=Homo sapiens GN=KRT14 PE=1 SV=4 - [K1C14_HUMAN]	31	6	18	53	472	51.5	5.16
P04259	Keratin, type II cytoskeletal 6B OS=Homo sapiens GN=KRT6B PE=1 SV=5 - [K2C6B_HUMAN]	10	1	20	43	564	60.0	8.00
B4DWU6	cDNA FLJ51361, highly similar to Keratin, type II cytoskeletal 6A OS=Homo sapiens PE=2 SV=1 - [B4DWU6_HUMAN]	18	2	21	37	520	55.8	6.48
P13647	Keratin, type II cytoskeletal 5 OS=Homo sapiens GN=KRT5 PE=1 SV=3 - [K2C5_HUMAN]	15	8	18	37	590	62.3	7.74
M0QZP4	Branched-chain-amino-acid aminotransferase OS=Homo sapiens GN=BCAT2 PE=1 SV=1 - [M0QZP4_HUMAN]	7	3	3	16	313	34.9	6.98

Q04695	Keratin, type I cytoskeletal 17 OS=Homo sapiens GN=KRT17 PE=1 SV=2 - [K1C17_HUMAN]	27	3	12	20	432	48.1	5.0 2
A0A024R0Y2	HCG30204, isoform CRA_a OS=Homo sapiens GN=hCG_30204 PE=4 SV=1 - [A0A024R0Y2_HUMAN]	11	8	8	11	2268	257.1	6.6 1
Q14CN4	Keratin, type II cytoskeletal 72 OS=Homo sapiens GN=KRT72 PE=1 SV=2 - [K2C72_HUMAN]	11	1	4	8	511	55.8	6.8 9
A0A087WYF5	Salivary acidic proline-rich phosphoprotein 1/2 (Fragment) OS=Homo sapiens GN=PRH1 PE=4 SV=1 - [A0A087WYF5_HUMAN]	8	1	1	3	140	14.0	11. 46
B3KPS3	cDNA FLJ32131 fis, clone PEBLM2000267, highly similar to Tubulin alpha-ubiquitous chain OS=Homo sapiens PE=2 SV=1 - [B3KPS3_HUMAN]	38	6	6	7	416	46.2	5.1 2
B4E2A0	cDNA FLJ61543, highly similar to Desmoplakin OS=Homo sapiens PE=2 SV=1 - [B4E2A0_HUMAN]	6	4	4	6	1350	156. 2	7.4 3
A0A087WWT3	Serum albumin OS=Homo sapiens GN=ALB PE=1 SV=1 - [A0A087WWT3_HUMAN]	14	3	3	6	396	45.1	6.1 0
Q53HF2	Heat shock 70kDa protein 8 isoform 2 variant (Fragment) OS=Homo sapiens PE=1 SV=1 - [Q53HF2_HUMAN]	40	4	4	5	493	53.5	5.8 6
Q8N1N4	Keratin, type II cytoskeletal 78 OS=Homo sapiens GN=KRT78 PE=2 SV=2 - [K2C78_HUMAN]	3	1	2	4	520	56.8	6.0 2
Q45KI0	Trypsin I (Fragment) OS=Homo sapiens GN=PRSS1 PE=3 SV=1 - [Q45KI0_HUMAN]	17	1	1	3	84	9.2	9.9 9
P81605	Dermcidin OS=Homo sapiens GN=DCD PE=1 SV=2 - [DCD_HUMAN]	1	3	3	4	110	11.3	6.5 4
Q19KS2	Lactoferrin (Fragment) OS=Homo sapiens PE=2 SV=1 - [Q19KS2_HUMAN]	15	4	4	5	353	39.1	9.0 3
I3L1U9	Actin, cytoplasmic 2 (Fragment) OS=Homo sapiens GN=ACTG1 PE=1 SV=1 - [I3L1U9_HUMAN]	48	3	3	4	214	23.8	5.4 4
O75556	Mammaglobin-B OS=Homo sapiens GN=SCGB2A1 PE=1 SV=1 - [SG2A1_HUMAN]	1	2	2	2	95	10.9	5.7 8
Q86W20	Protease serine 1 (Fragment) OS=Homo sapiens GN=PRSS1 PE=3 SV=1 - [Q86W20_HUMAN]	6	1	1	2	84	9.2	10. 27
B3KX99	cDNA FLJ45019 fis, clone BRAWH3015825 OS=Homo sapiens PE=2 SV=1 - [B3KX99_HUMAN]	2	1	1	3	333	38.5	8.9 7
Q9GZZ8	Extracellular glycoprotein lacritin OS=Homo sapiens GN=LACRT PE=1 SV=1 - [LACRT_HUMAN]	2	2	2	2	138	14.2	5.5 0
P61626	Lysozyme C OS=Homo sapiens GN=LYZ PE=1 SV=1 - [LYSC_HUMAN]	3	3	3	3	148	16.5	9.1 6
J3QRT3	Uncharacterized protein KIAA0195 (Fragment) OS=Homo sapiens GN=KIAA0195 PE=1 SV=5 - [J3QRT3_HUMAN]	1	1	1	2	89	9.5	6.7 6
B2R4M6	Protein S100 OS=Homo sapiens PE=2 SV=1 - [B2R4M6_HUMAN]	2	2	2	3	114	13.2	6.1 3

Q02413	Desmoglein-1 OS=Homo sapiens GN=DSG1 PE=1 SV=2 - [DSG1_HUMAN]	1	1	1	3	1049	113.7	5.03
A0A024R1X8	Junction plakoglobin, isoform CRA_a OS=Homo sapiens GN=JUP PE=4 SV=1 - [A0A024R1X8_HUMAN]	2	1	1	2	745	81.7	6.14
Q7Z612	Acidic ribosomal phosphoprotein P1 OS=Homo sapiens PE=2 SV=1 - [Q7Z612_HUMAN]	4	1	1	1	113	11.4	4.36
H0YGI8	Stress-induced-phosphoprotein 1 (Fragment) OS=Homo sapiens GN=STIP1 PE=1 SV=1 - [H0YGI8_HUMAN]	3	1	1	1	137	15.9	6.19
O95968	Secretoglobin family 1D member 1 OS=Homo sapiens GN=SCGB1D1 PE=1 SV=1 - [SG1D1_HUMAN]	1	1	1	1	90	9.9	9.25
Q5VSP4	Putative lipocalin 1-like protein 1 OS=Homo sapiens GN=LCN1P1 PE=5 SV=1 - [LC1L1_HUMAN]	2	1	1	1	162	17.9	5.00
P31151	Protein S100-A7 OS=Homo sapiens GN=S100A7 PE=1 SV=4 - [S10A7_HUMAN]	1	1	1	1	101	11.5	6.77
A0A087WYX2	Histone lysine demethylase PHF8 OS=Homo sapiens GN=PHF8 PE=1 SV=1 - [A0A087WYX2_HUMAN]	2	1	1	1	303	33.8	10.08
F8WE04	Heat shock protein beta-1 OS=Homo sapiens GN=HSPB1 PE=1 SV=1 - [F8WE04_HUMAN]	2	1	1	1	186	20.4	9.06
F8WCJ1	Eukaryotic translation initiation factor 5A OS=Homo sapiens GN=EIF5A2 PE=1 SV=1 - [F8WCJ1_HUMAN]	8	1	1	1	105	11.7	9.14
Q590G7	UTY (Fragment) OS=Homo sapiens GN=UTY PE=4 SV=1 - [Q590G7_HUMAN]	83	1	1	1	226	23.2	7.96
Q9HB00	Desmocollin 1, isoform CRA_b OS=Homo sapiens GN=DSC1 PE=4 SV=1 - [Q9HB00_HUMAN]	2	1	1	1	840	93.8	5.53
B4DYE2	Kinesin-like protein OS=Homo sapiens PE=2 SV=1 - [B4DYE2_HUMAN]	2	1	1	1	1234	139.8	6.13
Q7Z350	Putative uncharacterized protein DKFZp686L0695 OS=Homo sapiens GN=DKFZp686L0695 PE=2 SV=1 - [Q7Z350_HUMAN]	1	1	1	1	549	62.1	6.37
B7Z639	cDNA FLJ54938, weakly similar to Mus musculus transmembrane and tetratricopeptide repeat containing 1 (Tmtc1), mRNA OS=Homo sapiens PE=2 SV=1 - [B7Z639_HUMAN]	3	1	1	1	591	66.7	8.76
Q4ZG32	Putative uncharacterized protein EPB41L5 (Fragment) OS=Homo sapiens GN=EPB41L5 PE=4 SV=1 - [Q4ZG32_HUMAN]	2	1	1	1	533	60.6	7.96
A8K651	cDNA FLJ75700, highly similar to Homo sapiens complement component 1, q subcomponent binding protein (C1QBP), nuclear gene encoding mitochondrial protein, mRNA OS=Homo sapiens PE=2 SV=1 - [A8K651_HUMAN]	2	1	1	2	282	31.4	4.84
A0A087WTG3	Cullin-3 OS=Homo sapiens GN=CUL3 PE=1 SV=1 - [A0A087WTG3_HUMAN]	1	1	1	1	342	39.1	9.48
I3L1H9	Zymogen granule protein 16 homolog B (Fragment) OS=Homo sapiens GN=ZG16B PE=1 SV=1 - [I3L1H9_HUMAN]	5	1	1	1	69	7.5	9.32
Q7Z5L4	Spermatogenesis-associated protein 19, mitochondrial OS=Homo sapiens GN=SPATA19 PE=2 SV=2 - [SPT19_HUMAN]	1	1	1	1	167	19.2	6.96

Q15203	Prothymosin alpha OS=Homo sapiens PE=4 SV=2 - [Q15203_HUMAN]	18	1	1	1	73	8.2	3.76
A0A075B6Z2	Protein TRAJ56 (Fragment) OS=Homo sapiens GN=TRAJ56 PE=4 SV=1 - [A0A075B6Z2_HUMAN]	2	1	1	2	21	2.2	10.29
Q96PE2	Rho guanine nucleotide exchange factor 17 OS=Homo sapiens GN=ARHGEF17 PE=1 SV=1 - [ARHGH_HUMAN]	1	1	1	1	2063	221.5	6.29
B7Z5R3	Src family associated phosphoprotein 2, isoform CRA_c OS=Homo sapiens GN=SCAP2 PE=2 SV=1 - [B7Z5R3_HUMAN]	3	1	1	1	187	21.6	4.46
B3KM59	cDNA FLJ10361 fis, clone NT2RM2001256, highly similar to Anaphase-promoting complex subunit 1 OS=Homo sapiens PE=2 SV=1 - [B3KM59_HUMAN]	1	1	1	1	306	32.9	7.40
Q562R1	Beta-actin-like protein 2 OS=Homo sapiens GN=ACTBL2 PE=1 SV=2 - [ACTBL_HUMAN]	1	1	1	1	376	42.0	5.59
B3KPM8	cDNA FLJ31974 fis, clone NT2RP7008167, weakly similar to 85.1 kDa PROTEIN IN GREB-FEOA INTERGENIC REGION OS=Homo sapiens PE=2 SV=1 - [B3KPM8_HUMAN]	2	1	1	1	995	111.7	8.72
Q96QW8	DJ576K7.1 (FK506 binding protein 12-rapamycin associated protein 1) (Fragment) OS=Homo sapiens GN=FRAP1 PE=4 SV=1 - [Q96QW8_HUMAN]	3	1	1	1	895	102.9	7.28
H0Y8C6	Importin-5 (Fragment) OS=Homo sapiens GN=IPO5 PE=1 SV=1 - [H0Y8C6_HUMAN]	1	1	1	1	1099	123.8	5.06
Q0KH84	Kell blood group antigen Cellano (Fragment) OS=Homo sapiens GN=KEL PE=4 SV=1 - [Q0KH84_HUMAN]	9	1	1	1	177	20.4	5.91
Q8TC04	Keratin 23 (Histone deacetylase inducible) OS=Homo sapiens GN=KRT23 PE=2 SV=1 - [Q8TC04_HUMAN]	1	1	1	1	422	48.1	6.54
Q6ZSX8	cDNA FLJ45139 fis, clone BRAWH3039623 OS=Homo sapiens PE=2 SV=1 - [Q6ZSX8_HUMAN]	1	1	1	1	136	15.5	10.07

IGFR-1

Accession	Description	# Proteins	# Unique Peptides	# Peptides	# PSMs	# AAs	MW [kDa]	calc . pI
P13645	Keratin, type I cytoskeletal 10 OS=Homo sapiens GN=KRT10 PE=1 SV=6 - [K1C10_HUMAN]	23	29	32	159	584	58.8	5.21
H6VRF8	Keratin 1 OS=Homo sapiens GN=KRT1 PE=3 SV=1 - [H6VRF8_HUMAN]	14	27	31	149	644	66.0	8.12
P35527	Keratin, type I cytoskeletal 9 OS=Homo sapiens GN=KRT9 PE=1 SV=3 - [K1C9_HUMAN]	2	31	31	125	623	62.0	5.24

P08779	Keratin, type I cytoskeletal 16 OS=Homo sapiens GN=KRT16 PE=1 SV=4 - [K1C16_HUMAN]	32	15	26	71	473	51.2	5.05
P35908	Keratin, type II cytoskeletal 2 epidermal OS=Homo sapiens GN=KRT2 PE=1 SV=2 - [K22E_HUMAN]	8	16	25	68	639	65.4	8.00
P02533	Keratin, type I cytoskeletal 14 OS=Homo sapiens GN=KRT14 PE=1 SV=4 - [K1C14_HUMAN]	34	6	21	56	472	51.5	5.16
P04259	Keratin, type II cytoskeletal 6B OS=Homo sapiens GN=KRT6B PE=1 SV=5 - [K2C6B_HUMAN]	10	3	22	53	564	60.0	8.00
B4DWU6	cDNA FLJ51361, highly similar to Keratin, type II cytoskeletal 6A OS=Homo sapiens PE=2 SV=1 - [B4DWU6_HUMAN]	15	2	21	42	520	55.8	6.48
P13647	Keratin, type II cytoskeletal 5 OS=Homo sapiens GN=KRT5 PE=1 SV=3 - [K2C5_HUMAN]	14	8	16	35	590	62.3	7.74
Q04695	Keratin, type I cytoskeletal 17 OS=Homo sapiens GN=KRT17 PE=1 SV=2 - [K1C17_HUMAN]	29	3	14	21	432	48.1	5.02
A0A024R0Y2	HCG30204, isoform CRA_a OS=Homo sapiens GN=hCG_30204 PE=4 SV=1 - [A0A024R0Y2_HUMAN]	17	10	10	13	2268	257.1	6.61
Q0IIN1	Keratin 77 OS=Homo sapiens GN=KRT77 PE=1 SV=1 - [Q0IIN1_HUMAN]	9	1	4	12	578	61.8	5.85
B3KPS3	cDNA FLJ32131 fis, clone PEBLM2000267, highly similar to Tubulin alpha-ubiquitous chain OS=Homo sapiens PE=2 SV=1 - [B3KPS3_HUMAN]	31	6	6	9	416	46.2	5.12
Q53HF2	Heat shock 70kDa protein 8 isoform 2 variant (Fragment) OS=Homo sapiens PE=1 SV=1 - [Q53HF2_HUMAN]	40	6	6	10	493	53.5	5.86
Q9GZZ8	Extracellular glycoprotein lacritin OS=Homo sapiens GN=LACRT PE=1 SV=1 - [LACRT_HUMAN]	2	3	3	6	138	14.2	5.50
A0A087WWT3	Serum albumin OS=Homo sapiens GN=ALB PE=1 SV=1 - [A0A087WWT3_HUMAN]	14	2	2	5	396	45.1	6.10
Q14CN4	Keratin, type II cytoskeletal 72 OS=Homo sapiens GN=KRT72 PE=1 SV=2 - [K2C72_HUMAN]	13	1	4	6	511	55.8	6.89
Q45KI0	Trypsin I (Fragment) OS=Homo sapiens GN=PRSS1 PE=3 SV=1 - [Q45KI0_HUMAN]	17	1	1	3	84	9.2	9.99
I3L1U9	Actin, cytoplasmic 2 (Fragment) OS=Homo sapiens GN=ACTG1 PE=1 SV=1 - [I3L1U9_HUMAN]	48	3	3	5	214	23.8	5.44
Q8N1N4	Keratin, type II cytoskeletal 78 OS=Homo sapiens GN=KRT78 PE=2 SV=2 - [K2C78_HUMAN]	1	2	3	4	520	56.8	6.02
Q86YZ3	Hornerin OS=Homo sapiens GN=HRNR PE=1 SV=2 - [HORN_HUMAN]	1	2	2	3	2850	282.2	10.04
C9JL25	60 kDa heat shock protein, mitochondrial (Fragment) OS=Homo sapiens GN=HSPD1 PE=1 SV=1 - [C9JL25_HUMAN]	7	1	1	2	175	19.2	9.73
A0A0A0MRQ5	Peroxiredoxin-1 OS=Homo sapiens GN=PRDX1 PE=1 SV=1 - [A0A0A0MRQ5_HUMAN]	6	2	2	3	97	10.7	8.72
B2R4M6	Protein S100 OS=Homo sapiens PE=2 SV=1 - [B2R4M6_HUMAN]	2	2	2	3	114	13.2	6.13

O75556	Mammaglobin-B OS=Homo sapiens GN=SCGB2A1 PE=1 SV=1 - [SG2A1_HUMAN]	1	2	2	2	95	10.9	5.78
E5RJN0	Heparan-alpha-glucosaminide N-acetyltransferase OS=Homo sapiens GN=HGSNAT PE=1 SV=1 - [E5RJN0_HUMAN]	2	1	1	2	352	38.9	8.32
Q02413	Desmoglein-1 OS=Homo sapiens GN=DSG1 PE=1 SV=2 - [DSG1_HUMAN]	1	2	2	2	1049	113.7	5.03
O14942	Heat shock protein beta (Fragment) OS=Homo sapiens PE=4 SV=1 - [O14942_HUMAN]	12	1	1	2	130	14.1	4.79
B3KX99	cDNA FLJ45019 fis, clone BRAWH3015825 OS=Homo sapiens PE=2 SV=1 - [B3KX99_HUMAN]	2	1	1	3	333	38.5	8.97
P61626	Lysozyme C OS=Homo sapiens GN=LYZ PE=1 SV=1 - [LYSC_HUMAN]	3	3	3	3	148	16.5	9.16
P81605	Dermcidin OS=Homo sapiens GN=DCD PE=1 SV=2 - [DCD_HUMAN]	1	2	2	2	110	11.3	6.54
A0A087WTG3	Cullin-3 OS=Homo sapiens GN=CUL3 PE=1 SV=1 - [A0A087WTG3_HUMAN]	1	1	1	2	342	39.1	9.48
Q5VSP4	Putative lipocalin 1-like protein 1 OS=Homo sapiens GN=LCN1P1 PE=5 SV=1 - [LC1L1_HUMAN]	2	2	2	2	162	17.9	5.00
Q19KS2	Lactoferrin (Fragment) OS=Homo sapiens PE=2 SV=1 - [Q19KS2_HUMAN]	15	2	2	2	353	39.1	9.03
P25311	Zinc-alpha-2-glycoprotein OS=Homo sapiens GN=AZGP1 PE=1 SV=2 - [ZA2G_HUMAN]	1	1	1	2	298	34.2	6.05
P15924	Desmoplakin OS=Homo sapiens GN=DSP PE=1 SV=3 - [DESP_HUMAN]	5	2	2	2	2871	331.6	6.81
Q86W20	Protease serine 1 (Fragment) OS=Homo sapiens GN=PRSS1 PE=3 SV=1 - [Q86W20_HUMAN]	6	1	1	1	84	9.2	10.27
J3QSA3	Polyubiquitin-B (Fragment) OS=Homo sapiens GN=UBB PE=1 SV=1 - [J3QSA3_HUMAN]	37	1	1	1	43	4.9	5.19
F8WF65	Elongation factor 1-beta OS=Homo sapiens GN=EEF1B2 PE=1 SV=1 - [F8WF65_HUMAN]	4	1	1	1	29	3.1	4.46
M0R1I1	Tubulin beta-4A chain (Fragment) OS=Homo sapiens GN=TUBB4A PE=1 SV=1 - [M0R1I1_HUMAN]	27	1	1	1	74	7.8	4.94
P12004	Proliferating cell nuclear antigen OS=Homo sapiens GN=PCNA PE=1 SV=1 - [PCNA_HUMAN]	7	2	2	2	261	28.8	4.69
H7C2X0	Translation initiation factor eIF-2B subunit epsilon (Fragment) OS=Homo sapiens GN=EIF2B5 PE=1 SV=1 - [H7C2X0_HUMAN]	4	1	1	1	92	9.4	9.41
G3V361	Calmodulin (Fragment) OS=Homo sapiens GN=CALM1 PE=1 SV=1 - [G3V361_HUMAN]	8	1	1	1	98	11.1	4.25
Q7Z612	Acidic ribosomal phosphoprotein P1 OS=Homo sapiens PE=2 SV=1 - [Q7Z612_HUMAN]	4	1	1	1	113	11.4	4.36

A0A0A0MRX7	Transcription factor TFIIIB component B" homolog OS=Homo sapiens GN=BDP1 PE=1 SV=1 - [A0A0A0MRX7_HUMAN]	5	1	1	1	846	95.5	8.15
J3QRT3	Uncharacterized protein KIAA0195 (Fragment) OS=Homo sapiens GN=KIAA0195 PE=1 SV=5 - [J3QRT3_HUMAN]	1	1	1	1	89	9.5	6.76
P01040	Cystatin-A OS=Homo sapiens GN=CSTA PE=1 SV=1 - [CYTA_HUMAN]	1	1	1	1	98	11.0	5.50
B4E1W3	cDNA FLJ51732, highly similar to Peroxisomal NADH pyrophosphatase NUDT12 (EC 3.6.1.22) OS=Homo sapiens PE=2 SV=1 - [B4E1W3_HUMAN]	3	1	1	1	444	50.0	6.79
F8WE04	Heat shock protein beta-1 OS=Homo sapiens GN=HSPB1 PE=1 SV=1 - [F8WE04_HUMAN]	2	1	1	1	186	20.4	9.06
A0A087WXD2	Membrane-associated guanylate kinase, WW and PDZ domain-containing protein 1 OS=Homo sapiens GN=MAGI1 PE=1 SV=1 - [A0A087WXD2_HUMAN]	7	1	1	1	980	106.8	6.46
Q5HY57	Emerin OS=Homo sapiens GN=EMD PE=1 SV=1 - [Q5HY57_HUMAN]	2	1	1	1	219	24.9	5.02
Q9HB00	Desmocollin 1, isoform CRA_b OS=Homo sapiens GN=DSC1 PE=4 SV=1 - [Q9HB00_HUMAN]	2	1	1	1	840	93.8	5.53
Q59H71	Sodium channel protein type II alpha subunit variant (Fragment) OS=Homo sapiens PE=2 SV=1 - [Q59H71_HUMAN]	7	1	1	1	1315	149.2	5.49
Q5ZEY3	Glyceraldehyde-3-phosphate dehydrogenase (Fragment) OS=Homo sapiens GN=GAPD PE=2 SV=1 - [Q5ZEY3_HUMAN]	6	1	1	1	86	9.2	9.72
B7Z5R3	Src family associated phosphoprotein 2, isoform CRA_c OS=Homo sapiens GN=SCAP2 PE=2 SV=1 - [B7Z5R3_HUMAN]	3	1	1	1	187	21.6	4.46
C9JWI2	A disintegrin and metalloproteinase with thrombospondin motifs 9 OS=Homo sapiens GN=ADAMTS9 PE=4 SV=1 - [C9JWI2_HUMAN]	2	1	1	1	488	55.0	7.62
P07737	Profilin-1 OS=Homo sapiens GN=PFN1 PE=1 SV=2 - [PROF1_HUMAN]	2	1	1	1	140	15.0	8.27
V9GZN0	Histone H2A gene (lambda-HHG55) (Fragment) OS=Homo sapiens PE=4 SV=1 - [V9GZN0_HUMAN]	19	1	1	1	47	5.0	11.90
E9PN51	NADH dehydrogenase [ubiquinone] iron-sulfur protein 8, mitochondrial (Fragment) OS=Homo sapiens GN=NDUFS8 PE=1 SV=1 - [E9PN51_HUMAN]	6	1	1	1	110	12.4	9.98
P31151	Protein S100-A7 OS=Homo sapiens GN=S100A7 PE=1 SV=4 - [S10A7_HUMAN]	1	1	1	1	101	11.5	6.77
Q75MN6	Putative uncharacterized protein MLL3 (Fragment) OS=Homo sapiens GN=MLL3 PE=4 SV=1 - [Q75MN6_HUMAN]	4	1	1	1	2185	239.3	6.06
B2RDE0	cDNA, FLJ96567, highly similar to Homo sapiens propionyl Coenzyme A carboxylase, alpha polypeptide(PCCA), mRNA OS=Homo sapiens PE=2 SV=1 - [B2RDE0_HUMAN]	2	1	1	1	703	77.4	7.06
Q96QC0	Serine/threonine-protein phosphatase 1 regulatory subunit 10 OS=Homo sapiens GN=PPP1R10 PE=1 SV=1 - [PP1RA_HUMAN]	1	1	1	1	940	99.0	9.17
A0A075B6Z2	Protein TRAJ56 (Fragment) OS=Homo sapiens GN=TRAJ56 PE=4 SV=1 - [A0A075B6Z2_HUMAN]	2	1	1	1	21	2.2	10.29

Q16378	Proline-rich protein 4 OS=Homo sapiens GN=PRR4 PE=1 SV=3 - [PROL4_HUMAN]	2	1	1	1	134	15.1	7.06
P05109	Protein S100-A8 OS=Homo sapiens GN=S100A8 PE=1 SV=1 - [S10A8_HUMAN]	1	2	2	2	93	10.8	7.03
Q9UL72	Myosin-reactive immunoglobulin heavy chain variable region (Fragment) OS=Homo sapiens PE=2 SV=1 - [Q9UL72_HUMAN]	5	1	1	1	118	12.9	6.58
B4DJN9	cDNA FLJ57508, highly similar to Eukaryotic translation initiation factor 3 subunit 3 OS=Homo sapiens PE=2 SV=1 - [B4DJN9_HUMAN]	1	1	1	1	153	16.8	5.29
A0A087WUP6	Transmembrane and coiled-coil domain-containing protein 3 (Fragment) OS=Homo sapiens GN=TMCO3 PE=1 SV=1 - [A0A087WUP6_HUMAN]	5	1	1	1	145	16.9	4.97
E9PNW5	Uncharacterized protein C4orf50 OS=Homo sapiens GN=C4orf50 PE=4 SV=1 - [E9PNW5_HUMAN]	1	1	1	1	750	83.0	6.28
J3QQW9	Polycomb protein SUZ12 OS=Homo sapiens GN=SUZ12 PE=1 SV=1 - [J3QQW9_HUMAN]	3	1	1	1	716	80.3	8.76
A9NIU4	Obscurin isoform B (Fragment) OS=Homo sapiens GN=OBSCN PE=2 SV=1 - [A9NIU4_HUMAN]	4	1	1	1	1960	212.3	6.35
A8K651	cDNA FLJ75700, highly similar to Homo sapiens complement component 1, q subcomponent binding protein (C1QBP), nuclear gene encoding mitochondrial protein, mRNA OS=Homo sapiens PE=2 SV=1 - [A8K651_HUMAN]	1	1	1	2	282	31.4	4.84
A0A0A0MQU1	Inverted formin-2 (Fragment) OS=Homo sapiens GN=INF2 PE=1 SV=1 - [A0A0A0MQU1_HUMAN]	6	1	1	1	717	78.8	5.58

IGFR-2

Accession	Description	# Proteins	# Unique Peptides	# Peptides	# PSMs	# AAs	MW [kDa]	calc . pI
P35527	Keratin, type I cytoskeletal 9 OS=Homo sapiens GN=KRT9 PE=1 SV=3 - [K1C9_HUMAN]	2	31	32	257	623	62.0	5.24
P13645	Keratin, type I cytoskeletal 10 OS=Homo sapiens GN=KRT10 PE=1 SV=6 - [K1C10_HUMAN]	23	31	35	172	584	58.8	5.21
H6VRF8	Keratin 1 OS=Homo sapiens GN=KRT1 PE=3 SV=1 - [H6VRF8_HUMAN]	16	33	38	191	644	66.0	8.12
P35908	Keratin, type II cytoskeletal 2 epidermal OS=Homo sapiens GN=KRT2 PE=1 SV=2 - [K22E_HUMAN]	7	26	35	119	639	65.4	8.00
P02533	Keratin, type I cytoskeletal 14 OS=Homo sapiens GN=KRT14 PE=1 SV=4 - [K1C14_HUMAN]	32	9	26	64	472	51.5	5.16
P08779	Keratin, type I cytoskeletal 16 OS=Homo sapiens GN=KRT16 PE=1 SV=4 - [K1C16_HUMAN]	33	11	24	59	473	51.2	5.05

P13647	Keratin, type II cytoskeletal 5 OS=Homo sapiens GN=KRT5 PE=1 SV=3 - [K2C5_HUMAN]	16	11	22	49	590	62.3	7.7 4
B4DRR0	cDNA FLJ53910, highly similar to Keratin, type II cytoskeletal 6A OS=Homo sapiens PE=2 SV=1 - [B4DRR0_HUMAN]	19	7	20	37	535	57.8	8.0 0
Q04695	Keratin, type I cytoskeletal 17 OS=Homo sapiens GN=KRT17 PE=1 SV=2 - [K1C17_HUMAN]	27	3	15	24	432	48.1	5.0 2
Q0IIN1	Keratin 77 OS=Homo sapiens GN=KRT77 PE=1 SV=1 - [Q0IIN1_HUMAN]	7	4	7	19	578	61.8	5.8 5
Q6KB66	Keratin, type II cytoskeletal 80 OS=Homo sapiens GN=KRT80 PE=1 SV=2 - [K2C80_HUMAN]	9	1	2	15	452	50.5	5.6 7
A0A024R0Y2	HCG30204, isoform CRA_a OS=Homo sapiens GN=hCG_30204 PE=4 SV=1 - [A0A024R0Y2_HUMAN]	13	10	10	13	2268	257.1	6.6 1
Q86Y46	Keratin, type II cytoskeletal 73 OS=Homo sapiens GN=KRT73 PE=1 SV=1 - [K2C73_HUMAN]	11	2	5	12	540	58.9	7.2 3
Q53HF2	Heat shock 70kDa protein 8 isoform 2 variant (Fragment) OS=Homo sapiens PE=1 SV=1 - [Q53HF2_HUMAN]	22	5	7	8	493	53.5	5.8 6
B3KPS3	cDNA FLJ32131 fis, clone PEBLM2000267, highly similar to Tubulin alpha-ubiquitous chain OS=Homo sapiens PE=2 SV=1 - [B3KPS3_HUMAN]	35	4	4	7	416	46.2	5.1 2
Q45KI0	Trypsin I (Fragment) OS=Homo sapiens GN=PRSS1 PE=3 SV=1 - [Q45KI0_HUMAN]	17	1	1	3	84	9.2	9.9 9
J3QRT3	Uncharacterized protein KIAA0195 (Fragment) OS=Homo sapiens GN=KIAA0195 PE=1 SV=5 - [J3QRT3_HUMAN]	1	1	1	5	89	9.5	6.7 6
F6KPG5	Albumin (Fragment) OS=Homo sapiens PE=2 SV=1 - [F6KPG5_HUMAN]	14	3	3	5	585	66.5	6.0 4
B4DFN9	cDNA FLJ54303, highly similar to Heat shock 70 kDa protein 1 OS=Homo sapiens PE=2 SV=1 - [B4DFN9_HUMAN]	30	3	5	5	572	62.4	5.6 9
B7Z597	cDNA FLJ54373, highly similar to 60 kDa heat shock protein, mitochondrial OS=Homo sapiens PE=2 SV=1 - [B7Z597_HUMAN]	9	2	2	3	564	60.0	5.7 4
P81605	Dermcidin OS=Homo sapiens GN=DCD PE=1 SV=2 - [DCD_HUMAN]	1	3	3	4	110	11.3	6.5 4
Q8TBA7	HSP90AA1 protein (Fragment) OS=Homo sapiens GN=HSP90AA1 PE=2 SV=2 - [Q8TBA7_HUMAN]	15	4	4	5	638	73.8	5.1 6
Q7Z612	Acidic ribosomal phosphoprotein P1 OS=Homo sapiens PE=2 SV=1 - [Q7Z612_HUMAN]	4	1	1	3	113	11.4	4.3 6
Q8N1N4	Keratin, type II cytoskeletal 78 OS=Homo sapiens GN=KRT78 PE=2 SV=2 - [K2C78_HUMAN]	3	3	5	5	520	56.8	6.0 2
I3L1U9	Actin, cytoplasmic 2 (Fragment) OS=Homo sapiens GN=ACTG1 PE=1 SV=1 - [I3L1U9_HUMAN]	65	4	4	4	214	23.8	5.4 4
Q86YZ3	Hornerin OS=Homo sapiens GN=HRNR PE=1 SV=2 - [HORN_HUMAN]	1	2	2	2	2850	282. 2	10. 04
A0A087WUV8	Basigin OS=Homo sapiens GN=BSG PE=1 SV=1 - [A0A087WUV8_HUMAN]	6	1	1	2	189	20.5	6.6 8

B3KX99	cDNA FLJ45019 fis, clone BRAWH3015825 OS=Homo sapiens PE=2 SV=1 - [B3KX99_HUMAN]	2	1	1	4	333	38.5	8.9 7
O75556	Mammaglobin-B OS=Homo sapiens GN=SCGB2A1 PE=1 SV=1 - [SG2A1_HUMAN]	1	2	2	2	95	10.9	5.7 8
B4E2A0	cDNA FLJ61543, highly similar to Desmoplakin OS=Homo sapiens PE=2 SV=1 - [B4E2A0_HUMAN]	6	3	3	3	1350	156. 2	7.4 3
Q86W20	Protease serine 1 (Fragment) OS=Homo sapiens GN=PRSS1 PE=3 SV=1 - [Q86W20_HUMAN]	6	1	1	2	84	9.2	10. 27
Q19KS2	Lactoferrin (Fragment) OS=Homo sapiens PE=2 SV=1 - [Q19KS2_HUMAN]	15	2	2	3	353	39.1	9.0 3
Q02413	Desmoglein-1 OS=Homo sapiens GN=DSG1 PE=1 SV=2 - [DSG1_HUMAN]	1	2	2	2	1049	113. 7	5.0 3
Q5ZEY3	Glyceraldehyde-3-phosphate dehydrogenase (Fragment) OS=Homo sapiens GN=GAPD PE=2 SV=1 - [Q5ZEY3_HUMAN]	6	1	1	2	86	9.2	9.7 2
Q04656	Copper-transporting ATPase 1 OS=Homo sapiens GN=ATP7A PE=1 SV=3 - [ATP7A_HUMAN]	1	1	1	2	1500	163. 3	6.2 4
H0YKZ7	Annexin (Fragment) OS=Homo sapiens GN=ANXA2 PE=1 SV=1 - [H0YKZ7_HUMAN]	16	1	1	2	119	13.0	8.1 3
Q9GZZ8	Extracellular glycoprotein lacritin OS=Homo sapiens GN=LACRT PE=1 SV=1 - [LACRT_HUMAN]	2	2	2	2	138	14.2	5.5 0
B4DNE0	cDNA FLJ52573, highly similar to Elongation factor 1-alpha 1 OS=Homo sapiens PE=2 SV=1 - [B4DNE0_HUMAN]	35	2	2	3	395	42.6	9.0 1
A0A087WYX2	Histone lysine demethylase PHF8 OS=Homo sapiens GN=PHF8 PE=1 SV=1 - [A0A087WYX2_HUMAN]	2	1	1	4	303	33.8	10. 08
A0A0A0MRQ5	Peroxiredoxin-1 OS=Homo sapiens GN=PRDX1 PE=1 SV=1 - [A0A0A0MRQ5_HUMAN]	6	2	2	2	97	10.7	8.7 2
Q3SYB5	SERPINB12 protein OS=Homo sapiens GN=SERPINB12 PE=2 SV=1 - [Q3SYB5_HUMAN]	2	2	2	3	183	20.9	5.8 7
P31151	Protein S100-A7 OS=Homo sapiens GN=S100A7 PE=1 SV=4 - [S10A7_HUMAN]	1	1	1	2	101	11.5	6.7 7
B4DHR1	cDNA FLJ53009, highly similar to Calreticulin OS=Homo sapiens PE=2 SV=1 - [B4DHR1_HUMAN]	5	2	2	2	212	24.3	5.1 1
Q5VSP4	Putative lipocalin 1-like protein 1 OS=Homo sapiens GN=LCN1P1 PE=5 SV=1 - [LC1L1_HUMAN]	2	2	2	2	162	17.9	5.0 0
F8WF65	Elongation factor 1-beta OS=Homo sapiens GN=EEF1B2 PE=1 SV=1 - [F8WF65_HUMAN]	4	1	1	1	29	3.1	4.4 6
F8WE04	Heat shock protein beta-1 OS=Homo sapiens GN=HSPB1 PE=1 SV=1 - [F8WE04_HUMAN]	3	2	2	2	186	20.4	9.0 6
A0A024RC29	Desmocollin 3, isoform CRA_b OS=Homo sapiens GN=DSC3 PE=4 SV=1 - [A0A024RC29_HUMAN]	3	1	1	1	896	99.9	6.1 0

D6W507	HCG1990625, isoform CRA_a OS=Homo sapiens GN=hCG_1990625 PE=4 SV=1 - [D6W507_HUMAN]	11	1	1	1	146	16.6	6.13
G3V361	Calmodulin (Fragment) OS=Homo sapiens GN=CALM1 PE=1 SV=1 - [G3V361_HUMAN]	8	1	1	1	98	11.1	4.25
E5RJN0	Heparan-alpha-glucosaminide N-acetyltransferase OS=Homo sapiens GN=HGSNAT PE=1 SV=1 - [E5RJN0_HUMAN]	2	1	1	1	352	38.9	8.32
P07108	Acyl-CoA-binding protein OS=Homo sapiens GN=DBI PE=1 SV=2 - [ACBP_HUMAN]	5	1	1	1	87	10.0	6.57
Q8IXY4	PHLDB2 protein OS=Homo sapiens GN=PHLDB2 PE=2 SV=1 - [Q8IXY4_HUMAN]	1	1	1	1	519	56.9	8.78
A0A087WXD2	Membrane-associated guanylate kinase, WW and PDZ domain-containing protein 1 OS=Homo sapiens GN=MAGI1 PE=1 SV=1 - [A0A087WXD2_HUMAN]	7	1	1	1	980	106.8	6.46
F8W079	ATP synthase subunit beta, mitochondrial (Fragment) OS=Homo sapiens GN=ATP5B PE=1 SV=1 - [F8W079_HUMAN]	4	1	1	1	284	30.2	8.29
A9UFC0	Caspase 14 OS=Homo sapiens GN=CASP14 PE=2 SV=1 - [A9UFC0_HUMAN]	2	1	1	1	242	27.6	5.34
Q5TDG9	DnaJ (Hsp40) homolog, subfamily C, member 16, isoform CRA_a OS=Homo sapiens GN=DNAJC16 PE=1 SV=1 - [Q5TDG9_HUMAN]	4	1	1	1	595	69.3	7.15
B8ZZ54	10 kDa heat shock protein, mitochondrial OS=Homo sapiens GN=HSPE1 PE=1 SV=1 - [B8ZZ54_HUMAN]	4	1	1	1	47	5.2	4.72
D3VVK8	Ataxin 3 variant ref (Fragment) OS=Homo sapiens GN=ATXN3 PE=2 SV=1 - [D3VVK8_HUMAN]	1	1	1	1	329	37.8	4.82
B4DYE2	Kinesin-like protein OS=Homo sapiens PE=2 SV=1 - [B4DYE2_HUMAN]	2	1	1	1	1234	139.8	6.13
B2R8Y4	cDNA, FLJ94117, highly similar to Homo sapiens actinin, alpha 3 (ACTN3), mRNA OS=Homo sapiens PE=1 SV=1 - [B2R8Y4_HUMAN]	4	1	1	1	901	103.2	5.60
A0JLQ0	AZGP1 protein (Fragment) OS=Homo sapiens GN=AZGP1 PE=2 SV=1 - [A0JLQ0_HUMAN]	3	1	1	1	159	18.7	8.97
P05387	60S acidic ribosomal protein P2 OS=Homo sapiens GN=RPLP2 PE=1 SV=1 - [RLA2_HUMAN]	1	1	1	1	115	11.7	4.54
S4R3R2	Ankyrin repeat domain-containing protein 10 (Fragment) OS=Homo sapiens GN=ANKRD10 PE=1 SV=1 - [S4R3R2_HUMAN]	1	1	1	1	121	13.4	5.08
Q9HB00	Desmocollin 1, isoform CRA_b OS=Homo sapiens GN=DSC1 PE=4 SV=1 - [Q9HB00_HUMAN]	2	2	2	3	840	93.8	5.53
F8WCJ1	Eukaryotic translation initiation factor 5A OS=Homo sapiens GN=EIF5A2 PE=1 SV=1 - [F8WCJ1_HUMAN]	8	1	1	1	105	11.7	9.14
A0A0C4DFV9	Protein SET OS=Homo sapiens GN=SET PE=1 SV=1 - [A0A0C4DFV9_HUMAN]	6	1	1	1	266	31.1	4.23
Q8NFF2	Sodium/potassium/calcium exchanger 4 OS=Homo sapiens GN=SLC24A4 PE=1 SV=2 - [NCKX4_HUMAN]	1	1	1	1	622	69.0	7.52

Q9HBT7	Zinc finger protein 287 OS=Homo sapiens GN=ZNF287 PE=2 SV=1 - [ZN287_HUMAN]	1	1	1	1	754	87.5	8.48
H9KV28	Protein diaphanous homolog 1 OS=Homo sapiens GN=DIAPH1 PE=1 SV=2 - [H9KV28_HUMAN]	5	1	1	1	1228	136.8	5.24
Q5HY57	Emerin OS=Homo sapiens GN=EMD PE=1 SV=1 - [Q5HY57_HUMAN]	2	1	1	1	219	24.9	5.02
Q15203	Prothymosin alpha OS=Homo sapiens PE=4 SV=2 - [Q15203_HUMAN]	18	1	1	1	73	8.2	3.76
A8K651	cDNA FLJ75700, highly similar to Homo sapiens complement component 1, q subcomponent binding protein (C1QBP), nuclear gene encoding mitochondrial protein, mRNA OS=Homo sapiens PE=2 SV=1 - [A8K651_HUMAN]	4	2	2	2	282	31.4	4.84
A0A024R3V9	HCG37498, isoform CRA_b OS=Homo sapiens GN=hCG_37498 PE=4 SV=1 - [A0A024R3V9_HUMAN]	5	1	1	1	92	11.0	9.74
B4DI19	cDNA FLJ59524, highly similar to Cysteinyl-tRNA synthetase (EC 6.1.1.16) OS=Homo sapiens PE=2 SV=1 - [B4DI19_HUMAN]	4	1	1	1	662	75.6	6.60
D3DXE0	HCG20684, isoform CRA_b OS=Homo sapiens GN=hCG_20684 PE=3 SV=1 - [D3DXE0_HUMAN]	1	1	1	1	296	33.2	7.21
E9PPR4	Transcriptional activator Myb OS=Homo sapiens GN=MYB PE=1 SV=1 - [E9PPR4_HUMAN]	25	1	1	1	103	12.4	6.19
P05109	Protein S100-A8 OS=Homo sapiens GN=S100A8 PE=1 SV=1 - [S10A8_HUMAN]	1	1	1	2	93	10.8	7.03
P01040	Cystatin-A OS=Homo sapiens GN=CSTA PE=1 SV=1 - [CYTA_HUMAN]	1	1	1	1	98	11.0	5.50
Q53RS7	Putative uncharacterized protein LBP-9 (Fragment) OS=Homo sapiens GN=LBP-9 PE=4 SV=1 - [Q53RS7_HUMAN]	1	1	1	1	32	3.6	4.89
A0A024R1X8	Junction plakoglobin, isoform CRA_a OS=Homo sapiens GN=JUP PE=4 SV=1 - [A0A024R1X8_HUMAN]	2	1	1	1	745	81.7	6.14
P07737	Profilin-1 OS=Homo sapiens GN=PFN1 PE=1 SV=2 - [PROF1_HUMAN]	2	1	1	1	140	15.0	8.27
I3L234	Ribosomal L1 domain-containing protein 1 (Fragment) OS=Homo sapiens GN=RSL1D1 PE=1 SV=1 - [I3L234_HUMAN]	1	1	1	1	98	11.6	9.74
M0R1V7	Ubiquitin-60S ribosomal protein L40 (Fragment) OS=Homo sapiens GN=UBA52 PE=1 SV=1 - [M0R1V7_HUMAN]	36	1	1	1	63	7.1	5.36
Q6ZSX8	cDNA FLJ45139 fis, clone BRAWH3039623 OS=Homo sapiens PE=2 SV=1 - [Q6ZSX8_HUMAN]	1	1	1	3	136	15.5	10.07
L0R5A1	Alternative protein CSF2RB OS=Homo sapiens GN=CSF2RB PE=4 SV=1 - [L0R5A1_HUMAN]	1	1	1	1	108	11.6	11.30
Q8TC57	Meiosis 1 arrest protein OS=Homo sapiens GN=M1AP PE=1 SV=1 - [M1AP_HUMAN]	1	1	1	1	530	59.3	6.87
D9ZHQ0	Neuregulin 3 variant 6 OS=Homo sapiens GN=NRG3 PE=2 SV=1 - [D9ZHQ0_HUMAN]	1	1	1	1	239	27.2	7.44

Q8WVQ1	Soluble calcium-activated nucleotidase 1 OS=Homo sapiens GN=CANT1 PE=1 SV=1 - [CANT1_HUMAN]	1	1	1	1	401	44.8	6.09
Q5KSL6	Diacylglycerol kinase kappa OS=Homo sapiens GN=DGKK PE=1 SV=1 - [DGKK_HUMAN]	1	1	1	1	1271	141.7	5.53
Q9NZP6	Nuclear pore-associated protein 1 OS=Homo sapiens GN=NPAP1 PE=1 SV=2 - [NPAP1_HUMAN]	1	1	1	1	1156	120.9	8.69
P12004	Proliferating cell nuclear antigen OS=Homo sapiens GN=PCNA PE=1 SV=1 - [PCNA_HUMAN]	3	1	1	1	261	28.8	4.69
Q4LDE5	Sushi, von Willebrand factor type A, EGF and pentraxin domain-containing protein 1 OS=Homo sapiens GN=SVEP1 PE=1 SV=3 - [SVEP1_HUMAN]	3	1	1	1	3571	389.9	5.50
F5GXD8	Stress-induced-phosphoprotein 1 OS=Homo sapiens GN=STIP1 PE=1 SV=1 - [F5GXD8_HUMAN]	4	1	1	1	138	15.6	8.25
F8W061	Iron-sulfur protein NUBPL (Fragment) OS=Homo sapiens GN=NUBPL PE=1 SV=1 - [F8W061_HUMAN]	5	1	1	1	133	14.3	8.10
A0A087WU05	C-Maf-inducing protein OS=Homo sapiens GN=CMIP PE=1 SV=1 - [A0A087WU05_HUMAN]	4	1	1	1	586	65.2	5.94
H3BR41	Exportin-6 (Fragment) OS=Homo sapiens GN=XPO6 PE=1 SV=5 - [H3BR41_HUMAN]	4	1	1	1	143	17.0	7.37
B4DHH8	cDNA FLJ56865, highly similar to Transcriptional regulator ATRX (EC 3.6.1.-) OS=Homo sapiens PE=2 SV=1 - [B4DHH8_HUMAN]	3	1	1	1	858	98.1	6.71
Q6ZRA8	cDNA FLJ46514 fis, clone THYMU3032798, highly similar to Focal adhesion kinase 2 (EC 2.7.1.112) OS=Homo sapiens PE=2 SV=1 - [Q6ZRA8_HUMAN]	1	1	1	1	596	68.0	5.60
A8MXP8	Reticulocalbin-2 OS=Homo sapiens GN=RCN2 PE=1 SV=1 - [A8MXP8_HUMAN]	2	1	1	1	216	24.8	4.42
Q68DE6	Putative uncharacterized protein DKFZp781A0353 (Fragment) OS=Homo sapiens GN=DKFZp781A0353 PE=2 SV=1 - [Q68DE6_HUMAN]	3	1	1	1	1017	116.7	6.74
H0Y6T0	Nuclear receptor coactivator 7 (Fragment) OS=Homo sapiens GN=NCOA7 PE=1 SV=1 - [H0Y6T0_HUMAN]	9	1	1	1	177	20.7	7.15
H7C1F9	Ral GTPase-activating protein subunit alpha-2 (Fragment) OS=Homo sapiens GN=RALGAPA2 PE=1 SV=1 - [H7C1F9_HUMAN]	2	1	1	1	1740	194.9	5.90
F2WJ44	Cytochrome c oxidase subunit 1 OS=Homo sapiens GN=COX1 PE=3 SV=1 - [F2WJ44_HUMAN]	1	1	1	1	513	57.0	6.70

PDGFRB-1

Accession	Description	# Proteins	# Unique Peptides	# Peptides	# PSMs	# AAs	MW [kDa]	calc . pI
P35527	Keratin, type I cytoskeletal 9 OS=Homo sapiens GN=KRT9 PE=1 SV=3 - [K1C9_HUMAN]	2	30	31	204	623	62.0	5.24
H6VRF8	Keratin 1 OS=Homo sapiens GN=KRT1 PE=3 SV=1 - [H6VRF8_HUMAN]	17	30	34	196	644	66.0	8.12
P13645	Keratin, type I cytoskeletal 10 OS=Homo sapiens GN=KRT10 PE=1 SV=6 - [K1C10_HUMAN]	22	28	32	140	584	58.8	5.21
P35908	Keratin, type II cytoskeletal 2 epidermal OS=Homo sapiens GN=KRT2 PE=1 SV=2 - [K22E_HUMAN]	9	23	32	98	639	65.4	8.00
P02533	Keratin, type I cytoskeletal 14 OS=Homo sapiens GN=KRT14 PE=1 SV=4 - [K1C14_HUMAN]	36	7	23	56	472	51.5	5.16
P08779	Keratin, type I cytoskeletal 16 OS=Homo sapiens GN=KRT16 PE=1 SV=4 - [K1C16_HUMAN]	32	3	16	43	473	51.2	5.05
P13647	Keratin, type II cytoskeletal 5 OS=Homo sapiens GN=KRT5 PE=1 SV=3 - [K2C5_HUMAN]	19	9	20	37	590	62.3	7.74
B4DRR0	cDNA FLJ53910, highly similar to Keratin, type II cytoskeletal 6A OS=Homo sapiens PE=2 SV=1 - [B4DRR0_HUMAN]	20	4	16	27	535	57.8	8.00
Q04695	Keratin, type I cytoskeletal 17 OS=Homo sapiens GN=KRT17 PE=1 SV=2 - [K1C17_HUMAN]	26	1	13	19	432	48.1	5.02
Q0IIN1	Keratin 77 OS=Homo sapiens GN=KRT77 PE=1 SV=1 - [Q0IIN1_HUMAN]	7	2	5	15	578	61.8	5.85
Q86Y23	Hornerin OS=Homo sapiens GN=HRNR PE=1 SV=2 - [HORN_HUMAN]	1	2	2	5	2850	282.2	10.04
Q14CN4	Keratin, type II cytoskeletal 72 OS=Homo sapiens GN=KRT72 PE=1 SV=2 - [K2C72_HUMAN]	8	1	4	11	511	55.8	6.89
F6KPG5	Albumin (Fragment) OS=Homo sapiens PE=2 SV=1 - [F6KPG5_HUMAN]	14	3	3	5	585	66.5	6.04
P81605	Dermcidin OS=Homo sapiens GN=DCD PE=1 SV=2 - [DCD_HUMAN]	1	3	3	5	110	11.3	6.54
Q45KI0	Trypsin I (Fragment) OS=Homo sapiens GN=PRSS1 PE=3 SV=1 - [Q45KI0_HUMAN]	17	1	1	3	84	9.2	9.99
Q99456	Keratin, type I cytoskeletal 12 OS=Homo sapiens GN=KRT12 PE=1 SV=1 - [K1C12_HUMAN]	1	1	3	5	494	53.5	4.78
Q8N1N4	Keratin, type II cytoskeletal 78 OS=Homo sapiens GN=KRT78 PE=2 SV=2 - [K2C78_HUMAN]	4	2	3	4	520	56.8	6.02
Q86W20	Protease serine 1 (Fragment) OS=Homo sapiens GN=PRSS1 PE=3 SV=1 - [Q86W20_HUMAN]	6	1	1	3	84	9.2	10.27
A0A075B6Z2	Protein TRAJ56 (Fragment) OS=Homo sapiens GN=TRAJ56 PE=4 SV=1 - [A0A075B6Z2_HUMAN]	2	1	1	18	21	2.2	10.29

B4E2A0	cDNA FLJ61543, highly similar to Desmoplakin OS=Homo sapiens PE=2 SV=1 - [B4E2A0_HUMAN]	6	4	4	4	1350	156.2	7.43
F8WCJ1	Eukaryotic translation initiation factor 5A OS=Homo sapiens GN=EIF5A2 PE=1 SV=1 - [F8WCJ1_HUMAN]	8	2	2	3	105	11.7	9.14
Q9GZZ8	Extracellular glycoprotein lacritin OS=Homo sapiens GN=LACRT PE=1 SV=1 - [LACRT_HUMAN]	2	3	3	3	138	14.2	5.50
O75556	Mammaglobin-B OS=Homo sapiens GN=SCGB2A1 PE=1 SV=1 - [SG2A1_HUMAN]	1	2	2	2	95	10.9	5.78
Q7Z612	Acidic ribosomal phosphoprotein P1 OS=Homo sapiens PE=2 SV=1 - [Q7Z612_HUMAN]	4	1	1	2	113	11.4	4.36
J3QSA3	Polyubiquitin-B (Fragment) OS=Homo sapiens GN=UBB PE=1 SV=1 - [J3QSA3_HUMAN]	37	1	1	2	43	4.9	5.19
Q9HB00	Desmocollin 1, isoform CRA_b OS=Homo sapiens GN=DSC1 PE=4 SV=1 - [Q9HB00_HUMAN]	2	3	3	3	840	93.8	5.53
J3QRT3	Uncharacterized protein KIAA0195 (Fragment) OS=Homo sapiens GN=KIAA0195 PE=1 SV=5 - [J3QRT3_HUMAN]	1	1	1	2	89	9.5	6.76
F8VV32	Lysozyme OS=Homo sapiens GN=LYZ PE=1 SV=1 - [F8VV32_HUMAN]	3	2	2	2	104	11.5	9.07
L0R5A1	Alternative protein CSF2RB OS=Homo sapiens GN=CSF2RB PE=4 SV=1 - [L0R5A1_HUMAN]	1	1	1	3	108	11.6	11.30
Q5VSP4	Putative lipocalin 1-like protein 1 OS=Homo sapiens GN=LCN1P1 PE=5 SV=1 - [LC1L1_HUMAN]	2	1	1	2	162	17.9	5.00
A0A087WXD2	Membrane-associated guanylate kinase, WW and PDZ domain-containing protein 1 OS=Homo sapiens GN=MAGI1 PE=1 SV=1 - [A0A087WXD2_HUMAN]	7	1	1	2	980	106.8	6.46
H9KV28	Protein diaphanous homolog 1 OS=Homo sapiens GN=DIAPH1 PE=1 SV=2 - [H9KV28_HUMAN]	5	1	1	2	1228	136.8	5.24
B4DK31	cDNA FLJ54634, highly similar to Acetyl-CoA carboxylase 1 (EC 6.4.1.2) OS=Homo sapiens PE=2 SV=1 - [B4DK31_HUMAN]	9	2	2	2	306	35.6	6.38
F8VRZ4	Tubulin alpha-1A chain (Fragment) OS=Homo sapiens GN=TUBA1A PE=4 SV=1 - [F8VRZ4_HUMAN]	30	2	2	2	112	12.2	5.77
Q5HY57	Emerin OS=Homo sapiens GN=EMD PE=1 SV=1 - [Q5HY57_HUMAN]	2	2	2	2	219	24.9	5.02
C9JTX5	Actin, cytoplasmic 1 (Fragment) OS=Homo sapiens GN=ACTB PE=1 SV=1 - [C9JTX5_HUMAN]	44	2	2	2	80	8.5	5.35
Q19KS2	Lactoferrin (Fragment) OS=Homo sapiens PE=2 SV=1 - [Q19KS2_HUMAN]	12	1	1	2	353	39.1	9.03
B4DHW6	cDNA FLJ54930, highly similar to Homo sapiens Dbf4-related factor 1 (DRF1), transcript variant 2, mRNA OS=Homo sapiens PE=2 SV=1 - [B4DHW6_HUMAN]	3	1	1	2	154	16.7	10.27
B3KX99	cDNA FLJ45019 fis, clone BRAWH3015825 OS=Homo sapiens PE=2 SV=1 - [B3KX99_HUMAN]	2	1	1	2	333	38.5	8.97

Q3SYB5	SERPINB12 protein OS=Homo sapiens GN=SERPINB12 PE=2 SV=1 - [Q3SYB5_HUMAN]	2	1	1	1	183	20.9	5.87
Q6UXS9	Inactive caspase-12 OS=Homo sapiens GN=CASP12 PE=2 SV=2 - [CASPC_HUMAN]	1	1	1	1	341	38.8	6.02
A0A087WUV8	Basigin OS=Homo sapiens GN=BSG PE=1 SV=1 - [A0A087WUV8_HUMAN]	6	1	1	1	189	20.5	6.68
G3V361	Calmodulin (Fragment) OS=Homo sapiens GN=CALM1 PE=1 SV=1 - [G3V361_HUMAN]	8	1	1	1	98	11.1	4.25
C9IYG1	BRCA1-associated RING domain protein 1 (Fragment) OS=Homo sapiens GN=BARD1 PE=1 SV=1 - [C9IYG1_HUMAN]	9	1	1	2	216	24.4	8.47
Q7RTY7	Ovochymase-1 OS=Homo sapiens GN=OVCH1 PE=2 SV=2 - [OVCH1_HUMAN]	1	1	1	1	1134	125.0	8.32
B4DNE0	cDNA FLJ52573, highly similar to Elongation factor 1-alpha 1 OS=Homo sapiens PE=2 SV=1 - [B4DNE0_HUMAN]	35	2	2	2	395	42.6	9.01
A8K651	cDNA FLJ75700, highly similar to Homo sapiens complement component 1, q subcomponent binding protein (C1QBP), nuclear gene encoding mitochondrial protein, mRNA OS=Homo sapiens PE=2 SV=1 - [A8K651_HUMAN]	2	1	1	1	282	31.4	4.84
P05109	Protein S100-A8 OS=Homo sapiens GN=S100A8 PE=1 SV=1 - [S10A8_HUMAN]	1	1	1	1	93	10.8	7.03
A0A087WUI6	Progesterone-induced-blocking factor 1 OS=Homo sapiens GN=PIBF1 PE=1 SV=1 - [A0A087WUI6_HUMAN]	2	1	1	1	698	83.1	5.62
H3BQB6	Stathmin domain-containing protein 1 OS=Homo sapiens GN=STMND1 PE=2 SV=1 - [STMD1_HUMAN]	1	1	1	1	276	31.0	8.47
E9PN25	Heat shock cognate 71 kDa protein (Fragment) OS=Homo sapiens GN=HSPA8 PE=1 SV=1 - [E9PN25_HUMAN]	35	1	1	1	132	14.6	6.55
Q96MA3	cDNA FLJ32709 fis, clone TESTI2000695, weakly similar to KINESIN HEAVY CHAIN (Fragment) OS=Homo sapiens PE=2 SV=1 - [Q96MA3_HUMAN]	4	1	1	1	648	73.5	5.31
Q2Y0W8	Electroneutral sodium bicarbonate exchanger 1 OS=Homo sapiens GN=SLC4A8 PE=1 SV=1 - [S4A8_HUMAN]	1	1	1	1	1093	122.9	6.68
A0A024R1X8	Junction plakoglobin, isoform CRA_a OS=Homo sapiens GN=JUP PE=4 SV=1 - [A0A024R1X8_HUMAN]	2	1	1	1	745	81.7	6.14
P12004	Proliferating cell nuclear antigen OS=Homo sapiens GN=PCNA PE=1 SV=1 - [PCNA_HUMAN]	3	1	1	1	261	28.8	4.69
Q8TC57	Meiosis 1 arrest protein OS=Homo sapiens GN=M1AP PE=1 SV=1 - [M1AP_HUMAN]	1	1	1	1	530	59.3	6.87
P07737	Profilin-1 OS=Homo sapiens GN=PFN1 PE=1 SV=2 - [PROF1_HUMAN]	2	1	1	1	140	15.0	8.27
Q16378	Proline-rich protein 4 OS=Homo sapiens GN=PRR4 PE=1 SV=3 - [PROL4_HUMAN]	2	1	1	1	134	15.1	7.06
P47989	Xanthine dehydrogenase/oxidase OS=Homo sapiens GN=XDH PE=1 SV=4 - [XDH_HUMAN]	1	1	1	1	1333	146.3	7.66

Q3KRF4	Uncharacterized protein OS=Homo sapiens GN=LOC285033 PE=2 SV=1 - [Q3KRF4_HUMAN]	1	1	1	1	121	13.2	9.89
Q53SG8	Putative uncharacterized protein FLJ22527 (Fragment) OS=Homo sapiens GN=FLJ22527 PE=4 SV=1 - [Q53SG8_HUMAN]	6	1	1	1	199	22.8	9.92
B2R4M6	Protein S100 OS=Homo sapiens PE=2 SV=1 - [B2R4M6_HUMAN]	2	1	1	1	114	13.2	6.13
A0JLQ0	AZGP1 protein (Fragment) OS=Homo sapiens GN=AZGP1 PE=2 SV=1 - [A0JLQ0_HUMAN]	3	1	1	1	159	18.7	8.97
Q53GS1	MutS homolog 2 variant (Fragment) OS=Homo sapiens PE=2 SV=1 - [Q53GS1_HUMAN]	1	1	1	1	878	98.2	5.63
Q4ZG84	Putative uncharacterized protein LRP2 (Fragment) OS=Homo sapiens GN=LRP2 PE=4 SV=1 - [Q4ZG84_HUMAN]	4	1	1	1	3881	435.5	5.14
H7C2J5	Piezo-type mechanosensitive ion channel component 1 (Fragment) OS=Homo sapiens GN=PIEZO1 PE=1 SV=1 - [H7C2J5_HUMAN]	4	1	1	1	88	10.5	7.24
Q5TCD1	Isoleucine--tRNA ligase, cytoplasmic (Fragment) OS=Homo sapiens GN=IARS PE=1 SV=1 - [Q5TCD1_HUMAN]	5	1	1	1	330	38.3	6.19
H7C1F9	Ral GTPase-activating protein subunit alpha-2 (Fragment) OS=Homo sapiens GN=RALGAPA2 PE=1 SV=1 - [H7C1F9_HUMAN]	2	1	1	1	1740	194.9	5.90
Q6ZSX8	cDNA FLJ45139 fis, clone BRAWH3039623 OS=Homo sapiens PE=2 SV=1 - [Q6ZSX8_HUMAN]	1	1	1	2	136	15.5	10.07

PDGFRB-2

Accession	Description	# Proteins	# Unique Peptides	# Peptides	# PSMs	# AAs	MW [kDa]	calc . pI
P35527	Keratin, type I cytoskeletal 9 OS=Homo sapiens GN=KRT9 PE=1 SV=3 - [K1C9_HUMAN]	2	31	32	181	623	62.0	5.24
P13645	Keratin, type I cytoskeletal 10 OS=Homo sapiens GN=KRT10 PE=1 SV=6 - [K1C10_HUMAN]	21	26	31	156	584	58.8	5.21
H6VRF8	Keratin 1 OS=Homo sapiens GN=KRT1 PE=3 SV=1 - [H6VRF8_HUMAN]	16	30	35	164	644	66.0	8.12
P35908	Keratin, type II cytoskeletal 2 epidermal OS=Homo sapiens GN=KRT2 PE=1 SV=2 - [K22E_HUMAN]	8	24	33	87	639	65.4	8.00
P02533	Keratin, type I cytoskeletal 14 OS=Homo sapiens GN=KRT14 PE=1 SV=4 - [K1C14_HUMAN]	41	13	24	63	472	51.5	5.16

P08779	Keratin, type I cytoskeletal 16 OS=Homo sapiens GN=KRT16 PE=1 SV=4 - [K1C16_HUMAN]	32	4	16	49	473	51.2	5.0 5
P13647	Keratin, type II cytoskeletal 5 OS=Homo sapiens GN=KRT5 PE=1 SV=3 - [K2C5_HUMAN]	17	10	20	38	590	62.3	7.7 4
B4DRR0	cDNA FLJ53910, highly similar to Keratin, type II cytoskeletal 6A OS=Homo sapiens PE=2 SV=1 - [B4DRR0_HUMAN]	20	3	15	26	535	57.8	8.0 0
Q0IIN1	Keratin 77 OS=Homo sapiens GN=KRT77 PE=1 SV=1 - [Q0IIN1_HUMAN]	7	3	6	14	578	61.8	5.8 5
A0A024R0Y2	HCG30204, isoform CRA_a OS=Homo sapiens GN=hCG_30204 PE=4 SV=1 - [A0A024R0Y2_HUMAN]	11	13	13	15	2268	257.1	6.6 1
Q6KB66	Keratin, type II cytoskeletal 80 OS=Homo sapiens GN=KRT80 PE=1 SV=2 - [K2C80_HUMAN]	9	1	2	9	452	50.5	5.6 7
Q14CN4	Keratin, type II cytoskeletal 72 OS=Homo sapiens GN=KRT72 PE=1 SV=2 - [K2C72_HUMAN]	8	1	4	9	511	55.8	6.8 9
F6KPG5	Albumin (Fragment) OS=Homo sapiens PE=2 SV=1 - [F6KPG5_HUMAN]	14	4	4	7	585	66.5	6.0 4
P15924	Desmoplakin OS=Homo sapiens GN=DSP PE=1 SV=3 - [DESP_HUMAN]	6	5	5	9	2871	331. 6	6.8 1
Q45KI0	Trypsin I (Fragment) OS=Homo sapiens GN=PRSS1 PE=3 SV=1 - [Q45KI0_HUMAN]	17	1	1	5	84	9.2	9.9 9
Q86YZ3	Hornerin OS=Homo sapiens GN=HRNR PE=1 SV=2 - [HORN_HUMAN]	1	2	2	4	2850	282. 2	10. 04
Q8N1N4	Keratin, type II cytoskeletal 78 OS=Homo sapiens GN=KRT78 PE=2 SV=2 - [K2C78_HUMAN]	5	3	5	6	520	56.8	6.0 2
Q53HF2	Heat shock 70kDa protein 8 isoform 2 variant (Fragment) OS=Homo sapiens PE=1 SV=1 - [Q53HF2_HUMAN]	41	5	5	7	493	53.5	5.8 6
F8WCJ1	Eukaryotic translation initiation factor 5A OS=Homo sapiens GN=EIF5A2 PE=1 SV=1 - [F8WCJ1_HUMAN]	8	3	3	5	105	11.7	9.1 4
Q9GZZ8	Extracellular glycoprotein lacritin OS=Homo sapiens GN=LACRT PE=1 SV=1 - [LACRT_HUMAN]	2	4	4	5	138	14.2	5.5 0
P81605	Dermcidin OS=Homo sapiens GN=DCD PE=1 SV=2 - [DCD_HUMAN]	1	3	3	4	110	11.3	6.5 4
O75556	Mammaglobin-B OS=Homo sapiens GN=SCGB2A1 PE=1 SV=1 - [SG2A1_HUMAN]	1	2	2	3	95	10.9	5.7 8
Q2M2I5	Keratin, type I cytoskeletal 24 OS=Homo sapiens GN=KRT24 PE=1 SV=1 - [K1C24_HUMAN]	16	1	3	4	525	55.1	4.9 6
Q8N532	TUBA1C protein OS=Homo sapiens GN=TUBA1C PE=2 SV=1 - [Q8N532_HUMAN]	34	3	3	4	325	36.6	7.9 6
Q99456	Keratin, type I cytoskeletal 12 OS=Homo sapiens GN=KRT12 PE=1 SV=1 - [K1C12_HUMAN]	1	1	3	5	494	53.5	4.7 8
Q02413	Desmoglein-1 OS=Homo sapiens GN=DSG1 PE=1 SV=2 - [DSG1_HUMAN]	1	2	2	4	1049	113. 7	5.0 3

Q8TBA7	HSP90AA1 protein (Fragment) OS=Homo sapiens GN=HSP90AA1 PE=2 SV=2 - [Q8TBA7_HUMAN]	14	2	2	3	638	73.8	5.16
A0A087WYX2	Histone lysine demethylase PHF8 OS=Homo sapiens GN=PHF8 PE=1 SV=1 - [A0A087WYX2_HUMAN]	2	1	1	6	303	33.8	10.08
F8VV32	Lysozyme OS=Homo sapiens GN=LYZ PE=1 SV=1 - [F8VV32_HUMAN]	3	2	2	3	104	11.5	9.07
Q19KS2	Lactoferrin (Fragment) OS=Homo sapiens PE=2 SV=1 - [Q19KS2_HUMAN]	12	2	2	3	353	39.1	9.03
Q5HY57	Emerin OS=Homo sapiens GN=EMD PE=1 SV=1 - [Q5HY57_HUMAN]	2	2	2	3	219	24.9	5.02
A0A024R1X8	Junction plakoglobin, isoform CRA_a OS=Homo sapiens GN=JUP PE=4 SV=1 - [A0A024R1X8_HUMAN]	2	2	2	3	745	81.7	6.14
B2R4M6	Protein S100 OS=Homo sapiens PE=2 SV=1 - [B2R4M6_HUMAN]	2	1	1	2	114	13.2	6.13
V9GZN0	Histone H2A gene (lambda-HHG55) (Fragment) OS=Homo sapiens PE=4 SV=1 - [V9GZN0_HUMAN]	19	1	1	2	47	5.0	11.90
J3QRT3	Uncharacterized protein KIAA0195 (Fragment) OS=Homo sapiens GN=KIAA0195 PE=1 SV=5 - [J3QRT3_HUMAN]	1	1	1	2	89	9.5	6.76
C9IYG1	BRCA1-associated RING domain protein 1 (Fragment) OS=Homo sapiens GN=BARD1 PE=1 SV=1 - [C9IYG1_HUMAN]	9	1	1	2	216	24.4	8.47
Q08ES8	Cell growth-inhibiting protein 34 OS=Homo sapiens PE=2 SV=1 - [Q08ES8_HUMAN]	4	2	2	2	177	20.1	9.60
B4DNE0	cDNA FLJ52573, highly similar to Elongation factor 1-alpha 1 OS=Homo sapiens PE=2 SV=1 - [B4DNE0_HUMAN]	35	2	2	3	395	42.6	9.01
A0A087WTG3	Cullin-3 OS=Homo sapiens GN=CUL3 PE=1 SV=1 - [A0A087WTG3_HUMAN]	1	1	1	2	342	39.1	9.48
A0A0A0MRQ5	Peroxiredoxin-1 OS=Homo sapiens GN=PRDX1 PE=1 SV=1 - [A0A0A0MRQ5_HUMAN]	6	2	2	2	97	10.7	8.72
Q7Z350	Putative uncharacterized protein DKFZp686L0695 OS=Homo sapiens GN=DKFZp686L0695 PE=2 SV=1 - [Q7Z350_HUMAN]	1	1	1	2	549	62.1	6.37
A1L378	STRC protein OS=Homo sapiens GN=STRC PE=2 SV=1 - [A1L378_HUMAN]	4	1	1	2	1002	110.6	5.17
F8WF65	Elongation factor 1-beta OS=Homo sapiens GN=EEF1B2 PE=1 SV=1 - [F8WF65_HUMAN]	4	1	1	1	29	3.1	4.46
Q96MA3	cDNA FLJ32709 fis, clone TESTI2000695, weakly similar to KINESIN HEAVY CHAIN (Fragment) OS=Homo sapiens PE=2 SV=1 - [Q96MA3_HUMAN]	4	1	1	2	648	73.5	5.31
B3KX99	cDNA FLJ45019 fis, clone BRAWH3015825 OS=Homo sapiens PE=2 SV=1 - [B3KX99_HUMAN]	2	1	1	2	333	38.5	8.97
Q7Z612	Acidic ribosomal phosphoprotein P1 OS=Homo sapiens PE=2 SV=1 - [Q7Z612_HUMAN]	4	1	1	1	113	11.4	4.36

Q5SQH5	DEAH (Asp-Glu-Ala-His) box polypeptide 16, isoform CRA_a OS=Homo sapiens GN=DHX16 PE=1 SV=1 - [Q5SQH5_HUMAN]	3	1	1	1	560	63.5	6.76
Q86W20	Protease serine 1 (Fragment) OS=Homo sapiens GN=PRSS1 PE=3 SV=1 - [Q86W20_HUMAN]	6	1	1	1	84	9.2	10.27
Q5VSP4	Putative lipocalin 1-like protein 1 OS=Homo sapiens GN=LCN1P1 PE=5 SV=1 - [LC1L1_HUMAN]	2	1	1	1	162	17.9	5.00
A0A087WUV8	Basigin OS=Homo sapiens GN=BSG PE=1 SV=1 - [A0A087WUV8_HUMAN]	6	1	1	1	189	20.5	6.68
J3QSA3	Polyubiquitin-B (Fragment) OS=Homo sapiens GN=UBB PE=1 SV=1 - [J3QSA3_HUMAN]	37	1	1	1	43	4.9	5.19
M0R1I1	Tubulin beta-4A chain (Fragment) OS=Homo sapiens GN=TUBB4A PE=1 SV=1 - [M0R1I1_HUMAN]	27	1	1	1	74	7.8	4.94
Q6UXS9	Inactive caspase-12 OS=Homo sapiens GN=CASP12 PE=2 SV=2 - [CASPC_HUMAN]	1	1	1	1	341	38.8	6.02
A0A0A0MS48	DENN domain-containing protein 1A OS=Homo sapiens GN=DENND1A PE=1 SV=1 - [A0A0A0MS48_HUMAN]	4	1	1	1	459	52.0	8.50
J3KSP2	60S ribosomal protein L38 (Fragment) OS=Homo sapiens GN=RPL38 PE=1 SV=1 - [J3KSP2_HUMAN]	4	1	1	1	21	2.6	9.99
F8WCH0	Actin, gamma-enteric smooth muscle OS=Homo sapiens GN=ACTG2 PE=1 SV=1 - [F8WCH0_HUMAN]	43	1	1	1	52	5.6	6.49
H0YKZ7	Annexin (Fragment) OS=Homo sapiens GN=ANXA2 PE=1 SV=1 - [H0YKZ7_HUMAN]	16	1	1	1	119	13.0	8.13
B7Z532	cDNA FLJ51028, highly similar to 60 kDa heat shock protein, mitochondrial OS=Homo sapiens PE=2 SV=1 - [B7Z532_HUMAN]	7	2	2	2	245	26.7	5.22
Q59GI5	Dynamin 1 isoform 2 variant (Fragment) OS=Homo sapiens PE=2 SV=1 - [Q59GI5_HUMAN]	4	1	1	1	600	68.8	7.68
H0YGI8	Stress-induced-phosphoprotein 1 (Fragment) OS=Homo sapiens GN=STIP1 PE=1 SV=1 - [H0YGI8_HUMAN]	3	1	1	1	137	15.9	6.19
Q5ZEY3	Glyceraldehyde-3-phosphate dehydrogenase (Fragment) OS=Homo sapiens GN=GAPD PE=2 SV=1 - [Q5ZEY3_HUMAN]	6	1	1	1	86	9.2	9.72
Q5TDG9	DnaJ (Hsp40) homolog, subfamily C, member 16, isoform CRA_a OS=Homo sapiens GN=DNAJC16 PE=1 SV=1 - [Q5TDG9_HUMAN]	4	1	1	1	595	69.3	7.15
Q3SYB5	SERPINB12 protein OS=Homo sapiens GN=SERPINB12 PE=2 SV=1 - [Q3SYB5_HUMAN]	2	1	1	1	183	20.9	5.87
P10599	Thioredoxin OS=Homo sapiens GN=TXN PE=1 SV=3 - [THIO_HUMAN]	1	1	1	1	105	11.7	4.92
Q7Z5L4	Spermatogenesis-associated protein 19, mitochondrial OS=Homo sapiens GN=SPATA19 PE=2 SV=2 - [SPT19_HUMAN]	1	1	1	1	167	19.2	6.96
P31151	Protein S100-A7 OS=Homo sapiens GN=S100A7 PE=1 SV=4 - [S10A7_HUMAN]	1	1	1	1	101	11.5	6.77

B4DL87	cDNA FLJ52243, highly similar to Heat-shock protein beta-1 OS=Homo sapiens PE=2 SV=1 - [B4DL87_HUMAN]	3	1	1	1	170	18.5	6.9 5
P05109	Protein S100-A8 OS=Homo sapiens GN=S100A8 PE=1 SV=1 - [S10A8_HUMAN]	1	1	1	2	93	10.8	7.0 3
Q96L96	Alpha-protein kinase 3 OS=Homo sapiens GN=ALPK3 PE=2 SV=2 - [ALPK3_HUMAN]	1	1	1	2	1907	201. 1	7.5 8
Q9H700	cDNA: FLJ21617 fis, clone COL07481 OS=Homo sapiens PE=2 SV=1 - [Q9H700_HUMAN]	1	1	1	1	244	27.6	9.2 2
B4DHW6	cDNA FLJ54930, highly similar to Homo sapiens Dbf4-related factor 1 (DRF1), transcript variant 2, mRNA OS=Homo sapiens PE=2 SV=1 - [B4DHW6_HUMAN]	3	1	1	1	154	16.7	10. 27
L0R5A1	Alternative protein CSF2RB OS=Homo sapiens GN=CSF2RB PE=4 SV=1 - [L0R5A1_HUMAN]	1	1	1	1	108	11.6	11. 30
B3KM59	cDNA FLJ10361 fis, clone NT2RM2001256, highly similar to Anaphase-promoting complex subunit 1 OS=Homo sapiens PE=2 SV=1 - [B3KM59_HUMAN]	1	1	1	1	306	32.9	7.4 0
Q96PE2	Rho guanine nucleotide exchange factor 17 OS=Homo sapiens GN=ARHGEF17 PE=1 SV=1 - [ARHGH_HUMAN]	1	1	1	1	2063	221. 5	6.2 9
H0YEU5	Histone-binding protein RBBP4 (Fragment) OS=Homo sapiens GN=RBBP4 PE=1 SV=1 - [H0YEU5_HUMAN]	10	1	1	1	167	19.0	5.5 3
A6NCS4	Homeobox protein Nkx-2.6 OS=Homo sapiens GN=NKX2-6 PE=1 SV=1 - [NKX26_HUMAN]	1	1	1	1	301	32.1	9.8 8
I3L234	Ribosomal L1 domain-containing protein 1 (Fragment) OS=Homo sapiens GN=RSL1D1 PE=1 SV=1 - [I3L234_HUMAN]	1	1	1	1	98	11.6	9.7 4
A0A075B6Z2	Protein TRAJ56 (Fragment) OS=Homo sapiens GN=TRAJ56 PE=4 SV=1 - [A0A075B6Z2_HUMAN]	2	1	1	2	21	2.2	10. 29
Q96AY2	Crossover junction endonuclease EME1 OS=Homo sapiens GN=EME1 PE=1 SV=2 - [EME1_HUMAN]	1	1	1	1	570	63.2	7.0 5
P12004	Proliferating cell nuclear antigen OS=Homo sapiens GN=PCNA PE=1 SV=1 - [PCNA_HUMAN]	3	1	1	1	261	28.8	4.6 9
P05387	60S acidic ribosomal protein P2 OS=Homo sapiens GN=RPLP2 PE=1 SV=1 - [RLA2_HUMAN]	1	1	1	1	115	11.7	4.5 4
Q53SG8	Putative uncharacterized protein FLJ22527 (Fragment) OS=Homo sapiens GN=FLJ22527 PE=4 SV=1 - [Q53SG8_HUMAN]	6	1	1	4	199	22.8	9.9 2
H7C1L6	Cullin-3 (Fragment) OS=Homo sapiens GN=CUL3 PE=1 SV=1 - [H7C1L6_HUMAN]	3	1	1	1	192	22.6	8.6 9
E5RGW4	Nucleophosmin (Fragment) OS=Homo sapiens GN=NPM1 PE=1 SV=1 - [E5RGW4_HUMAN]	3	1	1	1	59	6.9	4.4 8
H7C0X2	Major facilitator superfamily domain-containing protein 6 (Fragment) OS=Homo sapiens GN=MFSD6 PE=1 SV=1 - [H7C0X2_HUMAN]	1	1	1	1	271	30.1	5.9 4
F8VSC5	SCY1-like protein 2 (Fragment) OS=Homo sapiens GN=SCYL2 PE=1 SV=1 - [F8VSC5_HUMAN]	2	1	1	1	681	77.0	7.0 5

I3L1H9	Zymogen granule protein 16 homolog B (Fragment) OS=Homo sapiens GN=ZG16B PE=1 SV=1 - [I3L1H9_HUMAN]	5	1	1	1	69	7.5	9.3 2
B4E3A8	cDNA FLJ53963, highly similar to Leukocyte elastase inhibitor OS=Homo sapiens PE=2 SV=1 - [B4E3A8_HUMAN]	2	1	1	1	341	38.7	6.6 7
H7C1F9	Ral GTPase-activating protein subunit alpha-2 (Fragment) OS=Homo sapiens GN=RALGAPA2 PE=1 SV=1 - [H7C1F9_HUMAN]	2	1	1	1	1740	194. 9	5.9 0
H0YHR3	Protein phosphatase Slingshot homolog 1 (Fragment) OS=Homo sapiens GN=SSH1 PE=1 SV=1 - [H0YHR3_HUMAN]	2	1	1	1	95	11.0	4.9 4
Q6ZSX8	cDNA FLJ45139 fis, clone BRAWH3039623 OS=Homo sapiens PE=2 SV=1 - [Q6ZSX8_HUMAN]	1	1	1	3	136	15.5	10. 07
A8K651	cDNA FLJ75700, highly similar to Homo sapiens complement component 1, q subcomponent binding protein (C1QBP), nuclear gene encoding mitochondrial protein, mRNA OS=Homo sapiens PE=2 SV=1 - [A8K651_HUMAN]	2	1	1	1	282	31.4	4.8 4

Control peptide 1

Accession	Description	# Proteins	# Unique Peptides	# Peptides	# PSMs	# AAs	MW [kDa]	calc. pI
H6VRF8	Keratin 1 OS=Homo sapiens GN=KRT1 PE=3 SV=1 - [H6VRF8_HUMAN]	15	24	27	142	644	66.0	8.12
P35527	Keratin, type I cytoskeletal 9 OS=Homo sapiens GN=KRT9 PE=1 SV=3 - [K1C9_HUMAN]	2	25	25	126	623	62.0	5.24
P13645	Keratin, type I cytoskeletal 10 OS=Homo sapiens GN=KRT10 PE=1 SV=6 - [K1C10_HUMAN]	7	25	26	78	584	58.8	5.21
P35908	Keratin, type II cytoskeletal 2 epidermal OS=Homo sapiens GN=KRT2 PE=1 SV=2 - [K22E_HUMAN]	12	16	23	66	639	65.4	8.00
P02533	Keratin, type I cytoskeletal 14 OS=Homo sapiens GN=KRT14 PE=1 SV=4 - [K1C14_HUMAN]	18	5	13	47	472	51.5	5.16
P08779	Keratin, type I cytoskeletal 16 OS=Homo sapiens GN=KRT16 PE=1 SV=4 - [K1C16_HUMAN]	16	7	13	41	473	51.2	5.05
B4DRR0	cDNA FLJ53910, highly similar to Keratin, type II cytoskeletal 6A OS=Homo sapiens PE=2 SV=1 - [B4DRR0_HUMAN]	17	8	16	26	535	57.8	8.00
P13647	Keratin, type II cytoskeletal 5 OS=Homo sapiens GN=KRT5 PE=1 SV=3 - [K2C5_HUMAN]	15	9	16	27	590	62.3	7.74
F5GWP8	Keratin, type I cytoskeletal 17 OS=Homo sapiens GN=KRT17 PE=1 SV=2 - [F5GWP8_HUMAN]	13	1	7	12	349	40.3	4.94
Q14CN4	Keratin, type II cytoskeletal 72 OS=Homo sapiens GN=KRT72 PE=1 SV=2 - [K2C72_HUMAN]	13	1	4	7	511	55.8	6.89
Q6KB66	Keratin, type II cytoskeletal 80 OS=Homo sapiens GN=KRT80 PE=1 SV=2 - [K2C80_HUMAN]	10	2	3	6	452	50.5	5.67

Q9GZ28	Extracellular glycoprotein lacritin OS=Homo sapiens GN=LACRT PE=1 SV=1 - [LACRT_HUMAN]	2	3	3	5	138	14.2	5.50
P81605	Dermcidin OS=Homo sapiens GN=DCD PE=1 SV=2 - [DCD_HUMAN]	1	3	3	4	110	11.3	6.54
B4E2A0	cDNA FLJ61543, highly similar to Desmoplakin OS=Homo sapiens PE=2 SV=1 - [B4E2A0_HUMAN]	6	4	4	5	1350	156.2	7.43
Q45KI0	Trypsin I (Fragment) OS=Homo sapiens GN=PRSS1 PE=3 SV=1 - [Q45KI0_HUMAN]	17	1	1	3	84	9.2	9.99
Q86YZ3	Hornerin OS=Homo sapiens GN=HRNR PE=1 SV=2 - [HORN_HUMAN]	1	2	2	3	2850	282.2	10.04
P61626	Lysozyme C OS=Homo sapiens GN=LYZ PE=1 SV=1 - [LYSC_HUMAN]	3	3	3	5	148	16.5	9.16
A0A024R0Y2	HCG30204, isoform CRA_a OS=Homo sapiens GN=hCG_30204 PE=4 SV=1 - [A0A024R0Y2_HUMAN]	13	3	3	3	2268	257.1	6.61
Q86W20	Protease serine 1 (Fragment) OS=Homo sapiens GN=PRSS1 PE=3 SV=1 - [Q86W20_HUMAN]	6	1	1	2	84	9.2	10.27
B3KX99	cDNA FLJ45019 fis, clone BRAWH3015825 OS=Homo sapiens PE=2 SV=1 - [B3KX99_HUMAN]	2	1	1	3	333	38.5	8.97
Q19KS2	Lactoferrin (Fragment) OS=Homo sapiens PE=2 SV=1 - [Q19KS2_HUMAN]	15	2	2	3	353	39.1	9.03
B2R4M6	Protein S100 OS=Homo sapiens PE=2 SV=1 - [B2R4M6_HUMAN]	2	2	2	2	114	13.2	6.13
A0A075B6Z2	Protein TRAJ56 (Fragment) OS=Homo sapiens GN=TRAJ56 PE=4 SV=1 - [A0A075B6Z2_HUMAN]	2	1	1	14	21	2.2	10.29
Q5VSP4	Putative lipocalin 1-like protein 1 OS=Homo sapiens GN=LCN1P1 PE=5 SV=1 - [LC1L1_HUMAN]	2	2	2	2	162	17.9	5.00
A0A0A0MS99	Multidrug resistance-associated protein 1 OS=Homo sapiens GN=ABCC1 PE=1 SV=1 - [A0A0A0MS99_HUMAN]	5	1	1	2	1215	134.9	6.46
I3L1U9	Actin, cytoplasmic 2 (Fragment) OS=Homo sapiens GN=ACTG1 PE=1 SV=1 - [I3L1U9_HUMAN]	47	2	2	2	214	23.8	5.44
Q5HY57	Emerin OS=Homo sapiens GN=EMD PE=1 SV=1 - [Q5HY57_HUMAN]	2	1	1	1	219	24.9	5.02
Q9HB00	Desmocollin 1, isoform CRA_b OS=Homo sapiens GN=DSC1 PE=4 SV=1 - [Q9HB00_HUMAN]	2	1	1	1	840	93.8	5.53
J3KSP2	60S ribosomal protein L38 (Fragment) OS=Homo sapiens GN=RPL38 PE=1 SV=1 - [J3KSP2_HUMAN]	4	1	1	1	21	2.6	9.99
J3QRT3	Uncharacterized protein KIAA0195 (Fragment) OS=Homo sapiens GN=KIAA0195 PE=1 SV=5 - [J3QRT3_HUMAN]	1	1	1	1	89	9.5	6.76
Q16378	Proline-rich protein 4 OS=Homo sapiens GN=PRR4 PE=1 SV=3 - [PROL4_HUMAN]	2	2	2	2	134	15.1	7.06
J3QSA3	Polyubiquitin-B (Fragment) OS=Homo sapiens GN=UBB PE=1 SV=1 - [J3QSA3_HUMAN]	37	1	1	1	43	4.9	5.19
O75556	Mammaglobin-B OS=Homo sapiens GN=SCGB2A1 PE=1 SV=1 - [SG2A1_HUMAN]	1	1	1	1	95	10.9	5.78
Q02413	Desmoglein-1 OS=Homo sapiens GN=DSG1 PE=1 SV=2 - [DSG1_HUMAN]	1	1	1	1	1049	113.7	5.03
A9UFC0	Caspase 14 OS=Homo sapiens GN=CASP14 PE=2 SV=1 - [A9UFC0_HUMAN]	2	1	1	1	242	27.6	5.34

H0YCE4	Uncharacterized protein C1orf105 (Fragment) OS=Homo sapiens GN=C1orf105 PE=4 SV=1 - [H0YCE4_HUMAN]	2	1	1	1	125	14.4	9.25
Q762B6	ATP7A protein OS=Homo sapiens GN=ATP7A PE=2 SV=1 - [Q762B6_HUMAN]	3	1	1	2	274	30.1	6.87
Q9NXJ9	cDNA FLJ20203 fis, clone COLF1334 OS=Homo sapiens PE=2 SV=1 - [Q9NXJ9_HUMAN]	3	1	1	1	697	77.6	5.50
P05109	Protein S100-A8 OS=Homo sapiens GN=S100A8 PE=1 SV=1 - [S10A8_HUMAN]	1	1	1	1	93	10.8	7.03
C9IYG1	BRCA1-associated RING domain protein 1 (Fragment) OS=Homo sapiens GN=BARD1 PE=1 SV=1 - [C9IYG1_HUMAN]	9	1	1	1	216	24.4	8.47
P31151	Protein S100-A7 OS=Homo sapiens GN=S100A7 PE=1 SV=4 - [S10A7_HUMAN]	1	1	1	1	101	11.5	6.77
A0PJ54	PEX12 protein (Fragment) OS=Homo sapiens GN=PEX12 PE=2 SV=1 - [A0PJ54_HUMAN]	1	1	1	1	324	36.9	9.98
Q8N1N4	Keratin, type II cytoskeletal 78 OS=Homo sapiens GN=KRT78 PE=2 SV=2 - [K2C78_HUMAN]	1	1	1	1	520	56.8	6.02
H7C013	Serum albumin (Fragment) OS=Homo sapiens GN=ALB PE=1 SV=1 - [H7C013_HUMAN]	9	1	1	1	197	22.8	6.34
F5H1K5	DNA repair protein RAD52 homolog OS=Homo sapiens GN=RAD52 PE=1 SV=1 - [F5H1K5_HUMAN]	9	1	1	1	99	10.8	6.25
A0A087WYX2	Histone lysine demethylase PHF8 OS=Homo sapiens GN=PHF8 PE=1 SV=1 - [A0A087WYX2_HUMAN]	2	1	1	1	303	33.8	10.08
E5RHF2	COP9 signalosome complex subunit 5 (Fragment) OS=Homo sapiens GN=COPS5 PE=1 SV=1 - [E5RHF2_HUMAN]	4	1	1	1	151	16.6	5.06
U3KQU9	POU domain, class 2, transcription factor 2 (Fragment) OS=Homo sapiens GN=POU2F2 PE=1 SV=1 - [U3KQU9_HUMAN]	10	1	1	1	65	6.9	5.78
H0YCG5	Serine/threonine-protein kinase PAK 1 (Fragment) OS=Homo sapiens GN=PAK1 PE=1 SV=1 - [H0YCG5_HUMAN]	11	1	1	1	244	27.2	4.77
Q96MA3	cDNA FLJ32709 fis, clone TESTI2000695, weakly similar to KINESIN HEAVY CHAIN (Fragment) OS=Homo sapiens PE=2 SV=1 - [Q96MA3_HUMAN]	4	1	1	1	648	73.5	5.31
B4DNN6	cDNA FLJ52003, highly similar to Homo sapiens nucleoredoxin (NXN), mRNA OS=Homo sapiens PE=2 SV=1 - [B4DNN6_HUMAN]	2	1	1	1	126	14.2	4.48
L0R5A1	Alternative protein CSF2RB OS=Homo sapiens GN=CSF2RB PE=4 SV=1 - [L0R5A1_HUMAN]	1	1	1	1	108	11.6	11.30
A6NNE9	E3 ubiquitin-protein ligase MARCH11 OS=Homo sapiens GN=MARCH11 PE=2 SV=3 - [MARHB_HUMAN]	1	1	1	1	402	43.8	6.92
Q53GE3	Pyruvate dehydrogenase E1 component subunit alpha (Fragment) OS=Homo sapiens PE=2 SV=1 - [Q53GE3_HUMAN]	1	1	1	1	390	43.2	8.06
E9PF46	Acylphosphatase OS=Homo sapiens GN=ACYP2 PE=1 SV=1 - [E9PF46_HUMAN]	2	1	1	1	97	10.3	8.69
G3V507	Protein arginine N-methyltransferase 5 OS=Homo sapiens GN=PRMT5 PE=1 SV=1 - [G3V507_HUMAN]	8	1	1	1	42	4.0	6.39
G3V3Y2	Fibulin-5 (Fragment) OS=Homo sapiens GN=FBLN5 PE=1 SV=1 - [G3V3Y2_HUMAN]	5	1	1	3	91	9.9	6.37
G3V3C9	Unconventional myosin-Va OS=Homo sapiens GN=MYO5A PE=1 SV=1 - [G3V3C9_HUMAN]	10	1	1	1	47	5.4	5.29

H0YI30	Growth/differentiation factor 11 (Fragment) OS=Homo sapiens GN=GDF11 PE=1 SV=1 - [H0YI30_HUMAN]	2	1	1	1	380	42.3	8.06
B4DSC8	cDNA FLJ53181, highly similar to Probable global transcription activator SNF2L2 (EC 3.6.1.-) (Fragment) OS=Homo sapiens PE=2 SV=1 - [B4DSC8_HUMAN]	3	1	1	1	715	83.4	8.59
E5RJS1	Protein EFR3 homolog A (Fragment) OS=Homo sapiens GN=EFR3A PE=1 SV=1 - [E5RJS1_HUMAN]	2	1	1	1	133	15.2	7.09
Q6ZSX8	cDNA FLJ45139 fis, clone BRAWH3039623 OS=Homo sapiens PE=2 SV=1 - [Q6ZSX8_HUMAN]	1	1	1	1	136	15.5	10.07
B4DZ83	cDNA FLJ59792, highly similar to Homo sapiens outer dense fiber of sperm tails 2-like (ODF2L), transcript variant 1, mRNA OS=Homo sapiens PE=2 SV=1 - [B4DZ83_HUMAN]	2	1	1	1	582	67.4	6.60
A0A096LNN3	Transcriptional regulator ATRX (Fragment) OS=Homo sapiens GN=ATRX PE=1 SV=1 - [A0A096LNN3_HUMAN]	5	1	1	1	528	59.4	6.34

Control Peptide 2

Accession	Description	# Proteins	# Unique Peptides	# Peptides	# PSMs	# AAs	MW [kDa]	calc. pI
H6VRF8	Keratin 1 OS=Homo sapiens GN=KRT1 PE=3 SV=1 - [H6VRF8_HUMAN]	16	27	30	154	644	66.0	8.12
P35527	Keratin, type I cytoskeletal 9 OS=Homo sapiens GN=KRT9 PE=1 SV=3 - [K1C9_HUMAN]	2	27	27	141	623	62.0	5.24
P13645	Keratin, type I cytoskeletal 10 OS=Homo sapiens GN=KRT10 PE=1 SV=6 - [K1C10_HUMAN]	25	23	26	87	584	58.8	5.21
P35908	Keratin, type II cytoskeletal 2 epidermal OS=Homo sapiens GN=KRT2 PE=1 SV=2 - [K22E_HUMAN]	12	20	28	77	639	65.4	8.00
P02533	Keratin, type I cytoskeletal 14 OS=Homo sapiens GN=KRT14 PE=1 SV=4 - [K1C14_HUMAN]	42	6	15	57	472	51.5	5.16
P08779	Keratin, type I cytoskeletal 16 OS=Homo sapiens GN=KRT16 PE=1 SV=4 - [K1C16_HUMAN]	39	4	11	45	473	51.2	5.05
P13647	Keratin, type II cytoskeletal 5 OS=Homo sapiens GN=KRT5 PE=1 SV=3 - [K2C5_HUMAN]	16	9	17	34	590	62.3	7.74
B4DRR0	cDNA FLJ53910, highly similar to Keratin, type II cytoskeletal 6A OS=Homo sapiens PE=2 SV=1 - [B4DRR0_HUMAN]	17	2	11	22	535	57.8	8.00
Q04695	Keratin, type I cytoskeletal 17 OS=Homo sapiens GN=KRT17 PE=1 SV=2 - [K1C17_HUMAN]	31	1	7	13	432	48.1	5.02
Q14CN4	Keratin, type II cytoskeletal 72 OS=Homo sapiens GN=KRT72 PE=1 SV=2 - [K2C72_HUMAN]	13	1	4	10	511	55.8	6.89
A0A024R0Y2	HCG30204, isoform CRA_a OS=Homo sapiens GN=hCG_30204 PE=4 SV=1 - [A0A024R0Y2_HUMAN]	13	4	4	6	2268	257.1	6.61
Q9GZZ8	Extracellular glycoprotein lacritin OS=Homo sapiens GN=LACRT PE=1 SV=1 - [LACRT_HUMAN]	2	3	3	6	138	14.2	5.50

Q86YZ3	Hornerin OS=Homo sapiens GN=HRNR PE=1 SV=2 - [HORN_HUMAN]	1	3	3	4	2850	282.2	10.04
Q45KI0	Trypsin I (Fragment) OS=Homo sapiens GN=PRSS1 PE=3 SV=1 - [Q45KI0_HUMAN]	17	1	1	4	84	9.2	9.99
P81605	Dermcidin OS=Homo sapiens GN=DCD PE=1 SV=2 - [DCD_HUMAN]	1	3	3	3	110	11.3	6.54
A0A087WWT3	Serum albumin OS=Homo sapiens GN=ALB PE=1 SV=1 - [A0A087WWT3_HUMAN]	14	3	3	3	396	45.1	6.10
B3KX99	cDNA FLJ45019 fis, clone BRAWH3015825 OS=Homo sapiens PE=2 SV=1 - [B3KX99_HUMAN]	2	1	1	3	333	38.5	8.97
A0PJ54	PEX12 protein (Fragment) OS=Homo sapiens GN=PEX12 PE=2 SV=1 - [A0PJ54_HUMAN]	1	1	1	3	324	36.9	9.98
Q19KS2	Lactoferrin (Fragment) OS=Homo sapiens PE=2 SV=1 - [Q19KS2_HUMAN]	15	3	3	3	353	39.1	9.03
B2R4M6	Protein S100 OS=Homo sapiens PE=2 SV=1 - [B2R4M6_HUMAN]	2	1	1	2	114	13.2	6.13
F8VV32	Lysozyme OS=Homo sapiens GN=LYZ PE=1 SV=1 - [F8VV32_HUMAN]	3	2	2	2	104	11.5	9.07
Q8N532	TUBA1C protein OS=Homo sapiens GN=TUBA1C PE=2 SV=1 - [Q8N532_HUMAN]	25	2	2	2	325	36.6	7.96
Q5HY57	Emerin OS=Homo sapiens GN=EMD PE=1 SV=1 - [Q5HY57_HUMAN]	2	2	2	2	219	24.9	5.02
Q5VSP4	Putative lipocalin 1-like protein 1 OS=Homo sapiens GN=LCN1P1 PE=5 SV=1 - [LC1L1_HUMAN]	2	2	2	3	162	17.9	5.00
I3L1U9	Actin, cytoplasmic 2 (Fragment) OS=Homo sapiens GN=ACTG1 PE=1 SV=1 - [I3L1U9_HUMAN]	47	2	2	2	214	23.8	5.44
M0R1I1	Tubulin beta-4A chain (Fragment) OS=Homo sapiens GN=TUBB4A PE=1 SV=1 - [M0R1I1_HUMAN]	27	1	1	1	74	7.8	4.94
F8WF65	Elongation factor 1-beta OS=Homo sapiens GN=EEF1B2 PE=1 SV=1 - [F8WF65_HUMAN]	4	1	1	1	29	3.1	4.46
H0YDD8	60S acidic ribosomal protein P2 (Fragment) OS=Homo sapiens GN=RPLP2 PE=1 SV=1 - [H0YDD8_HUMAN]	2	1	1	1	92	9.1	4.46
M0QZK8	Uncharacterized protein OS=Homo sapiens PE=4 SV=1 - [M0QZK8_HUMAN]	4	1	1	1	103	11.6	4.92
Q5D862	Filaggrin-2 OS=Homo sapiens GN=FLG2 PE=1 SV=1 - [FILA2_HUMAN]	1	1	1	1	2391	247.9	8.31
Q3SYB5	SERPINB12 protein OS=Homo sapiens GN=SERPINB12 PE=2 SV=1 - [Q3SYB5_HUMAN]	2	2	2	2	183	20.9	5.87
Q86W20	Protease serine 1 (Fragment) OS=Homo sapiens GN=PRSS1 PE=3 SV=1 - [Q86W20_HUMAN]	6	1	1	1	84	9.2	10.27
O95968	Secretoglobin family 1D member 1 OS=Homo sapiens GN=SCGB1D1 PE=1 SV=1 - [SG1D1_HUMAN]	1	1	1	1	90	9.9	9.25
P12273	Prolactin-inducible protein OS=Homo sapiens GN=PIP PE=1 SV=1 - [PIP_HUMAN]	1	1	1	1	146	16.6	8.05
J3QSA3	Polyubiquitin-B (Fragment) OS=Homo sapiens GN=UBB PE=1 SV=1 - [J3QSA3_HUMAN]	37	1	1	1	43	4.9	5.19
Q6UXS9	Inactive caspase-12 OS=Homo sapiens GN=CASP12 PE=2 SV=2 - [CASPC_HUMAN]	1	1	1	1	341	38.8	6.02
P01040	Cystatin-A OS=Homo sapiens GN=CSTA PE=1 SV=1 - [CYTA_HUMAN]	1	1	1	1	98	11.0	5.50
A8MXP8	Reticulocalbin-2 OS=Homo sapiens GN=RCN2 PE=1 SV=1 - [A8MXP8_HUMAN]	2	1	1	1	216	24.8	4.42

A8K2T2	cDNA FLJ75519 (Fragment) OS=Homo sapiens PE=2 SV=1 - [A8K2T2_HUMAN]	4	1	1	1	1173	130.7	9.01
Q9HB00	Desmocollin 1, isoform CRA_b OS=Homo sapiens GN=DSC1 PE=4 SV=1 - [Q9HB00_HUMAN]	2	1	1	1	840	93.8	5.53
G3V4X3	Protein NDRG2 OS=Homo sapiens GN=NDRG2 PE=1 SV=1 - [G3V4X3_HUMAN]	1	1	1	1	77	8.9	7.21
P31151	Protein S100-A7 OS=Homo sapiens GN=S100A7 PE=1 SV=4 - [S10A7_HUMAN]	1	1	1	1	101	11.5	6.77
A0A0A0MRQ5	Peroxiredoxin-1 OS=Homo sapiens GN=PRDX1 PE=1 SV=1 - [A0A0A0MRQ5_HUMAN]	6	1	1	1	97	10.7	8.72
Q8N1N4	Keratin, type II cytoskeletal 78 OS=Homo sapiens GN=KRT78 PE=2 SV=2 - [K2C78_HUMAN]	1	1	1	1	520	56.8	6.02
E5RG02	Putative serine protease 46 OS=Homo sapiens GN=PRSS46 PE=5 SV=1 - [PRS46_HUMAN]	1	1	1	1	174	19.3	9.10
B4DKX6	cDNA FLJ53584, highly similar to Desmoplakin (Fragment) OS=Homo sapiens PE=2 SV=1 - [B4DKX6_HUMAN]	4	1	1	1	954	112.2	6.73
F8W7D1	C3 and PZP-like alpha-2-macroglobulin domain-containing protein 8 OS=Homo sapiens GN=CPAMD8 PE=1 SV=1 - [F8W7D1_HUMAN]	4	1	1	2	503	56.0	7.84
A0A075B6G4	Protein crumbs homolog 1 OS=Homo sapiens GN=CRB1 PE=4 SV=1 - [A0A075B6G4_HUMAN]	6	1	1	1	674	74.6	5.59
A9UFC0	Caspase 14 OS=Homo sapiens GN=CASP14 PE=2 SV=1 - [A9UFC0_HUMAN]	2	2	2	2	242	27.6	5.34
Q8TDD1	ATP-dependent RNA helicase DDX54 OS=Homo sapiens GN=DDX54 PE=1 SV=2 - [DDX54_HUMAN]	1	1	1	1	881	98.5	10.02
Q02413	Desmoglein-1 OS=Homo sapiens GN=DSG1 PE=1 SV=2 - [DSG1_HUMAN]	1	1	1	1	1049	113.7	5.03
Q08AM8	SH3 domain containing ring finger 2 OS=Homo sapiens GN=SH3RF2 PE=1 SV=1 - [Q08AM8_HUMAN]	2	1	1	1	729	79.3	9.96
A0A075B6Z2	Protein TRAJ56 (Fragment) OS=Homo sapiens GN=TRAJ56 PE=4 SV=1 - [A0A075B6Z2_HUMAN]	2	1	1	10	21	2.2	10.29
Q9H6A9	Pecanex-like protein 3 OS=Homo sapiens GN=PCNXL3 PE=1 SV=2 - [PCX3_HUMAN]	1	1	1	1	2034	221.9	6.64
P05109	Protein S100-A8 OS=Homo sapiens GN=S100A8 PE=1 SV=1 - [S10A8_HUMAN]	1	1	1	1	93	10.8	7.03
Q9H4H8	Protein FAM83D OS=Homo sapiens GN=FAM83D PE=1 SV=3 - [FA83D_HUMAN]	2	1	1	1	585	64.4	6.54
Q59F77	Phosphoinositide phospholipase C (Fragment) OS=Homo sapiens PE=1 SV=1 - [Q59F77_HUMAN]	2	1	1	1	901	101.7	6.42
B7Z2C0	cDNA FLJ59621, highly similar to Liprin-beta-2 OS=Homo sapiens PE=2 SV=1 - [B7Z2C0_HUMAN]	5	1	1	1	520	57.9	8.91
A0A087WWF0	Protein IGHV3-64 OS=Homo sapiens GN=IGHV3-64 PE=1 SV=1 - [A0A087WWF0_HUMAN]	9	1	1	1	75	8.3	8.73
H7C1F9	Ral GTPase-activating protein subunit alpha-2 (Fragment) OS=Homo sapiens GN=RALGAPA2 PE=1 SV=1 - [H7C1F9_HUMAN]	2	1	1	1	1740	194.9	5.90

Appendix B: Table of accession numbers from MS

Proteins detected by mass spec which showed up in sample duplicates ordered by the accession number and uniprot description

Accession	Description	Expressed in HEK293T	SH3 domain	Comment
A0A024R0Y2	HCG30204, isoform CRA_a OS=Homo sapiens GN=hCG_30204 PE=4 SV=1 - [A0A024R0Y2_HUMAN]	Y	N	
A0A024R1X8	Junction plakoglobin, isoform CRA_a OS=Homo sapiens GN=JUP PE=4 SV=1 - [A0A024R1X8_HUMAN]	Y	N	
A0A024RC29	Desmocollin 3, isoform CRA_b OS=Homo sapiens GN=DSC3 PE=4 SV=1 - [A0A024RC29_HUMAN]	N	-	Contamination
A0A075B6Z2	Protein TRAJ56 (Fragment) OS=Homo sapiens GN=TRAJ56 PE=4 SV=1 - [A0A075B6Z2_HUMAN]	-	-	21 amino acid long peptide

A0A087WTG3	Cullin-3 OS=Homo sapiens GN=CUL3 PE=1 SV=1 - [A0A087WTG3_HUMAN]	Y	N	
A0A087WUV8	Basigin OS=Homo sapiens GN=BSG PE=1 SV=1 - [A0A087WUV8_HUMAN]	Y	N	
A0A087WWT3	Serum albumin OS=Homo sapiens GN=ALB PE=1 SV=1 - [A0A087WWT3_HUMAN]	N	-	Contamination
A0A087WXD2	Membrane-associated guanylate kinase, WW and PDZ domain-containing protein 1 OS=Homo sapiens GN=MAGI1 PE=1 SV=1 - [A0A087WXD2_HUMAN]	Y	N	Has WW domain which binds proline-rich motifs
A0A0A0MRQ5	Peroxiredoxin-1 OS=Homo sapiens GN=PRDX1 PE=1 SV=1 - [A0A0A0MRQ5_HUMAN]	Y	N	
A8K651	cDNA FLJ75700, highly similar to Homo sapiens complement component 1, q subcomponent binding protein (C1QBP), nuclear gene encoding mitochondrial protein, mRNA OS=Homo sapiens PE=2 SV=1 - [A8K651_HUMAN]	-	N	

A9UFC0	Caspase 14 OS=Homo sapiens GN=CASP14 PE=2 SV=1 - [A9UFC0_HUMAN]	N		Contamination
B2R4M6	Protein S100 OS=Homo sapiens PE=2 SV=1 - [B2R4M6_HUMAN]	-	N	
B3KPS3	cDNA FLJ32131 fis, clone PEBLM2000267, highly similar to Tubulin alpha-ubiquitous chain OS=Homo sapiens PE=2 SV=1 - [B3KPS3_HUMAN]	Y	N	
B3KRK8	cDNA FLJ34494 fis, clone HLUNG2005030, highly similar to VIMENTIN OS=Homo sapiens PE=2 SV=1 - [B3KRK8_HUMAN]	-	N	
B3KX99	cDNA FLJ45019 fis, clone BRAWH3015825 OS=Homo sapiens PE=2 SV=1 - [B3KX99_HUMAN]	-	N	
B4DHW6	cDNA FLJ54930, highly similar to Homo sapiens Dbf4-related factor 1 (DRF1), transcript variant 2, mRNA OS=Homo sapiens PE=2 SV=1 - [B4DHW6_HUMAN]	-	N	

B4DNE0	cDNA FLJ52573, highly similar to Elongation factor 1-alpha 1 OS=Homo sapiens PE=2 SV=1 - [B4DNE0_HUMAN]	-	N	
B4DRR0	cDNA FLJ53910, highly similar to Keratin, type II cytoskeletal 6A OS=Homo sapiens PE=2 SV=1 - [B4DRR0_HUMAN]	-	N	
B4DVQ0	cDNA FLJ58286, highly similar to Actin, cytoplasmic 2 OS=Homo sapiens PE=2 SV=1 - [B4DVQ0_HUMAN]	-	N	
B7Z1V3	cDNA FLJ54733, highly similar to General transcription factor 3C polypeptide 5 OS=Homo sapiens PE=2 SV=1 - [B7Z1V3_HUMAN]	-	N	
B7Z597	cDNA FLJ54373, highly similar to 60 kDa heat shock protein, mitochondrial OS=Homo sapiens PE=2 SV=1 - [B7Z597_HUMAN]	-	N	
B7Z5E7	cDNA FLJ51046, highly similar to 60 kDa heat shock protein, mitochondrial OS=Homo sapiens PE=2 SV=1 - [B7Z5E7_HUMAN]	-	N	

C9IYG1	BRCA1-associated RING domain protein 1 (Fragment) OS=Homo sapiens GN=BARD1 PE=1 SV=1 - [C9IYG1_HUMAN]	Y	N	
E5RJN0	Heparan-alpha-glucosaminide N- acetyltransferase OS=Homo sapiens GN=HGSNAT PE=1 SV=1 - [E5RJN0_HUMAN]	Y	N	
E9PN25	Heat shock cognate 71 kDa protein (Fragment) OS=Homo sapiens GN=HSPA8 PE=1 SV=1 - [E9PN25_HUMAN]	Y	N	
F6KPG5	Albumin (Fragment) OS=Homo sapiens PE=2 SV=1 - [F6KPG5_HUMAN]	N	-	Contamination
F8VV32	Lysozyme OS=Homo sapiens GN=LYZ PE=1 SV=1 - [F8VV32_HUMAN]	N	-	Contamination
F8WCH0	Actin, gamma-enteric smooth muscle OS=Homo sapiens GN=ACTG2 PE=1 SV=1 - [F8WCH0_HUMAN]	N		Contamination
F8WCJ1	Eukaryotic translation initiation factor 5A OS=Homo sapiens GN=EIF5A2 PE=1 SV=1 - [F8WCJ1_HUMAN]	Y	N	

F8WE04	Heat shock protein beta-1 OS=Homo sapiens GN=HSPB1 PE=1 SV=1 - [F8WE04_HUMAN]	Y	N	
F8WF65	Elongation factor 1-beta OS=Homo sapiens GN=EEF1B2 PE=1 SV=1 - [F8WF65_HUMAN]	Y	-	29 amino acid long peptide
G3V361	Calmodulin (Fragment) OS=Homo sapiens GN=CALM1 PE=1 SV=1 - [G3V361_HUMAN]	Y	N	EF hand motifs, calcium binding
G3V3Y2	Fibulin-5 (Fragment) OS=Homo sapiens GN=FBLN5 PE=1 SV=1 - [G3V3Y2_HUMAN]	N	-	Contamination Calcium-binding EGF domain
H0YDD8	60S acidic ribosomal protein P2 (Fragment) OS=Homo sapiens GN=RPLP2 PE=1 SV=1 - [H0YDD8_HUMAN]	Y	N	
H6VRF8	Keratin 1 OS=Homo sapiens GN=KRT1 PE=3 SV=1 - [H6VRF8_HUMAN]	N	-	Contamination
H7C1F9	Ral GTPase-activating protein subunit alpha-2 (Fragment) OS=Homo sapiens	Y	N	

	GN=RALGAPA2 PE=1 SV=1 - [H7C1F9_HUMAN]			
H7C2X0	Translation initiation factor eIF-2B subunit epsilon (Fragment) OS=Homo sapiens GN=EIF2B5 PE=1 SV=1 - [H7C2X0_HUMAN]	Y	N	
I3L1U9	Actin, cytoplasmic 2 (Fragment) OS=Homo sapiens GN=ACTG1 PE=1 SV=1 - [I3L1U9_HUMAN]	Y	N	
J3QRT3	Uncharacterized protein KIAA0195 (Fragment) OS=Homo sapiens GN=KIAA0195 PE=1 SV=5 - [J3QRT3_HUMAN]	Y	N	
J3QSA3	Polyubiquitin-B (Fragment) OS=Homo sapiens GN=UBB PE=1 SV=1 - [J3QSA3_HUMAN]	Y	N	43 amino acid peptide
L0R5A1	Alternative protein CSF2RB OS=Homo sapiens GN=CSF2RB PE=4 SV=1 - [L0R5A1_HUMAN]	N		Contamination

L8ECQ7	Alternative protein C10orf112 OS=Homo sapiens GN=C10orf112 PE=4 SV=1 - [L8ECQ7_HUMAN]	-	N	
O75531	Barrier-to-autointegration factor OS=Homo sapiens GN=BANF1 PE=1 SV=1 - [BAF_HUMAN]	Y	N	HhH domain, bind DNA
O75556	Mammaglobin-B OS=Homo sapiens GN=SCGB2A1 PE=1 SV=1 - [SG2A1_HUMAN]	N	-	Contamination
O95968	Secretoglobin family 1D member 1 OS=Homo sapiens GN=SCGB1D1 PE=1 SV=1 - [SG1D1_HUMAN]	N	-	Contamination
P01040	Cystatin-A OS=Homo sapiens GN=CSTA PE=1 SV=1 - [CYTA_HUMAN]	Y, very low levels	N	Intracellular thiol proteinase inhibitor
P02533	Keratin, type I cytoskeletal 14 OS=Homo sapiens GN=KRT14 PE=1 SV=4 - [K1C14_HUMAN]	N	-	Contamination
P05089	Arginase-1 OS=Homo sapiens GN=ARG1 PE=1 SV=2 - [ARGI1_HUMAN]	N	-	Contamination

P05109	Protein S100-A8 OS=Homo sapiens GN=S100A8 PE=1 SV=1 - [S10A8_HUMAN]	N	-	EF-hand domains
P07737	Profilin-1 OS=Homo sapiens GN=PFN1 PE=1 SV=2 - [PROF1_HUMAN]	Y	N	Binds actin
P08779	Keratin, type I cytoskeletal 16 OS=Homo sapiens GN=KRT16 PE=1 SV=4 - [K1C16_HUMAN]	N	-	Contamination
P12004	Proliferating cell nuclear antigen OS=Homo sapiens GN=PCNA PE=1 SV=1 - [PCNA_HUMAN]	Y	N	Phosphorylated by EGFR, DNA replication and DNA repair
P13645	Keratin, type I cytoskeletal 10 OS=Homo sapiens GN=KRT10 PE=1 SV=6 - [K1C10_HUMAN]	Y	N	
P13647	Keratin, type II cytoskeletal 5 OS=Homo sapiens GN=KRT5 PE=1 SV=3 - [K2C5_HUMAN]	N	-	Contamination
P31151	Protein S100-A7 OS=Homo sapiens GN=S100A7 PE=1 SV=4 - [S10A7_HUMAN]	N	-	EF-hand

P35527	Keratin, type I cytoskeletal 9 OS=Homo sapiens GN=KRT9 PE=1 SV=3 - [K1C9_HUMAN]	N	-	Contamination
P35908	Keratin, type II cytoskeletal 2 epidermal OS=Homo sapiens GN=KRT2 PE=1 SV=2 - [K22E_HUMAN]	N	-	Contamination
P50402	Emerin OS=Homo sapiens GN=EMD PE=1 SV=1 - [EMD_HUMAN]	Y	N	Stimulates actin polymerisation
P61626	Lysozyme C OS=Homo sapiens GN=LYZ PE=1 SV=1 - [LYSC_HUMAN]	N	-	Contamination
P81605	Dermcidin OS=Homo sapiens GN=DCD PE=1 SV=2 - [DCD_HUMAN]	Y	N	
Q02413	Desmoglein-1 OS=Homo sapiens GN=DSG1 PE=1 SV=2 - [DSG1_HUMAN]	N	-	Contamination
Q04695	Keratin, type I cytoskeletal 17 OS=Homo sapiens GN=KRT17 PE=1 SV=2 - [K1C17_HUMAN]	Y, very low levels	N	
Q0IIN1	Keratin 77 OS=Homo sapiens GN=KRT77 PE=1 SV=1 - [Q0IIN1_HUMAN]	N	-	Contamination

Q14CN4	Keratin, type II cytoskeletal 72 OS=Homo sapiens GN=KRT72 PE=1 SV=2 - [K2C72_HUMAN]	N	-	Contamination
Q15203	Prothymosin alpha OS=Homo sapiens PE=4 SV=2 - [Q15203_HUMAN]	Y	N	
Q16378	Proline-rich protein 4 OS=Homo sapiens GN=PRR4 PE=1 SV=3 - [PROL4_HUMAN]	N	-	Possible recognised from one of the peptides
Q19KS2	Lactoferrin (Fragment) OS=Homo sapiens PE=2 SV=1 - [Q19KS2_HUMAN]	-	N	
Q3SYB5	SERPINB12 protein OS=Homo sapiens GN=SERPINB12 PE=2 SV=1 - [Q3SYB5_HUMAN]	N	-	Contamination
Q45KI0	Trypsin I (Fragment) OS=Homo sapiens GN=PRSS1 PE=3 SV=1 - [Q45KI0_HUMAN]	N	-	Contamination
Q53HF2	Heat shock 70kDa protein 8 isoform 2 variant (Fragment) OS=Homo sapiens PE=1 SV=1 - [Q53HF2_HUMAN]	Y	N	
Q53SG8	Putative uncharacterized protein FLJ22527 (Fragment) OS=Homo sapiens	-	N	

	GN=FLJ22527 PE=4 SV=1 - [Q53SG8_HUMAN]			
Q59H57	Fusion (Involved in t(12;16) in malignant liposarcoma) isoform a variant (Fragment) OS=Homo sapiens PE=2 SV=1 - [Q59H57_HUMAN]	-	N	
Q5D862	Filaggrin-2 OS=Homo sapiens GN=FLG2 PE=1 SV=1 - [FILA2_HUMAN]	N	-	Contamination
Q5HY57	Emerin OS=Homo sapiens GN=EMD PE=1 SV=1 - [Q5HY57_HUMAN]	N	-	Contamination
Q5VSP4	Putative lipocalin 1-like protein 1 OS=Homo sapiens GN=LCN1P1 PE=5 SV=1 - [LC1L1_HUMAN]	-	N	
Q5ZEY3	Glyceraldehyde-3-phosphate dehydrogenase (Fragment) OS=Homo sapiens GN=GAPD PE=2 SV=1 - [Q5ZEY3_HUMAN]	Y	N	
Q6B823	Histone H4 (Fragment) OS=Homo sapiens PE=3 SV=1 - [Q6B823_HUMAN]	-	N	43 amino acid peptide

Q6KB66	Keratin, type II cytoskeletal 80 OS=Homo sapiens GN=KRT80 PE=1 SV=2 - [K2C80_HUMAN]	N	-	Contamination
Q6UXS9	Inactive caspase-12 OS=Homo sapiens GN=CASP12 PE=2 SV=2 - [CASPC_HUMAN]	-	N	
Q6ZSX8	cDNA FLJ45139 fis, clone BRAWH3039623 OS=Homo sapiens PE=2 SV=1 - [Q6ZSX8_HUMAN]	-	N	
Q7Z612	Acidic ribosomal phosphoprotein P1 OS=Homo sapiens PE=2 SV=1 - [Q7Z612_HUMAN]	-	N	
Q86W20	Protease serine 1 (Fragment) OS=Homo sapiens GN=PRSS1 PE=3 SV=1 - [Q86W20_HUMAN]	N	-	Contamination
Q86YZ3	Hornerin OS=Homo sapiens GN=HRNR PE=1 SV=2 - [HORN_HUMAN]	N	-	EF hand domains
Q8N1N4	Keratin, type II cytoskeletal 78 OS=Homo sapiens GN=KRT78 PE=2 SV=2 - [K2C78_HUMAN]	N	-	Contamination

Q96MA3	cDNA FLJ32709 fis, clone TESTI2000695, weakly similar to KINESIN HEAVY CHAIN (Fragment) OS=Homo sapiens PE=2 SV=1 - [Q96MA3_HUMAN]	-	N	
Q99456	Keratin, type I cytoskeletal 12 OS=Homo sapiens GN=KRT12 PE=1 SV=1 - [K1C12_HUMAN]	N	-	Contaminaton
Q9BRJ0	HECTD1 protein (Fragment) OS=Homo sapiens GN=HECTD1 PE=2 SV=2 - [Q9BRJ0_HUMAN]	Y	N	
Q9GZZ8	Extracellular glycoprotein lacritin OS=Homo sapiens GN=LACRT PE=1 SV=1 - [LACRT_HUMAN]	N	-	Contamination
Q9HB00	Desmocollin 1, isoform CRA_b OS=Homo sapiens GN=DSC1 PE=4 SV=1 - [Q9HB00_HUMAN]	N	-	Contamination
V9GZN0	Histone H2A gene (lambda-HHG55) (Fragment) OS=Homo sapiens PE=4 SV=1 - [V9GZN0_HUMAN]	-	N	47 amino acid peptide

Appendix C: C58 amino acid sequences

C58:

GGSPYPGIPVEELFKLLKEGHRMDKPANCTNELYMMMRDCWHA VPSQRPTFKQLVEDLDRILTLTTNEEYLD
LSQPLEQYS PSYPDTRSSCSSGDDSVFSPDPMPYEPCLPQYPHINGSVKT

C58 P800A:

GGSPYPGIPVEELFKLLKEGHRMDKPANCTNELYMMMRDCWHA VPSQRPTFKQLVEDLDRILTLTTNEEYLD
LSQPLEQYS PSYPDTRSSCSSGDDSVFSAADPMPYEPCLPQYPHINGSVKT

C58 P802A:

GGSPYPGIPVEELFKLLKEGHRMDKPANCTNELYMMMRDCWHA VPSQRPTFKQLVEDLDRILTLTTNEEYLD
LSQPLEQYS PSYPDTRSSCSSGDDSVFSPDAAMPYEPCLPQYPHINGSVKT

C58 P804A:

GGSPYPGIPVEELFKLLKEGHRMDKPANCTNELYMMMRDCWHA VPSQRPTFKQLVEDLDRILTLTTNEEYLD
LSQPLEQYS PSYPDTRSSCSSGDDSVFSPDMAAYEPCLPQYPHINGSVKT

C58 P807A:

GGSPYPGIPVEELFKLLKEGHRMDKPANCTNELYMMMRDCWHA VPSQRPTFKQLVEDLDRILTLTTNEEYLD
LSQPLEQYS PSYPDTRSSCSSGDDSVFSPDPMPYEAACLPQYPHINGSVKT

C58 P810A:

GGSPYPGIPVEELFKLLKEGHRMDKPANCTNELYMMMRDCWHA VPSQRPTFKQLVEDLDRILTLTTNEEYLD
LSQPLEQYS PSYPDTRSSCSSGDDSVFSPDPMPYEPCLAQYPHINGSVKT

C58 P813A:

GGSPYPGIPVEELFKLLKEGHRMDKPANCTNELYMMMRDCWHA VPSQRPTFKQLVEDLDRILTLTTNEEYLD
LSQPLEQYS PSYPDTRSSCSSGDDSVFSPDPMPYEPCLPQYAHINGSVKT

C58 Δ3:

GGSPYPGIPVEELFKLLKEGHRMDKPANCTNELYMMMRDCWHA VPSQRPTFKQLVEDLDRILTLTTNEEYLD
LSQPLEQYS PSYPDTRSSCSSGDDSVFSPDPMPYEPCLPQYPHINGSVKT

C58 Δ6:

GGSPYPGIPVEELFKLLKEGHRMDKPANCTNELYMMMRDCWHA VPSQRPTFKQLVEDLDRILTLTTNEEYLD
LSQPLEQYS PSYPDTRSSCSSGDDSVFSPDPMPYEPCLPQYPHI

C58 Δ9:

GGSPYPGIPVEELFKLLKEGHRMDKPANCTNELYMMMRDCWHA VPSQRPTFKQLVEDLDRILTLTTNEEYLD
LSQPLEQYS PSYPDTRSSCSSGDDSVFSPDPMPYEPCLPQY

C58 Δ12:

GGSPYPGIPVEELFKLLKEGHRMDKPANCTNELYMMMRDCWHA VPSQRPTFKQLVEDLDRILTLTTNEEYLD
LSQPLEQYS PSYPDTRSSCSSGDDSVFSPDPMPYEPCL

C58 Δ15:

GGSPYPGIPVEELFKLLKEGHRMDKPANCTNELYMMMRDCWHA VPSQRPTFKQLVEDLDRILTLTTNEEYLD
LSQPLEQYS PSYPDTRSSCSSGDDSVFSPDPMPYE

C58 Δ23:

GGSPYPGIPVEELFKLLKEGHRMDKPANCTNELYMMMRDCWHA VPSQRPTFKQLVEDLDRILTLTTNEEYLD
LSQPLEQYS PSYPDTRSSCSSGDDSVF